



Tissue engineering strategies for the development of a
human 3D model of the neuromuscular junction.

By

Lucia Marani

A thesis submitted in partial fulfilment of the
requirements for the reward of

Doctor of Philosophy

Loughborough University

November 2018

Table of Contents

ABSTRACT.....	VIII
ACKNOWLEDGMENTS	X
LIST OF FIGURES	XI
LIST OF TABLES	XV
LIST OF ABBREVIATIONS.....	XVI
1 INTRODUCTION	1
1.1 Neurons.....	1
1.1.1 The nervous system.....	1
1.1.2 Cellular components of the nervous system and synapses.....	4
1.1.3 Motor neurons	5
1.1.4 Neuromuscular junction development <i>in vivo</i>	6
1.1.5 Neuromuscular junction formation	6
1.1.6 Pathophysiology of the neuromuscular junction	10
1.1.7 Neurons in culture	11
1.1.8 SH-SY5Y human neuroblastoma cell line	12
1.1.8.1 Differentiation of SH-SY5Ys: an ‘eclectic’ line.....	13
1.2 Pluripotent stem cells.....	17
1.3 Muscle	17
1.3.1 Skeletal muscle gross structure and development.....	18
1.3.2 Skeletal muscle microstructure and physiology.....	20
1.3.3 Skeletal muscle force generation.....	23
1.3.4 Skeletal muscle in culture	25
1.3.4.1 C2C12 murine myoblast cell line.....	25
1.3.4.2 Human skeletal muscle.....	25

1.4	3D tissue engineering constructs	28
1.4.1	Fibrin gels.....	28
1.4.2	Collagen gels	29
1.4.3	The use of 3D constructs for functional studies	30
1.5	Conclusions and considerations.....	30
2	GENERAL METHODS.....	32
2.1	2D cell culture methods	32
2.1.1	Cell culture: C2C12.....	32
2.1.2	Cell culture: SH-SY5Y.....	32
2.1.3	Cell resuscitations: C2C12, SH-SY5Y and hSkM.....	33
2.1.4	Cell culture: hSkM cells	33
2.1.5	Cell passage and count: C2C12 and SH-SY5Y	34
2.1.6	Cryopreservation: C2C12, SH-SY5Y and hSkM.....	34
2.1.7	Cell culture and resuscitation of induced pluripotent stem cell-derived motor neurons progenitors.....	35
2.1.7.1	SureBond™ coating	35
2.1.7.2	SureBond™+ReadySet coating.....	36
2.1.7.3	Cell passage: MNPs	36
2.2	3D cell culture methods	37
2.2.1	Gel scans and gel width measurement	37
2.2.2	Fibrin gel constructs	37
2.2.3	Collagen gel constructs	38
2.2.3.1	Collagen only constructs	39
2.2.3.2	Collagen & Matrigel® constructs	40
2.3	Methods for biological analysis.....	40
2.3.1	Immunofluorescent staining.....	40

2.3.1.1	Fixation of cells in 2D.....	40
2.3.1.2	Fixation of cells in 3D.....	41
2.3.1.3	Permeabilisation of cells.....	41
2.3.1.4	Rhodamine phalloidin.....	41
2.3.1.5	β -III Tubulin.....	41
2.3.1.6	Choline Acetyltransferase.....	42
2.3.1.7	Islet 1.....	42
2.3.1.8	α -Bungarotoxin.....	42
2.3.1.9	Synaptic vesicle 2.....	43
2.3.2	Quantitative measurement of myotube width and neurite length.....	43
2.3.3	RNA extraction.....	44
2.3.4	RNA quantification.....	44
2.3.5	RT-qPCR.....	45
2.3.6	RT-qPCR data analysis.....	45
2.4	Statistical analysis.....	48
3	C2C12 & SH-SY5Y: OPTIMISING A CHIMERIC MUSCLE-NERVE CO-CULTURE IN 2D.....	49
3.1	Introduction.....	49
3.1.1	The effect of retinoic acid on C2C12 and SH-SY5Y cells.....	50
3.1.2	The use of agrin to increase muscle-nerve interactions.....	51
3.2	Aims & objectives of the chapter.....	51
3.3	Materials & Methods.....	53
3.3.1	Co-culture medium optimisation: different RA concentrations.....	53
3.3.2	Addition of agrin to mono and co-culture.....	54
3.3.3	Co-culture morphological staining: phalloidin & β -III Tubulin.....	55
3.3.4	Co-culture interaction staining: BTX & SV-2.....	55

3.3.5	Quantitative analysis: measurement of myotube width and neurite length ...	55
3.3.6	Statistical analysis	55
3.4	Results	56
3.4.1	Co-culture medium optimisation: the effect of the RA concentration on C2C12 and SH-SY5Y morphology.....	56
3.4.2	C2C12 and SH-SY5Y interactions: co-localisation of acetylcholine receptors and synaptic vesicle 2	62
3.4.3	The addition of agrin did not affect myotube width and muscle maturity.....	67
3.5	Discussion.....	79
3.5.1	A concentration of 1 μ M RA ensures both C2C12 and SH-SY5Y differentiation.....	79
3.5.2	NMJ formation between C2C12 and SH-SY5Y: finding a needle in a haystack	80
3.5.3	Agrin enhanced muscle maturity in co-cultures, and decreased it in monocultures.....	81
3.6	Chapter summary.....	82
4	C2C12 & SH-SY5Y CO-CULTURE: FROM 2D TO 3D.....	84
4.1	Introduction	84
4.2	Aims & objectives of the chapter	86
4.3	Materials & Methods	87
4.3.1	Co-culture in fibrin gels	87
4.3.2	Co-culture in 500 μ L collagen gels.....	87
4.3.3	Morphological staining of 3D constructs: phalloidin and β -III Tubulin.....	87
4.3.4	Statistical analysis	87
4.4	Results	88
4.4.1	C2C12 & SH-SY5Y co-culture in fibrin gels	88
4.4.2	C2C12 & SH-SY5Y co-culture in 500 μ L collagen gels.....	93

4.5	Discussion.....	97
4.5.1	C2C12 & SH-SY5Y differentiate and align in fibrin gel constructs.....	97
4.5.2	C2C12 & SH-SY5Y differentiate and align in 500 μ L collagen gel constructs 98	
4.6	Chapter summary.....	100
5	IPSC-DERIVED MOTOR NEURON PROGENITORS CHARACTERISATION .	102
5.1	Introduction	102
5.1.1	Sources of human motor neurons.....	102
5.1.2	Induced pluripotent stem cells for the generation of motor neurons.....	103
5.1.3	ChAT and Islet 1 as markers of mature MNs.....	104
5.2	Aims & objectives of the chapter	106
5.3	Materials & Methods	107
5.3.1	MNPs: expansion and differentiation at P1.....	107
5.3.1.1	MNPs: positivity to cholinergic markers	107
5.3.2	MNPs characterisation: expansion and differentiation at P2	107
5.4	Results	108
5.4.1	MNPs characterisation: expansion and differentiation at P1	108
5.4.1.1	MNPs characterisation: MN markers immunostaining.....	113
5.4.2	MNPs characterisation: expansion and differentiation at P2	118
5.5	Discussion.....	121
5.5.1	MNPs can be cultured and differentiated into MN-like cells.....	121
5.5.2	MNPs cannot be differentiated at P2.....	121
5.5.3	MNPs express cholinergic markers ChAT and Islet 1	122
5.6	Chapter summary.....	123
6	ESTABLISHING HUMAN MUSCLE-NERVE CO-CULTURES	124
6.1	Introduction	124

6.1.1	iPSC-derived MNs and human primary SkM co-cultures	124
6.2	Aims & objectives of the chapter	125
6.3	Materials & Methods	127
6.3.1	Human MNPs and human SkM co-culture	127
6.3.2	Human co-cultures in collagen/Matrigel® gels	129
6.3.3	Force measurement	130
6.3.4	Confocal imaging	130
6.3.5	Cross sections preparation.....	131
6.4	Results	132
6.4.1	MNPs & human primary SkM co-culture in monolayer.....	132
6.4.2	Hu028_1 & MNPs co-culture in monolayer: preliminary cues on substrate and media compatibility	132
6.4.2.1	Hu020, hu027 and hu028_2 & MNPs co-culture: how do MNs affect SkM?	137
6.4.3	The first attempt of a human muscle-nerve 3D co-culture.....	145
6.5	Discussion.....	159
6.5.1	Substrate and media compatibility for human SkM co-cultures with human MNs	159
6.5.2	Human muscle-nerve co-cultures in 2D: cues on SkM maturation and the influence of MNs	160
6.5.3	The first attempt to establish a human muscle-nerve co-culture in 3D.....	162
6.6	Chapter summary.....	164
7	GENERAL DISCUSSION	165
7.1	Key findings	166
7.2	Future directions	172
7.3	Conclusions	175
8	BIBLIOGRAPHY	176

9	SUPPLEMENTARY INFORMATION	205
9.1	APPENDIX A: SH-SY5Y neurites alignment to C2C12 myotubes	205
9.2	APPENDIX B: Human skeletal muscle & SH-SY5Y co-culture.....	205
9.3	APPENDIX C: SH-SY5Y vs iPSC-derived MNs comparison.....	208
9.4	APPENDIX D: Media and substrate for human MNs: compatibility for hSkM.	212
9.5	APPENDIX E: Culture of Human iPSC-Derived Motor Neuron Progenitors....	217

ABSTRACT

In vitro models represent an important tool in the regenerative medicine research area. Great importance is given to utilising a representative system, which closely mimics the *in vivo* environment.

Developing a model of the neuromuscular junction (NMJ) is a promising step which will allow scientists to investigate the physiology and pathophysiology of the interface between skeletal muscles (SkM) and peripheral motor neurons (MNs). These cell types can be affected by degenerative disease such as amyotrophic lateral sclerosis (ALS), that leads to progressive paralysis and for which no treatment is available to this date. A human model of the NMJ could be used to study potential therapeutic agents and reduce the use of animals in research.

The main aim of this project was to “humanise” currently existing models of the NMJ using tissue engineered constructs. In the first part of the work, cell lines were used to establish a chimeric co-culture. Immunofluorescent staining, gene expression analysis and the evaluation of morphological features were used. As a result, the co-culture conditions for C2C12s and SH-SY5Ys were optimised, the expression of pre- and post-synaptic proteins was verified and agrin was not included in the medium for 3D cultures. Fibrin and collagen constructs allowed for the alignment of C2C12 fibres, and the addition of SH-SY5Ys to the culture did not affect matrix remodeling or myotube width. However, information on the cells distribution, training on the use of tissue engineered constructs and observations on the alignment of SH-SY5Ys were gathered. Subsequently, iPSC-derived MN progenitors were differentiated for 35 days and showed typical MN morphology, as well as cholinergic markers expression. The culture of SkM on gelatin proved to be more effective for its differentiation, and donor-to-donor variability was observed when generating the co-culture with MNs. Despite the expression of NMJ markers and the use of 3D constructs, gene expression was depleted when the neurons were present in the culture, the distribution of the cells within collagen/Matrigel® gels did not allow for an increase in force generation and it was not possible to verify the presence of a NMJ.

The co-culture of human muscle and nerve in a 3D environment is a promising model which allows researchers to understand the mechanisms underpinning NMJ development and formation. Tissue engineered constructs are suitable systems as they allow for the cells to grow and interact in a matrix which mimics the *in vivo* conditions, while mechanically or electrically stimulate the cells. The work carried out for this thesis led to a great amount of future

developments using a novel co-culture system, which is an improvement compared to existing animal or embryonic models. This can be further optimised for applications such as drug screening, personalised medicine testing, or disease modeling.

ACKNOWLEDGMENTS

This work would have not been completed without the precious support of my supervisor, Professor Mark P Lewis, and co-supervisors. Thanks for being encouraging and for showing me how to appreciate every small achievement throughout my PhD. Mark, your passion and positivity was a constant lesson for me, and I will never forget your reassuring words, often spoken after a good drink. Thanks to our research group for the endless roundtables, the banter and the occasional distraction which made this journey fly. A particular thought goes to Dr Darren J Player and Dr Neil W Martin who were always available to share expertise and guidance, and to deal with my moments of discouragement. The sciencey ChATs with you were a fundamental part of this. Maria, you know everything.

Without the amazing “Trimonas” I met here in Loughborough, this would have been so much harder. You know who you are, you hold a special place in my heart and I am incredibly grateful for meeting you and receiving your support and understanding in moments of need. You came into my life as friends, now you are brothers and sisters away from home. Thanks to Holly and Chris too for being teachers more than students, for being proud of me and making this past year special.

At first I did not want to do a PhD, but I am grateful I did. I learned so much, not just about how to be a scientist, but mostly about myself. I understood how much I love research when I saw a myotube twitching and some motor neurons in culture, and that says it all. Other times I loved it less, but overcoming the frustration made it all worthwhile in the end.

Last but not least, thanks to my beautiful family who never stopped believing in me. Thanks for coping with the distance and doing the simplest things to make me feel loved. Mum, dad, after almost 10 years at uni, I am finally not a student anymore, but I would not have come this far without you. From the bottom of my heart, thanks for being the best family I could ever have wished for.

LIST OF FIGURES

Figure 1.1. Structural organisation of the nervous system.....	3
Figure 1.2. Structure of neurons.....	5
Figure 1.3. Motor unit structure.	7
Figure 1.4. Action potential in neurons.....	8
Figure 1.5. NMJ formation.	10
Figure 1.6. Skeletal muscle structure.	19
Figure 1.7. MRF in SkM maturation and differentiation.....	19
Figure 1.8. Schematic representation of the muscle fibre and its micro components.....	22
Figure 1.9. The force-frequency relationship in SkM.....	24
Figure 1.10. Schematic representation of the culture of myoblasts in fibrin gels.....	28
Figure 1.11. Schematic representation of the culture of myoblasts in collagen gels.....	29
Figure 2.2. 3D printed inserts for collagen gels preparation.....	39
Figure 3.1. Representative images of C2C12 and SH-SY5Y monocultures in optimal conditions.....	56
Figure 3.2. Monocultures differentiated with different concentrations of RA.	58
Figure 3.3. C2C12 and SH-SY5Y co-cultures differentiated with different concentrations of RA.	59
Figure 3.4. C2C12 myotube width (μm) when the cells are monocultured and co-cultured with SH-SY5Y in optimal conditions (control) and at different concentrations of RA.	60
Figure 3.5. SH-SY5Y neurite length (μm) when the cells are monocultured and co-cultured with myoblasts and myotubes at different concentrations of RA.	61
Figure 3.6. AChR's are expressed on C2C12 differentiated for 3 (3D), 5 (5D) or 7 (7D) days in MDM.	62
Figure 3.7. Detail of AChR's on the surface of C2C12 myotubes after 5 days of differentiation.	64

Figure 3.8. C2C12 and SH-SY5Y express pre- and post-synaptic structures in monolayer co-cultures.	65
Figure 3.9. C2C12 and SH-SY5Y cells interact and AChR's and SV-2 colocalise.	66
Figure 3.10. Morphological immunostaining of C2C12 monocultures and co-cultures with SH-SY5Y, in the presence or absence of agrin.	68
Figure 3.11. Myotube width of C2C12 in monoculture and co-culture, with or without agrin.	69
Figure 3.12. Interaction staining C2C12 myotubes in monoculture in the absence or presence of agrin, and in co-culture with SH-SY5Y in the presence or absence of agrin.	70
Figure 3.13. MyoD (development) mRNA expression in C2C12 cultured in different conditions.	72
Figure 3.14. MyoG (development) mRNA expression in C2C12 cultured in different conditions.	73
Figure 3.15. MyHC3 (embryonic) mRNA expression in C2C12 cultured in different conditions.	74
Figure 3.16. MyHC8 (neonatal) mRNA expression in C2C12 cultured in different conditions.	75
Figure 3.17. MyHC7 (slow) mRNA expression in in C2C12 cultured in different conditions.	76
Figure 3.18. MyHC1 (fast) mRNA expression in in C2C12 cultured in different conditions.	77
Figure 3.19. MyHC2 (fast) mRNA expression in C2C12 cultured in different conditions.	78
Figure 4.1. C2C12 myoblasts differentiate into myotubes in fibrin gel constructs.	88
Figure 4.2. Fibrin gels deformation over time in control conditions (C2C12 monoculture) and C2C12/SH-SY5Y co-culture.	89
Figure 4.3. Fibrin gels deformation.	90
Figure 4.4. C2C12 and SH-SY5Y co-culture in fibrin gel constructs.	92
Figure 4.5. Bundles of SH-SY5Y on fibrin gel constructs.	92

Figure 4.6. Myotube width of C2C12 cells monocultured in fibrin gels (control), and co-cultured with SH-SY5Y cells (co-culture).....	93
Figure 4.7. C2C12 myoblasts differentiate into myotubes in collagen gel constructs.....	94
Figure 4.8. Collagen gels deformation over time in control conditions (C2C12 monoculture) and C2C12/SH-SY5Y co-culture.....	95
Figure 4.9. Collagen gels deformation.....	95
Figure 4.10. C2C12 and SH-SY5Y co-culture in 500 μ L collagen gel constructs.....	96
Figure 4.11. Myotube width of C2C12 cells monocultured in 500 μ L collagen gels (control), and co-cultured with SH-SY5Y cells (co-culture).....	96
Figure 5.1. MNPs P1 proliferation after thawing.....	108
Figure 5.2. MNPs P1 did not adhere on gelatin upon thawing.	109
Figure 5.3. MNPs P1 differentiation in monolayer from day 0 to day 10.	110
Figure 5.4. MNPs P1 differentiation in monolayer from day 12 to day 22.	111
Figure 5.5. MNPs P1 differentiation in monolayer from day 24 to day 34.	112
Figure 5.6. MNPs are positive to ChAT immunostaining from day 5 to day 35.....	114
Figure 5.7. MNPs are positive to Islet 1 immunostaining at day 5, 7 and 14. The cells were immunostained for Islet 1 to identify the cholinergic marker (red), β -III Tubulin for the cytoskeleton (green) and DAPI to counterstain the nuclei (blue). Scale bars: 50 μ m.....	115
Figure 5.8. MNPs express the cholinergic marker ChAT in the nuclei after 5 days in MM.....	116
Figure 5.9. MNPs express the cholinergic marker Islet 1 in the nuclei after 5 days in MM.....	117
Figure 5.10. MNPs at passage P1 and P2 expansion upon thawing, from day 1 to day 5....	119
Figure 5.11. MNPs P2 did not adhere to SureBond™+ReadySet-coated glass after passage.	120
Figure 6.1. Co-culture protocol using hu020, hu027 and hu028_2 SkM cells.	129
Figure 6.2. Human primary SkM cells hu028_1 cultured on gelatin and SureBond™+ReadySet.	133
Figure 6.3. Human primary SkM cells hu028_1 and MNPs were co-cultured on gelatin and SureBond™+ReadySet.	134

Figure 6.4. Number of hu028_1 myotubes per frame.....	135
Figure 6.5. MNPs extend along and around hu028_1 myofibres (plate C).	136
Figure 6.6. Human muscle-nerve co-cultures using hu020, hu027 and hu028_2 SkM cells and MNPs.	138
Figure 6.7. Myotube width (μm) of hu020, hu027 and hu028_2 in control, MM and co-culture conditions.....	139
Figure 6.8. Interaction immunostaining of pre- and post-synaptic markers in human co-cultures.	140
Figure 6.9. MyHC8 (neonatal) mRNA expression in human SkM hu027 and hu028_2.....	142
Figure 6.10. MyHC7 (fast) mRNA expression in human SkM hu027 and hu028_2.	143
Figure 6.11. MyHC1 (fast) mRNA expression in human SkM hu027 and hu028_2.	144
Figure 6.12. Collagen gels (50 μL) with hu028_2 and MNs.	146
Figure 6.13. Collagen/Matrigel® gels deformation.....	147
Figure 6.14. 3D culture of hu028_2 and MNs.	148
Figure 6.15. Myotube width (μm) of hu028_2 cultured in 50 μL collagen/Matrigel® gels.	149
Figure 6.16. Contractility of hu028_2 cells in 50 μL collagen/Matrigel® gels.....	151
Figure 6.17. Tile scans of human 50 μL collagen/Matrigel® constructs.	153
Figure 6.18. Morphological tile scan image of human co-culture gels.....	155
Figure 6.19. Z stack of co-culture gels acquired via confocal imaging.....	156
Figure 6.20. Cross sectional images of hu028_2 and MNs co-culture constructs.	158
Figure 7.1. Process to develop a personalised 3D muscle-nerve in vitro model.	174
Figure S9.1. hu035 and SH-SY5Y co-culture in monolayer.	206
Figure S9.2. Number of hu035 myotubes per frame (n).....	207
Figure S5.12. Positivity to ChAT immunostaining in SH-SY5Y and MNs.	209
Figure S5.13. Morphological difference between SH-SY5Y and iPSC-derived MNs.....	210
Figure S5.14. SH-SY5Y neurite length (μm) in different culture conditions.....	211

Figure S9.3. hu029 proliferation on gelatin and SureBond™+ReadySet over a period of 4 days.	213
Figure S9.4. hu029 differentiation on gelatin (in control conditions, MDM and neuronal medium, MM) and SureBond™+ReadySet (in neuronal MM).	214
Figure S9.5. Number of hu029 cells per frame (n) during proliferation on gelatin or SureBond™+ReadySet.	215
Figure S9.6. Desmin positivity of hu029 cells cultured on gelatin or SureBond™+ReadySet, and differentiated in either MDM or MM.	216

LIST OF TABLES

Table 1.1. Summary of the techniques reported in the literature to induce differentiation of SH-SY5Y cells.	15
Table 1.2. MyHC isoforms in mouse and human during development and in adult SkM.....	23
Table 1.3. Summary of the applications of C2C12 cells as model for the NMJ.....	27
Table 2.4. Donors information for work using primary SkM cells.....	34
Table 2.5. Target genes and primer sequences utilised for RT-qPCR of mouse cells (C2C12).	46
Table 2.6. Target genes and primer sequences utilised for RT-qPCR of human cells (hu020, hu027, hu028_1 and hu028_2).	47
Table 3.1. Composition of gold standard media used to expand and differentiate C2C12 and SH-SY5Y.	53
Table 3.2. Composition of different media used with different concentrations of RA for the co- culture of C2C12 and SH-SY5Y.....	53
Table 3.3. Samples details for the addition of agrin to C2C12 monocultures and co-cultures with SH-SY5Y cells.....	54
Table 3.4. Myotube width (μm) and neurite length (μm) of C2C12 and SH-SY5Y.	57
Table 5.1. Summary of recent protocols used for the differentiation of hES and iPSCs into MNs.....	105
Table 6.1. Media abbreviations and compositions used for the MNPs & human primary SkM co-culture.	127
Table 6.2. Experimental setup for the MNPs/hu028_1 co-culture in monolayer. All samples were seeded both on SureBond™+ReadySet and gelatin.....	128
Table 6.3. Maximum force (μN) generated by hu028_2 cells in 50 μL collagen/Matrigel® constructs.	150
Table S9.1. Angle difference between the orientation of C2C12 muscle fibres and SH-SY5Y neurites.....	205
Table S9.2. Culture conditions for SH-SY5Y cells and MNPs.	208

LIST OF ABBREVIATIONS

3D	three-dimensional
AA	ascorbic acid
ACh	acetylcholine
AChE	acetylcholine esterase
AChR	acetylcholine receptor
ADP	adenosine diphosphate
ALS	amyotrophic lateral sclerosis
ATP	adenosine triphosphate
BDNF	brain-derived neurotrophic factor
bFGF	basic fibroblast growth factor
BTX	α -bungarotoxin
cAMP	cyclic adenosine monophosphate
cDNA	complementary deoxyribonucleic acid
Ch	choline
ChAT	choline acetyltransferase
CNS	central nervous system
cpdC	compound C
CNTF	ciliary neurotrophic factor
C_T	cycle threshold
DAPI	4',6-diamidino-2-phenylindole
DAT	dopamine transporter
DM	differentiation medium
DMEM	Dulbecco's Modified Eagle's medium
DMSO	dimethyl sulfoxide
DNA	deoxyribonucleic acid
dNTPs	deoxyribonucleotide triphosphate
DR2/DR3	dopaminergic receptor 2/3
ECM	extracellular matrix
ESCs	embryonic stem cells

FBS	foetal bovine serum
FDM	fused deposition modelling
GDNF	glial-derived neurotrophic factor
GM	growth medium
GS	goat serum
KOSR	knockout serum replacement
HS	horse serum
hSkM	human-derived skeletal muscle
ICC	immunocytochemistry
IGF-1	insulin-like growth factor 1
IHC	immunohistochemistry
iPSCs	induced pluripotent stem cells
MAb	monoclonal antibody
MAP2	microtubule-associated protein 2
MDM	muscle differentiation medium
MEFs	mouse embryonic fibroblasts
MEM	Eagle's minimal essential medium
MG	myasthenia gravis
MGM	muscle growth medium
MM	maintenance medium
MN	motor neuron
MNPs	motor neuron progenitors
MPP	1-methyl-4-phenyl-1,2,3,6-tetrahydropyridinium ion
ms	millisecond
MSCs	mesenchymal stem cells
MyHC	myosin heavy chain
MyLC	myosin light chain
MyoG	myogenin
NaOH	sodium hydroxide
NDM	neuronal differentiation medium
NEAA	non-essential amino acids
NGM	neuronal growth medium

nM	nanomolar
NMJ	neuromuscular junction
NSE	neuron specific enolase
P1	passage 1
P2	passage 2
PAb	polyclonal antibody
Pax	paired box
PBS	phosphate buffer saline
PCR	polymerase chain reaction
PEEK	polyether ether ketone
PNS	peripheral nervous system
PLA	poly(lactic acid)
Pur	purmorphamin
P/S	penicillin/streptomycin
RA	retinoic acid
RAR	retinoic acid receptor
RARE	retinoic acid responsive elements
RM	recovery medium
RNA	ribonucleic acid
RT	room temperature
RT-qPCR	reverse transcriptase quantitative polymerase chain reaction
RXR	retinoic X receptor
SkM	skeletal muscle
SMA	spinal muscular atrophy
ssDNA	single strand deoxyribonucleic acid
SV-2	synaptic vesicle 2
Syn	synapsin
TBS	tris buffered saline
TH	tyrosine hydroxylase
TPA	12-O-tetradecanoyl-phorbol-13-acetate
Tuj1	β -III Tubulin
UV	ultraviolet

VMAT	vesicular monoamine transporter
μL	microliter
μm	micrometer
μM	micromolar
μN	micronewton

1 INTRODUCTION

The experiments described in this thesis represent an attempt to develop a three-dimensional model of the neuromuscular junction using human cells. Therefore, this introduction will focus on what is currently known regarding skeletal muscle, motor neurons, the interface between the two, and tissue engineering approaches to establish a co-culture model. The aim of this section is to give the reader an insight into the general structure and physiology of either tissues, while providing details which will be useful to understand the experimental design and development of each chapter that follows.

1.1 Neurons

1.1.1 The nervous system

The nervous system is a complex network of neurons and glia cells which are responsible for the transmission of signals throughout the body, via electro-chemical pathways. The structure of the nervous system is represented in **Figure 1.1**. In mammals, it has two main divisions: the central nervous system (CNS) conducts and interprets signals and stimuli to the peripheral nervous system (PNS). The CNS includes the brain (cerebrum, cerebellum and brain stem), the spinal cord, optic, olfactory and auditory systems; the PNS transmits sensory and excitatory stimuli to and from the spinal cord. It comprises cranial (from the brain), spinal (from the spinal cord) and sensory nerves which interconnect the CNS to the body (Schmidt and Leach, 2003). The PNS is divided into somatic and visceral regions. The somatic region includes spinal nerves which innervate skin, joints and voluntary muscles. Here lie motor neurons (MNs), specialised neurons which command muscle contraction within the body. The soma of MNs (i.e. cell body) is located in the CNS (spinal cord), whilst the axons extending from them are mostly located in the PNS. The visceral PNS, also called autonomic, is formed by neurons which innervate internal organs, glands and blood vessels (Bear et al., 2001). It is subdivided into the sympathetic and parasympathetic regions, which are responsible for opposing responses. While the sympathetic division is triggered in moments of stress or danger commonly known as the ‘fight or flight response’, the parasympathetic system is in charge of relaxing the body as a reaction to the sympathetic trigger, known as the ‘rest and digest’ response (Alberts et al., 2002; Lodish et al., 2000).

From a functional point of view, the nervous system is divided into sensory systems and motor systems. Sensory systems are appointed to acquire and process information from the surrounding environment, utilising sensory ganglia, nerves and receptors within the body. The motor systems include autonomic ganglia and nerves, and MNs, which respond to central information and target peripheral structures (smooth, cardiac and skeletal muscles, and glands) (Purves et al., 2004).

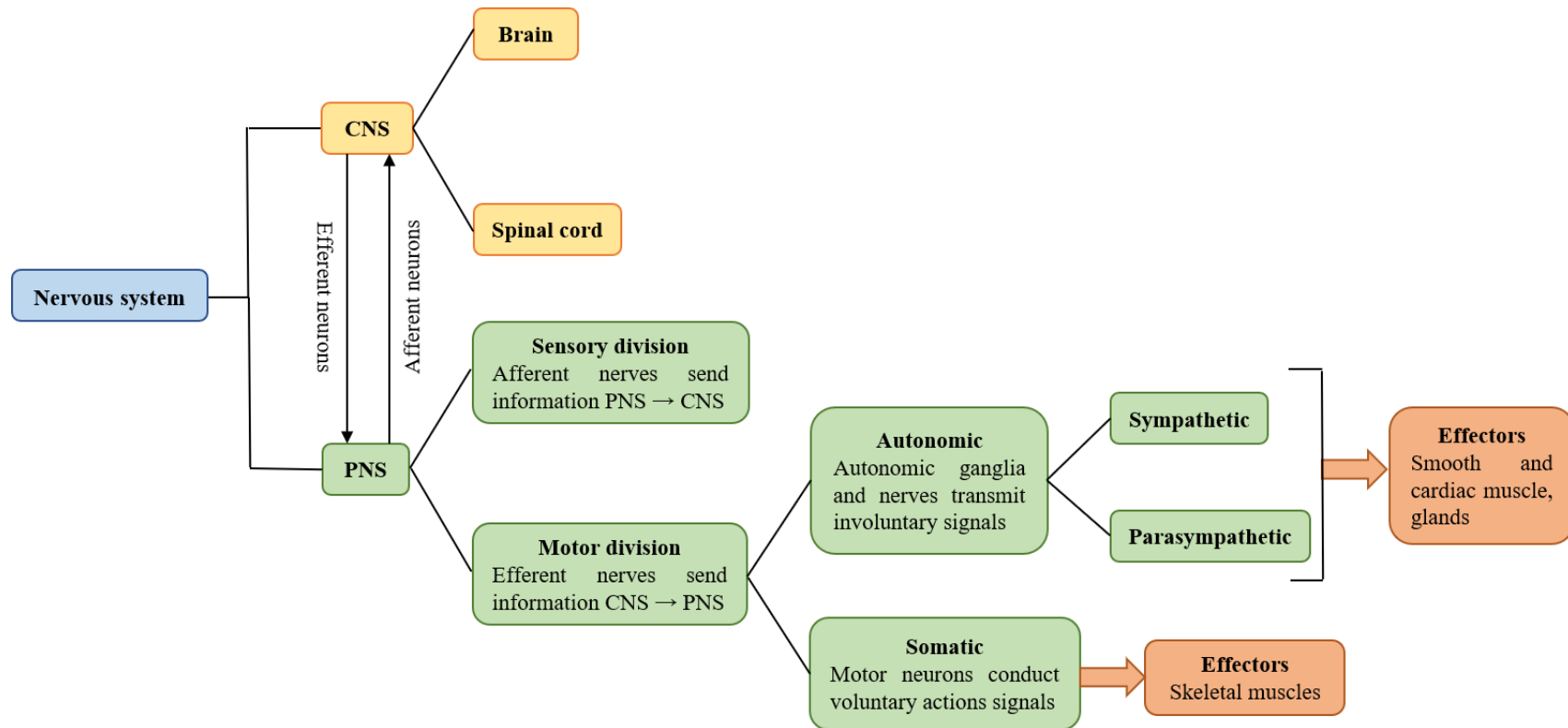


Figure 1.1. Structural organisation of the nervous system. The nervous system is divided into the central nervous system (CNS), which includes the brain and spinal cord, and the peripheral nervous system (PNS). This comprises a sensory division which functions as a connection between the PNS and the CNS, and a motor division, which runs in the opposite direction. The motor division, is subdivided into autonomic (involuntary signals which target smooth muscle, cardiac muscle and glands) and somatic (voluntary signals which target skeletal muscles). The part of the autonomic system referred to as sympathetic is responsible for the ‘fight or flight’ response, whereas the parasympathetic is responsible for the ‘rest and digest’ response.

1.1.2 Cellular components of the nervous system and synapses

The nervous system is mainly composed of two cell types: neurons and glial cells. These differ in structure and function across CNS and PNS. Generally, neurons represent the structural and functional elements of the nervous system, while glial cells act as support for neurons and mediate processes such as development and regeneration (Schmidt and Leach, 2003).

Neurons (**Figure 1.2**) are specialised cells capable of conducting electrical signals over long distances. This section will elaborate mainly on peripheral neurons as they are relevant to this work. Although neurons vary in size and shape depending on their function, their structure is consistent: neurons are made of a cell body (soma) and its extensions (dendrites and axons). Signal from other cells are picked up by dendrites and transmitted to the soma, whereas outgoing signals travel along the axons and are diffused via the axon terminals (Purves et al., 2004). Axons are surrounded by myelinated Schwann cells, which represent the glial cell population. These cells are essential to the survival and function of neurons by secreting trophic agents (Bhatheja and Field, 2006; Son and Thompson, 1995), besides being involved in debris clearance and cytokine release during axonal regeneration (Schmidt and Leach, 2003). Individual axons and myelin sheaths are enclosed in the endoneurium, a complex membrane which sustains neurons. Bundles of axons form fascicles around which the perineurium lies as a layer of fibroblasts and collagen. Lastly, multiple fascicles are grouped into a large nerve cable surrounded by a fibrocollagenous tissue called epineurium (Schmidt and Leach, 2003; Winter and Schmidt, 2002). The highly organised and aligned structure of neurons resemble the one found in skeletal muscles (SkM), which will be discussed further in section 1.3.

The signal transmission occurs via an impulse, which is triggered by a change in the membrane potential. When neurons are at resting potential, their inner charge equals -70 mV and is stabilised by sodium and potassium pumps. If the neuron receives a signal which is powerful enough to modify this potential, voltage-gated ion channels open on the surface of the cell and allow for a positively-charged ion flow to enter it, thus depolarising the cell (depolarisation). Return to the resting potential occurs through hyperpolarisation and the release of positive ions (Alberts et al., 2002; Lodish et al., 2015). The presence of myelin around the axons gives rise to the so-called saltatory conduction: impulses jump faster and more effectively from one node of Ranvier to another, as myelin represents a non-conductive layer (Purves et al., 2004).

A synapse is the mechanisms through which neurons communicate with other neurons or cell types. These signal transmissions can be either chemical or electrical. Chemical synapses involve the release of vesicles containing the chemicals by the axon terminals and fuse to the post-synaptic membrane to trigger a response. These chemicals are called neurotransmitters, and have different effects depending on their class (Alberts et al., 2002; Purves et al., 2004). Particularly relevant to this thesis is acetylcholine (ACh), a neurotransmitter released by MNs which binds to SkM fibres to trigger muscle contraction. This interaction, referred to as a neuromuscular junction (NMJ) will be addressed in detail below (see section 1.1.5).

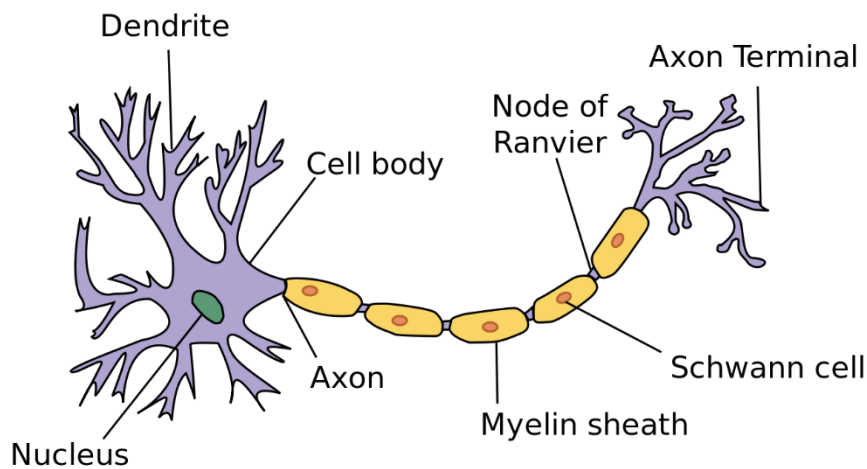


Figure 1.2. Structure of neurons. The cell body of neurons is called soma. Dendrites are responsible for receiving stimuli from other cells to the soma, whereas axons transmit information from the soma to other cells. Axons are surrounded by intermittent regions of myelin sheaths which insulate and protect them while allowing for a quicker transmission. The electrical impulse travels from node to node of Ranvier, thus reaching the axon terminals quicker than unmyelinated sheaths. Image from Wikimedia.org.

1.1.3 Motor neurons

Peripheral MNs are efferent neurons which develop from the neuroepithelium in the notochord, and reside in the somatic portion of the motor division (DeLapeyriere and Henderson, 1997). During development, MNs extend axons towards SkM fibres in a process controlled by a complex network of chemoattractants and repellents (reviewed by DeLapeyriere and Henderson, 1997). Mature MNs are subdivided into three types, α , β and γ . The most abundant ones are α -MNs, the function of which is to innervate extrafusal SkM fibres to trigger contraction. The γ subtype innervate intrafusal fibres and are involved in motor control, while

β -MNs innervate both fibre types and have, as yet, a poorly understood role in muscle contraction (Kanning et al., 2010).

1.1.4 Neuromuscular junction development *in vivo*

For a NMJ to form, the development of both SkM and MNs must be complete. These cell types generate from two different germ lines, MNs from the ectoderm and SkM from the mesoderm. Around the 3rd week of gestation, the outer layer of the embryo (i.e. the ectoderm) thickens and forms a neural plate which progressively folds to fuse into the neural tube at the end of the 4th week. As development progresses, different portions of the tube will give rise to different areas of the nervous system. The patterning process determines the dorso-ventral and rostro-caudal axes, and early MNs originate to then mature and synapse with SkM fibres. These fibres are fully formed at the end of the 12th week of gestation, and evidence of NMJ formation was observed within that time (Molina et al., 2010). In the mesoderm, MyoD and Myf5 expression triggers the generation of myogenic precursors which then mature into myoblasts thanks to an increase in Myogenin and Mrf4. Further expression of Mrf4, MyoD and MyoG allows for the fusion of myoblasts into multinucleated cells called myotubes. This process is explained in detail in section 1.3.1.

Understanding how either cell type originates is crucial when establishing a co-culture, and particularly important during the generation of MNs from pluripotent stem cells. Such information can give clues on which factors can be used for the differentiation, as well as on which cell type can be added to the culture first, if not at the same time.

1.1.5 Neuromuscular junction formation

The motor unit is the elementary component of motor control, which includes α -MNs, their axons and the muscle fibre they innervate (**Figure 1.3**) (Heckman and Enoka, 2004). The mechanism through which a MN innervates a SkM fibre and triggers contraction is called neuromuscular junction (NMJ) formation.

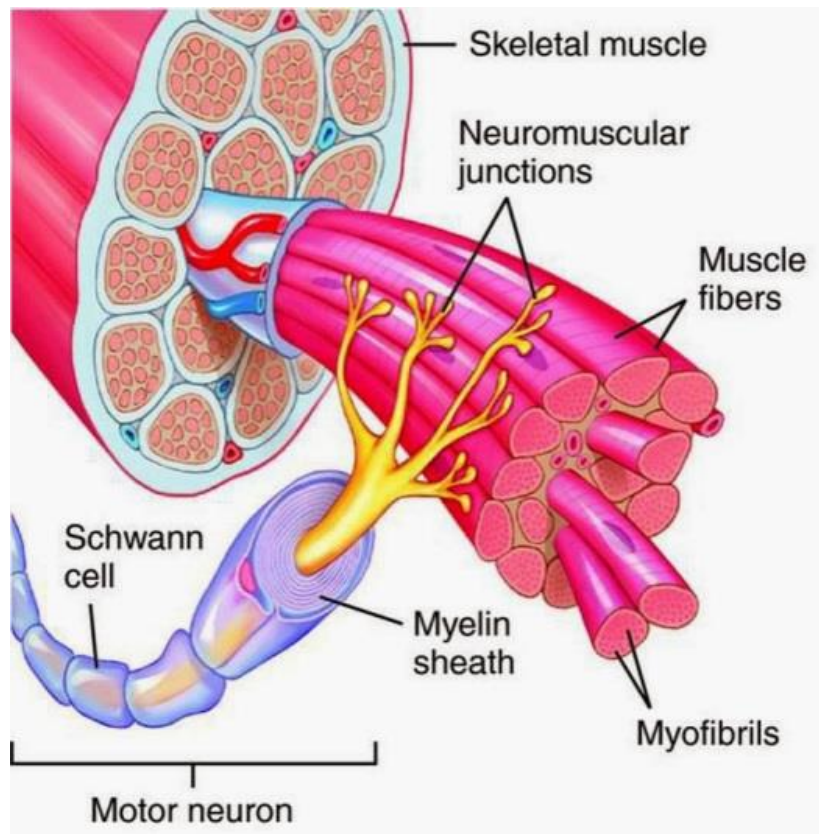


Figure 1.3. Motor unit structure. Lower MNs cell bodies reside in the grey matter of the spinal cord. Their axons project out of the spinal cord and travel towards SkM's to form the motor unit. The axon terminals which interact with the SkM fibres generate muscle contraction via the formation of a process known as NMJ. Image from physiopolis.wordpress.com.

A schematic representation of NMJ formation and its constituent elements is shown in **Figure 1.5**. Essentially, the NMJ controls a very brief release of vesicles containing the neurotransmitter ACh, which travels through the synaptic cleft (the space between the axon terminal and the muscle fibre) and binds to ACh receptors (AChR's) on the post-synaptic membrane (Colquhoun and Sakmann, 1998; Witzemann, 2006). At their resting potential, neurons maintain a membrane potential of -70 mV. If the summation of the inputs coming from other neurons is greater than the threshold potential, this triggers the generation of an action potential which travels down the axon, reaches the axon terminals and induces release of ACh (**Figure 1.4**).

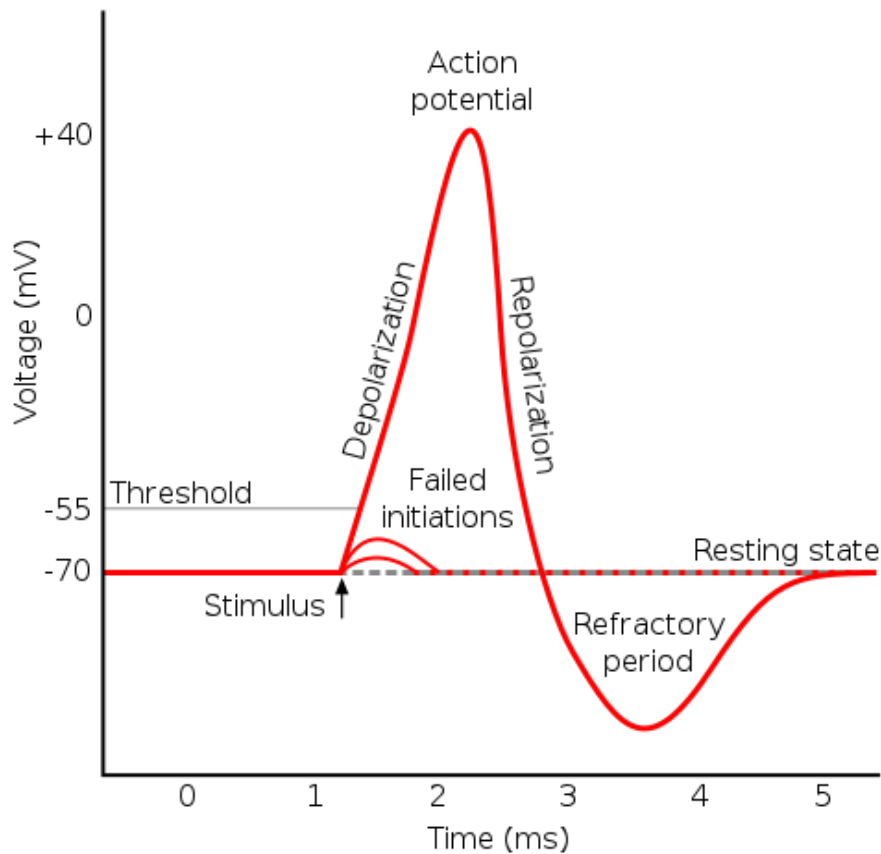


Figure 1.4. Action potential in neurons. Neurons maintain a resting potential of -70 mV thanks to the sodium-potassium pump. When a stimulus is received, depolarisation starts, and at the threshold of -55 mV, the sodium channels open and allow ions to flood inside the cell. This process continues until potassium channels open at +40 mV. This triggers repolarisation and exit of potassium ions. After a refractory period in which sodium gates remain closed, the cell returns to its resting potential. Image from Wikimedia.org.

The binding of ACh to the surface of the muscle causes the release of Ca^{2+} from the sarcoplasmic reticulum. Meanwhile, the Na^+ channels located on the post-synaptic membrane open and Na^+ ions enter the muscle fibres, thus creating the end plate potential which spreads through the muscle fibres and causes contraction (Hall and Guyton, 2016). This process continues for as long as ACh is available in the synaptic space. Two events block further excitation of the ACh receptors: first, some of the ACh diffuses away from the synaptic space. Second, the enzyme acetylcholinesterase (AChE) splits ACh into an acetate ion and choline, which can be reabsorbed into the neural terminal to be re-used when more ACh is needed (Hall and Guyton, 2016). The mechanism of muscle contraction will be further discussed in section

1.3.1 (Bear et al., 2001; Guyton and Hall, 2005). The NMJ process has been investigated for several years, and the role of other cell types and proteins was found to be crucial. During muscle formation, the pre-patterning process leads to clustering of AChR's in the central regions of the myofibres (Witzemann, 2006). The AChR's are stabilised by rapsyn (Wu et al., 2010), agrin and the activation of a muscle-specific kinase (MuSK) even before innervation (Burden et al., 2013; Legay and Mei, 2017). In fact, the presence of MuSK drives the axonal extension towards the muscle (DeChiara et al., 1996) because studies in mice lacking MuSK showed loss of AChR's and aberrant neuronal growth (Hesser et al., 2006). The activation of MuSK occurs via phosphorylation induced by R-spondin 2 (Rspo2), an activator of the Wnt signalling which is produced by MNs and binds to receptors on the muscle membrane called Lgr5 (Nakashima et al., 2016). Once bonded, this mediates AChR clustering, which is then stabilised by the structural protein rapsyn, similarly to the mechanism of action of agrin. Agrin is a proteoglycan expressed both by neurons and muscles, although neuronal agrin is known to be much more powerful than its muscle counterpart in inducing accumulation of AChR's at the synaptic sites (Witzemann, 2006). Agrin binds to the receptor Lrp4 and also mediates the activation of MuSK (Weatherbee et al., 2006). An inducible Lrp4 mutant mouse model was generated to investigate the NMJ maintenance (Barik et al., 2014). Prolonged absence of Lrp4 causes muscle weakness, body weight loss, reduced AChR intensity and fragmented AChR clusters, suggesting that Lrp4 is essential for NMJ maintenance in adults (Barik et al., 2014). However, Lrp4 can bind to MuSK independently from agrin (Kim et al., 2008; Zhang et al., 2011). In fact it was found that even in the absence of innervation, MuSK was activated, perhaps due to the muscle agrin counterpart (Schaeffer et al., 2001).

Extensive studies carried out in the past 50 years have generated fundamental knowledge on the formation of the NMJ, a crucial mechanisms for survival and locomotion which involves different cell types and molecules. However, research on the pathophysiology of this interface is still limited by the requirement of a human source of MNs which can be used to generate a model of the NMJ *in vitro*.

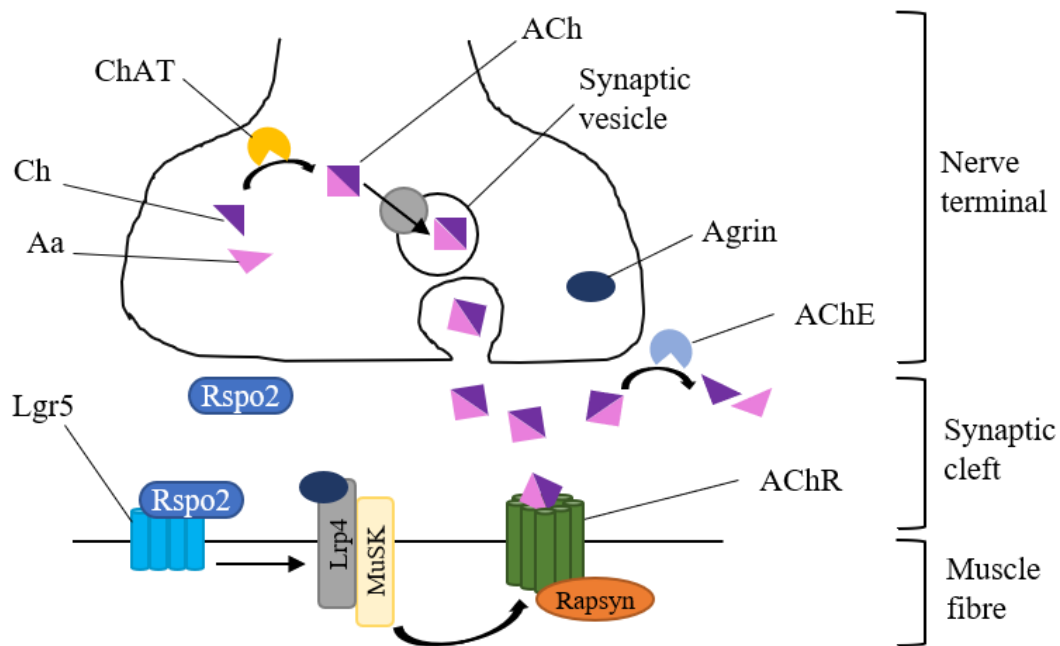


Figure 1.5. NMJ formation. The enzyme ChAT (choline acetyltransferase) is responsible for the generation of ACh (acetylcholine) by binding Ch (choline) to Aa (acetic acid). ACh is internalised in synaptic vesicles which are exocytosed by the nerve terminal into the synaptic cleft. Here, ACh travels to AChR's (acetylcholine receptors) on the surface of the muscle fibre. These receptors are stabilised by rapsyn and MuSK, which are activated when neuronal agrin binds to its receptor on the post-synaptic membrane (Lrp4). Further activation of MuSK comes from the bound of Rspo2 (R-spondin 2) to the transmembrane receptor Lgr5. The excess ACh is split into Ch and Aa by AChE (acetylcholinesterase).

1.1.6 Pathophysiology of the neuromuscular junction

Malfunctioning of the NMJ apparatus results in serious consequences for patients. Toxins (i.e. black widow spider venom, botulinum toxin or cobratoxin) can bind to AChR's, blocking them and causing paralysis which can quickly lead to death. The NMJ can also be affected by a pathological disorder. Myasthenia gravis (MG) is an autoimmune disease in which the patient's immune system attacks acetylcholine receptors, resulting in progressive muscle weakness and difficulty in completing every day actions (Miralles, 2016). More common than MG are amyotrophic lateral sclerosis (ALS) and spinal muscular atrophy (SMA). ALS occurs predominately in males over the age of 60, with a frequency of 2 individuals out of 100,000/year in the United Kingdom (UK). This disorder hits neurons in the cortex, corticospinal tract, brain stem and spinal cord. At the moment there are no clear evidences of

the factors which lead to the development of the disease. Only a mutation in the SOD1 gene on chromosome 13 has been shown to be related to it (Wijesekera and Leigh, 2009). SMA targets the MNs of the spinal cord, leading to progressive loss of function of the muscles which are innervated by the neurons. The disease hits 1 out of 10,000 children and causes death by the second year of life in the most severe cases. The patients who reach adult age live quite normally, but experience motor impairment. SMA is caused by the disruption of the gene SMN1 (survival motor neuron 1), which causes degeneration of α -MNs (Ebert et al., 2009). For neither of these diseases is there, to date, a cure. (Vitte et al., 2009). Therefore, all current treatments aim to improve the patients symptoms and slow down the progression of the degeneration. Studying the NMJ in a representative *in vitro* model is crucial to both understand the mechanisms underpinning the pathophysiology of such conditions, and to test novel therapeutics and explore personalised medicine for those who undergo treatment.

1.1.7 Neurons in culture

Cell lines which express neuronal properties are useful tools for studying the nervous system and interactions between neurons and other tissues (i.e. SkM). The use of cell lines ensures reproducibility and availability at a much lower cost and ethical implications than when utilising primary cells. This paragraph briefly describes the most widely used neuronal lines.

The neuronal cell line PC12 was first isolated from a tumor in the adrenal medulla of a rat in 1976. The cells were treated with neuronal growth factor (NGF) to generate dopamine- and noradrenalin-releasing neurons, thus proving to be suitable for studies on the sympathetic division of the PNS (Greene and Tischler, 1976). The presence of ACh was also reported in small vesicles inside PC12's (Howard and Melega, 1981; Schubert et al., 1980), and the treatment with Luteolin, an active compound found in *Rosmarinus officinalis*, induced PC12 differentiation and cholinergic activities (El Omri et al., 2012). A PC12 co-culture with the murine myoblast line C2C12 reported higher muscle maturity, differentiation and expression of neuromuscular markers (Ostrovidov et al., 2017), thus showing the suitability of this cell line for various neuronal studies. However, PC12s are an animal cell line, and as such, not the primary choice when designing a human *in vitro* model.

Studies have also been conducted using another cell line, NSC-34 (Maier et al., 2013; Matusica et al., 2008). This line is mouse-derived, and it is undifferentiated. Therefore, specific protocols

for differentiation into MNs are necessary and unpractical. It has recently suggested that NSC-34 cells cannot be considered a valid model for studies related to MNs (Hounoum et al., 2016).

A human neuronal alternative to PC12 cells is the neuronal line NT2, which was derived from a human embryonic teratocarcinoma (Andrews et al., 1984). These cells possess typical markers of dopaminergic neurons (Zigova et al., 1999), and the release of dopamine was later confirmed (Iacovitti et al., 2001). The versatility of these cells lies in their pluripotency, thus showing their potential to differentiate into different neuronal types. Previous work generated a mixed population including glial cells to sustain the differentiated glutamatergic neurons (Langlois and Duval, 1997). Others obtained a subpopulation of glutamatergic cells and a major portion of neurons which appeared cholinergic (Podrygajlo et al., 2009). The potential to derive both a neuronal population (NT2N) and a glial population (particularly astrocytes, NT2A), allowed for the generation of a co-culture where several aspects were analysed: morphology, electrical activity, response to the neurotransmitter glutamate and to Tetrodotoxin (a neurotoxin) were investigated and revealed a co-dependance between NT2N and NT2A. This confirmed the versatility of this cell line, as well as reiterate the supportive role of a glial population in neuronal cultures (Hill et al., 2012). All in all, NT2's represent an adaptable neuronal population which can be utilised for several studies.

1.1.8 SH-SY5Y human neuroblastoma cell line

Another versatile source of human neurons is the neuroblastoma line SH-SY5Y, a neuroblastoma line. Neuroblastoma is the most common malignant tumor affecting neuronal crest-derived cells (Joshi et al., 2006). This cell line was first derived by a bone marrow biopsy of the tumor (SK-N-SH) in 1973 (Biedler et al., 1973). SK-N-SH cells were characterised by the presence of three different cell types: neuronal (N), Schwannian (S) and intermediary (I). However, SH-SY5Ys are a homogenous population of N-type cells (Hong-rong et al., 2010). SH-SY5Ys can be used as neuronal model because they grow continuously in an undifferentiated state, presenting a neuronal-like morphology and expressing immature neuronal markers such as nestin (Smith et al., 2013). Given the availability of SH-SY5Ys and their extensive use in our laboratory, co-culture studies were performed in this work, particularly to determine the culture conditions and the interaction between human neurons and murine skeletal muscle. Certainly, these cells present limitations too, but as a primary human

source of MNs is not obtainable, SH-SY5Ys were proven to be sufficient for preliminary studies in this thesis.

1.1.8.1 Differentiation of SH-SY5Ys: an ‘eclectic’ line

SH-SY5Y cells are a versatile cell line which can be used to generate dopaminergic, adrenergic or cholinergic neurons. Different factors can be used to guide the SH-SY5Y cells towards such phenotypes. The most commonly used are retinoic acid (RA) and phorbol esters (Smith et al., 2013). RA is a derivate of vitamin A which is used to guide the cells to exit the cell cycle, therefore stopping them from proliferating and inducing differentiation (Joshi et al., 2006). It plays an essential role in neurite outgrowth and development of the nervous system (Clagett-dame et al., 2006); it was also linked to peripheral nerve regeneration, therefore representing a key element of neuronal physiology (Mey and McCaffery, 2004). Furthermore, RA is involved in the development and functional maintenance of vital organs in adults (Zhu et al., 2009).

RA’s mechanism of action involves the binding of this compound to two families of nuclear receptors: the RA receptors (RAR’s) and the retinoid X receptors (RXR’s) (Joshi et al., 2006). The so-formed heterodimers then bind to RA responsive elements (RARE) and activate transcription via the Wnt signaling pathway (Hong-rong et al., 2010).

In the majority of reported works, RA was used at a concentration of 10 μ M, but different protocols were also proposed (Adem et al., 1987). RA can lead to a cholinergic phenotype, which can be verified by the expression of markers such as choline acetyl esterase (ChAT) and vesicular monoamine transporter (VMAT) (Ichikawa et al., 1997). Some studies, however, suggest that when RA was used in combination with other factors like phorbol esters (Presgraves et al., 2004) or cholesterol (Sarkanen et al., 2007), the expression of dopaminergic receptors (D2R and D3R) and the dopamine transporter DAT increased. These markers were positive also in the undifferentiated SH-SY5Y cells, but the dopaminergic characteristics significantly increased upon differentiation. Phorbol esters like 12-O-tetradecanoyl-phorbol-13-acetate (TPA) enhanced the cellular noradrenaline content (Påhlman et al., 1984), therefore inducing an adrenergic phenotype (Murphy et al., 1991; Scott et al., 1986). In fact, one study analysed the differences between differentiated SH-SY5Ys in the presence of RA or TPA alone, and the combination of both. The treatment with RA and TPA increased the number of differentiated cells which also had longer neurites than the ones treated with RA or TPA only. The same applied to the inhibition of cell proliferation. The neuron-specific enolase (NSE)

activity was similar among the three conditions. RA caused a 4-fold increase in noradrenalin concentration, whereas TPA caused a 200-fold increase. When treated with RA and TPA, the levels of noradrenalin were comparable to the untreated control (Påhlman et al., 1984). Following this work, the same research group investigated the effect of RA and TPA on muscarinic receptors on the membrane of SH-SY5Ys. Moreover, the treatment with both RA and TPA caused an increase in AChE and choline acetyltransferase (ChAT) activity. Overall, the use of RA caused a major cholinergic phenotype than TPA.

In contrast with the majority of studies which indicate that RA causes SH-SY5Y cells to differentiate into cholinergic cells, one study showed that the administration of 1 μ m RA produced an increase in dopaminergic markers (Korecka et al., 2013). The expression of 50 genes which are involved in development and differentiation was investigated after treatment with RA. These were more expressed in the treated samples, confirming the role of RA in the differentiation process. TFAP2B, Isl-1, SIX3 and ATF5 are negative regulators of neuronal differentiation and were downregulated upon treatment with RA. The group did not observe significant differences in the expression of transcription factors typical of the early stage of development of dopaminergic neurons. However, the cells expressed the enzymes which are crucial during synthesis and degradation of dopamine, a characteristic which is typical of mature dopaminergic neurons. Despite these results, there was no significant difference between the levels of these markers before or after RA treatment, indicating perhaps that the cells already possessed dopaminergic features and that RA did not affect them. The same applies to the expression of cholinergic neurotransmitters. It is clear, then, that SH-SY5Y cells present an heterogeneous phenotype which is not always affected by the presence of RA in a significant manner (Korecka et al., 2013).

Although it can be generally said that the population of undifferentiated SH-SY5Ys is made of N-type cells (Hong-rong et al., 2010), a previous study (Encinas et al., 2000) showed that differentiated cells presented characteristics of S-type cells after 8-10 days in RA. RA was used in combination with brain-derived neurotrophic factor (BDNF), which had an anti-apoptotic effect. Therefore, 3-5 days appeared to be the best interval to keep the cells in RA. For the work presented in this instance, 5 days in differentiating medium were considered. To date, SH-SY5Y cells represent a valid cell line to study neurons with different phenotypes. A summary of the approaches which have been used to differentiate SH-SY5Y cells, the investigated markers and the resulting phenotypes can be found in **Table 1.1**.

Table 1.1. Summary of the techniques reported in the literature to induce differentiation of SH-SY5Y cells.

Abbreviations: RA = retinoic acid; TPA = 12-0-tetradecanoylphorbol-13-acetate; NSE = neuron-specific enolase; AChE = acetylcholinesterase; ChAT = choline acetyltransferase; MPP = 1-methyl-4-phenyl-1,2,3,6-tetrahydropyridinium ion; DAT = dopamine transporter; TH = tyrosine hydroxylase; DRD2 = dopamine receptor D2; DRD3 = dopamine receptor D3; VMAT = vesicular monoamine transporter; dBcAMP = Dibutyryl-cyclic adenosine monophosphate; SypI = synaptophysin I; AM1-43 = activity-dependent fluorescent nerve terminal probe; FGF-8 = fibroblast growth factor 8; Nkx2.2 = homeobox protein Nkx2.2; Nkx6.1 = homeobox protein Nkx6.1; SHH = sonic hedgehog; Sox2 = sex-determining region Y; TGF- β = Transforming growth factor beta; Wnt-1 = protooncogene protein; COMT = Catechol-O-methyltransferase; DDC = dopamine decarboxylase; GCH1 = Guanosine triphosphate cyclohydrolase; MAO-A = Monoamine oxidase A; MAO-B = Monoamine oxidase B; PTS = 6-pyruvoyltetrahydropterin synthase; VMAT2 = vesicular monoamine transporter 2; DMEM HG = Dulbecco's Modified Eagle's Medium high glucose; BDNF = brain-derived neurotrophic factor; 6-OHDA = oxidopamine.

Reference	Methods	Markers	Phenotype
(Påhlman et al., 1984)	10 μ M RA; 16 nM TPA; RA + TPA. All for 10 days.	Number of differentiated cells; proliferation rate; NSE activity; noradrenalin concentration.	Cholinergic.
(Adem et al., 1987)	0.1 μ M RA; 16 nM TPA.	Characterisation of muscarinic receptors; AChE and ChAT activity.	Cholinergic.
(Presgraves et al., 2004)	10 μ M RA for 6 days; 80 nM TPA for 6 days; RA for 3 days and then TPA for 3 days.	Sensitivity to the neurotoxin MPP ⁺ and DAT. Expression of TH, DRD ₂ and DRD ₃ and VMAT.	The cells treated with RA only presented characteristics typical of cholinergic neurons. A dopaminergic portion was observed after treatment with RA/TPA or TPA only.
(Sarkanen et al., 2007)	20 nmol/L TPA; 50 μ mol/L dBcAMP; 5 μ mol/L RA; 10 μ g/mL cholesterol; 5 μ mol/L RA+ 5 μ g/mL cholesterol. All for 14 days.	Neurite length; SypI and AM1-43 co-localisation.	Dopaminergic.

(Korecka et al., 2013)	1 μ M RA for 8 days.	Early stage dopaminergic markers (FGF-8, Nkx2.2, Nkx6.1, SHH, Sox2, TGF- β , Wnt-1). Dopamine synthesis and turnover markers (COMT, DDC, GCH1, MAO-A, MAO-B, PTS, VMAT2, DAT, TH). Dopaminergic neuron markers and neurotransmitter receptors.	Dopaminergic characteristics, not significantly different from the non-treated samples.
(Forster et al., 2016)	First, DMEM HG, l-glutamine and 10 μ M RA. Then, Neurobasal medium, l-glutamine, N2 supplement and BDNF.	Markers of undifferentiated and differentiated state. Analysis of the plasma membrane potential. Response to 6-OHDA.	No dopaminergic phenotype was observed.

1.2 Pluripotent stem cells

Stem cells are cells capable of self-renewal and differentiation into specific cell types (Hanna et al., 2010). There are different levels of potency, depending on how many cell types can originate from a stem cell. Totipotent stem cells are solely those in the blastocyst at the 3rd day of gestation, which can give rise to the entire organism and to extra-embryonic cells (i.e. the placenta). Pluripotent cells can generate the entire body and include both embryonic (ESCs) and induced pluripotent stem cells (iPSCs). Multipotent stem cells, such as hematopoietic stem cells, can differentiate into a limited amount of cell types. Finally, unipotent stem cells are only capable of generating one cell type, as satellite cells do in SkM (Singh et al., 2016).

Pluripotent cells can differentiate into the three germ layers: mesoderm, ectoderm and endoderm (Binder et al., 2009). Just over a decade ago pluripotent cells from human adult cells were generated (Takahashi and Yamanaka, 2006). Both these and ESCs were utilised to generate human neurons (Shi et al., 2012), but the use of iPSCs has the promising advantage of not requiring embryos, together with the possibility to derive specific cell types from a patient.

During the maturation of MNs *in vitro*, pluripotent cells acquire cell polarity and migrate to form rosettes (Elkabetz et al., 2008; Yonemura et al., 1993), which eventually give rise to MNs (Delli Carri et al., 2013). This process depends on the activation of Sonic Hedgehog (SHH) and Notch pathways, following which the neuronal rosettes become positive for neuroectodermal markers such as Pax6 and Sox1 (Elkabetz et al., 2008). Therefore, the rosettes can differentiate into the three cell lineages of the nervous system: neurons, oligodendrocytes and astrocytes (Elkabetz et al., 2008). Although there are no specific markers for mature MNs, one that can be used is nestin (a neuroprogenitor indicator) (Zhang et al., 2001) and others which are typical for neural plate and tube formation in the neuroectoderm, such as Pax6 and Sox1 (Pevny et al., 1998). In order to confirm the presence of mature MNs in culture, the following markers are often used; HB9 (Arber et al., 1999), ChAT, Islet 1 (Ericson et al., 1992), Islet 2 (Tanabe et al., 1998), and Olig2 (Shirasaki and Pfaff, 2002).

1.3 Muscle

Muscle is a soft tissue which can be of three types: cardiac, smooth or skeletal. Cardiac muscle (or myocardium) constitutes the heart and has involuntary contractile properties. Smooth

muscles are also involuntary muscles which are found in certain organs like the skin, stomach, intestines, uterus and urinary bladder, as well as in the walls of arteries and veins (Gray, 1960). This section will focus on the development and physiology of skeletal muscle (SkM) as it is relevant to the work carried out in this thesis.

1.3.1 Skeletal muscle gross structure and development

SkM is a striated, contractile tissue which is connected to bones via tendons. It covers a range of functions including maintaining posture, voluntary movement, breathing and is responsible for the generation of heat which contributes to keeping body temperature stable. By interacting with MNs and other components of the musculoskeletal system, it contracts and allows locomotion (Lumley et al., 1980). The gross structure of SkM is shown in **Figure 1.6**. Muscles are covered by a layer of connective tissue called epimysium. They are made of several, highly aligned substructures called fascicles, covered by the endomysium. Each fascicle is made of organised and elongated fibres. Muscle fibres are characterised by even smaller structures called myofibrils (Sciote and Morris, 2000).

SkM cells secrete a series of components which support the tissue from a structural and mechanical point of view. These components constitute the SkM extracellular matrix (ECM). The main component of this ECM is collagen; the outer layer of the muscle primarily formed by collagen type I. The other two layers (epymisium and endomysium) are made of collagen type I and III (Gillies and Lieber, 2012). In the ECM there is also a large portion of proteoglycans (*i.e.* decorin) and glycoproteins (Kjær, 2004). The complex architecture of the ECM and its interaction with nearby tissues such as tendons or neurons is a crucial aspect of SkM structure. Tissue engineering can help create a more complex environment in which SkM cells grow, differentiate and interact with other cell types.

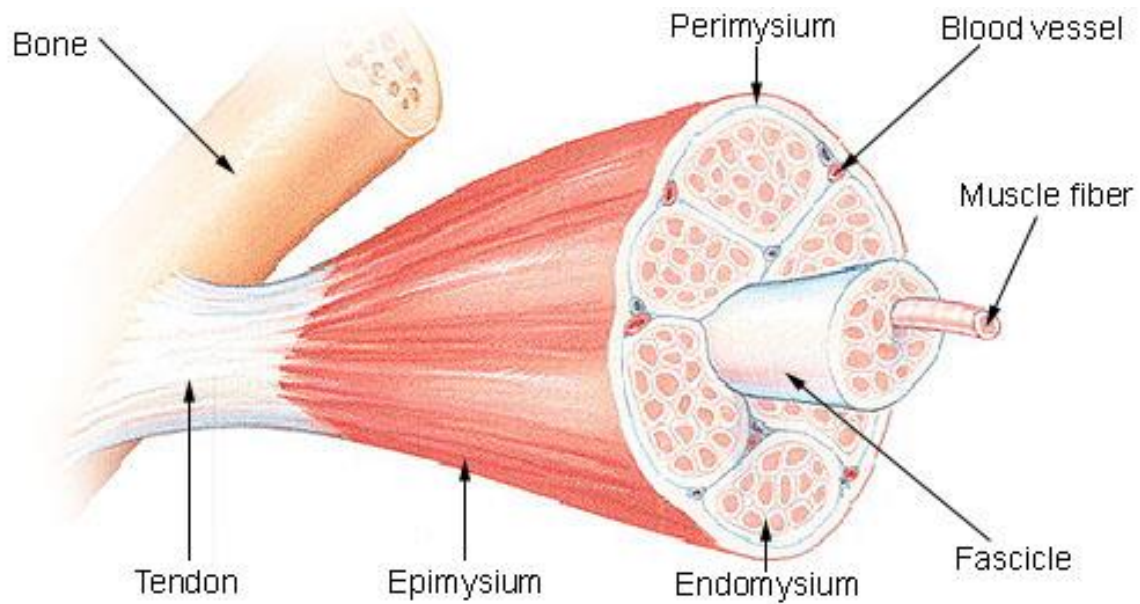


Figure 1.6. Skeletal muscle structure. The whole muscle is surrounded by the epimysium. The perimysium surrounds bundles of fibres. The endomysium is the internal membrane which covers the multinucleated fibres. Image from Wikimedia.org.

SkM derives from the embryonic lineage of mesoderm: stem cells in this germ line give rise to immature muscle cells called myoblasts. During the commitment to the myogenic lineage, specific transcription factors are expressed in these muscle progenitors. These are called myogenic regulatory factors (MRFs) and they alternately appear and disappear in the differentiation process (**Figure 1.7**).

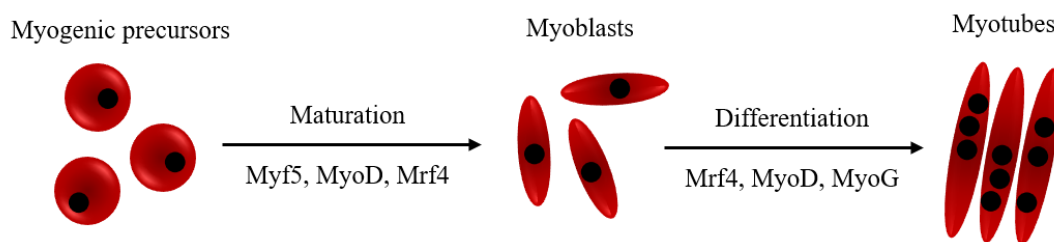


Figure 1.7. MRF in SkM maturation and differentiation. During the maturation process, there is activation of Myf5, MyoD and Mrf4. Mrf4 remains active also during the differentiation step, together with MyoG. The morphology of the cells also varies. Myogenic precursors appear round-shaped and they elongate during development. At the mature stage of myotubes, they fuse to fibre-like, multinucleated structures.

The best characterised MRFs are MyoD, Myf-5, Mrf4 and myogenin (MyoG), as well as the paired box (Pax) transcription factors Pax 3 and Pax 7 (Buckingham and Relaix, 2007; Burattini et al., 2004; Rudnicki et al., 1993). Initially, myogenic precursors express Pax 3 which is downregulated during maturation to myoblasts, which form thanks to the activation of Myf5, MyoD and Mrf4 by the SHH and Wnt pathways (Cossu and Borello, 1999). Mrf4, MyoD and MyoG then promote the differentiation of myoblasts into myotubes, which form a continuous layer of aligned cells (Olson and Klein, 1994). Further growth of the SkM tissue is facilitated by Pax 3 and Pax 7 positive cells which are mainly Myf5 and MyoD positive and therefore myogenic. These cells fuse with existing fibres and create bigger structures (Buckingham and Relaix, 2007). Towards the end of fetal development, a subpopulation of Pax 3 and Pax 7 positive cells form the mammalian postnatal satellite population. Satellite cells are the stem cell population of SkM, although they express SkM markers which suggest commitment of the myogenic lineage even prior to their activation (Beauchamp et al., 2000; Irintchev et al., 1994). Satellite cells lie between the sarcolemma and the basal lamina of SkM fibres and they are activated upon SkM injury, where repair is required (Charge and Rudnicki, 2004). A small population of satellite cells remains undifferentiated in order to replenish the fibre's satellite pool, thus enabling future response to traumatic events (Ten Broek et al., 2010).

1.3.2 Skeletal muscle microstructure and physiology

When several myoblasts fuse together, they share their cytoplasm and become a whole multinucleated cell called a myotube. Myotubes run parallel to the line of muscle action and range in length from 1 mm to several cm (Sciote and Morris, 2000). Myotubes do not proliferate, but produce muscle contractile proteins and elements of the ECM which allow interaction with MNs and the generation of a functional NMJ (Blau et al., 1985). Within myotubes, elements such as nuclei, mitochondria and other organelles are pushed to the periphery to allow myofibrils to occupy most of the intracellular space (Sciote and Morris, 2000). These are cylindrical structures made up of long chains of repeated contractile units, the sarcomeres (Alberts et al., 2002). Sarcomeres are responsible for the striated appearance of SkM, due to the presence of alternated thick and thin filaments made of the most abundant proteins within the muscle: actin (thin filament) and myosin (thick filament). These proteins interact in the core of the muscle to initiate contraction (Bell et al., 1980). Sarcomeres are linked end to end through the attachment of the myofibril, and the junction points are called Z lines. Attached to the Z lines are strands of actin and myosin. The muscle isotropic bands consist of actin filaments

which spirally run along a protein called tropomyosin. This works together with troponin to block the binding sites for actin, on the myosin filaments. Thus, when the muscle is relaxed, the sites for the actin to bind to myosin are occupied (Franzini-Armstrong and Peachy, 1981; Huxley, 1953). The actin filaments are bound at their plus end to a Z disc, while the capped minus ends extend into the anisotropic band where they interlock with myosin filaments (Alberts et al., 2002). The process of contraction is shown in **Figure 1.8**. Actin is made of a double chain which can bind to myosin during contraction. Thin and thick filaments slide towards each other, in the presence of adenosine triphosphate (ATP), which is hydrolysed to adenosine diphosphate (ADP) and an inorganic phosphate (P_i), and Ca^{2+} . ATP is used as source of energy to lift the actin heads towards the myosin. Intracellular Ca^{2+} increases due to the arrival of an action potential from MNs which causes depolarisation of the post synaptic cell (Alberts et al., 2002). The influx of Ca^{2+} in the cell triggers the removal of troponin and tropomyosin from the binding sites for actin, thus allowing the myosin heads to bind to the thick filaments. After actin binds to myosin, it slides the myosin, therefore reducing the length of the sarcomere. When this process occurs in several muscle fibres simultaneously, the contraction of a whole muscle or groups of muscles allows movement of the skeleton (Lieber, 2009). Relaxation occurs again when cytosolic Ca^{2+} is sequestered and the actin-tropomyosin structure returns to its original conformation, blocking the myosin heads from binding to the actin filaments (Gomes et al., 2002). A third key protein in the sarcomere is titin, also known as connectin. Titin holds together the basic structure of the sarcomere and helps maintain its shape, while transmitting force from the contractile proteins to the Z lines (Heckman and Enoka, 2004). Even though titin is not directly involved in the contraction process, it provides stiffness to the muscle fibre when the sarcomere is elongated past its resting length (Heckman and Enoka, 2004).

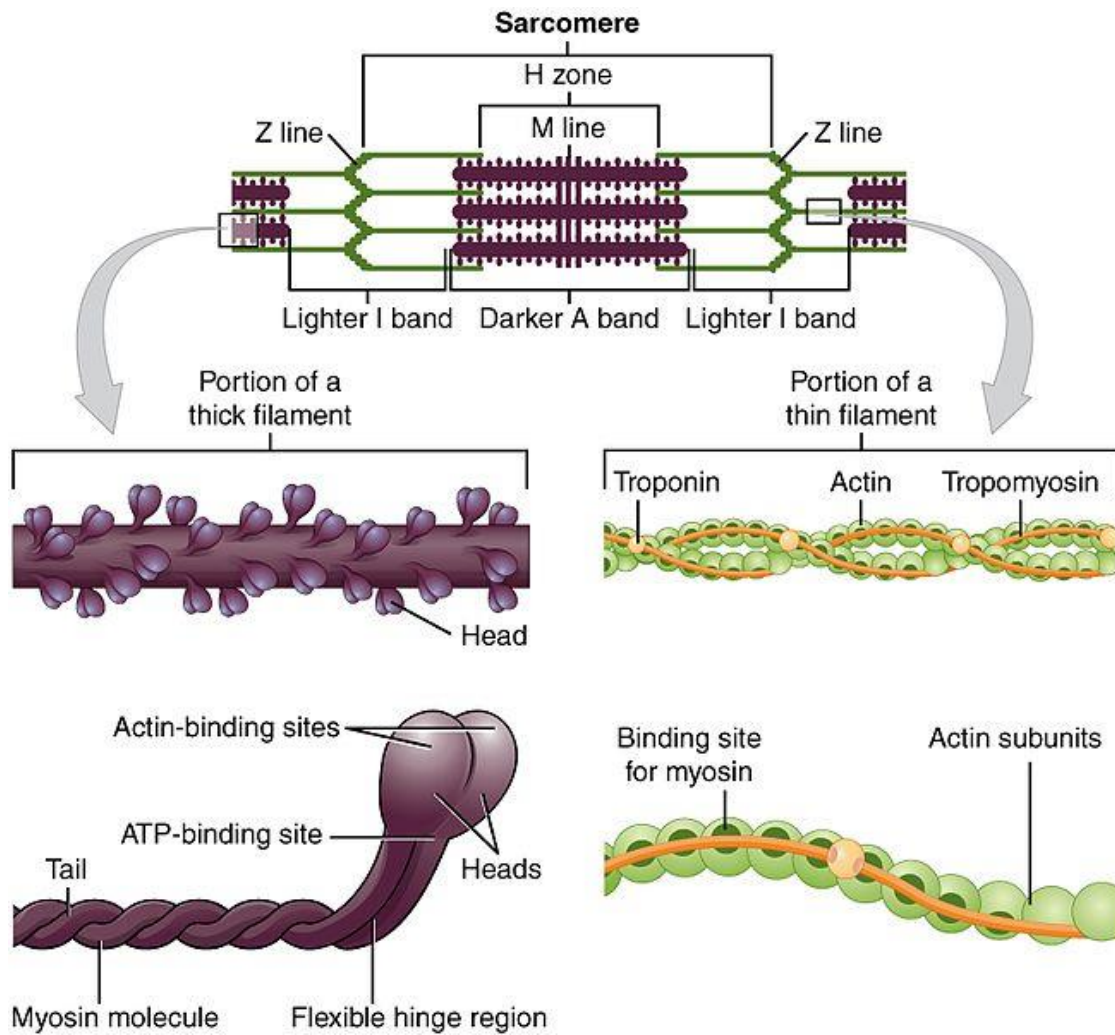


Figure 1.8. Schematic representation of the muscle fibre and its micro components. Contraction occurs when thick myosin filaments interact with thin actin filaments. Actin filaments are capped at their minus end by Tropomodulin and interact with CapZ at their plus end to bind the filament to the Z disc. Titin is a highly elastic protein which connects the myosin filaments to the Z disc and changes length to allow contraction and relaxation of the sarcomere. B) Interaction of actin and myosin enables sarcomeric shortening. Synchronised shortening of thousands of sarcomeres lying end to end in each myofibril facilitates rapid contraction of the SkM tissue. Image from Wikimedia.org.

What gives SkM its contractile properties are different isoforms of myosin proteins within their myofibrils (Sciote and Morris, 2000). Myosin is a large molecule made of 2 myosin heavy chains (MyHC) and 2 pairs of non-identical myosin light chains (MyLC) (Allison Weiss et al., 1999). MyHC's cover different roles within the muscle, from structural support during contraction, to the enzymatic hydrolysis of ATP (Pette and Staron, 2000). In particular, different MyHC isoforms determine the nature of the excitation-contraction coupling during sarcomere shortening and the force-velocity characteristics of the muscle fibres, which were characterised (Barany, 1967; Sciote and Morris, 2000). The major SkM MyHC isoforms and their relative fibre types in mouse and human are reported below in **Table 1.2**. A total of nine fibre types were identified in SkM: type I, α , extra-ocular, neonatal, embryonic, Iia, Iib, Iix and Iim. The expression of the different isoforms during development and in the adult muscle are conserved across mouse and human (Weiss et al., 1999), but a few differences were identified. For example, MyHC2 encodes for type Iia fibres which are expressed in the fetal stage in human, but later in the early postnatal phase in mouse (Schiaffino et al., 2015).

Table 1.2. MyHC isoforms in mouse and human during development and in adult SkM.

Gene	Fibre type	Development	Adul muscle
MyHC3	Embryonic	Embryonic and foetal	Specialised muscles only
MyHC8	Neonatal	Embryonic and foetal	Specialised muscles only
MyHC7	Type I, slow	Embryonic and foetal	Type I fibres and ventricles
MyHC2	Type Iia, fast	Foetal (human) Early postnatal (mouse)	Type Iia
MyHC1	Type Iix, faster	Embryonic	Fast muscle

1.3.3 Skeletal muscle force generation

Muscles contract upon a number of events which follow neuronal signalling, via a process called excitation contraction coupling. When MNs release ACh, towards a muscle fibre, the neurotransmitter crosses the synaptic cleft and reaches its receptors on the post-synaptic membrane (Lieber, 2009). The action potential which causes depolarisation and eventually triggers contraction must be transmitted from the pre-synaptic membrane (MNs) to the muscle fibre. It is the depolarisation of the sarcolemma in muscle cells which allows the propagation of the action potential. When this reaches the sarcoplasmic reticulum, dihydropyridine

receptors sense this change in voltage and release Ca^{2+} , which can then bind to troponin, allowing myosin to bind to actin and generate force which causes contraction of the fibres (MacIntosh et al., 2006; Schiaffino and Reggiani, 2011). Once the stimulus ceases, Ca^{2+} is pumped from the sarcoplasm back into the sarcoplasmic reticulum so that troponin can go back to its inhibitory role on the actin molecule (MacIntosh et al., 2006).

As shown in **Figure 1.9**, the activation of SkM through this mechanism lasts about 5 milliseconds (ms), whereas the relaxation step in which Ca^{2+} returns to the sarcoplasmic reticulum takes up to 100 ms (Lieber, 2009). The coupling of this type of contraction/relaxation is known as unfused tetanus. If, however, MNs fire repetitive stimuli to the muscle, there is not enough time for the Ca^{2+} to return to its resting location, thus triggering a second contraction and an increase in the amount of force produced (Lieber, 2009). This causes the so-called fused tetanus. Finally, when the stimulus occurs at low frequency, single twitches are observed.

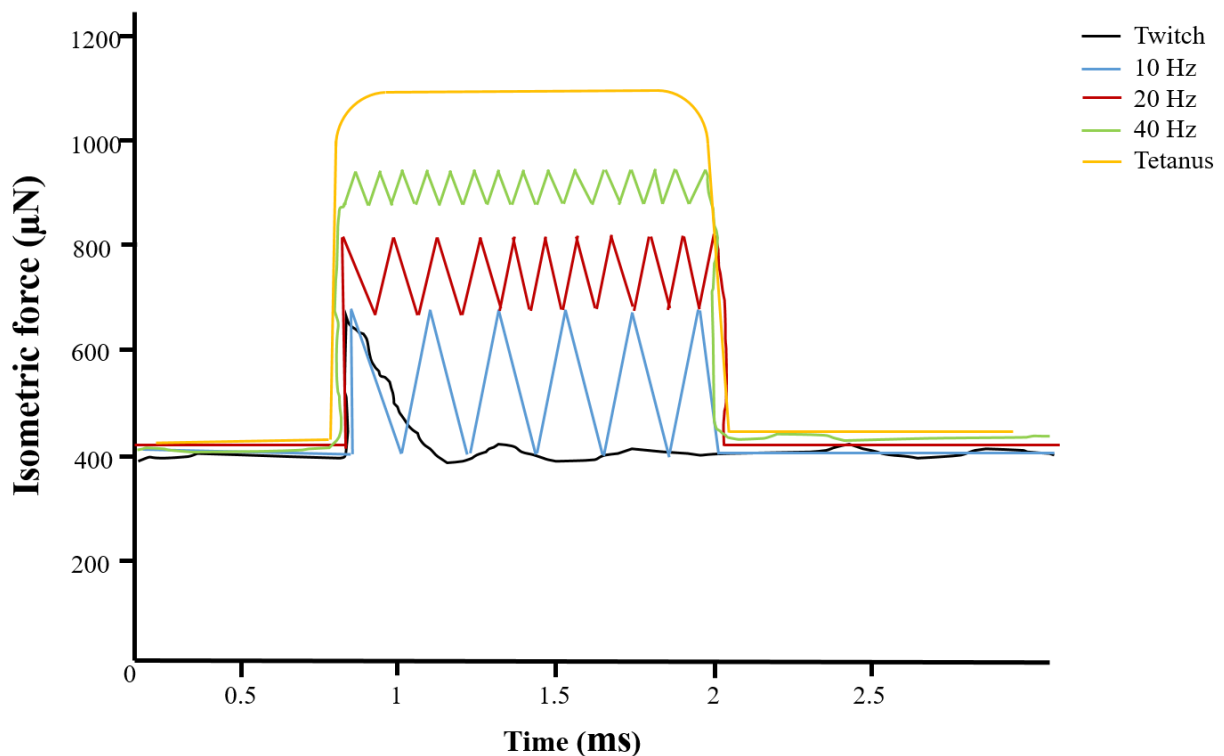


Figure 1.9. The force-frequency relationship in SkM. Low frequency stimuli generate single twitches (brown and green lines). When the frequency of stimulation from MNs is higher, summation occurs leading to unfused (red line) and subsequently fused tetanus (blue line), which results in increased force.

1.3.4 Skeletal muscle in culture

The culture of SkM *in vitro* presents less challenges if compared to MNs cultures. This is simply due to the much larger availability of primary SkM tissue, which can be obtained without permanently damaging the tissue. On the other hand, the removal of great portions of nerves could cause an irreparable injury which would not differentiate and would require auto- or allografts. Thus, cultures of primary human and rat SkM were established several decades ago using various methods for cell extraction (Bischoff, 1974; Yasin et al., 1977).

1.3.4.1 C2C12 murine myoblast cell line

The murine cell line C2C12 was firstly isolated for its ability to rapidly differentiate and produce mature myotubes. These myotubes contract and express SkM proteins (Blau et al., 1985). C2C12 were derived from satellite cells. Therefore, their characteristics correspond to the ones of a progenitor lineage (Burattini et al., 2004).

The use of C2C12 as a SkM model was widely reported (Burattini et al., 2004; Manabe et al., 2012; Sharples et al., 2012). Several studies also showed that this line is suitable for modelling the NMJ. A summary of these works can be found in **Table 1.3**.

The extensive use of C2C12 cells as model for the SkM shows effective differentiation and NMJ formation when cultured with MNs. However, being an animal-derived cell type, it presents limitations for human-related studies such as disease modelling or drug screening. Models of the NMJ which are based on human cells are therefore a promising alternative (Guo et al., 2011).

1.3.4.2 Human skeletal muscle

The use of primary hSkM is reported in the literature (Brady et al., 2008; Mouly et al., 2005), whereby a small portion of muscle is removed from the *vastus lateralis* (quadriceps) and minced into pieces in the presence of muscle growth medium (MGM). Over the following days, a population of cells migrates from the tissue sample onto the culture dish. These cells are a mix of muscle precursor cells, which retain the potential to form multinucleated myotubes, and non-myogenic cells which will not differentiate (i.e. fibroblasts and pericytes) (Asakura et al., 2001; Machida et al., 2004). Ideally, the population of myogenic cells should be predominant, but not necessarily the sole component, as other cell types sustain muscle growth and differentiation.

Alternatively to the mince approach, enzymes such as trypsin and collagenase can be used to digest the connective tissue and release the cells (A. S. T. Smith et al., 2012). Whichever the method, the culture of primary hSkM remains the same and the donor-to-donor variability plays an important role in the amount of myogenic cells that can be obtained, thus varying the outcome of experimental work carried out with such cells.

When plated on glass or tissue culture plastic, primary muscle adheres to a stiff surface which differs from the native environment it is derived from. In fact, maturation of these cells was shown to be poor as much as on very soft substrates, whereas mimicking the *in vivo* stiffness of the tissue using hydrogels could ensure higher maturation (Engler et al., 2004). The timing of primary cultures is also variable and each experiment has to take this under consideration.

Despite the challenges that are intrinsic to using primary cells, moving from cell lines to these alternatives is a promising step towards personalised screening tests and disease studies. In addition, this approach helps reducing, refining and replacing animals and animal-derived cells in research (<https://www.nc3rs.org.uk/the-3rs>).

Table 1.3. Summary of the applications of C2C12 cells as model for the NMJ.

Abbreviations: MNs = motor neurons; BTX = α -bungarotoxin, AChR = acetylcholine receptor; iPSC = induced pluripotent stem cell; ESC = embryonic stem cell; ChAT = choline acetyltransferase.

Reference	Methods	Results
(Tong et al., 2014)	Mouse embryonic MNs were co-cultured with C2C12 in a microfluidic device which allows neurites extension.	MNs extended axons towards the myotubes after 7-10 days in culture. Staining with BTX identified AChR's, Myosin II was used for C2C12 and β -III Tubulin for MNs.
(Hu et al., 2010)	Human iPSC-derived MNs were co-cultured with C2C12 in monolayer.	After 2 weeks in culture, the neurites bound to the myotubes, which contracted. Staining with BTX and confocal analysis confirmed the presence of a synapsis.
(Li et al., 2005)	C2C12 were plated on top of human ESC-derived MNs. Also, ventral progenitor cells were plated on top of the myotubes.	The BTX staining was positive after 4 days in culture and more evident after 2 weeks. The myotubes were innervated by ChAT ⁺ fibres. After 3 weeks, C2C12 cultured alone did not show contraction, which was instead present in the co-culture.
(Son et al., 2011)	Mouse and human fibroblasts-derived MNs were purified by flow cytometry and cultured with C2C12 cells for 7-14 days.	The MNs projected axons towards the myotubes, which twitched in the co-culture, but not when cultured separately from the neurons. After adding a contraction inhibitor to the culture, the frequency of myotubes contraction declined.
(Martin et al., 2015)	Primary mouse-derived MNs were cultured with C2C12s to determine whether the presence of the neurons would affect the myotubes morphology and contractile force generation in tissue engineering constructs.	The MNs did not affect the differentiation of the muscle precursors, but enhanced the cytoskeleton organisation of C2C12 cells, which plays a key role in the improved force generation within the constructs.
(Hester et al., 2011)	Human iPSC-derived MNs were co-cultured with C2C12	Complete myotube maturation was confirmed by the positivity to the marker α -actinin. Staining with BTX also showed interaction between the two cell types.
(Du et al., 2015)	Human iPSC-derived MNs were co-cultured with mature C2C12 for 7 days.	BTX ⁺ receptors were overlapped with ChAT ⁺ neurites, suggesting the formation of NMJs.

1.4 3D tissue engineering constructs

Tissue engineering is the branch of science which focusses on generating materials and or tissues which can be integrated *in vivo* or used to study physiology and pathophysiology *in vitro*. This field is vast and incorporates several types of biocompatible materials (metals, polymers, ceramics, hydrogels) which can be used as scaffolds to sustain cell growth before and after implantation. This section will introduce two particular types of tissue engineering constructs which are used for SkM cultures and are suitable for studies on the NMJ.

1.4.1 Fibrin gels

Fibrin is the product of polymerisation of fibrinogen by thrombin, and it represents the main constituent of a blood clot (Mosesson, 2005). Fibrin gels have a similar stiffness to muscle tissue and provide a matrix onto which tissue engineered SkM can be formed, as previously reported (Bian and Bursac, 2009; Boonen et al., 2010; Huang et al., 2005; Khodabukus and Baar, 2009). Within similar collagen-based constructs, myotubes develop and mature whilst aligning to the pins which hold the gel on a sylgard coated dish (Strohman et al., 1990). Similarly, this was repeated using laminin, strongly suggesting that myoblasts embedded in a matrix anchored to two fixed points allows myotube formation and resembles the *in vivo* muscle architecture (Dennis and Kosnik, 2000).

A schematic representation of the constructs is shown in **Figure 1.10**.

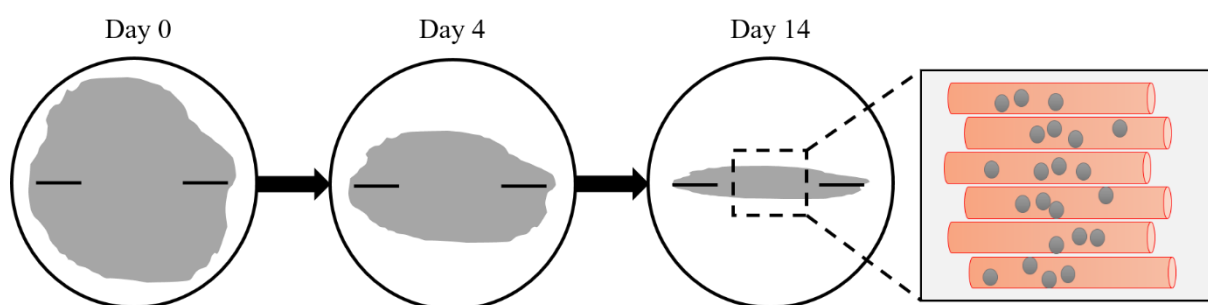


Figure 1.10. Schematic representation of the culture of myoblasts in fibrin gels. The gel (grey) contracts over time, until it aligns to the pins. The cells expand until day 4, when they are exposed to differentiation medium. During the last 10 days in culture, myoblasts fuse into multinucleated fibres which follow the alignment of the gel to the pins.

Fibrin gels have also been used for rat primary SkM/MN co-cultures, showing the ability of neurites to extend through the matrix, reach myotubes and form a functional NMJ (Martin et al., 2015). This is particularly relevant to this work, as the co-culture of muscle and neurons in a matrix which allows cell-cell interaction is fundamental. In addition, these constructs can be used for functional studies, described in details below (1.4.3).

1.4.2 Collagen gels

Collagens are components of extracellular matrices, and comprise up to 10% of muscle dry mass (Gillies and Lieber, 2012). Together with other proteins such as laminin, fibronectin and tenascin (Lewis et al., 2001), collagens provide a supporting matrix to which the muscle connects to exploit its physiological function (Smith et al., 2010). Collagen type IV is particularly abundant in the basal lamina, whereas type I, III and V are most abundant in the epi-, peri- and endomysium of connective tissues (Kjaer, 2004). Therefore, collagen-based constructs represent a suitable matrix for the culture of myoblasts *in vitro*. These hydrogels were first described in 1979 (Vandenburg and Kaufman, 1979) and subsequently have been proven to improve SkM maturation (Vandenburg et al., 1988). Similarly to fibrin constructs, the principle behind the alignment of the myotubes lies in the directional cues given by the fixed points (Eastwood et al., 1998, 1994). In addition, collagen gels can undergo mechanical stimulation to simulate exercise and record SkM response (Passey et al., 2011).

A schematic representation of the constructs is shown in **Figure 1.11**.

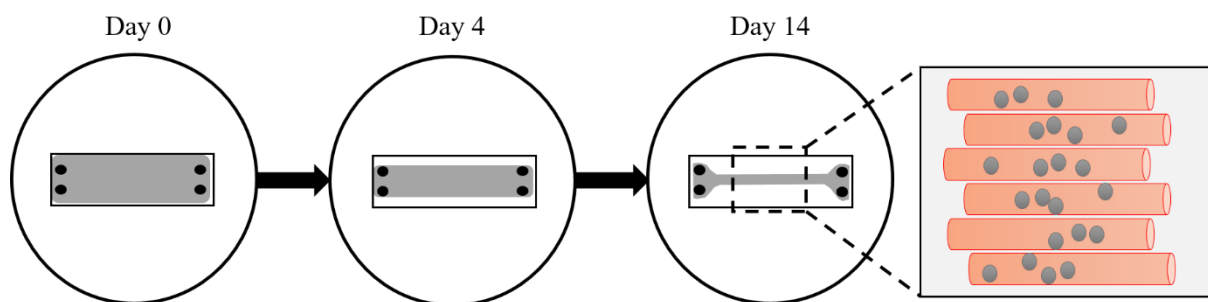


Figure 1.11. Schematic representation of the culture of myoblasts in collagen gels. The gel (grey) is cast into the 3D-printed chamber and contracts over time, until it aligns to the posts. The cells expand until day 4, when they are exposed to differentiation medium. During the last 10 days in culture, myoblasts fuse into multinucleated fibres which follow the alignment of the gel to the posts.

1.4.3 The use of 3D constructs for functional studies

In order to engineer a functional tissue *in vitro*, it is key to generate a biomimetic microenvironment in which the cells find a tissue specific ECM, together with the biochemical and mechanical stimuli that encourage maturation and functionality (Khodabukus et al., 2018). The fibrin and collagen gels described above are able to provide this matrix for SkM to grow and differentiate, as well as to be investigated from a functional perspective. As shown in section 1.3.3, depending on the stimulus generated by MNs, SkM contracts in different ways and generates more or less force. The quantification of this force can be achieved by performing functional studies, which are important in tissue engineering to determine whether the cells or tissues retain their capabilities to function and interact with other cell types *in vitro*, as they do *in vivo*. Force generation in SkM is the main functional aspect that can be investigated, and being able to do this using the fibrin and collagen constructs described above is an advantage. For example, collagen/Matrigel® gels were used to generate an artificial SkM model and electrically stimulate it to investigate the effect of insulin growth factor 1 (IGF-1) on the contractile force of C2C12 (Sato et al., 2011). This study showed that IGF-1 was able to induce hypertrophy and higher force generation if compared to untreated C2C12. Similarly, another compound, Leucine, was added to C2C12 cultures to determine its effect on muscle maturity and functionality when cultured in fibrin gels. It was observed that the supplement increased contractile force, thus showing the suitability of fibrin constructs for functional studies (Martin et al., 2017). More importantly, these gels can not only be used for SkM studies, but also to generate a functional interaction between SkM and MNs (i.e. NMJ). This was recently achieved using primary rat cells, and the fibrin constructs proved to be appropriate when determining that the presence of MNs enhanced SkM contractility (Martin et al., 2015). The previous use of these constructs for force generation measurements shows their potential as tissue engineering platforms for the study of SkM/MNs functionality.

1.5 Conclusions and considerations

Given the background provided in this first chapter, the reader should have gathered knowledge on the key aspects of MNs, SkM and the neuromuscular junction. This will help understanding the aims and rationale behind the experiments conducted in this work. Information on NMJ development and formation are key to generate SkM/MN co-cultures, both using cell lines and primary cells. Components of the motor unit such as agrin can be added to the culture to

facilitate NMJ formation, and SkM markers expression can be investigated following the information provided on SkM development, maturation and differentiation. Using a tissue engineering approach for the generation of this model is essential, and information on the composition of collagen and fibrin constructs, together with their applications for muscle-nerve co-cultures, together with applications for functional studies, justify their use for this work. Finally, background on the culture of each cell type, available lines and stem cells is important to understand why C2C12s, SH-SY5Ys, primary human SkM and iPSC-derived MNs were utilised in this work. Further literature and background specific to each results chapter will be provided at the beginning of each of them.

Regarding the applications for this model, different ones can be identified. The general aim for this work was to generate a biologically-relevant muscle-nerve co-culture, and to do this in 3D constructs which are suitable for different kinds of studies. Therefore, additional optimisation and modifications may be carried out in the future to adapt the model to the intended application. In order to study the effect of a treatment on specific patients' cells, the differentiation of iPSCs into either SkM or MNs would be improved to allow for a more efficient model. For drug testing, cost may be reduced by using less growth factors (e.g. eliminating Matrigel®) and making the process for the gels preparation automated and reproducible. However, if the aim for this model is to study how the NMJ forms and neuromuscular diseases arise, it will need to closely mimic the in vivo muscle-nerve interface (e.g. by adding more cell types to the model, or adjust the muscle:nerve cells ration).

2 GENERAL METHODS

2.1 2D cell culture methods

For the fulfilment of this work, different cell types, including cell lines and primary human cells were used. C2C12 murine skeletal muscle myoblasts and SH-SY5Y human neuroblastoma were used as cell lines. For the culture of primary human cells, skeletal muscle-derived myoblasts (hSkM) and induced pluripotent stem cell-derived motor neuron Progenitors (MNPs) were utilised.

2.1.1 Cell culture: C2C12

The murine SkM myoblast line C2C12 (ATCC, USA) was cultured in T75/T175 flasks in a humidified 5% CO₂ atmosphere at 37° C in muscle growth medium (MGM), composed of: 79% Dulbecco's Modified Eagle Medium (DMEM, Merk, UK), 20% Foetal Bovine Serum (FBS, PAN Biotech UK Laboratories, UK), and 1% penicillin-streptomycin (P/S, PenStrep: 100 units/mL penicillin and 100 µg/mL streptomycin, Thermo Fisher Scientific, UK). The incubators used for the culture were Thermo Scientific HERAcell 240i, and the cell culture cabinets utilised were ThermoScientific HERAsafe. The cells were expanded to 75% confluence before passaging (see section 2.1.5) and to 100% confluence for experimental work. To induce myotubes formation, the cells were washed 3x in sterile phosphate buffered saline (PBS, Thermo Fisher Scientific BioReagents™ Phosphate Buffered Saline Tablet, dissolved in dH₂O) solution and the medium was switched to muscle differentiation medium (MDM) composed of 97% DMEM, 2% Horse Serum, (HS, Merk, UK) and 1% P/S. For optimal differentiation, the cells were used between passage 6 and 10.

2.1.2 Cell culture: SH-SY5Y

The human neuroblastoma cell line SH-SY5Y (ATCC, USA) was cultured in T75/T175 flasks in a humidified 5% CO₂ atmosphere at 37° C in neuronal growth medium (NGM) composed of: 89% Glutamax (DMEM 1X + Glutamax™ - Gibco, UK), 10% heat inactivated FBS (NFBS, Merk, UK), and 1% P/S. The incubators used for the culture were Thermo Scientific HERAcell 240i, and the cell culture cabinets utilised were ThermoScientific HERAsafe. The cells were grown until they reached 60% confluence. To induce neurite extension, the serum concentration in the medium was decreased to 2% and 1 µM Retinoic Acid, (≥98% (HPLC)),

powder all-*trans* RA, Merk, UK) was added to the neuronal differentiation medium (NDM). For optimal differentiation, the cells were used between passage 6 and 10.

2.1.3 Cell resuscitations: C2C12, SH-SY5Y and hSkM

When cells were needed from the liquid nitrogen storage, a cell culture flask was prepared by pipetting approx. 10 mL MGM or NGM into it. Then, the cells were removed from the liquid nitrogen and placed in a water bath (37° C) until the cell suspension was thawed. The cell suspension was then placed into the flask and incubated overnight at 37° C, 5% CO₂. The following day, the MGM or NGM was removed, the flask was washed 2x with sterile PBS and fresh MGM or NGM was pipetted into the flask.

2.1.4 Cell culture: hSkM cells

Primary hSkM cells were obtained by explant biopsy at Loughborough University. The samples were obtained from healthy males, between the ages of 18–55 reporting no recent injuries or intake of anti-inflammatory pharmaceuticals. Tissue was obtained via the Bergstrom biopsy procedure, with any visible connective tissue being removed (Bergstrom, 1975). Tissue samples were removed from the storage MGM solution and washed 3 times in a buffer solution (PBS, 1% P/S & 1% Amphotericin, Merk, UK). Once washed, tissue chunks were placed into a petri dish, suspended in 1 mL of MGM and mechanically minced using 2 scalpel blades until broken down into small sized pieces. Tissue was then seeded into 0.2% gelatin (Merk, UK) coated T25 flasks (approximately 4 pieces/flask) and suspended in 0.5 mL of MGM to ensure tissue was planted on the culture surface and not floating. Flasks were then placed in standard tissue culture incubators (Sanyo O₂/CO₂ incubator MCO-18AIC) for 7-10 days to allow cellular migration to occur with more MGM added to prevent flasks drying out. Migration of hSkM cells was monitored with the migrated cellular population passaged at 60% confluence to prevent spontaneous differentiation at low passage. Cells were dissociated with accutase (Corning®) before re-plating. The cells were then cultured through 3 passages to confirm myogenic capacity and increase cell quantity for experimental purposes. All SkM cells were used between passages 3 and 6 as previously published by our group (Martin et al., 2013). For experimental work, the cells were plated in gelatin-coated wellplates. To coat the culture vessels, a solution of gelatin was prepared (1:10 in sterile PBS). The solution was then used to cover the culture vessels at RT for 30 minutes. When the cells were seeded, the gelatin solution was removed and replaced by prewarmed warm, MGM. Differentiation medium was composed

of DMEM, 2% HS and 1% P/S. All cell culture work was done in a Airstream ESCO Class II Biological Safety Cabinet.

Information on the donors used for this work are reported below in **Table 2.4**.

Table 2.4. Donors information for work using primary SkM cells.

Donor code	Gender	Age
Hu020	M	22
Hu027	M	24
Hu028	M	25
Hu035	F	Unknown

2.1.5 Cell passage and count: C2C12 and SH-SY5Y

Prior experimentation, GM was removed from C2C12 and SH-SY5Y cells and the flask was washed 3x in PBS. A volume of 5 mL of trypsin/ethylenediaminetetraacetic acid (EDTA) was added to each flask and incubated for 5 minutes at 37° C, 5% CO₂. After checking that cells had detached from the tissue culture plastic, trypsin was neutralized with an equal amount of GM. For C2C12, the total volume was collected and transferred to a 15 mL centrifuge tube, which was then centrifuged at 600 xg for 5 minutes at room temperature (Thermo Fisher Scientific Heraeus Megafuge 11R). For SH-SY5Y, cells were centrifuged at 600 xg, for 5 minutes at room temperature. The supernatant was removed and the cells were re-suspended in 1 mL of GM for counting. After mixing the cell suspension thoroughly, 10 µL of suspension were added to 90 µL of Trypan Blue and mixed. Then, 10 µL was added to a hemocytometer (Neubauer, 0.0025 mm²).

2.1.6 Cryopreservation: C2C12, SH-SY5Y and hSkM

In order to cryopreserve C2C12, SH-SY5Y and hSkM cells, these were trypsinised and counted as described in section 2.1.5. A solution made of 90% MGM with 1x10⁶ cells, and 10% dimethyl sulfoxide (DMSO, Thermo Fisher Scientific BioReagents®) was prepared and immediately pipetted into a cryogenic vial (Corning®, UK). The vials were then placed into a freezing container (Mr Frosty™, Thermo Fisher Scientific) and placed at -80° C overnight. The day after, the cryovials were transferred into a liquid nitrogen storage dewar for long term preservation.

2.1.7 Cell culture and resuscitation of induced pluripotent stem cell-derived motor neurons progenitors

Human induced pluripotent stem cell-derived motor neuron progenitors (MNPs, Axol Bioscience, UK) from a healthy 74 years old male donor, were received in dry ice and kept in liquid nitrogen until needed. All cell culture work was done in a Airstream ESCO Class II Biological Safety Cabinet.

All protocols for thawing, expanding, passaging and differentiating MNPs were provided by the manufacturer and a copy can be found in the Supplementary section of this thesis. Updated protocols will be available at:

<https://www.axolbio.com/shop/product/human-ipsc-derived-motor-neuron-progenitors-5172>.

The day before thawing the MNPs, the culture vessels (T25 flasks) were prepared by coating them with SureBond™ (see section 1.8.1).

On the day of thawing the MNPs, motor neuron recovery medium (MN RM, Axol Bioscience) was prepared by adding Y-27632 (Selleck Chemicals) to a final concentration of 10 μ M, and Retinoic Acid (\geq 98% (HPLC), powder all-*trans* RA, Merk, UK) to a final concentration of 0.1 μ M. All medium and culture vessels were pre-warmed at 37°C prior to use. A volume of 4 mL of RM (+Y-27632 and RA) was added to a 15 mL sterile Falcon™ tube. To thaw the cells, the vial was submerged in a water bath set at 37°C. Once the vial was 2/3 thawed, the cell suspension was added dropwise to the 15 mL tube containing RM (+Y-27632 and RA). The cryogenic vial was washed with 1 mL of the same medium. The cells were then centrifuged at 200 \times g for 5 minutes at RT (Thermo Fisher Scientific Heraeus Megafuge 11R). The supernatant was discarded and the cells were counted as described in section 2.1.5. The coating solution which has previously been added to the wells (see section 2.1.7.1) was then removed from the wells and the cells were re-suspended in the appropriate volume of medium to obtain a seeding density ranging from 100,000-150,000 cells/cm².

The cells were incubated at 37° C, 5% CO₂ for 24 hours, and then the medium was changed to RM supplemented with 0.1 μ M RA. Every 2 days, the medium was replaced with fresh, pre-warmed RM supplemented with 0.1 μ M RA. The cells were ready to passage between day 5 and 7.

2.1.7.1 SureBond™ coating

SureBond™ (Axol Bioscience) was used to coat culture vessels upon resuscitation of iPSC-derived MNPs. Briefly, aliquots of SureBond™ coating solution were thawed over night at 4°C. The following day, the SureBond™ stock solution (50x) was diluted in Dulbecco's PBS

(1x) (DPBS, without calcium or magnesium, Thermo Fisher Scientific, UK). Specifically, one vial of SureBond™ (120 µL) was diluted in 6 mL of DPBS. The surface of the culture vessels was then coated with SureBond™ 1x working solution at a volume of 200 µL/cm² overnight at 37° C, 5% CO₂.

2.1.7.2 SureBond™+ReadySet coating

A combination of SureBond™+ReadySet (Axol Bioscience) was used to coat culture vessels for experimentation. The SureBond™ solution was thawed overnight at 4°C the day before coating. The culture vessels were pre-coated with ReadySet at a volume of 250 µL/cm², and incubated at 37° C, 5% CO₂ for 45 minutes. Then, the plates were washed 4x using an equal volume of sterile dH₂O. The SureBond™ solution was prepared as described in section 2.1.7.1 and the culture vessels were incubated with it for 1 hour at 37° C and 5% CO₂.

2.1.7.3 Cell passage: MNPs

When the culture was 70% confluent, the cells were ready to undergo passaging. The day before passaging, an aliquot of Unlock™ (Axol Bioscience) and Motor Neuron Maintenance Medium (MM, Axol Bioscience) were thawed at 4°C. On the day of passaging MNPs, the culture vessels were pre-coated with SureBond™+ReadySet (Axol Bioscience) as follows: SureBond™ was thawed overnight at 4°C the day before coating (2 days before passaging the cells). The culture vessels were then coated with ReadySet at a volume of 250 µL/cm². The vessels were incubated at 37°C, 5% CO₂ for 45 minutes. Then, the plate was washed thoroughly 4x using an equal volume of sterile dH₂O. Meanwhile, a 1x SureBond™ working solution was prepared as described in section 2.1.7.1. The surface of the culture vessels was then coated with SureBond™ at a volume of 200 µL/cm² for 1 hour at 37°C and 5% CO₂.

To detach the cells from the culture vessel, the medium was removed and the vessels were washed once with DPBS at a volume of 2 mL/10 cm². The DPBS was then removed and the cells were incubated with Unlock™ at RT (1 mL/10 cm²). The cells were then incubated for 5 minutes at 37°C, 5% CO₂. Once the cells were detached, a 4x volume of pre-warmed RM was added to the culture vessel and the cells were centrifuged at 200 xg for 5 minutes (Thermo Fisher Scientific Heraeus Megafuge 11R). Subsequently, the supernatant was discarded and the cells were re-suspended in 1 mL fresh RM to perform a cell count as described in section 2.1.5.

Finally, the coating solution was removed from the culture vessels and the cells were seeded at a density of 150,000-200,000 cells/cm². The day after plating, the medium was replaced with

MM supplemented with 0.5 μ M RA, 5 ng/mL brain-derived neurotrophic factor (BDNF, Peptrotech, UK) and ciliary neurotrophic factor (CNTF, Peptrotech). MM was changed every 2 days.

2.2 3D cell culture methods

Collagen and fibrin-based gels were used as 3D tissue engineering constructs for the completion of this work. The purpose of using these systems is that cells grow in a 3D environment *in vivo*, and thus, mimic a 3D structure *in vitro* could aid to obtain a more reliable response in terms of functionality. In addition, the use of these gels in particular make the cells align, which is especially important for SkM cells, as the fusion of myoblasts into myotubes ensures that the cells acquire an *in vivo*-like architecture.

2.2.1 Gel scans and gel width measurement

All constructs were imaged using a computer scanner (Epson Perfection V330 Photo). The images were processed using the software Fiji (Java 1.6.0_24, available to download at <https://imagej.net/Fiji/Downloads>) to measure the width of the gels.

2.2.2 Fibrin gel constructs

The cells were trypsinised and counted as described in section 2.1.5. Fibrin gels were prepared as previously described (Martin et al., 2013). Two 6 mm silk sutures were pinned into Sylgard 184-coated (Dow-Corning, UK) 35-mm plates 12 mm apart using 0.15 mm minuten pins (Entomoravia, Slavkov u Brna, Czech Republic). Plates were sterilized by washing with 70% ethanol and left to dry for 3 hours, followed by 1 hour exposure to the ultraviolet lamps of the cell culture cabinet (ThermoScientific HERAsafe). Each plate then received 500 mL of GM containing 10 units/mL thrombin (Merk, UK) and 80 mg/mL aprotinin (Merk, UK) which was spread evenly over the surface of the plate ensuring the sutures were fully covered. 200 μ L of 20 mg/mL stock fibrinogen (Merk, UK) solution was then added to the plate, agitated gently to ensure even distribution and then left to incubate for 10 minutes at room temperature before being incubated at 37°C, 5% CO₂ for 1 hour. Once the gel had set, 1×10^5 C2C12 cells were evenly plated on top of the gel surface in 2 mL of MGM containing 0.25 mg/mL 6-aminocaproic acid (Merk, UK) to prevent fibrin degradation. Culture medium was replaced every other day for the duration of experimentation. Once the cells within the gels became

confluent (typically 4 days of culture), the medium was switched to MDM containing 0.25 mg/mL 6-aminocaproic acid.

For co-culture fibrin gels, the procedure remains unchanged. However, after 4 days of MGM, the neurons (SH-SY5Y) were passaged as described in sections 2.1.5. MGM was removed from the culture vessels and the gels were washed 3x in sterile PBS. Then, a total of 100,000 cells/gel in 50 μ L NGM were seeded on the fibrin layer. The cell suspension was left to adhere at 37°C, 5% CO₂ for 30 minutes, and then NDM was added until the end of the culture period (14 days).

2.2.3 Collagen gel constructs

Collagen gel constructs were prepared using different protocols. Optimisation and scaling down of the process were performed in the laboratory to achieve smaller gels, requiring less cells and consumables, and ultimately making the system more representative of the physiological architecture of the tissue. Matrigel® (Corning™ Matrigel™ Membrane Matrix)

was added to 50 μ L gel mixture to facilitate the migration of neurites through the matrix. Two different types of 3D printed inserts were used to perform the 3D cell culture (**Figure 2.1**).

The 50 μ L constructs were assembled in 2-parts with a removable barrier. The external geometries of the part were designed to fit into a standard 6 or 12 well culture plate. All 3D modelling was performed using computer aided design (CAD) Siemens NX software (version 8.5) with completed .stl files verified using Materialise MiniMagics. FDM printing utilised a commercially available Ultimaker 2+ system (Ultimaker, Netherlands). For FDM, completed .stl files were processed using the in-house Cura Software for Ultimaker 2+ (version 3.2). FDM parts were printed using PLA and were extruded onto the standard glass build plate, at previously published settings (Rimington et al., 2017). LS parts were printed using an EOS Formiga P100™ (EOS GmbH, Germany) from PA-12. The powder used was a mixture of recycled and virgin powder (20% recycled, 80% virgin); well within manufacturer recommendations. Samples were removed from the build chamber and cleaned using a soft abrasive brush to remove un-sintered powder. All samples were sterilised via UV for \geq 1 h, prior to being adhered to culture well plates using an in-house bio-adhesive which has been found to be completely compatible (Rimington et al., 2017). Once adhered, samples were rinsed with 70 % IMS and left for the remaining solvent to evaporate prior to use.

The designs of the 500 μ L mold mold are available at https://figshare.com/articles/500uL_Mould_FDM/6969851; the designs for the 50 μ L mold

and inserts are available at https://figshare.com/articles/50uL_Mould_FDM/6969710 and https://figshare.com/articles/50uL_FDM_removable_insert/6969707.

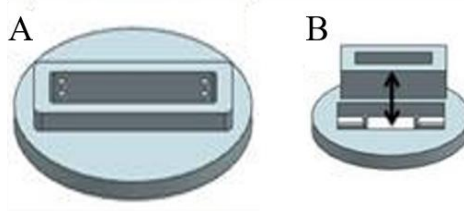


Figure 2.1. 3D printed inserts for collagen gels preparation. A) 500 μ L insert. B) 2-part 50 μ L insert (Rimington et al., 2018b, 2018a).

2.2.3.1 Collagen only constructs

Prior to collagen/myoblast construct setup, muscle cells (both C2C12 and primary SkM) were passaged as described in section 2.1.5. The collagen gels protocol was adapted from previous work (A. S. T. Smith et al., 2012). Although different volume gels were used for this work (500 μ L and 50 μ L), the preparation remained the same. For 500 μ L gels, 20% of the total volume minimal essential media (MEM; Gibco) was added to 85% type 1 rat-tail collagen (First Link, UK; dissolved in 0.1 M acetic acid, protein at 2.035 mg/mL). NaOH was used to neutralise the solution for polymerisation until the mixture fully changed colour from yellow to bright pink. Following neutralisation, the cells suspended in 5% volume of MGM and then added to the collagen solution, at a final concentration of 4×10^6 /mL. The tube was swirled to ensure homogeneous distribution of the components and then the collagen solution was pipetted into 3D printed moulds described in section 2.2.3.

The resulting construct was allowed to polymerise for 30 minutes at 37°C, 5% CO₂. Once set, the compliant construct was physically detached from the chamber and floated in 6 mL MGM for the 2 mL gels, 5 mL MGM for the 500 μ L gels and 2 mL for the 50 μ L gels. Following 4 days of culture in MGM, the constructs were transferred to DM to promote myoblast differentiation. A further 10 days of culture allowed for the maturation of the constructs and the differentiation of myoblasts into multinucleated myotubes.

For co-culture gels, the procedure remains unchanged. However, after 4 days of MGM, the neurons (SH-SY5Y and MNPs) were passaged as described in sections 2.1.5 and 2.1.7.3, respectively. MGM was removed from the culture vessels and the gels were washed 3x in sterile PBS. Then, a total of 1×10^6 SH-SY5Y cells/gel were seeded on the 2 mL collagen gels,

in 200 μ L NGM; 250,000 cells/gel were seeded on the 500 μ L collagen gels, in 100 μ L NGM; 100,000 cells/gel were seeded on the 50 μ L collagen gels, in 50 μ L NGM. The cell suspension was left to adhere at 37°C, 5% CO₂ for 30 minutes, and then NGM was added for 24h. The following day, the medium was changed to NDM until the end of the culture period (14 days).

2.2.3.2 Collagen & Matrigel® constructs

While working with Matrigel®, the solution and the centrifuge tubes were kept on ice at all times. The collagen/Matrigel® mixture was only used for 50 μ L gels. The preparation was based on the protocol described above (section 2.2.3.1). However, the collagen concentration in the gel was reduced from 85% to 60%, and 20% Matrigel® (Corning™ Matrigel™ Membrane Matrix) was added to the gel mixture.

2.3 Methods for biological analysis

The morphological and quantitative analysis for this work was performed mainly using immunofluorescent staining procedures. The outputs of this were morphological analysis and measurement of cell features such as myotube width and neurite length. Furthermore, the gene expression analysis was used to reveal muscle maturity in the presence of absence of neurons and other factors such as agrin.

2.3.1 Immunofluorescent staining

For the completion of this work, immunofluorescent staining was used to verify the expression of both morphological and cell-cell interaction specific markers. Particularly, Rhodamine Phalloidin was used to stain the actin filaments in C2C12 and SH-SY5Y cells. Anti- β -III Tubulin was used to stain neuronal microtubules (SH-SY5Y and MNPs). Choline acetyltransferase (ChAT) and Islet 1 were used as MN markers in MNPs. The neurotoxin α -bungarotoxin (BTX) bound to acetylcholine receptors (AChR's) on muscle fibres (both C2C12 and primary SkM).

Each staining protocol required fixation and permeabilisation first; the protocols for these steps slightly differ for cells cultured in 2D or 3D. For indirect methods, a blocking stage was performed before the incubation with the primary antibody (β -III Tubulin, ChAT and Islet 1).

2.3.1.1 Fixation of cells in 2D

The immunostaining of both C2C12 and SH-SY5Y cells was performed after fixation. Briefly, GM or DM was removed from the chamber and the cells were washed 3x in PBS. Then, a

solution of 3.7% paraformaldehyde in PBS was incubated onto the glass coverslips for 15 minutes. After removal of the fixative, the coverslips were washed 3x and left in PBS for short term storage at 4°C.

2.3.1.2 Fixation of cells in 3D

The immunostaining of collagen and fibrin gels was performed upon fixation. Briefly, GM or DM was removed from the chamber and the cells were washed 3x in PBS. Then, half of the total volume used for the washes was added to the chambers, and the remaining 50% was added dropwise to the chamber (a cold solution of methanol:acetone (v/v 1:1)). The gels were left at RT for 30 minutes, after which the volume was removed from the chamber and substituted by a total amount of methanol:acetone (v/v 1:1) for further 30 minutes. At the end of the fixing period, the fixative was removed and the wells were washed 3x with sterile PBS. For short term storage, the gels were left in PBS at 4°C.

2.3.1.3 Permeabilisation of cells

Before performing immunostaining, the cells were washed 3x with 1x tris-buffered saline (TBS, pH 8.5). Then, the cells were incubated in a 0.2% (v/v) Triton X-100 (Thermo Fisher Scientific) solution in 1x TBS for 30 minutes. This was done equally for cells culture in 2D and 3D.

2.3.1.4 Rhodamine phalloidin

For Rhodamine phalloidin staining (Life Technologies), the coverslips were washed 3x in 1x TBS and incubated with a 1x TBS solution containing 1:200 (v/v) Rhodamine-Phalloidin antibody and incubated for 2 hours. Then, the coverslips were incubated with 1 µL/mL 4',6-diamidino-2-phenylindole, DAPI (Thermo Fisher Scientific) to stain the nuclei for 10 minutes. Finally, the cells were washed 3x in 1x TBS and mounted onto glass slides using mounting medium (Fluoromount™ Aqueous Mounting Medium, Merk, UK). The coverslips were left to dry overnight and protected from light, before imaging. To stain 3D tissue engineering constructs, the antibody was incubated for 3 hours instead of 2.

2.3.1.5 β-III Tubulin

For the β-III Tubulin staining, the initial blocking solution was prepared using 5% goat serum (GS, Merk, UK), 0.2% Triton in 1x TBS and the coverslips were incubated for 30 minutes. Then, the coverslips were washed 3x and incubated for 1 hour in the I antibody (monoclonal anti-β-III Tubulin, Scientific Laboratory Supplies Ltd (SLS, Merk, UK) solution at a concentration of 1:200 and 2% GS. Then, the coverslips were washed 3x and incubated with

the secondary antibody solution containing 1:200 II antibody (AlexaFluor 488® goat anti-mouse, IgG, SLS, Merk, UK), 2% GS and 1 µL/mL for 1 hour. After the incubation, the cells were incubated for 10 minutes with a 1x TBS and 1:1000 (v/v) DAPI solution. Finally, the coverslips were washed 3x in 1x TBS and mounted onto glass slides using mounting medium. The coverslips were left to dry overnight and protected from light, before imaging.

2.3.1.6 Choline Acetyltransferase

The immunofluorescent staining for Choline Acetyltransferase (ChAT) was performed upon fixation (section 2.3.1.1) and then as follows: firstly, the cells were permeabilised in a solution of 1x TBS (pH 8.5) and 0.2% (v/v) Triton X-100 (Thermo Fisher Scientific) for 30 minutes. Then, the blocking step was done using a solution of 5% GS for 30 minutes. The cells were washed in TBS 1x, 3x for 5 minutes and then incubated for 1 hour with a solution of primary anti-ChAT antibody (abcam, UK) 1:100 (v/v), with 5% GS in 1x TBS. Then, after 3x washes (5 minutes each) in TBS 1x, the cells were incubated with the secondary antibody solution: goat anti-rabbit IgG H&L, conjugated with Alexa Fluor® 488 (abcam, UK), with 5% GS for 1 hour. After washing the cells 3x with TBS 1x, they were counterstained with a solution of TBS 1x and DAPI 1:1000 (v/v) for 10 minutes. At the end of the staining protocol, the cells were washed again 3x with TBS 1x and then mounted onto glass slides using Fluoromount™. The coverslips were left to dry overnight and protected from light, before imaging.

2.3.1.7 Islet 1

The Islet 1 staining (abcam, UK) staining was performed in one step, as the primary antibody was conjugated with the Alexa Fluor® 568 fluorophore. Upon fixation and permeabilisation (sections 2.3.1.1 and 2.3.1.3, respectively), the cells were incubated in a solution with 1x TBS and 1:1000 (v/v) Islet 1 for 2 hours. At the end of the incubation, the cells were washed 3x with 1x TBS before incubating with 1x TBS and DAPI 1:1000 (v/v) for 10 minutes. At the end of the incubation, the cells were washed with 1x TBS, 3x for 5 minutes and the coverslips were mounted onto glass slides using Fluoromount™. The coverslips were left to dry overnight, protected from light, before imaging.

2.3.1.8 α -Bungarotoxin

The α -Bungarotoxin (BTX, Merk, UK) staining was performed in order to determine the presence of acetylcholine receptors (AChR's) at different stages of differentiation of C2C12 cells (after 3, 5 and 7 days in DM).

Upon fixation of C2C12 cells (section 2.3.1.1), the wells were washed 3x with non-sterile 1x TBS and a solution of 1x TBS and 0.2% (v/v) Triton X-100 was added for 30 minutes. After washing the cells with 1x TBS, 3x for 5 minutes, a solution of 1x TBS and 1:1000 (v/v) Texas Red® conjugated BTX was added for 3 hours. At the end of the incubation, the cells were washed 3x with 1x TBS before incubating with 1x TBS and DAPI 1:1000 (v/v) for 10 minutes. At the end of the incubation, the cells were washed with 1x TBS, 3x for 5 minutes and the coverslips were mounted onto glass slides using Fluoromount™. The coverslips were left to dry overnight, protected from light, before imaging.

2.3.1.9 Synaptic vesicle 2

The C2C12/SH-SY5Y co-culture in monolayer was stained with α -BTX and synaptic vesicle 2 (SV-2, DSHB) in order to identify the co-localisation of vesicles containing the neurotransmitter acetylcholine (in SH-SY5Y cells) and clusters of acetylcholine receptors AChR's in C2C12 cells.

The co-culture was fixed (section 2.3.1.1) and the wells were washed 3x with non-sterile 1x TBS. A solution of 1x TBS and 0.2% (v/v) Triton X-100 was added for 30 minutes. Then, the cells were blocked by adding 1x TBS, 5% GS, and 0.2% (v/v) Triton X-100 for 1 hour. After washing the cells with 1x TBS, 3x for 5 minutes, the solution containing the primary antibody for SV-2 was prepared as follows: 1x TBS, 2% GS, 1:10 (v/v) SV-2 primary antibody. The primary antibody was incubated at RT for 3 hours. The cells were washed with 1x TBS, 3x for 5 minutes before adding 1x TBS, 2% GS, 1:100 AlexaFluor 488® goat anti-mouse IgG, 1:1000 (v/v) Texas Red® conjugated α -BTX for 3 hours. At the end of the incubation, the cells were washed with 1x TBS, 3x for 5 minutes and a solution of 1x TBS with DAPI (1:1000 v/v) was added for 10 minutes. Finally, the cells were washed with 1x TBS, 3x for 5 minutes and the coverslips were mounted onto glass slides using Fluoromount™. The coverslips were left to dry overnight, protected from light, before imaging.

Image acquisition was performed using a fluorescent microscope Leica DM2500 and the software LAS X. For coverslips imaging, 5 frames per coverslips were taken. Further image analysis is described in section 2.3.2.

2.3.2 Quantitative measurement of myotube width and neurite length

The morphological analysis was performed using the software Fiji (Java 1.6.0_24, available to download at <https://imagej.net/Fiji/Downloads>). A total of 10 myotubes and 10 neurites were measured in each image. The myotube width and neurite length from one image was averaged,

and then the value obtained was averaged with the remaining frames (5 frames per coverslip, 3 coverslips per well). The measured cells were picked randomly in the frames, but only myotubes with 3 or more nuclei were considered for myotube width measurement, and the middle of the myotube was taken for the measurement itself. Whenever possible, neurite length was measured from nucleus to the end of the neurite.

2.3.3 RNA extraction

In order to extract the RNA from cells cultured in monolayer, culture medium was removed from the culture wells and the cells were washed 3x with sterile PBS. Then, 1 mL TRI Reagent® (Trizol, Merk, UK) per 10 cm² of culture surface were added to each well. Using an upside-down 1 mL pipette tip, the culture surface was scraped in all directions to ensure detachment of the cells from tissue culture plastic and production of a lysate. This was then transferred to RNase-free tubes and stored at -80°C until needed.

On the day of the extraction, the samples were thawed at RT and let to set. Then, chloroform was added to the tubes (200 µL/mL Trizol used). The samples were shaken vigorously for 15 seconds and allowed to stand at RT for 15 minutes. The mixtures were then centrifuged at 12,000 xg for 15 minutes at 2-8°C (Thermo Fisher Scientific Heraeus Megafuge 11R). This step allows the formation of three phases; the upper phase, containing the RNA, was transferred to fresh RNase-free tubes, to which 2-propanol (Merk, UK) was added (500 µL/mL Trizol used). The samples were mixed by inversion and left to stand at RT for 10 minutes, then centrifuged at 12,000 xg for 10 minutes at 2-8°C. Subsequently, the supernatant was removed and the pellet was washed by adding 75% ethanol (1 mL/mL Trizol used). The samples were vortexed before being centrifuged at 7,500 xg for 5 minutes at 2-8°C. Finally, the ethanol was removed and the samples were left to dry for 5-10 minutes. To store the RNA samples, 50 µL of Storage Solution (Ambion, UK) were added to each sample and these were stored at -80°C unless immediately used for RNA quantification or RT-qPCR.

2.3.4 RNA quantification

The RNA quantification (260 nm) and purity (260/280 nm ratio) were determined spectrophotometrically using a NanoDrop 2000 (Thermo Scientific, UK). Only RNA samples which resulted in a 260/280 ratio between 1.8 and 2 were used. Briefly, 1 µL Storage Solution (Ambion, UK) was loaded into the machine as blank. Then, the samples were analysed using 1 µL per sample.

2.3.5 RT-qPCR

The genes analysed via RT-qPCR for mouse and human cells are reported in **Table 2.5** and **Table 2.6**, respectively.

Before setting up the PCR plate, the bench and pipettes were wiped using RNaseZap™ (Thermo Fisher Scientific). Reactions were prepared in triplicates in 384 well plates (Applied Biosystems, UK) using filtered pipette tips (Starlab, UK) The reactions consisted of 5 ng of RNA in 5 µL, and 5 µL of master mix consisting of 4.7 µL SYBR® Green, 0.1 µL of both forward and reverse primer and 0.1 µL of quantifast reverse transcriptase kit (Qiagen, UK). The reaction was carried out as follows: 50°C for 10 minutes and 95°C for 5 minutes, followed by 40 cycles of 95°C for 10 seconds and 60°C for 30 seconds.

2.3.6 RT-qPCR data analysis

Relative quantification of gene expression has been analysed in this thesis by the $2^{-\Delta\Delta C_T}$ method as previously described (Schmittgen and Livak, 2008). All methods and reagents were used based on previous RT-qPCR conducted in our laboratory. This analysis requires the use of a housekeeping gene (always expressed) to which the data is normalised. RPII was used as a reference gene, both for mouse and human samples. All primers were customised and supplied by Merk, UK. These were optimised in our laboratory, using the standard curve methods. Briefly, serial dilutions of RNA were run to generate a linear curve from which the primer efficiency was calculated. Only primers with an efficiency between 90-110% were used.

The amplification of RT-qPCR was assessed by using QuantiFast® SYBR® Green one step kit (Qiagen, UK) on ViiA™ 7 RUO Software.

Table 2.5. Target genes and primer sequences utilised for RT-qPCR of mouse cells (C2C12).

Target mRNA		Primer sequence 5'-3'	NCBI reference sequence
RPII	F R	GGTCAGAAGGGAACCTGTGGTAT GCATCATTAATGGAGTAGCGTC	NM_153798.2
MyoD	F R	CATTCCAACCCACAGAAC GGCGATAGAAGCTCCATA	NM_010866.2
MyoG	F R	CCAAGTGTGAGATTGTCTGTC GGTGTAGCCTTATGTGAAT	NM_031189.2
MyHC1	F R	CGCTTTGGTAAGTTCATCAG TAGATCCGGCTTCTTGTTAG	NM_030679.1
MyHC2	F R	CCTATCTGCTAGAGAAGTCC CTTCTTGTTGGATGTGATCTG	NM_001039545.2
MyHC3	F R	CATATCAGAGTGAGGAGGAC CTTGTAGGACTTGACTTTCAC	NM_002470.3
MyHC7	F R	GCAGAGTCAGTGAAGGGCAT CTTGGAGCTGGGTAGCACAA	NM_080728.2
MyHC8	F R	TGGATGATCTATACCTACTCAG TTGTCAGAGATGGAGAAGATG	NM_177369.3

Table 2.6. Target genes and primer sequences utilised for RT-qPCR of human cells (hu020, hu027, hu028_1 and hu028_2).

Target mRNA		Primer sequence 5'-3'	NCBI reference sequence
RPII	F R	AAGGCTTGGTTAGACAACAG TATCGTGGCGGTTCTTCA	NM_000938.1
MyHC1	F R	CGCTTTGGTAAGTTCATCAG TAGATCCGGCTTCTTGTTAG	NM_005963.3
MyHC7	F R	GCTTTGCCACATCTTGAT AATTGCTTTATTCTGCTTCCT	NM_000257.3
MyHC8	F R	ATTTCCACCAAGAACCCA AAAGGATTCTGCCTCTGG	NM_002472.2

2.4 Statistical analysis

GraphPad Prism 6.0 software was used for statistical data analysis. Specific statistical analyses performed in this thesis have been highlighted in the methods section of each chapter, as each experiment had specific analytical requirements.

3 C2C12 & SH-SY5Y: OPTIMISING A CHIMERIC MUSCLE-NERVE CO-CULTURE IN 2D

3.1 Introduction

In order to develop an *in vitro* model of the NMJ, preliminary studies using cell lines were performed. This first step ensured that the co-culture conditions were optimised before using human primary cells and the 3D tissue engineering models. Establishing suitable co-culture conditions presents several challenges. Integrating heterotypic cells within the same system requires optimisation of the culture conditions to allow both cell types to survive, differentiate and coexist (Grey, 2011). Other aspects are the seeding density and the timing of the cultures, which must be carefully planned to ensure that both cell types reach optimal confluence when needed. For the realisation of this co-culture, cell lines were chosen primarily because of their higher availability and lower cost, compared to primary cells. This is particularly relevant when considering the neuronal population, as human primary motor neurons (MNs) can only be obtained using stem cells, whereas primary muscle is easily extracted with a biopsy. In addition, establishing a chimeric co-culture (murine muscle and human neurons) represents a progression from the previously established mouse models (Morimoto et al., 2013).

The culture of different cell types in *in vitro* models is essential, as it provides researchers with a system that mimics the *in vivo* environment, allowing study of natural interactions occurring between cells and improves monocultures success (Goers et al., 2014). Although some of the mechanisms underpinning NMJ formation are still unclear, the formation of nerve-muscle contacts was characterised and extensively reviewed (Witzemann, 2006), explaining the role of the proteins involved in the NMJ formation process and sustaining the pre-patterning theory. Co-cultures mimic functional interactions between cell types (Grey, 2011; Smith et al., 2016). In particular, culturing MNs with skeletal muscle (SkM) showed enhancement of muscle contractility and maturity (Larkin et al., 2005; Martin et al., 2015).

Optimising a system whereby murine SkM and human neurons are cultured together represents a step forward if compared to animal cultures, and a platform for further studies with primary human cells. Besides the advantages of using cell lines, which are more reproducible, cheaper

and less time-consuming to use, this chimeric model will develop understanding of the physiological interaction between the cell types.

3.1.1 The effect of retinoic acid on C2C12 and SH-SY5Y cells.

The aim of this work was to combine human SkM cells and MNs. During the first stage, cell lines were used to generate a chimeric system (mouse/human). The human neuronal cell line (SH-SY5Y) was used in combination with murine myoblasts (C2C12). SH-SY5Y cells require retinoic acid (RA) to differentiate. RA is a major component of vitamin A and plays a key role in biological processes like cell growth, apoptosis, migration and differentiation. Every cell type requires specific growth and differentiation conditions, which may involve different media formulations, oxygen levels, supplementations etc. (Goers et al., 2014). Therefore, it is essential to establish the culture conditions when co-culturing heterotypic cells such as C2C12 and SH-SY5Y. The phenotype of RA-treated SH-SY5Y cells is the subject of controversy in the literature (Hong-rong et al., 2010). Being a versatile cell line, it can be used to generate dopaminergic, adrenergic or cholinergic neurons. Protocols in the literature differ, although generally, RA was found to promote a cholinergic phenotype in SH-SY5Y (Adem et al., 1987; Forster et al., 2016; Pählman et al., 1995).

While the role of RA in neurological development is essential (Rhinn and Dolle, 2012), its effect on SkM cells showed variable results in the literature. The influence of RA on SkM cells was studied in different species including quail (Maden et al., 2000), zebrafish (Hamade et al., 2006), chicken (Reijntjes et al., 2010) and rat (Arnold et al., 1992). In murine myoblasts, RA promoted MyoD expression and myoblast differentiation (Albagli-Curiel et al., 1993; Halevy and Lerman, 1993). The concentrations used to induce differentiation were as low as 0.0001 to 0.01 μM (Halevy and Lerman, 1993), suggesting that RA may be beneficial to myotube formation, if kept at low concentrations. Also, RA promoted C2C12 myotube formation and expression of myogenic markers upon treatment with concentrations ranging from 0.25 to 4 μM (Zhu et al., 2010). However, another study showed that concentrations between 0.1 and 10 μM induced a reduction in MyoD, Myogenin (MyoG) and myosin light chain MyLC1/3 expression, suggesting inhibition of the differentiation process (Xiao et al., 1995a). Recently, reduced myotube width was reported when C2C12 myoblasts were treated with 10 μM RA if compared to no RA at all, suggesting that the presence of RA induced muscle atrophy (Pardo-Figueres, 2017).

Another study (Yun et al., 2008) showed that RA is involved in cytoskeleton remodeling which allows the cells to change morphology and migrate. The process through which this occurs, involves the activation of a specific protein which is involved in the regulation of glucose uptake in SkM cells: AMP-activated protein kinase (AMPK). The authors also believed that RA did not affect C2C12 viability, but no results were shown to confirm this statement. This represents a limitation because qualitative and quantitative experiments would support such a declaration. In fact, it is not clear what exactly was not affected by RA (adhesion, proliferation, metabolic activity, differentiation).

In human myoblasts, the treatment with RA impaired SkM differentiation, but the inactivation of endogenous RA receptors enhanced myoblasts differentiation, showing that RA enhanced the expression of myogenic specification genes while inhibiting the expression of early and late muscle differentiation markers (El Haddad et al., 2017).

In conclusion, the variability in the literature reinforces the need to test the effect of RA on C2C12 and in co-cultures with SH-SY5Y cells, to ensure survival and differentiation of both cell types.

3.1.2 The use of agrin to increase muscle-nerve interactions

Agrin is a protein involved in the formation of the NMJ (Witzemann, 2006), found to play a role in synaptogenesis in the brain (Daniels, 2012). There are two main subtypes of agrin: neuronal agrin is responsible for the anchoring to the SkM fibres, stabilising AChR clustering and controlling axonal growth (Bian and Bursac, 2012; Hoch, 1999; Witzemann, 2006); muscle agrin is involved in synaptogenesis (Burgess et al., 1999). Lack of neuronal agrin *in vivo* can result in impaired synaptic development of the NMJ (Burgess et al., 1999). The use of agrin in muscle-nerve co-cultures aims to increase AChR's clustering and enhance interactions between the two cell types (Marangi et al., 2001; McMahan et al., 1992; Smith, 2012; Wallace, 1989), thus aiding NMJ formation.

3.2 Aims & objectives of the chapter

Co-culturing different cell types requires optimisation of the culture conditions (e.g. differentiation medium composition, amount of time the cells require to either fuse into multinucleated myotubes or extend neurites, seeding procedures...). In addition, the presence

of neurons (SH-SY5Y) in a SkM culture (C2C12) was hypothesised to enhance muscle maturity in terms of increased myotube size and expression of mature SkM markers. The reason for enhancing SkM maturity was to obtain an *in vitro* model which was functional, and this can only be obtained if the muscle is mature. Hence, the aim of this chapter was to test different differentiation medium compositions to allow both myotube formation and neurite extension, as well as to determine whether the presence of a neuronal population in the culture could cause larger C2C12 myotubes to form, suggesting a higher degree of maturation. Finally, the role of agrin in the co-culture was investigated to determine its effect on AChR's clustering and muscle markers expression. The results obtained in this chapter represent a helpful step to determine the conditions for the 3D co-cultures performed afterwards and to understand the potential of SH-SY5Y as an *in vitro* neuronal model and to increase C2C12 maturity.

The aims for this chapter were:

- Identifying the differentiation medium composition for C2C12/SH-SY5Y cells co-culture;
- Verifying the expression of pre- and post-synaptic proteins on C2C12s and SH-SY5Ys;
- Adding agrin to the culture to increase NMJ contacts and C2C12 cells' markers expression.

The objectives for this chapter were:

- To test three concentrations of RA and measure myotube width and neurite length as measurements of cell differentiation;
- To observe cell morphology, distribution and pre/post-synaptic markers expression using immunofluorescent staining;
- To test the addition of agrin to the culture and observe AChR expression on C2C12s, and gene expression of MyoD, MyoG, MyHC1, MyHC2, MyHC3, MyHC7 and MyHC8.

3.3 Materials & Methods

C2C12 murine myoblasts and SH-SY5Y neuroblastoma cells were routinely cultured, passaged and plated as described in section 2.1. The immunofluorescent stainings for morphological and synaptical markers were performed as described in **Error! Reference source not found.** and adjusted for the co-culture as explained in sections 3.3.3 and 3.3.4. Quantitative analysis of the images was done according to section 3.3.5 and gene expression analysis was investigated via RT-qPCR as reported in 2.3.5.

3.3.1 Co-culture medium optimisation: different RA concentrations

This experiment was conducted to establish the optimal differentiation medium. The aim was to determine which concentration of RA allowed for both myotube formation and neurite extension. Firstly, C2C12 and SH-SY5Y were monocultured in optimal conditions based on previous protocols (Pardo-Figueres, 2017; Turner et al., 2018) (**Table 3.1**). The cells were also monocultured in different compositions of differentiation medium (NDM), and three concentrations of RA: 1, 5 and 10 μM (**Table 3.2**).

Table 3.1. Composition of gold standard media used to expand and differentiate C2C12 and SH-SY5Y.

	GM	DM
C2C12	DMEM + 20% FBS + 1% P/S	DMEM + 2% HS + 1% P/S
SH-SY5Y	Glutamax + 10% NFBS + 1% P/S	Glutamax + 10% NFBS + 10 μM RA + 1% P/S

Table 3.2. Composition of different media used with different concentrations of RA for the co-culture of C2C12 and SH-SY5Y.

RA concentration	NDM
1 μM	Glutamax + 2% NFBS + 1 μM RA + 1% P/S
5 μM	Glutamax + 2% NFBS + 5 μM RA + 1% P/S
10 μM (control)	Glutamax + 2% NFBS + 10 μM RA + 1% P/S

The experiment was setup as follows: C2C12 were seeded in muscle GM (MGM) at the density of 10,000/cm² until they reached 100% confluency. Then, they were differentiated for 5 days in muscle DM (MDM). SH-SY5Y controls were seeded at the same density and differentiated when they reached 60% confluency. For the co-cultures, C2C12 were seeded in MGM at day 0 at the same density as in the monocultures and expanded until they reached 100% confluency. Then, an equal density of SH-SY5Y cells was seeded on top of the myoblast layer in neuronal GM (NGM) (Glutamax, 10% NFBS, 1% P/S) for 24h. The following day, neuronal DM (NDM) was removed and the co-culture was washed 3x with sterile PBS before adding to NDM (Glutamax, 2% NFBS, 1% P/S and 1, 5 or 10 μ M RA). The culture was carried on for further 5 days. At the end of the experiment, the cells were fixed and immunostained for morphological markers as described in sections 2.3.1.4 and 2.3.1.5. SH-SY5Y were also seeded on a layer of myoblasts (undifferentiated C2C12) which were subconfluent to prevent fusion into myotubes.

3.3.2 Addition of agrin to mono and co-culture

To induce AChR's clustering on C2C12 myotubes, agrin (Recombinant Rat Agrin Protein 100 μ g, R&D Systems, USA) was added to the culture at the point of differentiation in NDM, at a concentration of 200 ng/mL as previously described (Martin et al., 2015). C2C12 monocultures were used as control, then agrin was added to C2C12 monocultures (C2C12 +agrin); in C2C12/SH-SY5Y co-cultures, NDM was kept standard (co-culture -agrin) or supplemented with agrin (co-culture +agrin). The samples are defined in the table below (**Table 3.3**) for clarity. The differentiation was carried out for a 5 days.

Table 3.3. Samples details for the addition of agrin to C2C12 monocultures and co-cultures with SH-SY5Y cells.

Sample name	Growth	Differentiation
Control	MGM	MDM
C2C12 +agrin	MGM	MDM +agrin (200 ng/mL)
Co-culture -agrin	MGM (+24h NGM)	NDM
Co-culture +agrin	MGM (+24h NGM)	NDM +agrin (200 ng/mL)

3.3.3 Co-culture morphological staining: phalloidin & β -III Tubulin

Morphological immunostaining was performed according to 2.3.1.4 and 2.3.1.5. For the staining of co-cultures, a combination of such previously described methods was used.

3.3.4 Co-culture interaction staining: BTX & SV-2

Similarly to the morphological staining described in section 3.3.3, a combination of BTX and SV-2 immunostaining was based on individual protocols described in 2.3.1.8 and 2.3.1.9.

3.3.5 Quantitative analysis: measurement of myotube width and neurite length

The morphological analysis was performed using the software Fiji (Java 1.6.0_24, available to download at <https://imagej.net/Fiji/Downloads>). The quantitative analysis was done using the cumulative frequency method. The myotube width and neurite length from one image was averaged, and then the value obtained was averaged with the remaining frames (5 frames per coverslip, 3 coverslips per well). The measured cells were picked randomly in the frames. Only myotubes with 3 or more nuclei were considered for myotube width measurement. Whenever possible, neurite length was measured from the soma to the end of the neurite.

3.3.6 Statistical analysis

The statistical differences between the values in this chapter were analysed using the software GraphPad 6.0. The Shapiro-Wilkinson test was used to determine if the populations were normally distributed, and the homogeneity of the data was also tested.

Multiple comparison two-way ANOVA was used to determine differences between myotube width and neurite length the values of the cells in monoculture and co-culture, as well as to compare the experimental conditions to the control, considered as the cells cultured in gold standard conditions. Differences were considered significant at $p \leq 0.05$ (*), $p \leq 0.01$ (**) and $p \leq 0.001$ (***). The level of significance was adjusted according to the Bonferroni's correction. Gene expression were analysed using a 1 by 3 ANOVA with parametric results, and Kruskal Willis test for non-parametric results. All results are presented as average \pm standard deviation (SD).

3.4 Results

3.4.1 Co-culture medium optimisation: the effect of the RA concentration on C2C12 and SH-SY5Y morphology

In order to effectively co-culture C2C12 and SH-SY5Y cells, the co-culture medium required optimisation, particularly regarding the RA concentration, which was necessary for neurite extension and thus neuronal differentiation. C2C12 and SH-SY5Y were treated with different NDM compositions (**Table 3.2**). As controls, C2C12 and SH-SY5Y were monocultured and differentiated in gold standard conditions (**Table 3.1**) and showed myotube formation and neurite extension (**Figure 3.1**). Similarly, differentiation was observed when C2C12 and SH-SY5Y were monocultured in different NDM compositions (Table 3.2).

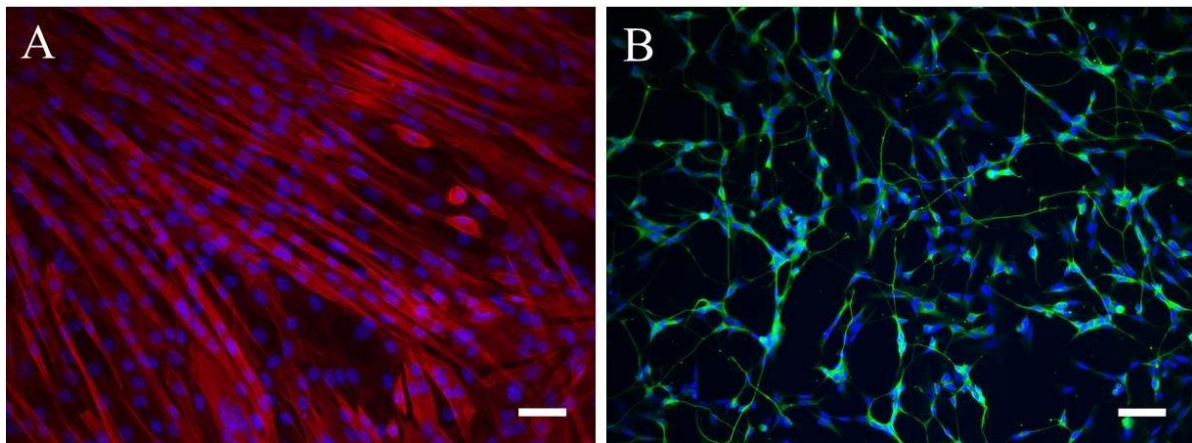


Figure 3.1. Representative images of C2C12 and SH-SY5Y monocultures in optimal conditions. C2C12 myoblasts (A) were immunostained with rhodamine phalloidin to show actin filaments (red) and DAPI for the nuclei (blue). SH-SY5Y (B) were immunostained with β -III Tubulin (green) and nuclei were counterstained with DAPI (blue). Scale bars: 50 μ m.

As controls, C2C12 and SH-SY5Y were monocultured and differentiated in gold standard conditions (**Table 3.1**) and showed myotube formation and neurite extension (**Figure 3.1**). Similarly, differentiation was observed when C2C12 and SH-SY5Y were monocultured in different NDM compositions (**Table 3.2**).

In the co-culture conditions, SH-SY5Y were co-cultured both with fully differentiated C2C12 (myotubes) and undifferentiated C2C12 (myoblasts) (**Figure 3.3**). Both in the monoculture and in the co-culture, C2C12 myotubes appeared smaller as the concentration of RA increased. SH-

SY5Y extended neurites at all culture conditions and RA concentrations. When SH-SY5Y were monocultured, the neurites did not extend in specific directions (**Figure 3.1B, Figure 3.2**) as opposed to the co-cultures (**Figure 3.3**), where they formed bundles which aligned to the direction of the myotubes. The values of myotube width and neurite length resulting from these co-cultures are reported in **Table 3.4** and represented in **Figure 3.4** and **Figure 3.5**.

Table 3.4. Myotube width (μm) and neurite length (μm) of C2C12 and SH-SY5Y.

The difference between average values was analysed using ANOVA and the Bonferroni correction. Results are shown as average \pm SD and were considered significant when $p \leq 0.05$.

	C2C12		SH-SY5Y		
	Monoculture	Co-culture	Monoculture	Co-culture (myoblasts)	Co-culture (myotubes)
1 μM RA	14.95 \pm 4.59	17.26 \pm 5.73	124.97 \pm 12.83	69.48 \pm 14.86	138.56 \pm 40.98
5 μM RA	14.91 \pm 5.08	13.92 \pm 2.80	89.42 \pm 13.98	81.4 \pm 12.81	106.68 \pm 33.70
10 μM RA	12.67 \pm 3.93	12.94 \pm 3.60	56.81 \pm 10.40	70.95 \pm 9.55	101.30 \pm 33.71

The myotube width did not show any statistical differences when compared to the optimal control. A general trend was observed when culturing the cells in the presence of RA, showing that increasing the concentration of RA led to a decrease in myotube width, and that the co-culture had larger myotubes at 1 and 10 μM RA, if compared to the monoculture. The myotube width values when the cells were monocultured in 1 μM RA were the closest to the optimal control (2% HS) (**Figure 3.4**). The longest neurites were observed when SH-SY5Y were monocultured and co-cultured with myotubes at 1 μM RA. Generally, the cells projected longer neurites when co-cultured with myotubes, if compared to co-cultures with myoblasts and monocultures. In particular, a significant difference in neurite length was observed between the monoculture at 1 μM and the monoculture at 10 μM RA; the co-culture with myoblasts and with myotubes at 1 μM RA; the co-culture with myotubes at 1 μM RA and the monoculture at 10 μM RA; finally, the co-culture with myotubes at 1 μM RA and the co-culture with myoblasts at 10 μM RA (**Figure 3.5**).

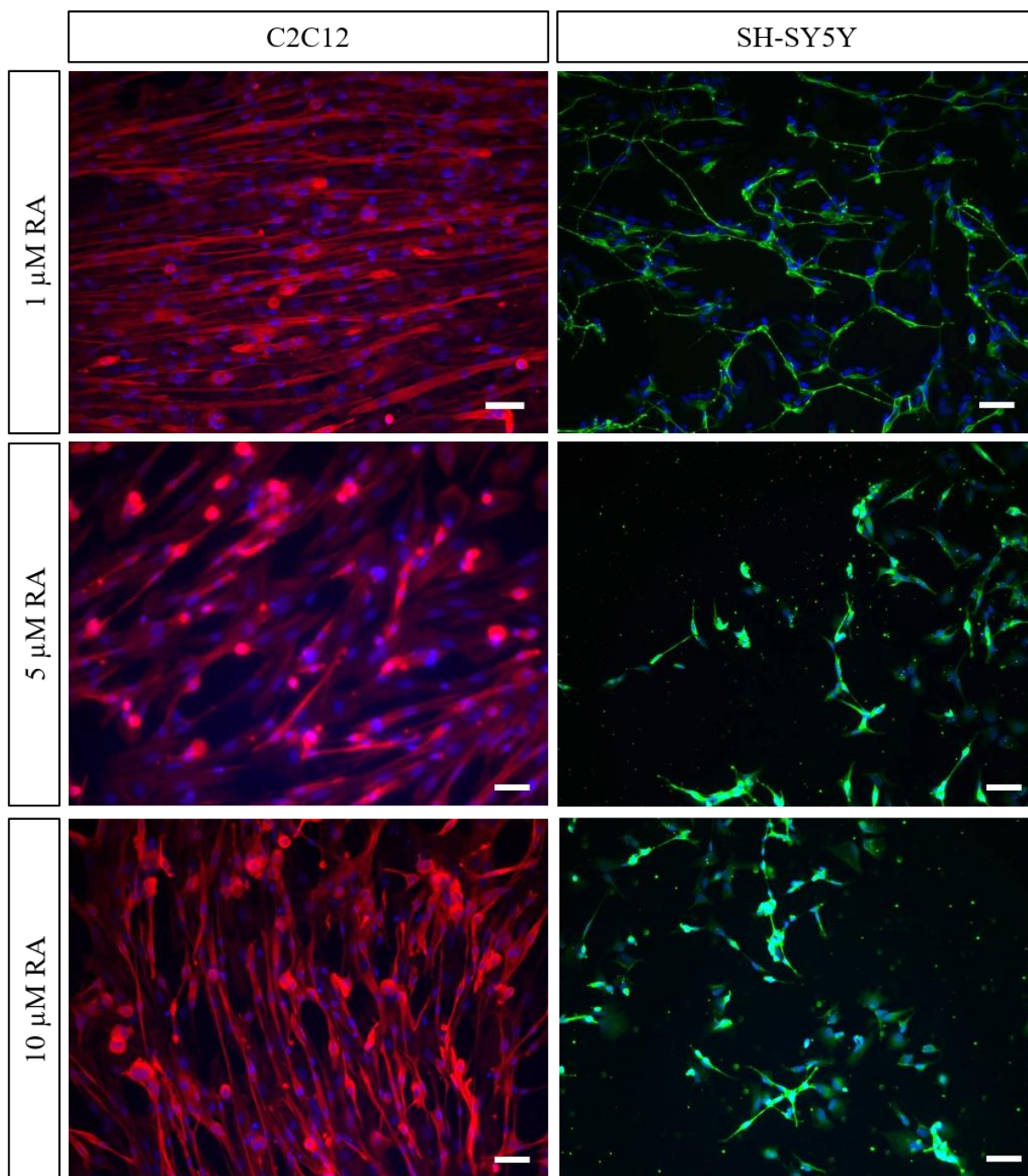


Figure 3.2. Monocultures differentiated with different concentrations of RA. The cells were fixed and immunostained with morphological markers: actin filaments were stained with rhodamine phalloidin (red), SH-SY5Y cytoskeleton was stained with β -III Tubulin (green) and nuclei were counterstained with DAPI (blue). Scale bars: 50 μ m.

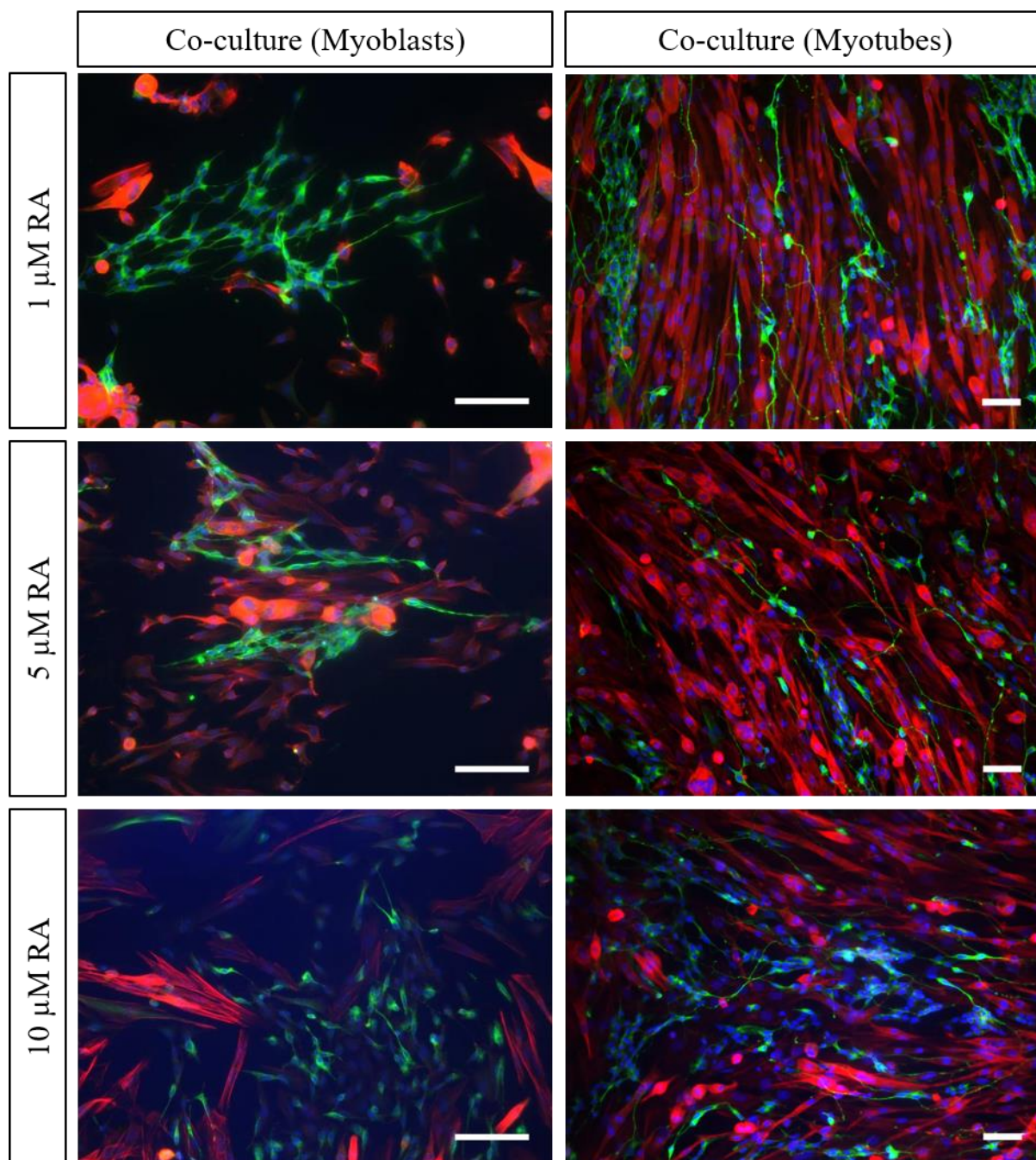


Figure 3.3. C2C12 and SH-SY5Y co-cultures differentiated with different concentrations of RA. The cells were fixed and immunostained with morphological markers: actin filaments were stained with rhodamine phalloidin (red), SH-SY5Y cytoskeleton was stained with β -III Tubulin (green) and nuclei were counterstained with DAPI (blue). Scale bars: 50 μ m.

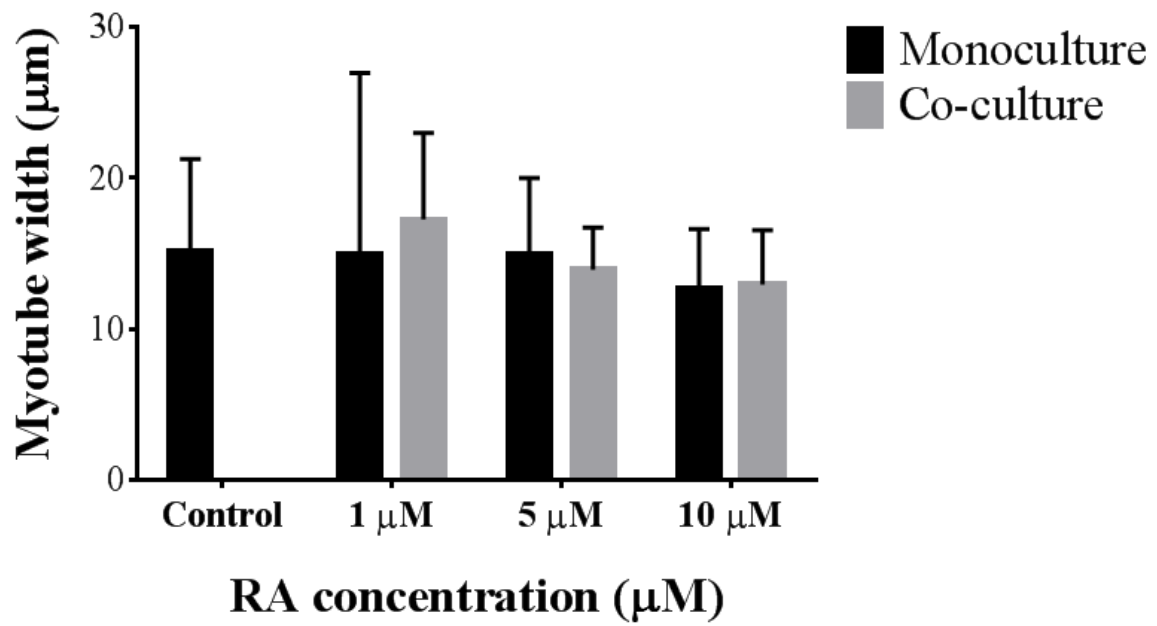


Figure 3.4. C2C12 myotube width (μm) when the cells are monocultured and co-cultured with SH-SY5Y in optimal conditions (control) and at different concentrations of RA. No significant differences were found across all samples. No significant differences between the average values were assessed using ANOVA statistical analysis. Results are shown as average \pm SD, $n=12$.

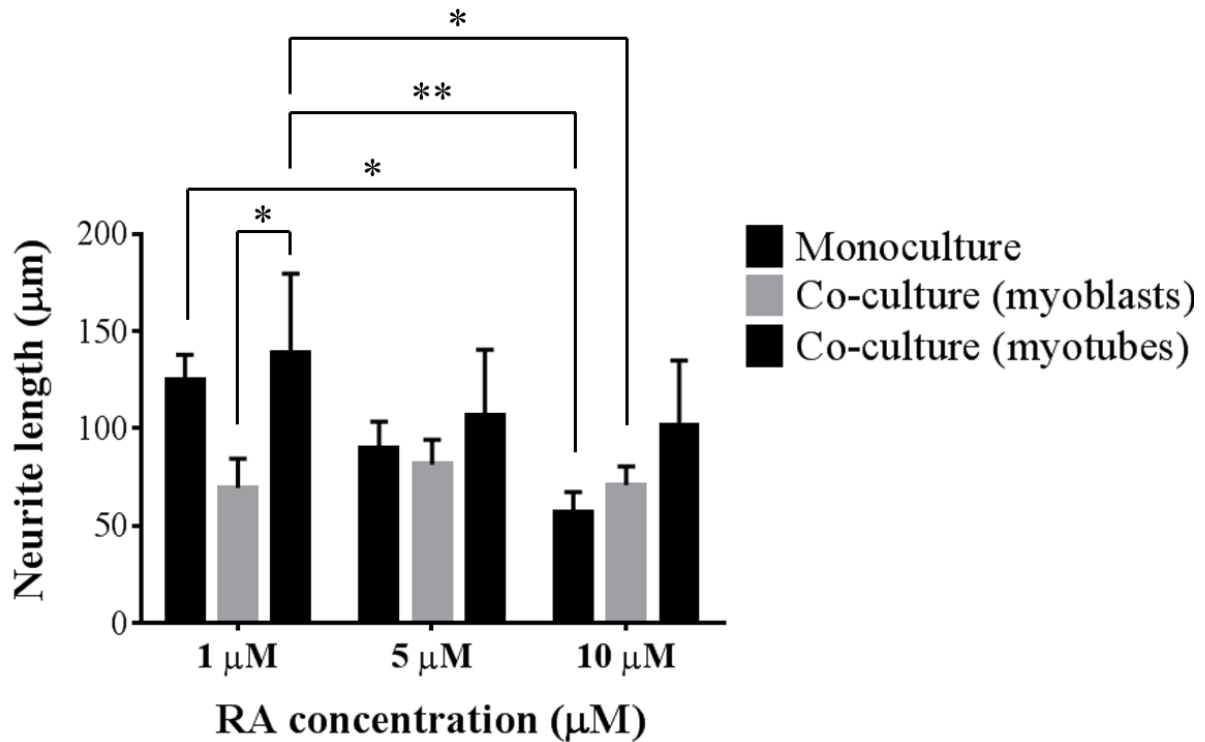


Figure 3.5. SH-SY5Y neurite length (μm) when the cells are monocultured and co-cultured with myoblasts and myotubes at different concentrations of RA. Asterisks indicate significant differences between samples: * = $p \leq 0.05$, ** = $p \leq 0.01$. Significant differences between the average values were assessed using ANOVA and the Bonferroni post-hoc test. Results are shown as average \pm SD, $n=12$.

3.4.2 C2C12 and SH-SY5Y interactions: co-localisation of acetylcholine receptors and synaptic vesicle 2

After establishing the composition of the NDM used for C2C12/SH-SY5Y co-cultures, the presence of AChR's on C2C12 myotubes and SV-2 positive vesicles on SH-SY5Y was investigated. This analysis allows the identification of pre- and post-synaptic markers which are physiologically interacting to form a NMJ *in vivo*, thus giving us an insight on the markers which are directly involved in NMJ formation. First, the presence of AChR's on differentiated C2C12 was verified by using α -Bungarotoxin (BTX) as an immunostaining marker. The cells showed clusters of AChR's after 3, 5 and 7 days in MDM (**Figure 3.6**).

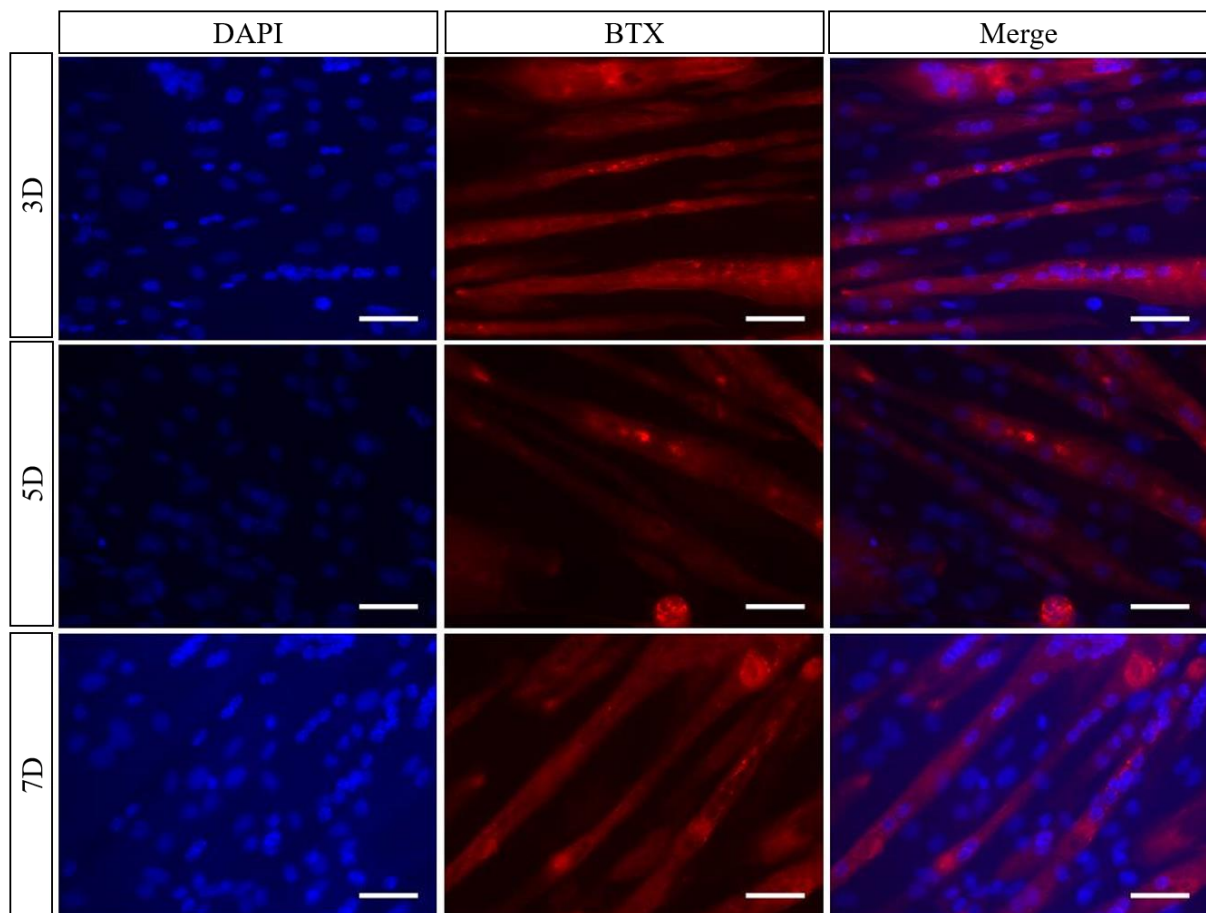


Figure 3.6. AChR's are expressed on C2C12 differentiated for 3 (3D), 5 (5D) or 7 (7D) days in MDM. The cells were fixed and immunostained: texas red-conjugated α -Bungarotoxin (BTX, red) was used for AChR clusters and nuclei were counterstained with DAPI (blue). Scale bars: 50 μ m.

The morphology of the myotubes was not stained, so the less intensively stained red areas were considered as background of the BTX immunostaining. A high magnification image (**Figure 3.7**), shows the receptors after 5 days in MDM with the arrows highlighting them. Subsequently, the co-culture was immunostained with BTX and anti-SV-2. SH-SY5Y were positively stained by SV-2 when co-cultured with C2C12 and C2C12 retained their positivity to BTX staining in the co-culture (**Figure 3.9**). SH-SY5Y projected SV-2-positive neurites towards C2C12 myofibres (**Figure 3.8**). In sporadic areas there was overlap between BTX and SV-2-positive areas, which may indicate co-localisation of the two markers, and therefore muscle-nerve interaction. These co-localisation spots appeared yellow and can be seen in **Figure 3.9**.

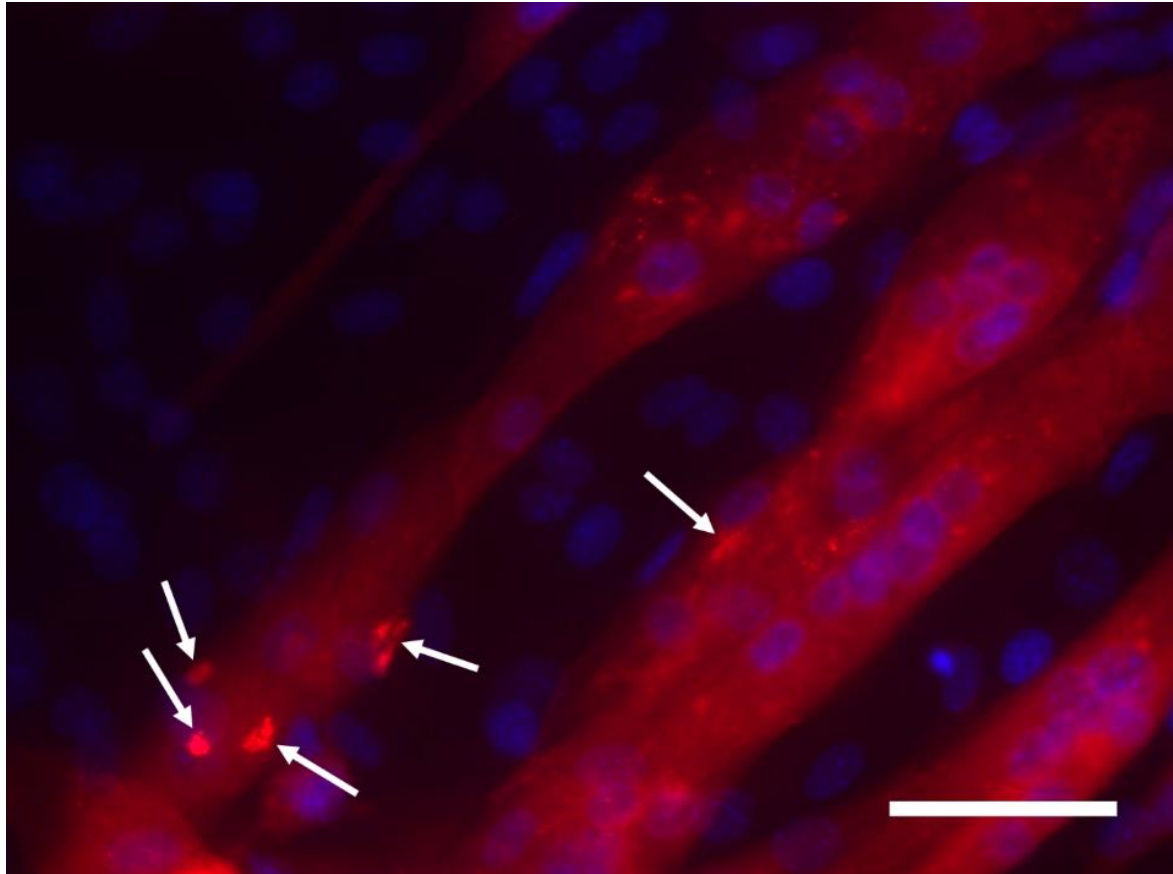


Figure 3.7. Detail of AChR's on the surface of C2C12 myotubes after 5 days of differentiation. The cells were fixed and immunostained: texas red-conjugated α -Bungarotoxin (BTX, red) was used for AChR clusters and nuclei were counterstained with DAPI (blue). The arrows highlight AChR clusters. Scale bar: 25 μ m.

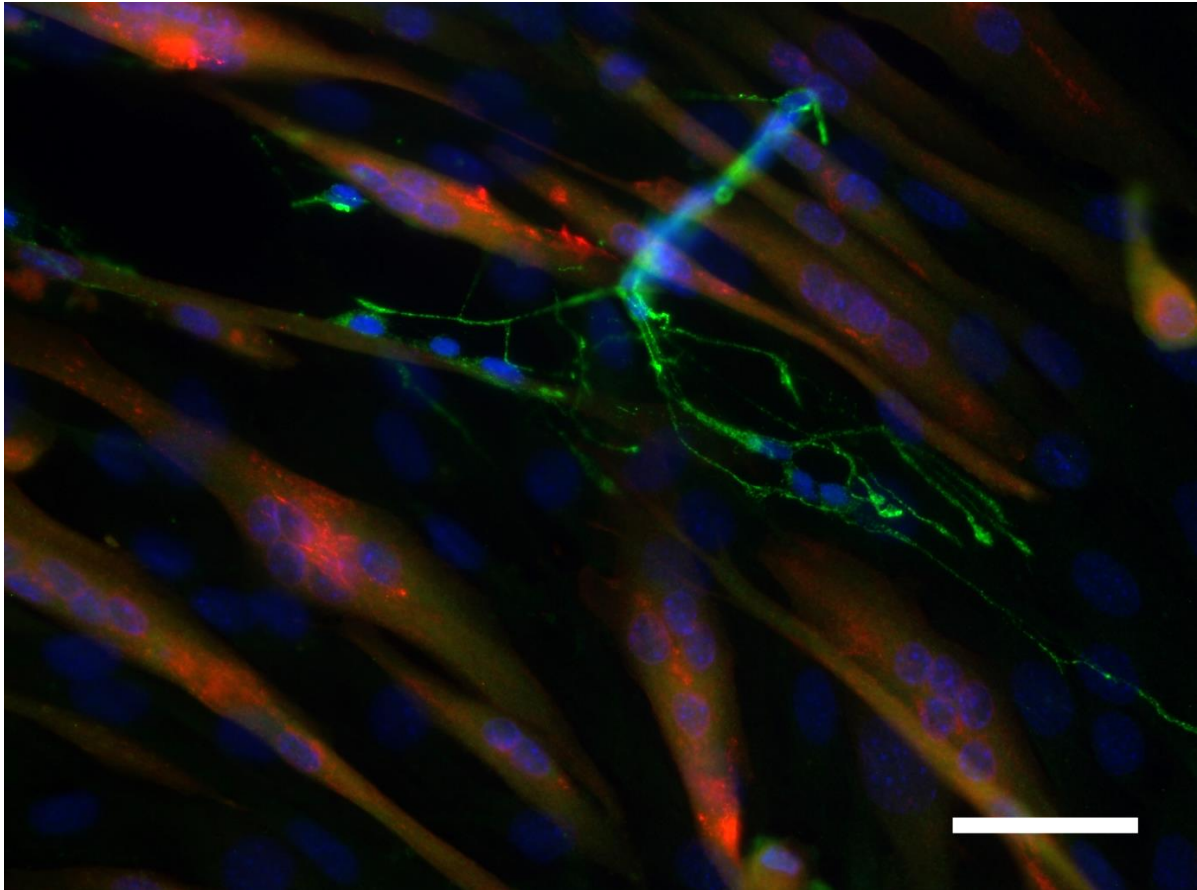


Figure 3.8. C2C12 and SH-SY5Y express pre- and post-synaptic structures in monolayer cocultures. The cells were fixed and immunostained with pre- and post-synaptic markers: texas red-conjugated α -Bungarotoxin (BTX, red) was used for AChR clusters, synaptic vesicle 2 (SV-2) was used for ACh-releasing vesicles in SH-SY5Y cells (green) and nuclei were counterstained with DAPI (blue). Scale bar: 50 μ m.

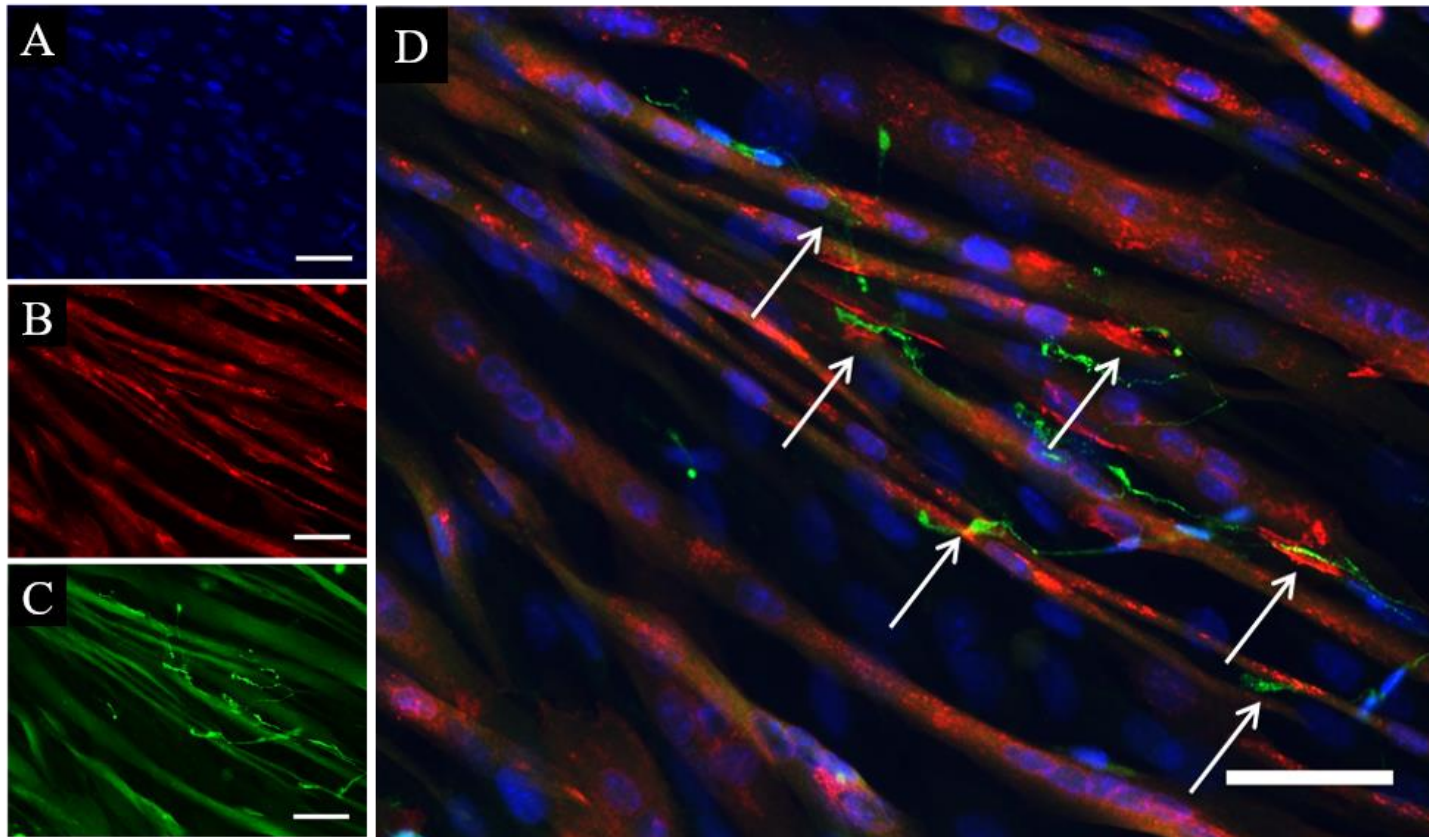


Figure 3.9. C2C12 and SH-SY5Y cells interact and AChR's and SV-2 colocalise. The cells were fixed and immunostained for pre- and post-synaptic markers: texas red-conjugated α -Bungarotoxin (BTX, red) was used for AChR clusters (B), synaptic vesicle 2 (SV-2) was used for ACh-releasing vesicles in SH-SY5Y cells (green, C) and nuclei were counterstained with DAPI (blue, A). The arrows in the merged picture (D) highlight the co-localisation of the two markers, which appeared yellow. Scale bars: 50 μ m.

3.4.3 The addition of agrin did not affect myotube width and muscle maturity

Agrin was added to NDM to both C2C12 in monoculture and in co-culture with SH-SY5Y. The rationale behind adding this compound to the differentiation stage was to increase AChR's clustering and enhance interactions between pre- and post-synaptic proteins (Smith, 2012). As outputs, the myotube width was measured, and the expression of 8 genes was tested to investigate muscle maturity across all conditions. The genes of interest were MyoD, MyoG and Myosin Heavy Chain (MyHC) 1, 2, 3, 4, 7 and 8. These were considered as they represent different stages of development (from embryonic to post-natal) and types of muscle fibres, thus providing important information on the maturity of the muscle.

In terms of morphology, agrin did not appear to influence neither C2C12 in monoculture or C2C12 and SH-SY5Y in co-culture (**Figure 3.10**). The cells differentiated in all conditions, forming myotubes which did not differ in terms of myotube width (**Figure 3.11**), although a slight increase in myotube width was observed when C2C12 were co-cultured with SH-SY5Y, instead of monocultured in control conditions.

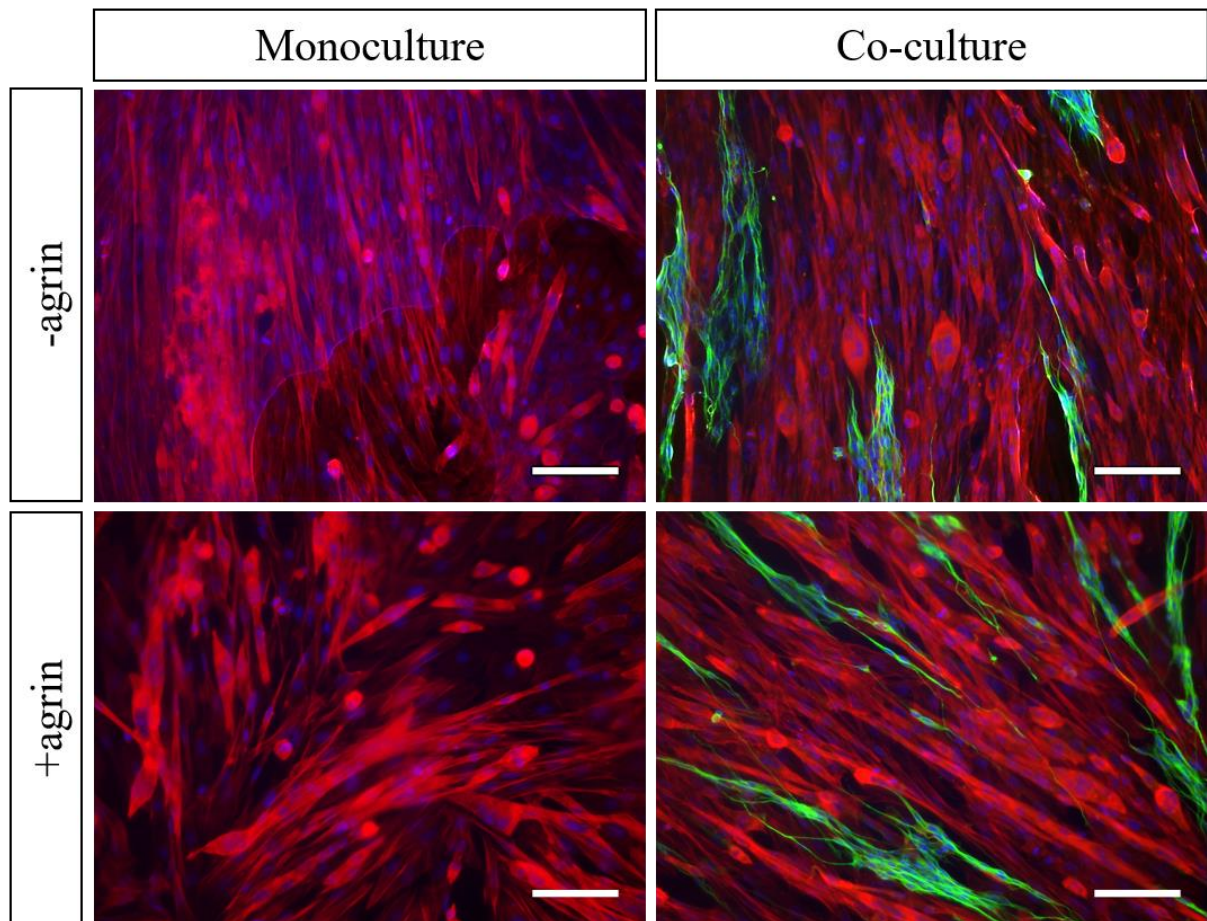


Figure 3.10. Morphological immunostaining of C2C12 monocultures and co-cultures with SH-SY5Y, in the presence or absence of agrin. The cells were fixed and immunostained for morphological markers: actin filaments were stained with rhodamine phalloidin (red), SH-SY5Y cytoskeleton was stained with β -III Tubulin (green) and nuclei were counterstained with DAPI (blue). Scale bars: 100 μ m.

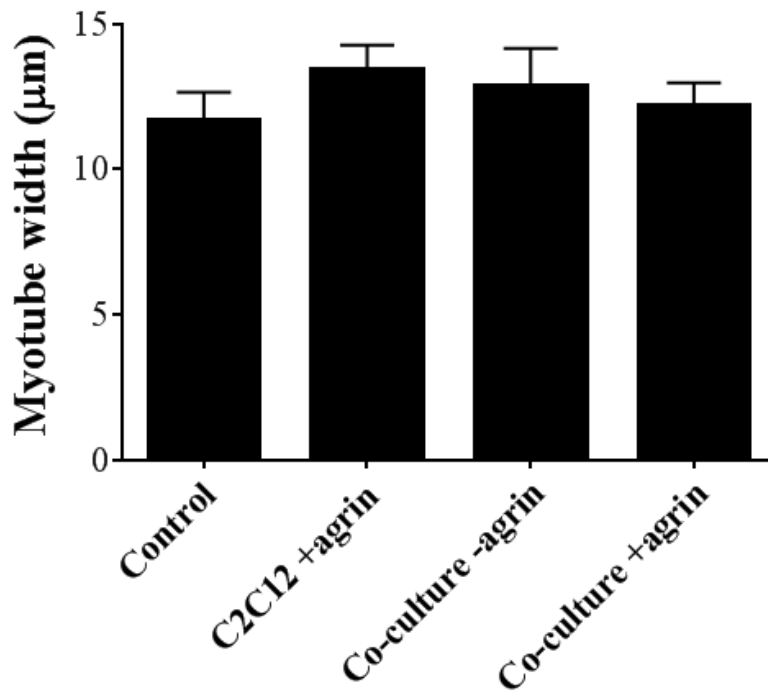


Figure 3.11. Myotube width of C2C12 in monoculture and co-culture, with or without agrin. The width of the myotubes was measured in control conditions (control, C2C12 monoculture without agrin), C2C12 monoculture with agrin, C2C12/SH-SY5Y co-culture without agrin and C2C12/SH-SY5Y co-culture with agrin. Student's t-Test did not reveal statistical difference across mean values. Results are shown as average \pm SD, n=6.

The immunostaining for AChR's was performed on C2C12 monocultures and an increase in the number of clusters was observed (**Figure 3.12**), but not quantified. The interaction immunostaining was performed to identify differences in the presence or absence of agrin, in the co-culture. Although AChR's were marked by BTX, the SV-2 immunostaining appeared aspecific, as it bound to the myotubes too, which appeared yellow/green instead of black/red. No interaction was recorded, but proximity of neurites and AChR's was observed.

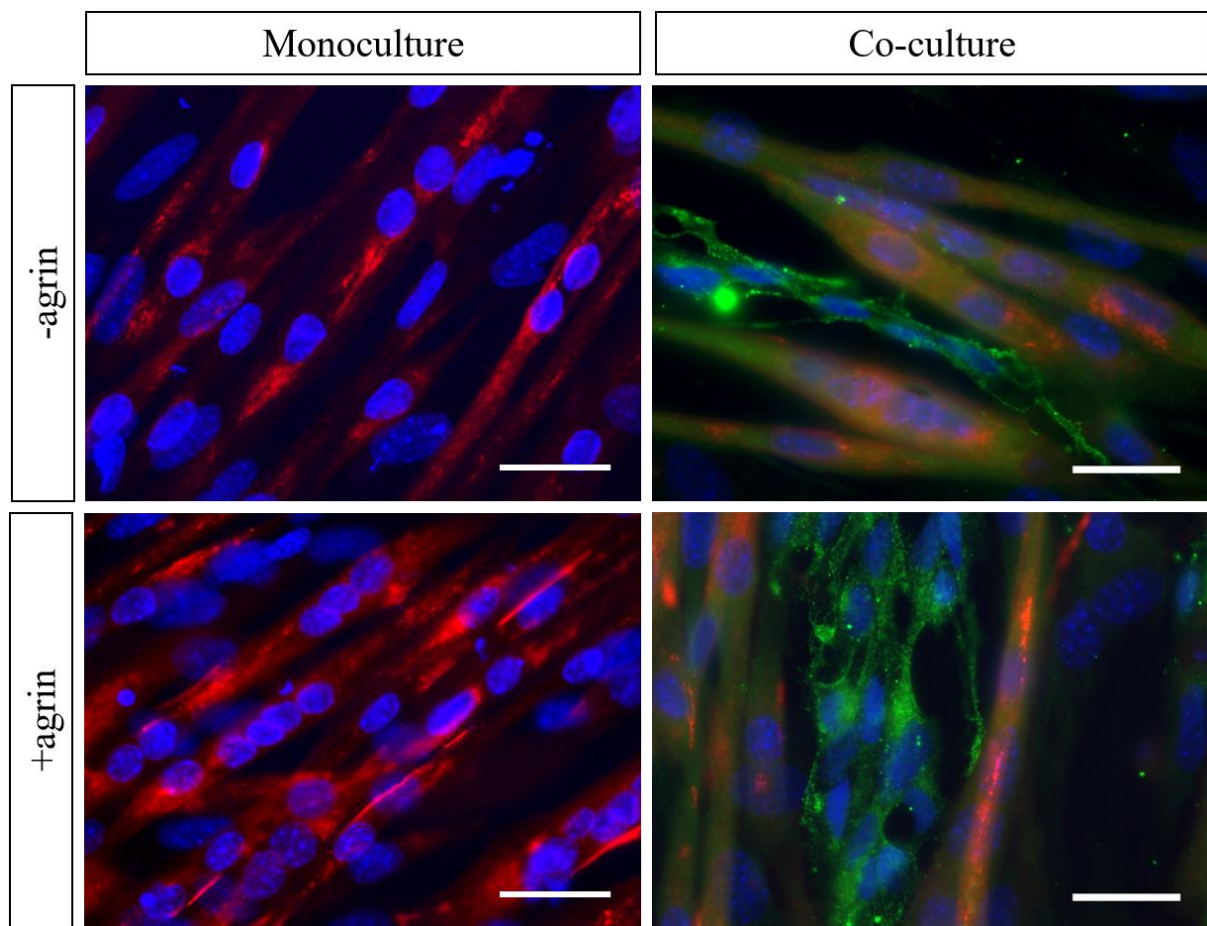


Figure 3.12. Interaction staining C2C12 myotubes in monoculture in the absence or presence of agrin, and in co-culture with SH-SY5Y in the presence or absence of agrin. The cells fixed and immunostained to highlight pre- and post-synaptic markers: AChR's were identified on C2C12 using texas red-conjugated α -Bungarotoxin (BTX, red), synaptic vesicle 2 on SH-SY5Y (SV-2) were stained in green, and nuclei were counterstained with DAPI (blue). Scale bars: 25 μ m.

Gene expression analysis of MyoD (**Figure 3.13**), MyoG (**Figure 3.14**), MyHC3 (**Figure 3.14**), MyHC8 (**Figure 3.15**), MyHC7 (**Figure 3.16**), MyHC1 (**Figure 3.18**) and MyHC2 (**Figure 3.19**) was investigated. Significant differences were found in MyoG expression between the monoculture +agrin and the co-culture +agrin ($p=0.037$), in MyHC3 between the monoculture +agrin and the co-culture+agrin ($p=0.006$). Differences were also observed in MyHC8 expression, between the monoculture +agrin and the co-culture -agrin ($p=0.04$), and the monoculture +agrin and the co-culture +agrin ($p=0.016$).

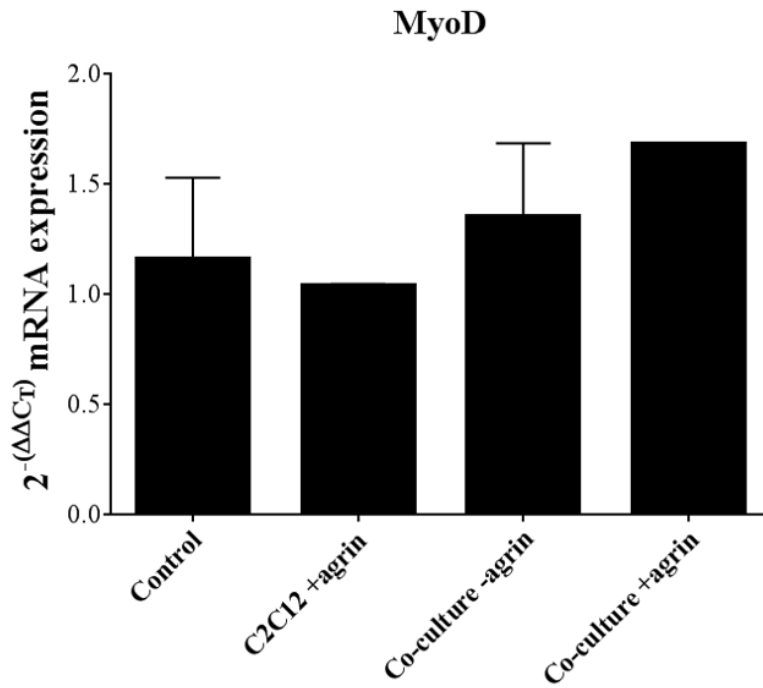


Figure 3.13. MyoD (development) mRNA expression in C2C12 cultured in different conditions. Control conditions (control, C2C12 monoculture without agrin), C2C12 monoculture with agrin (C2C12+agrin), C2C12/SH-SY5Y co-culture without agrin (co-culture -agrin) and C2C12/SH-SY5Y co-culture with agrin (co-culture +agrin). Student's t-Test did not reveal statistical difference across mean values. Results are shown as average \pm SD, n=6.

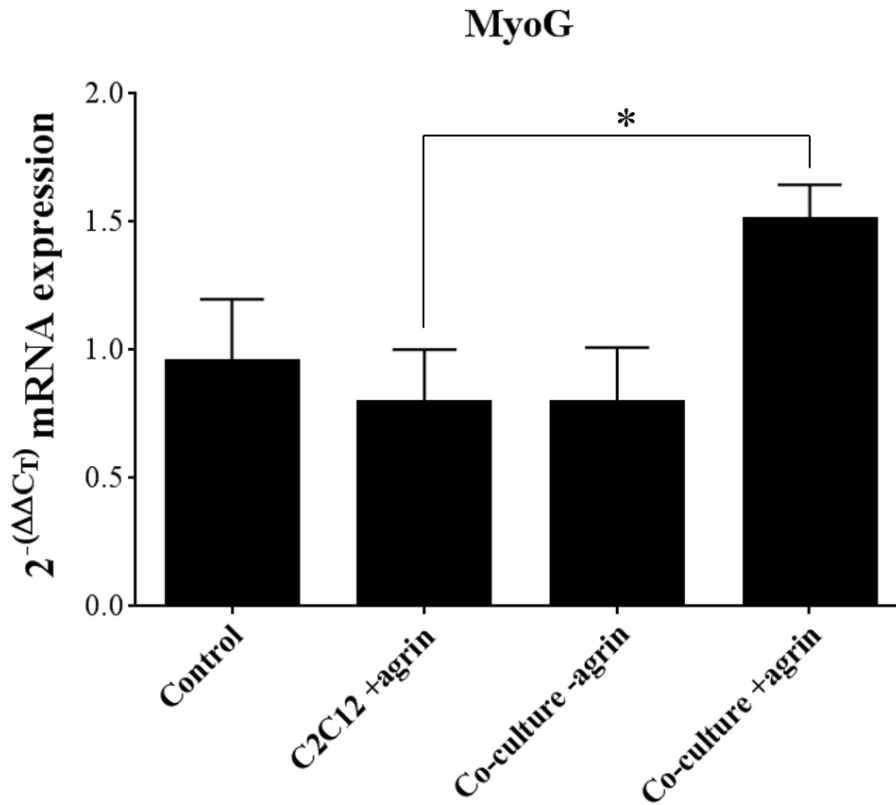


Figure 3.14. MyoG (development) mRNA expression in C2C12 cultured in different conditions. Control conditions (control, C2C12 monoculture without agrin), C2C12 monoculture with agrin (C2C12 + agrin), C2C12/SH-SY5Y co-culture without agrin (co-culture - agrin) and C2C12/SH-SY5Y co-culture with agrin (co-culture + agrin). Asterisks show significant difference between samples: * = $p \leq 0.05$. The statistical analysis was done using Student's t-Test. Results are shown as average \pm SD, n=6.

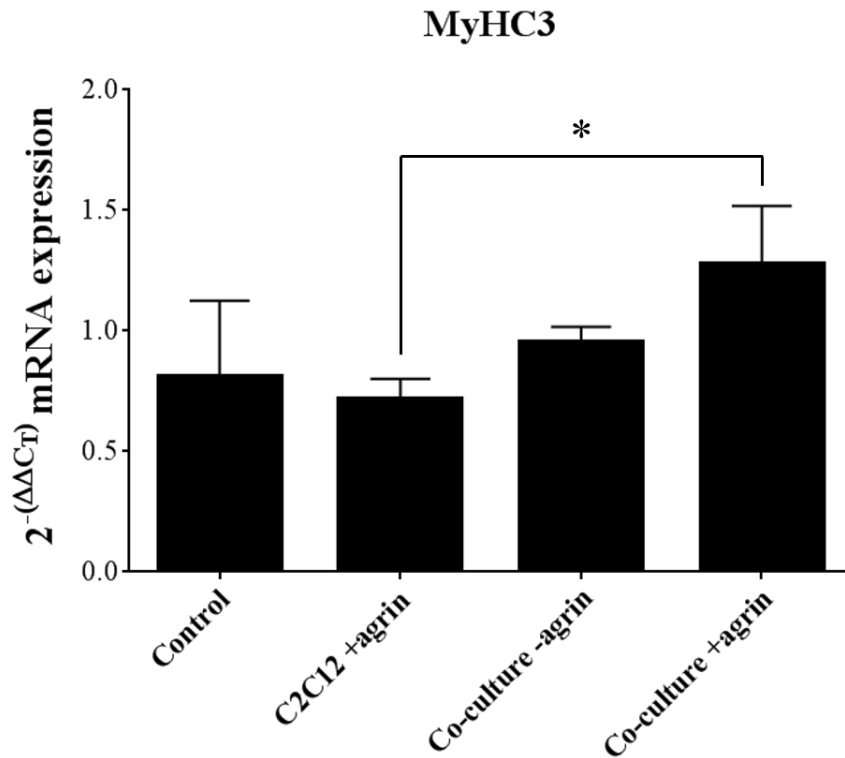


Figure 3.15. MyHC3 (embryonic) mRNA expression in C2C12 cultured in different conditions. Control conditions (control, C2C12 monoculture without agrin), C2C12 monoculture with agrin (C2C12 + agrin), C2C12/SH-SY5Y co-culture without agrin (co-culture - agrin) and C2C12/SH-SY5Y co-culture with agrin (co-culture + agrin). Asterisks show significant difference between samples: * = $p \leq 0.05$. The statistical analysis was done using Student's t-Test. Results are shown as average \pm SD, n=6.

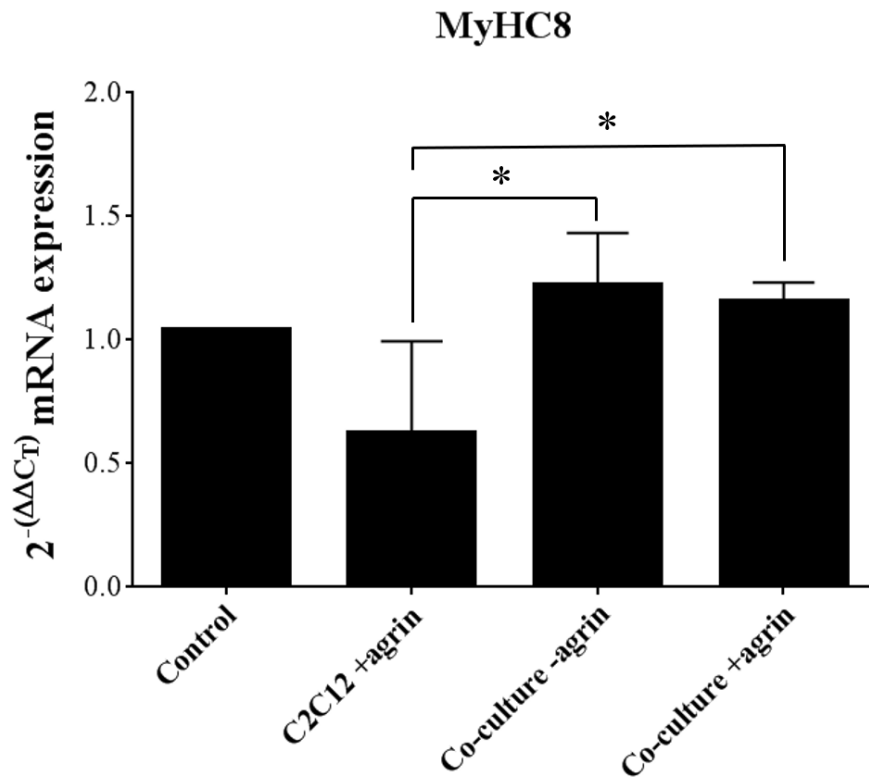


Figure 3.16. MyHC8 (neonatal) mRNA expression in C2C12 cultured in different conditions. Control conditions (control, C2C12 monoculture without agrin), C2C12 monoculture with agrin (C2C12 + agrin), C2C12/SH-SY5Y co-culture without agrin (co-culture - agrin) and C2C12/SH-SY5Y co-culture with agrin (co-culture + agrin). Asterisks show significant difference between samples: * = $p \leq 0.05$. The statistical analysis was done using Student's t-Test. Results are shown as average \pm SD, n=6.

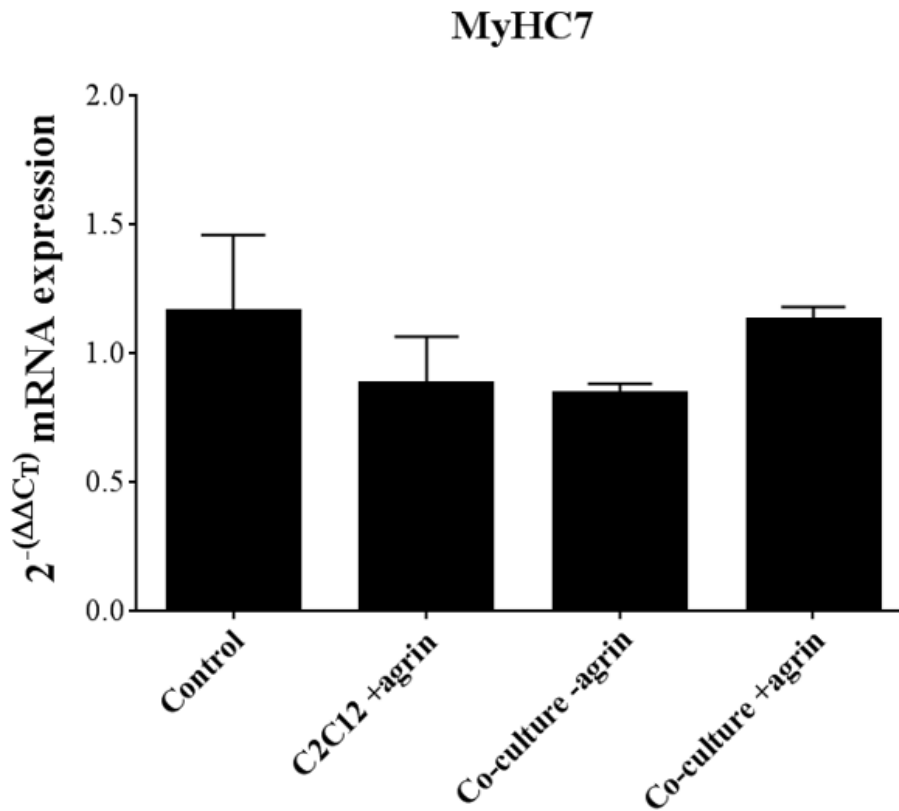


Figure 3.17. MyHC7 (slow) mRNA expression in C2C12 cultured in different conditions. Control conditions (control, C2C12 monoculture without agrin), C2C12 monoculture with agrin (C2C12 + agrin), C2C12/SH-SY5Y co-culture without agrin (co-culture - agrin) and C2C12/SH-SY5Y co-culture with agrin (co-culture + agrin). Student's t-Test did not reveal statistical difference across mean values. Results are shown as average \pm SD, n=6.

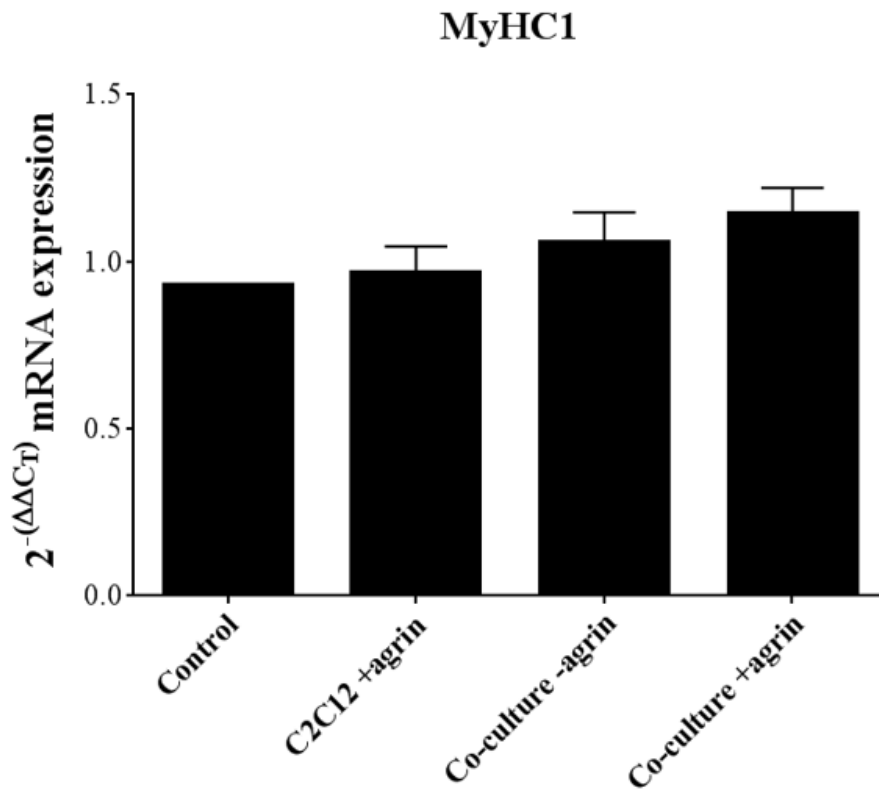


Figure 3.18. MyHC1 (fast) mRNA expression in in C2C12 cultured in different conditions. Control conditions (control, C2C12 monoculture without agrin), C2C12 monoculture with agrin (C2C12 + agrin), C2C12/SH-SY5Y co-culture without agrin (co-culture - agrin) and C2C12/SH-SY5Y co-culture with agrin (co-culture + agrin). Student's t-Test did not reveal statistical difference across mean values. Results are shown as average \pm SD, n=6.

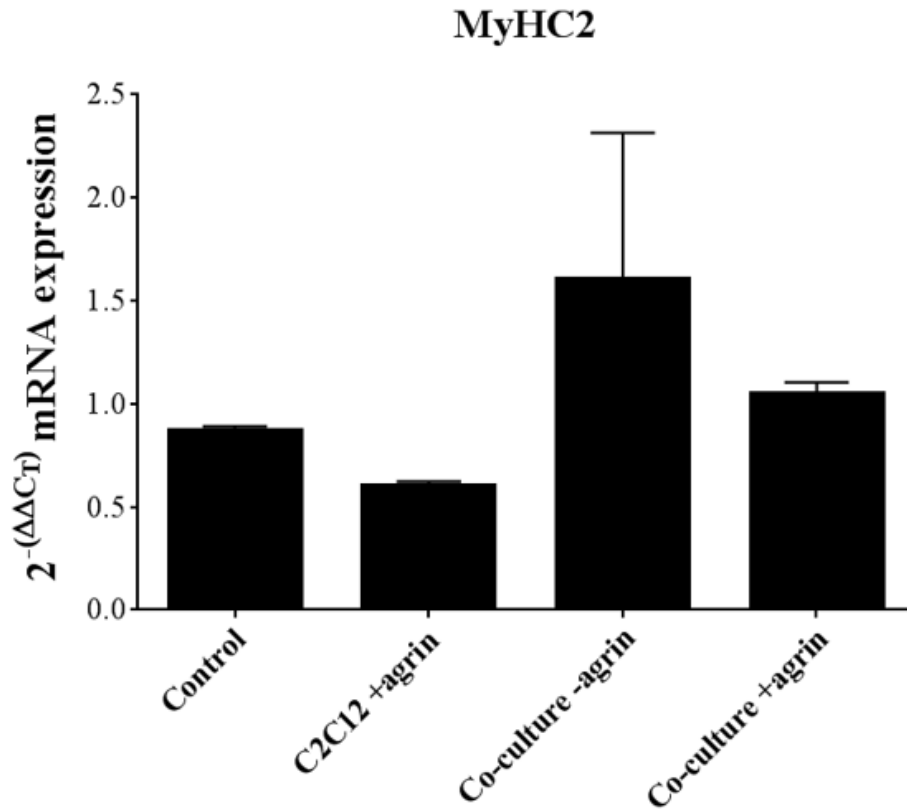


Figure 3.19. MyHC2 (fast) mRNA expression in C2C12 cultured in different conditions. Control conditions (control, C2C12 monoculture without agrin), C2C12 monoculture with agrin (C2C12 +agrin), C2C12/SH-SY5Y co-culture without agrin (co-culture -agrin) and C2C12/SH-SY5Y co-culture with agrin (co-culture +agrin). Asterisks show significant difference between samples: * = $p \leq 0.05$. Student's t-Test did not reveal statistical difference across mean values. Results are shown as average \pm SD, n=6.

3.5 Discussion

Establishing the conditions to co-culture different cell types is essential and represents a bottom-up approach whereby a tissue is gradually developed *in vitro* (Goers et al., 2014). Muscle-nerve co-cultures can provide scientists with information regarding the behavior of cells in a more complex environment, as well as laying the grounds for further analysis. Utilising cell lines to achieve this is a faster, cheaper and more reproducible fashion to perform preliminary studies, compared to primary cells. Limitations which are typical of primary cells, such as variability and cell number do not represent an issue when using cell lines. Furthermore, the use of a chimeric co-culture whereby murine muscle is cultured with human neurons represents a progression *versus* animal only co-cultures, implementing the ‘reduction, refinement and replacement’ approach that is vastly being embraced in nowadays’ research (<https://www.nc3rs.org.uk/the-3rs>).

3.5.1 A concentration of 1 μ M RA ensures both C2C12 and SH-SY5Y differentiation

C2C12 and SH-SY5Y cells require different culture conditions when cultured independently from one-another. Therefore, the medium compatibility results presented in this chapter determined a suitable differentiation protocol for both C2C12 and SH-SY5Y. In particular, C2C12 fuse into multinucleated myotubes when the serum concentration is reduced or totally removed (Burattini et al., 2004; Sharples et al., 2012), and/or when the species from which the serum is derived, changes (Manabe et al., 2012). On the other side, to promote neurite extension and induce a cholinergic phenotype in SH-SY5Y, the use of RA is required (Clagett-dame et al., 2006; Encinas et al., 2000; Hong-rong et al., 2010). Since the effect of RA on myogenesis is unclear (Xiao et al., 1995b; Zhu et al., 2010), testing different concentrations was used as an approach to determine what amount of RA promoted differentiation in both cell types, without causing muscle atrophy or hindering neuronal extension. Three doses of RA were investigated in this work, 1, 5 and 10 μ M, based on previous work where 1 μ M (Korecka et al., 2013) and 10 μ M (Påhlman et al., 1995; Presgraves et al., 2004) were used to induce a cholinergic phenotype. However, this data has not been compared within a single study. The results indicated that C2C12 monocultures differentiated in all conditions, without showing a statistical difference between the control (gold standard muscle differentiation medium) and the neuronal differentiation medium supplemented with RA. The presence of SH-SY5Y in culture did not significantly impact the width of the myotubes, although an increase in mean

value was observed at 1 and 10 μM . The measurement of SH-SY5Y neurite length was on cells which were monocultured and co-cultured both with undifferentiated C2C12 (myoblasts) and differentiated C2C12 (myotubes). A lower seeding density was used to prevent C2C12 from fusing into myotubes, therefore providing us with additional information. A trend in decreasing neurite length was observed when the concentration of RA was enhanced. The concentration reported in the literature to induce cholinergic differentiation of SH-SY5Y is 10 μM (Påhlman et al., 1984) and was therefore used as an initial control. In this work, neurite extension was obtained at all concentrations, but the neurite length was higher when the RA concentration was lower. Neurite extension is a determining factor for the contact between MNs and SkM fibres. Although it was not reported what the “standard” neurite length of differentiated SH-SY5Y should be, it was interesting to observe that the presence of myotubes in culture had an increasing effect on neurite length, compared to the neuronal monoculture. The longest neurites were observed in C2C12/SH-SY5Y co-cultures differentiated in 1 μM RA. This suggests that this concentration not only does not affect the size of the myotubes compared to the standard control, but allows projection of neurites which are essential for the cells to interact with one another. In conclusion, neuronal differentiation medium (NDM) supplemented with 1 μM RA was used for further C2C12/SH-SY5Y co-cultures.

3.5.2 NMJ formation between C2C12 and SH-SY5Y: finding a needle in a haystack

Immunostaining observations of C2C12 and SH-SY5Y co-cultures revealed that neurites typically extended in proximity of myotubes. This may indicate that the maturation of the muscle attracted neuronal extensions towards them. In order to determine whether the cells express pre- and post-synaptic proteins, specific co-localisation staining was performed. AChR's on the surface of C2C12 cells were found after 3, 5 and 7 days of differentiation in standard MDM. Following the co-culture protocol optimised in the first part of this chapter, C2C12 and SH-SY5Y were co-cultured for 5 days in NDM supplemented with 1 μM RA. As a result, C2C12 in co-culture with SH-SY5Y were also positive to AChR's-specific immunostaining (BTX). In addition, the neurons were positively stained by a marker for SV-2, the vesicles responsible for the release of ACh. Thin SV-2-positive neuronal projections were seen running alongside and projecting towards cultured myotubes, and are believed to indicate neurite growth in close proximity of AChR-expressing SkM cells (**Figure 3.8** and **Figure 3.9**). This outcome is comparable to what was previously observed (Smith, 2012). Although it was frequently observed that pre- and post-synaptic markers were in proximity of

one-another, the incidence of the co-localisation of AChR's and SV-2 was rare. A 3D culture, although more complex, could provide both cell types with a more physiologically-relevant niche. This could enhance the frequency at which these co-localisations appear, as reported in a similar work (Smith, 2012). The lack of directionality that is intrinsic in monolayer cultures did not promote organization of two cell types, which can be achieved by using patterned surfaces or 3D constructs (Pardo-Figueres, 2017; Tong et al., 2014).

3.5.3 Agrin enhanced muscle maturity in co-cultures, and decreased it in monocultures

Treatment of muscle cells with agrin has been previously shown to improve levels of post-synaptic patterning, characterised by a significant increase in clusters of AChR's on myotube membranes (Henriquez et al., 2008). The localisation of AChR clusters on the myotubes' surface requires the expression of agrin, which maintains the molecular architecture of the post-synaptic membrane (McConville and Vincent, 2002). The role of agrin is to stabilise the AChR's, prevent them from dispersing across the myotubes, and initiating the cascade of events which lead to the formation of a NMJ (Witzemann, 2006). The effect of agrin on C2C12 monocultures and C2C12/SH-SY5Y co-cultures was addressed in this work in order to determine whether this compound would have been necessary or not for the formation of a NMJ in 2D and, subsequently, in 3D. The addition of agrin did not appear to increase the interactions between C2C12 and SH-SY5Y, but it had some effect on the expressions of SkM-related genes. MyoD and MyoG are expressed during SkM development and regeneration (Brown et al., 2012; Schiaffino et al., 2015). Their levels decreased in the monoculture, from the control to the addition of agrin. In the co-culture, the levels of mRNA increased upon the addition of agrin, but these changes were non-significant. A similar trend was observed for MyoG, where agrin decreased its expression in the monoculture and increased in the co-culture. This time, the difference between the monoculture with agrin and the co-culture with agrin, was significant, indicating that the presence of the neurons and the agrin treatment encouraged muscle maturation. MyHC's expressed in mouse during the early stages of development are MyHC3 (embryonic), MyHC8 (neonatal) and MyHC7 (slow fibres) (Brown et al., 2012; Schiaffino et al., 2015). Although the addition of agrin did not significantly influence the expression of MyHC7, the co-culture did play a role in MyHC3 and MyHC8. The addition of agrin in the co-culture enhanced MyHC3 expression when compared to the monoculture +agrin. Since MyHC3 is the earliest heavy chain expressed during embryonic development and

regeneration (Brown et al., 2012), these results suggest that the treatment with agrin promoted development both in mono and in co-cultures. As for MyHC8, if compared to C2C12 monocultures with or without agrin, an increase in gene expression was observed, although it was only significant if compared to the monoculture with agrin. Finally, post-natal MyHC1 and MyHC2, which encode for fast fibres, were not influenced by the presence of agrin or the addition of SH-SY5Y to the culture. Although agrin is generally utilised in muscle-nerve co-cultures (Flanagan-Steet et al., 2005; Guo et al., 2011), it did not represent a determining factor in the maturation of C2C12. Observations of BTX-stained myotubes did not lead to include agrin in future 3D co-cultures, particularly considering that these co-cultures were firstly established using the chimera C2C12/SH-SY5Y.

Despite the observation of some changes in gene expression when adding agrin to the culture, an increase by 1 or 2 fold was not considered biologically relevant to justify the use of an additional compound in the culture in 3D. Indeed, the use of agrin was not perpetuated in the 3D cultures reported in the following chapter. It was hypothesised that the 3D environment and the potential to stimulate the constructs (mechanically, electrically or using drugs), could enhance cell-cell interactions and facilitate NMJ formation, rather than the addition of agrin.

3.6 Chapter summary

The work conducted in this chapter established successful muscle-nerve co-cultures using cell lines. C2C12, a widely used murine myoblast line, were co-cultured with the human neuroblastoma line SH-SY5Y. Optimisation of the differentiation conditions lead to the definition of a medium which can be used for further cultures in 3D tissue engineered constructs. This chimeric co-culture is a step forward from the mouse-mouse co-cultures reported in the literature, as the source of neurons was human. Even though working with cell lines includes several advantages (*i.e.* low cost of cells and reagents, high availability, high reproducibility, non-necessity for surface coatings), some limitations can also be highlighted. First, there is a possibility that different species may have played a role in the low number of interactions observed in the co-cultures, when AChR's and synaptic vesicles were immunostained. In addition, since SH-SY5Y may include different kinds of neurons, the cholinergic population will be lower than the one found in primary MNs. Despite that, these cells were previously found to be cholinergic if differentiated in the presence of RA, therefore representing a valid candidate for muscle-nerve human co-cultures, where no animal models

are used and a readily available source of human MNs is still not available. The addition of agrin to the culture was tested to investigate its role on the expression of muscle maturation markers and the clustering of AChR's. Although some significant differences were found, the increase in gene expression was no larger than two times the baseline value, thus not justifying the addition of another component to the co-culture medium.

Muscle and neurons require a complex matrix to be physiologically relevant and functionally active. Therefore, the use of tissue engineered constructs may provide the cells with a more suitable environment for NMJ formation. The preliminary studies carried out in this chapter were essential to establish the co-culture conditions in terms of medium composition, seeding density and timing. Tissue engineered constructs were extensively used in our laboratory for SkM culture (collagen gels) and SkM/MNs co-culture (fibrin gels). Information on morphology, cell distribution, cell-cell interaction and functionality can be obtained and will be a crucial aspect when establishing a primary human co-culture in 3D. Furthermore, training is required when using such constructs, which would be cheaper and more quickly completed with cell lines. The C2C12/SH-SY5Y co-culture will be briefly carried out in 3D in the following chapter.

4 C2C12 & SH-SY5Y CO-CULTURE: FROM 2D TO 3D

4.1 Introduction

Tissue engineering has been defined as “an interdisciplinary field that applies the principles of engineering and life sciences toward the development of biological substitutes that restore, maintain or improve function or a whole organ” (Nerem, 1992). Using tissue engineering as a tool for the development of an *in vitro* model would allow for the generation of a pre-clinical platform, alongside the use of animal models (or potentially, in the future, completely substituting them). Matrices of various types resemble the *in vivo* microenvironment more closely than monolayer cultures do (Edmondson et al., 2014), and therefore it is important to have a representative 3D (three dimensional) system which mimics human tissues. Within the field of tissue engineering, various tissues have been cultured in closed systems that allow nutrient and waste exchange while providing the cells with a 3D environment to grow in (Langer and Vacanti, 1993). Skeletal muscle (SkM) is a highly organised tissue (Gillies and Lieber, 2012), which features aligned fibres that must be achieved in 3D cultures. Biomaterials of different kinds can be utilised to guide SkM reorganisation, acting as a matrix in which cells can grow three-dimensionally, and mediating the delivery of bioactive factors or therapeutics in a controlled fashion (Qazi et al., 2015). Constructs such as using porous scaffolds, hydrogels, fibrous meshes and patterned substrates were used to culture SkM (Qazi et al., 2015). Among hydrogels, widely used ones are collagen gels (Passey et al., 2011; Player et al., 2014; Sharples et al., 2012; Smith et al., 2016), fibrin gels (Martin, 2012; Martin et al., 2015, 2013), combinations of collagen and Matrigel® (Powell et al., 2002), and collagen and alginate (Bach et al., 2004). Each of these constructs is suitable for SkM tissue engineering due to their biocompatibility and support role for the growth and differentiation of SkM *in vitro*. Besides a 3D environment and a construct which allows for the generation of aligned structures, the use of such gels can resemble *in vivo* tissues. Therefore, great importance is given to the suitability of 3D constructs for functional studies. External *stimuli* which enhance muscle maturation and contraction, such as mechanical (Goldspink et al., 1992; Noah et al., 2002; Tatsumi et al., 2001; Vandeburgh and Kaufman, 1979) and electrical stimulation (Dusterhoft and Pette, 1990; Wehrle et al., 1994) can be reproduced in tissue engineered constructs. These systems are important because SkM is an adaptable tissue which responds to conditions such as mechanical stress, physical activity, availability of nutrients and growth factors (Sandri, 2008). Thus, these

models could be used to understand the mechanisms behind the formation of the NMJ and how these are disrupted in pathological situations

The 3D tissue engineering constructs (collagen and fibrin gels) used in our laboratory were described in sections 1.4 of this thesis. The advantage of using these types of hydrogels *versus* polymeric scaffolds, is that they are highly biocompatible, being made out of the same constituents of SkM's extracellular matrix (ECM). Collagen is the main component in SkM (Alberts et al., 2002). In particular, collagen type I is mainly found in the perimysium, the ECM layer which surrounds groups of muscle cells (Gillies and Lieber, 2012); collagen type III is mainly found in epimysium (around the whole muscle) and endomysium (around single muscle cells). Other collagen subtypes are part of SkM's ECM. Collagen type IV makes up the basement membrane with smaller amounts of type VI, XV and XVIII. Although other components are present (proteoglycans, glycosaminoglycans, glycoproteins and matrix remodelling enzymes) (Gillies and Lieber, 2012), the abundance of collagen in SkM's ECM makes such constructs particularly suitable for supporting SkM growth and differentiation *in vitro*. The high collagen content required by muscle cells and intrinsic in the preparation of collagen constructs, together with the similar stiffness of fibrin gels to native muscle, make these constructs suitable for SkM tissue engineering. On the other hand, a suitable matrix for neuronal cultures should be made of other ECM proteins such as laminin or fibronectin.

Another crucial aspect of 3D cultures is being able to simulate basic functions and the electrical impulse coming from peripheral motor neurons (MNs) *in vitro*. This represents a powerful tool for physiology and pathophysiology studies. For instance, mechanical loading replicates physiological contraction and exercise *in vitro*, and has been shown to enhance myotube width and force generation (Powell et al., 2002) and the co-culture of primary rat muscle and MNs significantly increased spontaneous muscle twitching compared to muscle alone (Martin et al., 2015). Supporting both cell types within the construct is essential to enable matrix remodelling and cell-cell interactions. While collagen represents a valuable candidate for SkM culture, surfaces for neuronal 2D and 3D outgrowth can be based on collagen, fibrin and fibronectin (Alovskaya et al., 2007). Primary neurons require surface modifications or coatings such as poly-D-lysine/fibronectin or poly-D-lysine/laminin to adhere (Smith et al., 2013), as well as complex matrices (e.g. Matrigel®) (Yi et al., 2018). Therefore, establishing the 3D culture conditions for both SkM and MN differentiation is essential.

All in all, developing a stable 3D model of the NMJ is crucial to support the integration of multiple cell types in a more complex environment than the one found in 2D cultures, allowing for studies on cell-cell and cell-matrix interactions.

4.2 Aims & objectives of the chapter

Following the optimisation of the C2C12/SH-SY5Y co-culture in monolayer carried out in Chapter 3, this chapter focusses on the culture of these cell lines in 3D tissue engineered constructs. Utilising these cell lines provided important information on the cell-cell and cell-matrix interactions and also the set up the conditions used for the successful co-habiting of both cell types. Engineering the co-culture in collagen- and fibrin-based matrices enables the characterisation of muscle-nerve cells in a complex environment and can be used for functional studies or as a platform for drug testing. Achieving this co-culture aims to underpin how both cell types coexist in different types of materials, providing us with essential information on how the presence of the neurons may or may not affect muscle maturity, matrix remodelling or spontaneous muscle twitching. Finally, this chapter sets the grounds for engineering 3D cultures of human primary cells.

The aims for this chapter were:

- Culturing and differentiating C2C12 and SH-SY5Y cells in fibrin and collagen gels;
- Increasing matrix remodelling when SH-SY5Ys are added to the gels;
- Facilitating NMJ formation using tissue engineered constructs.

The objectives for this chapter were:

- To utilise immunofluorescent staining to observe the morphology and distribution of C2C12 and SH-SY5Y cells in collagen and fibrin constructs;
- To measure the gels width as an indication of the matrix remodelling performed by the cells and identify a difference when neurons are added;
- To measure C2C12 myotube width in the absence of presence of neurons

4.3 Materials & Methods

4.3.1 Co-culture in fibrin gels

The co-culture of SH-SY5Y and C2C12 in fibrin gels was carried out following the procedure described in 2.2.2. C2C12 myoblasts were expanded for 4 days in muscle growth medium (MGM), then SH-SY5Y cells were seeded on top of the gel in neuronal growth medium (NGM) and left to adhere for 15 minutes, before filling up the culture chamber with NGM. The following day, the medium was switched to neuronal differentiation medium (NDM) for a further 7 days. The gels which were used for the co-culture were chosen at the very beginning of the culture, in order to obtain unbiased results.

4.3.2 Co-culture in 500 μ L collagen gels

The co-culture in 500 μ L collagen gels was carried out following the procedure described in 2.2.3. C2C12 myoblasts were expanded for 4 days in MGM, then SH-SY5Y cells were seeded on top of the gel in NGM and left to adhere for 15 minutes, before filling up the culture chamber with NGM. The following day, the medium was switched to NDM for a further 7 days. The gels which were used for the co-culture were chosen at the very beginning of the culture, in order to obtain unbiased results.

4.3.3 Morphological staining of 3D constructs: phalloidin and β -III Tubulin

The morphological staining using rhodamine phalloidin for actin filaments and β -III Tubulin for the neuronal structure, was performed as described in 2.3.1.4 and 2.3.1.5. The only differences are the fixing process (2.3.1.2) and the fact that the antibodies were incubated for 3 hours instead of 2.

4.3.4 Statistical analysis

The data from the myotube width analysis was presented as average \pm SD. Statistical analysis was performed using the GraphPad Prism 6.0 software. An F-Test was used to determine if the variances of the two populations were equal. Then, the statistical difference between control and co-culture gel deformation, and the myotube width in control and co-culture gels were verified using an unpaired t-Test.

4.4 Results

4.4.1 C2C12 & SH-SY5Y co-culture in fibrin gels

Fibrin gels were used to co-culture C2C12 and SH-SY5Y cells in 3D. To do this, C2C12 were seeded within the fibrin matrix at day 0, and expanded in MGM until day 4. Then, SH-SY5Y were seeded in NGM on top of the gel, and the day after the medium was changed to NDM, based on the media optimisation carried out in Chapter 3.

C2C12 myoblasts were successfully monocultured in fibrin-based constructs. The cells differentiated into aligned myotubes, which can be seen in **Figure 4.1**. Over time, the gels width decreased in size as C2C12 remodeled the matrix, both in absence and presence of SH-SY5Y (**Figure 4.2**).

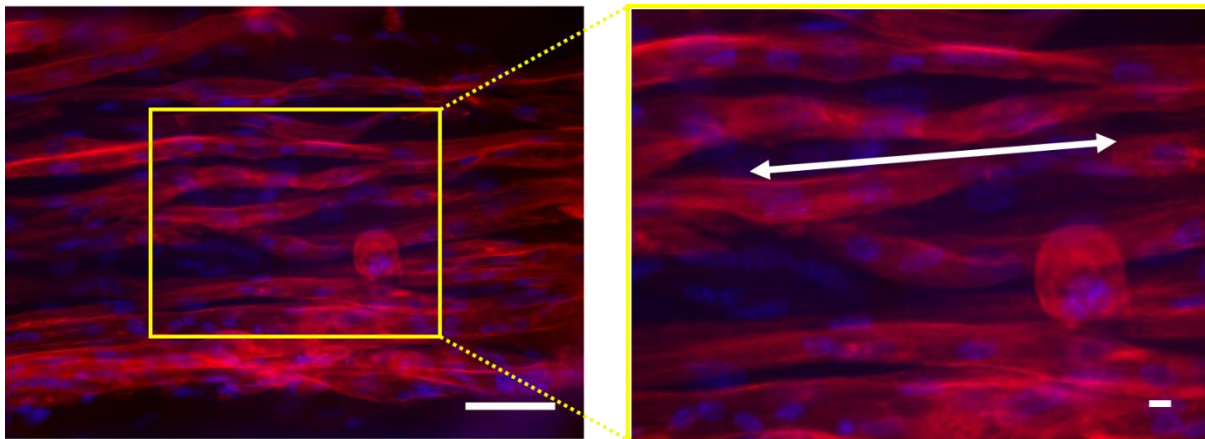


Figure 4.1. C2C12 myoblasts differentiate into myotubes in fibrin gel constructs. The gels were fixed and immunostained with morphological markers: actin filaments were stained with rhodamine phalloidin (red) and nuclei were counterstained with DAPI (blue). The arrow shows the alignment of the cells. Scale bars: 50 μm .

Quantitative analysis of the width of the gels revealed that this decreased at day 5, when the control gels were exposed to MDM for 24h and SH-SY5Y were seeded on co-culture gels. Control gels contracted more than co-culture gels, but the difference was not found to be significant. Further deformation was observed at the end of the culture (day 14), showing comparable values between control and co-culture gels (**Figure 4.3**).

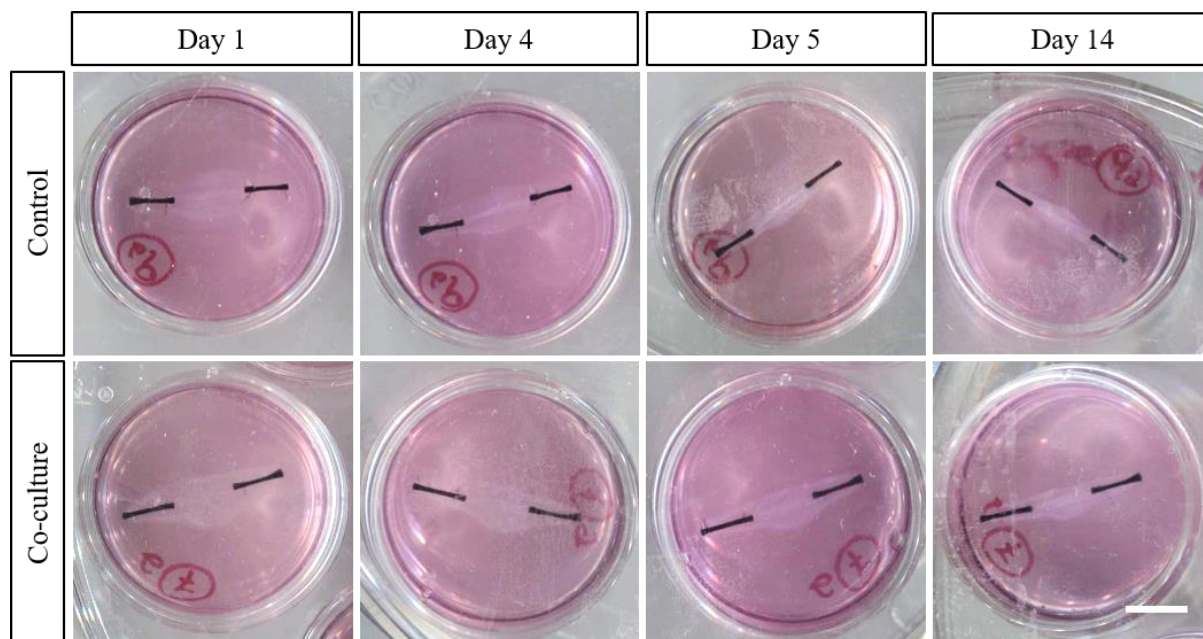


Figure 4.2. Fibrin gels deformation over time in control conditions (C2C12 monoculture) and C2C12/SH-SY5Y co-culture. Scale bar: 1 cm.

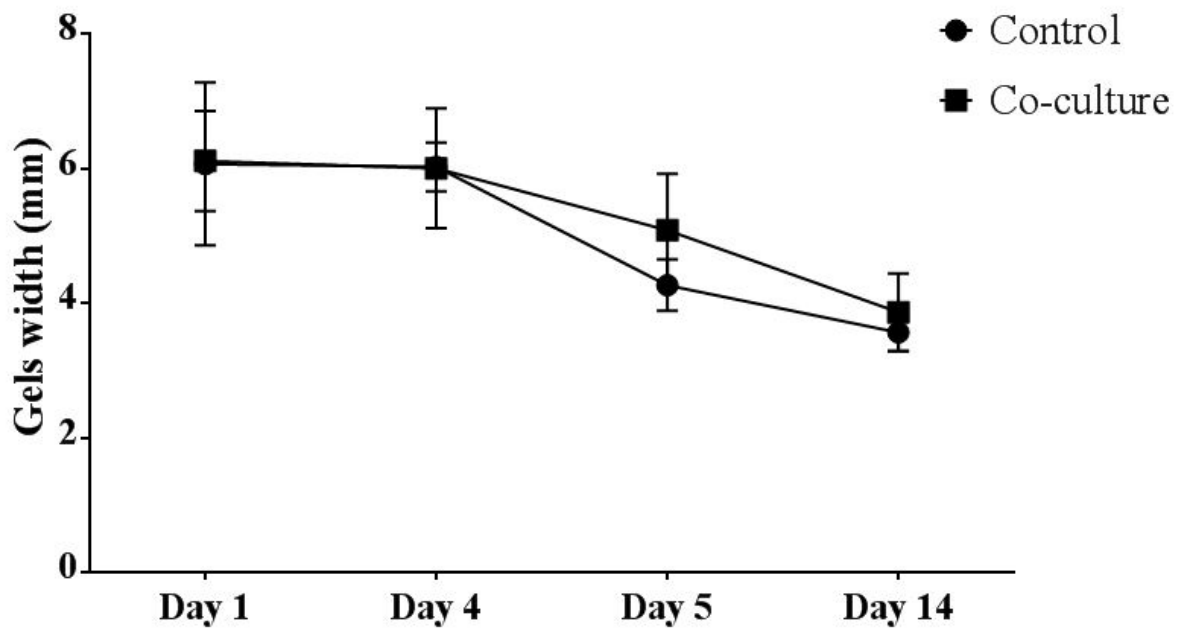


Figure 4.3. Fibrin gels deformation. Each gel was measured in the middle three times, and then averaged. Such values were then averaged to the other gels to obtain a final value. No difference was observed between control and co-culture gels using the Student's t-Test. Results are shown as average \pm SD, n=3.

From a cell distribution point of view, it was interesting to observe that SH-SY5Y seeded at day 4 differentiated extending neurites along the same direction as the myotubes, as highlighted by the arrows in **Figure 4.4**. The alignment was quantified and is reported in the supplementary section (**Table S9.1**). Both cell types coexisted until the end of the culture period (14 days) and in all co-culture gels certain features were observed. Firstly, although the seeding density was the same for C2C12 and SH-SY5Y, the neurons did not appear to be adhering to the matrix, or proliferate, as the amount found upon immunostaining the gels was limited. In fact, the neurons were seeded on top of the gel, whereas C2C12 were embedded in the matrix from day 0, as myoblasts require physical interactions to fuse into myotubes, and it was hypothesised that the presence of SH-SY5Y could have impaired this process. This resulted in a lower number of neurons at the end of the culture, although not quantified, possibly due to the lower amount of days that the neurons spent in growth medium (4 days for C2C12, 1 day for SH-SY5Y). The growth period was not prolonged because SH-SY5Y continue to proliferate in NDM and the remaining days in culture were necessary for the muscle to differentiate too. In addition, SH-SY5Y neurites formed into bundles, rather than extending in isolation on the gel (**Figure 4.5**).

The measurement of the width of myotubes in the gels revealed no difference between control and co-culture conditions (**Figure 4.6**). While in 2D the presence of the neurons influenced myotube width by increasing it (Chapter 3), in fibrin gels this was not observed. However, it is important to highlight that besides being in a 3D matrix which differs from 2D cultures, fibrin gels also require an additional compound. Aminocaproic acid (AA) must be added to the growth and differentiation stage to retain muscle cells from degrading the matrix, and this may have influenced the myotube width in 3D. Further work may be carried out to understand the effect of SH-SY5Y on C2C12 within a 3D tissue engineered construct. Gene expression analysis and functional work were not carried out on these gels, but interesting information may arise from these investigations.

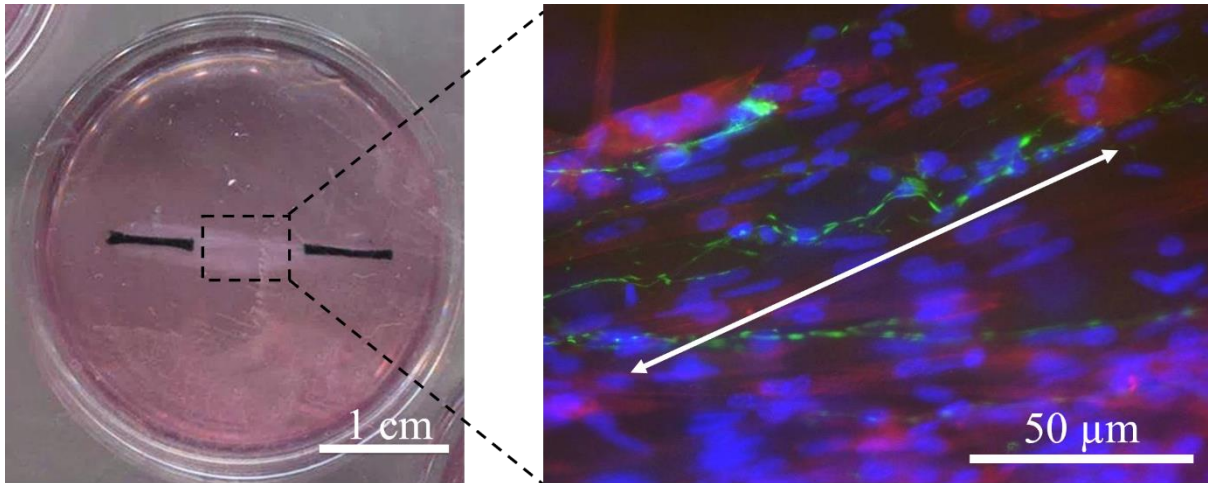


Figure 4.4. C2C12 and SH-SY5Y co-culture in fibrin gel constructs. The gels were fixed and immunostained with morphological markers: actin filaments were stained with rhodamine phalloidin (red), SH-SY5Y cytoskeleton was stained with β -III Tubulin (green) and nuclei were counterstained with DAPI (blue). The arrow shows the alignment of the cells.

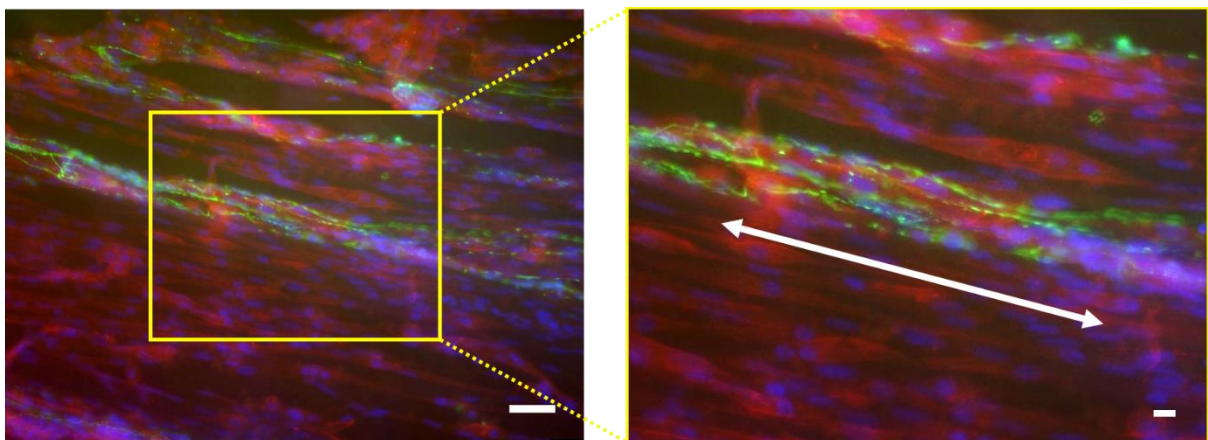


Figure 4.5. Bundles of SH-SY5Y on fibrin gel constructs. The gels were fixed and immunostained with morphological markers: actin filaments were stained with rhodamine phalloidin (red), SH-SY5Y cytoskeleton was stained with β -III Tubulin (green) and nuclei were counterstained with DAPI (blue). Scale bars: 50 μ m.

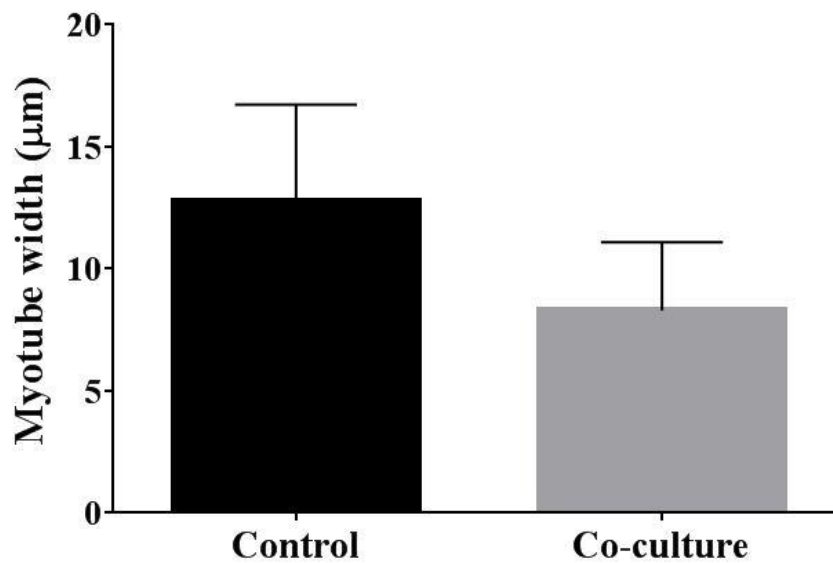


Figure 4.6. Myotube width of C2C12 cells monocultured in fibrin gels (control), and co-cultured with SH-SY5Y cells (co-culture). No significant differences were found between control and co-culture conditions using the Student's t-Test. Results are shown as average \pm SD, n=3.

4.4.2 C2C12 & SH-SY5Y co-culture in 500 μ L collagen gels

C2C12 myoblasts seeded in collagen gels differentiated into aligned myotubes, as shown in **Figure 4.7**. The presence of muscle cells within the matrix caused it to decrease in width over time (**Figure 4.8**) both in C2C12 monocultures and in C2C12/SH-SY5Y co-cultures. The co-culture did not have an effect on the gel width, as shown in **Figure 4.9**.

For the setup of the co-culture, the same experimental setup as fibrin gels was utilised. SH-SY5Y seeded on the surface of the constructs extended neurites along the axis of the anchor points, suggesting that they either followed the alignment of C2C12 embedded in the gel, or the tension generated by the two fixed points (**Figure 4.10**). Also for these constructs, the alignment was quantified and is reported in the supplementary section (**Table S9.1**). Quantification of the number of neurites on the gels, and the neurite extension was not carried out because of imaging limitations. In fact, the neurites present were bundled up similarly to

what was observed in the fibrin gels (**Figure 4.5**), therefore making it challenging to discern how many cells adhered on the gels and how to analyse neurite length.

Like in fibrin gels, the measurement of myotube width revealed no difference between the C2C12 monoculture and the co-culture with SH-SY5Y (**Figure 4.11**).

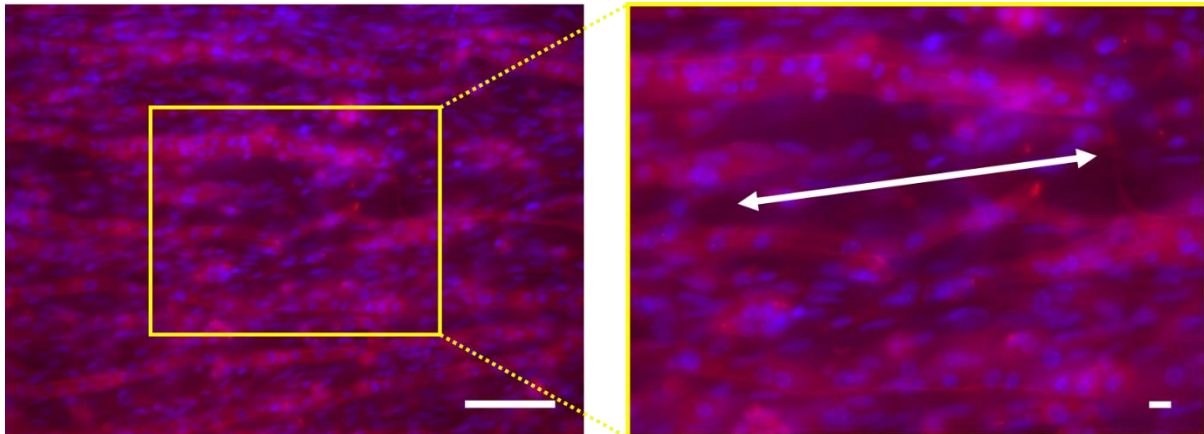


Figure 4.7. C2C12 myoblasts differentiate into myotubes in collagen gel constructs. The gels were fixed and immunostained with morphological markers: actin filaments were stained with rhodamine phalloidin (red) and nuclei were counterstained with DAPI (blue). The arrow shows the alignment of the cells. The gels were fixed and stained for morphological markers: rhodamine phalloidin (red) and DAPI (blue). Scale bars: 100 μm .

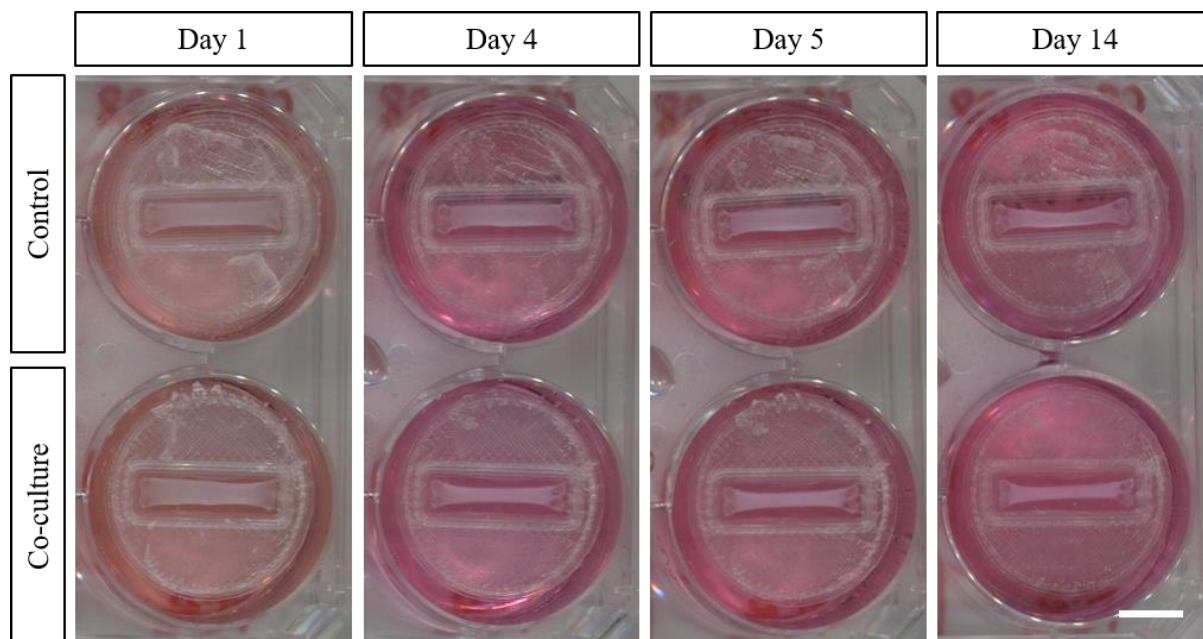


Figure 4.8. Collagen gels deformation over time in control conditions (C2C12 monoculture) and C2C12/SH-SY5Y co-culture. Scale bar: 1 cm.

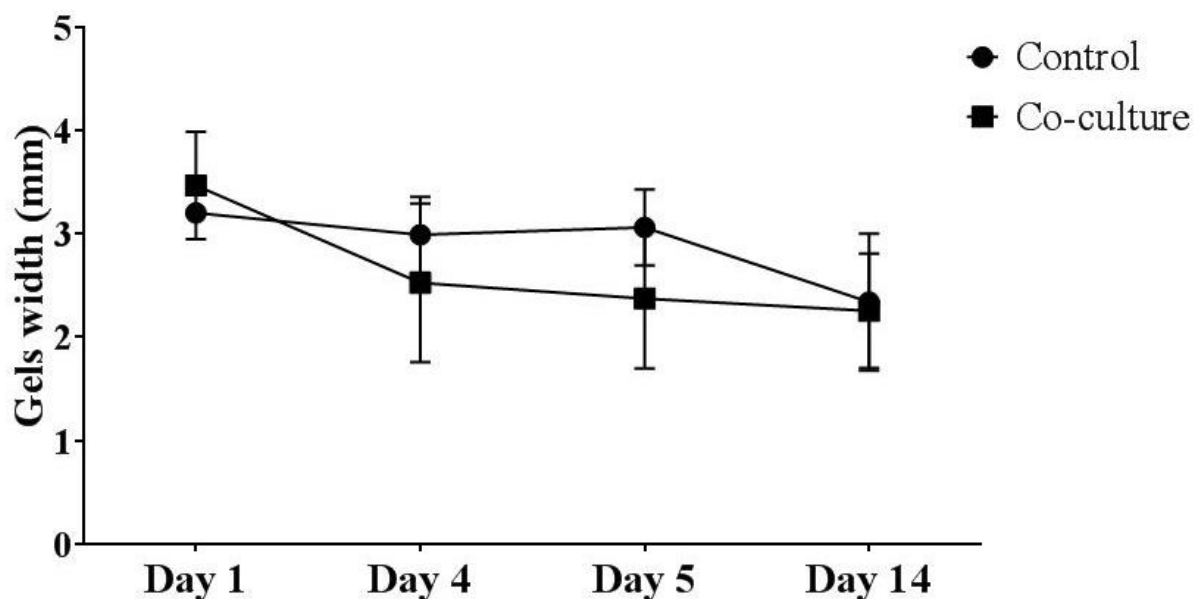


Figure 4.9. Collagen gels deformation. Each gel was measured in the middle three times, and then averaged. Such values were then averaged to the other gels to obtain a final value. No difference was observed between control and co-culture gels using the Student's t-Test. Results are shown as average \pm SD, n=4.

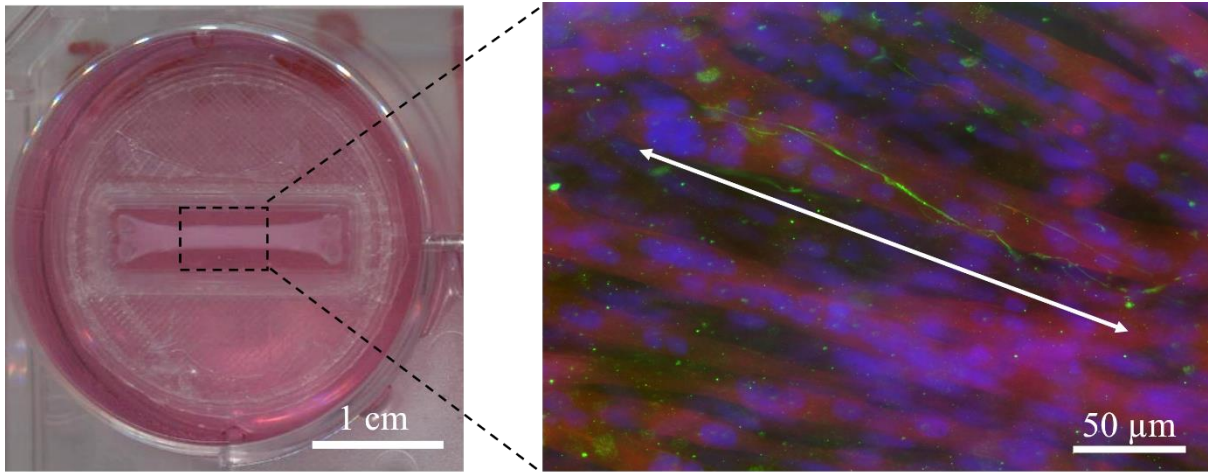


Figure 4.10. C2C12 and SH-SY5Y co-culture in 500 μL collagen gel constructs. The gels were fixed and immunostained with morphological markers: actin filaments were stained with rhodamine phalloidin (red), SH-SY5Y cytoskeleton was stained with β -III Tubulin (green) and nuclei were counterstained with DAPI (blue). The arrow shows the alignment of the cells.

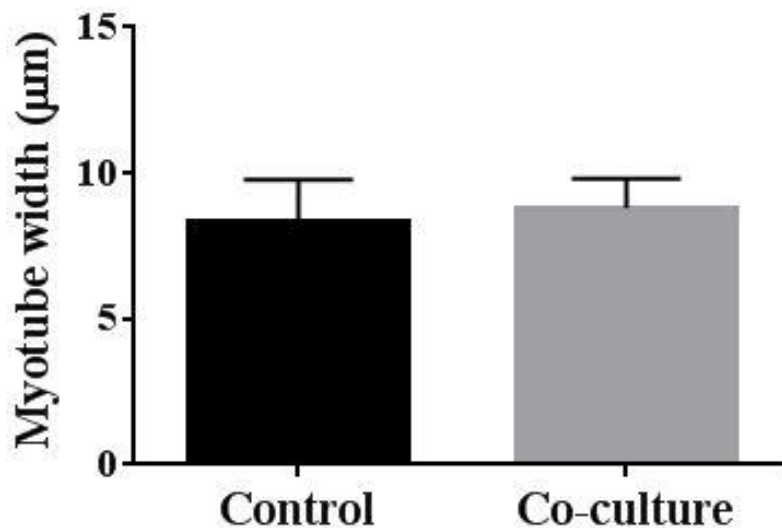


Figure 4.11. Myotube width of C2C12 cells monocultured in 500 μL collagen gels (control), and co-cultured with SH-SY5Y cells (co-culture). No significant differences were found between control and co-culture conditions when using the Student's t-Test. Results are shown as average \pm SD, $n=4$.

4.5 Discussion

The generation of 3D tissues *in vitro* which are physiologically relevant for biomedical studies is increasing. This approach is a promising tool to investigate development, as well as physiological and pathophysiological processes, whilst resembling the *in vivo* architecture (Dixon et al., 2018; Ostrovidov et al., 2014). The native cellular microenvironment comprises cell-cell and cell-matrix interactions which are not closely reproduced in 2D models (Griffith and Swartz, 2006; Kalman et al., 2015; Lund et al., 2009), therefore making 3D tissue engineered constructs a valuable platform for the development of *in vitro* models, which can be utilised for disease modelling, drug testing and functional studies (Dixon et al., 2018).

4.5.1 C2C12 & SH-SY5Y differentiate and align in fibrin gel constructs

Muscle-nerve co-cultures were previously reported in 3D constructs (Morimoto et al., 2013). In this work, the presence of two fixed points at each end of the gel created tension that allowed myotube formation, uniaxial alignment and gel deformation (**Figure 4.1, Figure 4.2, Figure 4.3**). This is in agreement with previous C2C12 cultures in fibrin gels (Khodabukus et al., 2007; Khodabukus and Baar, 2014, 2009) and acts as a fundamental muscle control when establishing co-cultures. Other types of fibrin constructs were reported for the 3D culture of human induced pluripotent stem cell-derived (hiPSC) SkM (Maffioletti et al., 2018), therefore showing that fibrin is a suitable matrix for primary human SkM as well as for the murine cell line used for this work. Fibrin gels were also used as a 3D matrix for the generation of a primary rat NMJ (Martin et al., 2015), but has never been reported with human MNs and human SkM cells.

The abrupt decrease in gel width at day 5 can be attributed to the decrease in serum concentration, both in the control differentiation medium and in the co-culture one. In fact, the cells were exposed to 20% fetal bovine serum (FBS) during the growth phase (day 0 to day 4) and then control gels were immersed in 2% horse serum (HS). The decrease in serum percentage, and the different species (from bovine to horse) is well known to be responsible for C2C12 differentiation (Burattini et al., 2004; Manabe et al., 2012), which may have caused greater gel deformation at the beginning of the differentiation window. Co-culture gels in NGM for 24h showed a lower deformation at day 5, perhaps due to a serum concentration equal to 10% (NFBS). This amount is half of what was used in the growth phase, but higher than the 2% used in the control. In fact, when the medium

was switched to NDM at day 5, the gels width was found to be comparable between control and co-cultures.

Preliminary co-culture work reported in this thesis showed that the human neuroblastoma line SH-SY5Y adhered to the constructs and aligned to the direction of the muscle fibres (**Figure 4.4**). Although single neurites were observed (**Figure 4.4**), it is unsure whether SH-SY5Y spread within the gel or not. The formation of bundles (**Figure 4.5**) on the surface of the construct may suggest that the neurons occupied the available space left by the muscle fibres, or adhered to one-another because they found the environment suboptimal for further neuronal extension. This did not permit the measurement of neurite length allowing comparison with 2D cultures or collagen constructs. In addition, it appeared to be challenging to be compared to the literature, as no co-cultures with these cell types in fibrin-based constructs have been previously reported. The measurement of myotube width represents a method to quantify muscle maturity morphologically, and ensure that the myofibres are not atrophic. SH-SY5Y did not significantly influence this parameter (**Figure 4.6** and **Figure 4.11**). The difference in species may have played a role in hindering the contact between C2C12 and SH-SY5Y since most MNs co-cultures with C2C12 were performed with a murine source of neurons (Morimoto et al., 2013; Tong et al., 2014). It is however interesting to observe that even in primary rat muscle-nerve co-culture carried out in these constructs, MNs did not affect myotube width (Martin et al., 2015). What was affected, was the percentage of striated myotubes, the generated force and the expression of myosin heavy chains 3 and 8 (MyH3, MyH8). These measurements were not acquired for this work due to the fibrinogen batch-to-batch variability, which caused subsequent results to be inconsistent and to an increased amount of gels which failed to set at the very start. Difficulties in using these constructs brought our laboratory to increasingly focus on collagen-based constructs, and to eventually use these for human muscle-nerve co-cultures (see Chapter 6).

4.5.2 C2C12 & SH-SY5Y differentiate and align in 500 μ L collagen gel constructs

Musculoskeletal tissues have been widely generated utilising collagen as a matrix, due to its abundance in SkM (Gillies and Lieber, 2012) in various isoforms. Collagen's high biocompatibility and low immunogenicity, as well as conservation across species, allows for its use for tissue engineering applications (Abou Neel et al., 2006). Previous work with collagen gels was carried out in our laboratory using larger gel volumes (2 mL) and cell numbers (8×10^6

cells/gel) (Player, 2013; Sharples et al., 2012). The setup was different and less reproducible than the more recent 500 μ L gels used in this work, and the greater amount of consumables and cells required represented a disadvantage compared to the smaller gels used for this work. However, the principle remains the same: the presence of anchor points creates tension and causes the myoblasts to differentiate into aligned myotubes (Sakar et al., 2012). The precursors of the tissue engineered constructs used for this work (A. S. T. Smith et al., 2012) were recently investigated in comparison with commercially available polyether ether ketone (PEEK) chambers (Jones et al., 2018). The manuscript revealed that C2C12 morphology and gene expression were comparable between the manufactured model and the custom-built system previously used in our laboratory. However, the matrix remodeling found in PEEK chambers was more consistent. The design of the 500 μ L collagen-based constructs used for this muscle-nerve co-culture resembles the PEEK chambers, therefore representing a much more reproducible system if compared to the old custom-built systems, or fibrin-based gels described above, also less consistent.

C2C12 myoblasts seeded in a type I collagen-based matrix formed aligned myotubes (**Figure 4.7**). Myotube formation was observed upon differentiation in MDM, similarly to what was found within the fibrin constructs (**Figure 4.1**) and previous work (Sharples et al., 2012; Smith, 2012).

Collagen-only based tissue engineered constructs for muscle-nerve co-cultures are not commonly used as they do not facilitate neuronal adherence. Collagen-laminin-coated microfluidic chambers were used to generate a NMJ *in vitro* (Southam et al., 2013), but do not represent a truly 3D model and cannot be compared to the collagen constructs utilised in this work.

When C2C12 and SH-SY5Y were co-cultured in 500 μ L collagen gels, it was challenging to find neurites on the surface of the gel, suggesting poor neuronal adhesion and/or proliferation (**Figure 4.10**). Gel remodeling occurred both in control and co-culture conditions (**Figure 4.8** and **Figure 4.9**), suggesting that this process was mainly dependant on the presence of C2C12 in the gels, rather than C2C12 and SH-SY5Y combined. The presence of the neurons in the gels and the use of a different kind of differentiation medium did not affect myotube width (**Figure 4.11**). Gel deformation (**Figure 4.9**) was observed mainly at the beginning of the culture (from day 0 to day 4) and can be appointed to the matrix remodeling done by C2C12.

At day 4 the neurons were seeded on top of the gels, and greater deformation was observed compared to control gels, although non-significant. Similarly to fibrin-based constructs, the decrease in serum concentration (Manabe et al., 2012) within the differentiation medium used for the co-cultures, may have affected the matrix remodelling process, which was more evident in co-culture conditions. However, this greater remodelling started earlier in the culture as it was already observable at day 4. No significant difference was observed between control and co-culture gels, and at the end of the culture period, these were comparable. Quantification of the neurite length was not performed due to the little amount of neurites observed on the surface of the gel, as seen in **Figure 4.10**. The limited adhesion of SH-SY5Y on the collagen matrix may be related to the nature of the matrix itself. Further optimisation of the collagen system carried out after these experiments were completed, led to the use of a mixture of matrices for the outgrowth of neurites, which could allow for higher adhesion and greater neurite extension in all directions, as previously shown (Sun et al., 2012). The use of laminin or Matrigel® is well reported in the literature to enhance neuronal adhesion in culture (Kleinman and Martin, 2005; Ma et al., 2008; Sun et al., 2012). Matrigel® was also found to increase muscle differentiation, if compared to collagen type I (Grefte et al., 2012).

In conclusion, carrying out the co-culture of C2C12 and SH-SY5Y in collagen gels highlighted some limitations that may be overcome by changing the composition of the gel itself, particularly by adding a percentage of Matrigel® to it. The use of collagen/Matrigel® hybrid gels was reported for muscle-only cultures (Dixon et al., 2018; Powell et al., 2002) and muscle-nerve co-cultures (Dixon et al., 2018). Matrigel®-based gels were also used to generate a mouse NMJ in a 3D model (Morimoto et al., 2013), even though these models are always based on mouse-derived cells, rather than on a chimeric mouse/human model that we proposed.

4.6 Chapter summary

Optimisation of co-culture conditions in 2D carried out in the previous chapter allowed for progression to 3D culture analysis. To the best of the author's knowledge, no C2C12/SH-SY5Y co-cultures were reported in the literature, although muscle-nerve co-cultures using C2C12 are common. Using C2C12 and SH-SY5Y cell lines ensured higher reproducibility to improve the co-culture conditions and observe muscle and nerve behavior in culture in a less expensive manner than when using primary cells. In this chapter, the co-culture was carried out using two different types of 3D tissue engineered constructs: fibrin- and type I collagen-based hydrogels.

The use of the same differentiation medium for the co-culture in 2D and 3D successfully led to myotube formation and neurite extension. With regards to the neuronal distribution on either gel types, preliminary results indicated that additional molecules to the collagen matrix may be key for SH-SY5Y cells to adhere and differentiate. Due to the neurons laying in a different focal plan than C2C12, it was hypothesised that there was no interaction between the two cell types. The fact that the nature of the collagen matrix hindered cell-cell interaction, indicated that further optimisation of this 3D model was required for primary human co-cultures. As for the fibrin-based constructs, the lack of successful gels due to fibrinogen batch-to-batch variability did not allow for extensive studies and thus, this approach was discarded. No significant difference in myotube width was observed when C2C12 were co-cultured with SH-SY5Y in either constructs. The different species may play a role in this lack of influence, even though the same outcome was previously observed in primary rat co-cultures (Martin et al., 2015).

The aim of this work was to set the conditions for muscle/nerve co-cultures in 3D gels, rather than to verify the effect of the neurons on the muscle population. Nevertheless, the encouraging coexistence of C2C12 and SH-SY5Y in 3D tissue engineering constructs is a promising first step towards the optimisation of a more complex muscle-nerve model. Due to time limitations, subsequent work did not focus on human co-cultures using primary SkM and SH-SY5Y cells. As iPSC-derived MNs became available, this neuronal source was tested to more closely mimic a human NMJ *in vitro*. Therefore, the following chapter will show the characterisation of such MNs.

5 IPSC-DERIVED MOTOR NEURON PROGENITORS CHARACTERISATION

5.1 Introduction

The advancements in stem cell biology led to the generation of an alternative source of human pluripotent stem cells than embryonic stem cells. Neurons generated via the process of de-differentiation and re-differentiation were characterised to assess their morphology and cholinergic features, in order to be used as substitutes of SH-SY5Ys.

5.1.1 Sources of human motor neurons

To develop a human *in vitro* model of the neuromuscular junction (NMJ), the search for human motor neurons (MNs) represents a challenge. Animal-derived and human embryonic stem cells (ESCs) have been the gold standard for several years (Lu et al., 2015; Hynek Wichterle et al., 2002). In addition, animals in research can be expensive to keep and take care of, besides being strongly affected by ethical issues, as well as ESCs do. However, the rapidly growing use of induced pluripotent stem cells (iPSCs) in research appears to be a promising alternative to generate human MNs. Since their innovative discovery just over a decade ago (Takahashi and Yamanaka, 2006; Yamanaka et al., 2007), iPSCs opened new avenues and applications for which the cells could be used (Dolmetsch and Geschwind, 2013). These range from the development of disease models (Lee et al., 2010) and cell therapies (Imberti et al., 2015), to drug screening platforms (Wheeler et al., 2015). Although some believe that the similarities between ESCs and iPSCs are still debatable (Yamanaka, 2012), others are confident that the cells have equal differentiation potential and the same protocols can be used for either (Chambers et al., 2009; Karumbayaram et al., 2009; Qu et al., 2014). Using iPSCs would provide researchers with an alternative method to generate human MNs. This approach primarily overcomes the availability and ethical issues which are typical of both animal-derived and ESCs. In addition, using iPSC-derived MNs represents a human source of highly specialised cells which can be used to generate a model for *in vitro* drug screening, personalised therapeutics testing and to study physiology and pathophysiology of the peripheral nervous system.

5.1.2 Induced pluripotent stem cells for the generation of motor neurons

The literature reports several recent works about the generation of human MNs from iPSCs. Despite the advantages listed above, there are still limitations to overcome, such as the long period of time required to generate MNs (Hu and Zhang, 2009), the low percentage of MNs in the cell population (Ebert et al., 2009) and the inconsistency of the process which can be influenced by various factors. In fact, there is often a substantial batch-to-batch variability (Zeng et al., 2010) and it is challenging to identify which aspects play an essential role in the success of the differentiation process (*i.e.* how long do the cells have to be exposed to a certain medium formulation, what factors or substrates can be used and at what concentration). As summarised in **Table 5.1**, the induction/differentiation protocols differ substantially between published examples. Some common methods can be identified across different protocol. For instance, the use of mouse embryonic fibroblasts (MEFs) (Dimos et al., 2008; Ebert et al., 2009; Karumbayaram et al., 2010) or Matrigel® (Du et al., 2015; Qu et al., 2014; Su et al., 2013) as substrates to sustain neuronal adhesion is reported in several publications. Similarly, the protocols to induce a neuronal phenotype include similar compounds (e.g. RA and N2 supplement). As for other media components, Rho kinase (ROCK) inhibitors (here reported as Y-27632) are generally used in critical steps such as thawing and plating. ROCKs are targets of the protein Rho, and the binding of the two is involved in several cell functions, such as motility, secretion, proliferation and gene expression (Liao et al., 2009). In stem cell cultures, ROCK inhibitors are routinely used to prevent dissociation-induced apoptosis when generating single-cell cultures from ESCs (Martin-Ibañez et al., 2008). They were shown to improve embryoid body formation (Ungrin et al., 2008) and increase the survival of cryopreserved ESCs after thawing (Li et al., 2009). Retinoic acid (RA), described in Chapters 1 and 3 of this thesis, is also a key factor during neuronal induction, and was shown to induce differentiation in the neuronal cell lines SH-SY5Y (Xun et al., 2012) and NT2 (Lee and Andrews, 1986). During the differentiation stage, the use of neurotrophic factors such as brain-derived neurotrophic factor (BDNF) and ciliary neurotrophic factor (CNTF) is also common. BDNF is a key neurotrophin during neurogenesis and differentiation of stem cells into MNs (Huang and Reichardt, 2009), and it has been seen to support neuronal survival (Acheson et al., 1995). Thus, it was used to generate MNs from iPSCs, often in combination with CNTF (Du et al., 2015; Su et al., 2013). CNTF is also involved in neuronal differentiation and survival, and was shown to help nerve recovery after injury (Sleeman et al., 2000).

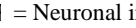
A recent protocol based on the use of small molecules to generate an adherent neuronal culture, allowed for the production of functional MNs which express the expected markers (β -III Tubulin, HB9, MAP2 and neurofilament) and do not express pluripotent markers which were observed in the early stages of the differentiation (Olig2, Pax6 and Sox1) (Bianchi et al., 2018). This protocol required 21 days for synapses between neurons and functional Ca^{2+} activity to be detected, and 5 weeks for the cells to be electrophysiologically active. The MNs were thoroughly characterised, but it is unclear whether they could be used for long-term studies such as *in vitro* modelling, thus highlighting how even the most recent works require optimisation.

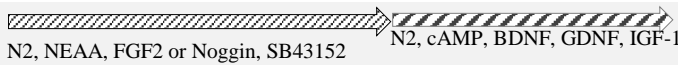
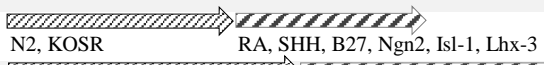
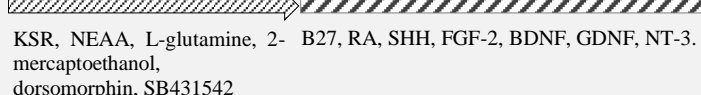
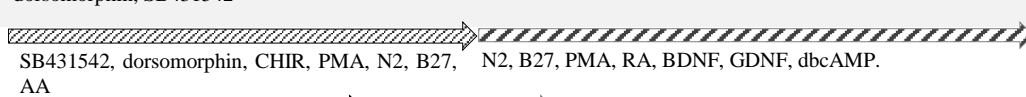
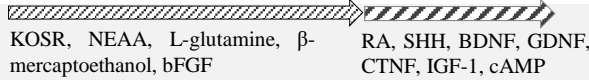
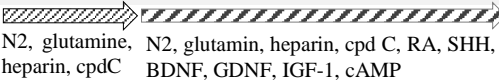
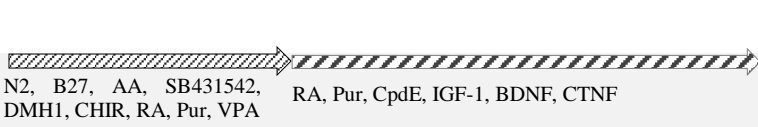
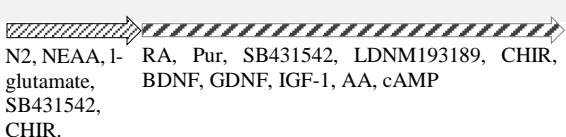
Even though similar features can be identified, methods to derive iPS from differentiated cells, substrates for iPS adhesion, media compositions for the neuronal induction and differentiation stages all differ. Thus, understanding what condition allows for the generation of a specific phenotype, at a certain timepoint, remains a challenge when attempting to define a reproducible protocol.

5.1.3 ChAT and Islet 1 as markers of mature MNs

Among the numerous markers that can be used to identify mature MNs, two are commonly utilised for iPSC-derived MNs in the literature, choline acetyltransferase (ChAT) (Dimos et al., 2008; Du et al., 2015; Ebert et al., 2009; Egawa et al., 2012) and Islet 1 (Chambers et al., 2009; Dimos et al., 2008). These are used alongside an antibody that marks the structure of the neuron, such as MAP-2 or β -III Tubulin. ChAT is the enzyme responsible for the synthesis of the cholinergic neurotransmitter acetylcholine (ACh) (Kasa et al., 1991; Necker, 2004). Neurons that are positively stained by anti-ChAT antibodies are considered spinal and cholinergic, thus suitable for co-cultures which aim to form a NMJ *in vitro*. Islet 1 is required for the formation of mature and functional MNs (Dimos et al., 2008; Qu et al., 2014) and expressed by all classes of MNs (Pfaff et al., 1996), therefore representing a valuable marker of MN generation.

Table 5.1. Summary of recent protocols used for the differentiation of hES and iPSCs into MNs.

Abbreviations: AA = ascorbic acid; BDNF = brain-derived neurotrophic factors; bFGF = basic fibroblast growth factor; cAMP = cyclic adenosine monophosphate; ChAT = choline acetyltransferase; cpdC = compound C; CTNF = ciliary neurotrophic factors; FGF2 = fibroblasts growth factor; GDNF = glial-derived neurotrophic factors; IGF1 = insulin-like growth factor 1; KOSR = knockout serum replacement; MAP2 = microtubule-associated protein 2; MEF = Mouse Embryonic Fibroblasts; MSCs = mesenchymal stem cells; NEAA = non-essential amino acids; Pur = Purmorphamin; RA = Retinoic Acid; SHH = Sonic hedgehog; SV-2 = synaptic vesicle 2; Syn = synapsin; Tuj1 = β -III Tubulin.  = Neuronal induction;  = MN differentiation.

Reference	Substrate	Characterisation	Protocol (days)																			
			0	2	4	6	8	10	12	14	16	18	20	22	24	26	28	30	32	34	36	38
(Dimos et al., 2008)	MEF	Tuj1, HB9, Islet																				
(Ebert et al., 2009)	MEF	Nestin, Tuj1, HOXB4, Olig2, Islet1, HB9, ChAT, SMI-32																				
(Karumbayaram et al., 2009)	MEF	Brn2, Sox3, Pax6, Nkx6.1, Olig2, Tuj1, electrophysiology																				
(Hu et al., 2010)	MEF	Olig2, HB9, Tuj1, HOXC8, biotin, ChAT, Syn, Btx, electrophysiology																				
(Hester et al., 2011)	MEF	HOX, HB9, ChAT, electrophysiology																				
(Egawa et al., 2012)	SNL feeder layer / Matrigel	Nanog, SSEA-4, Sox-17, Tuj1, Islet1, HB9, ChAT, synapsin, MAP2																				
(Reinhardt et al., 2013)	MEF / Gelatin / Matrigel	Islet1, HB9, ChAT, SMI-32, electrophysiology																				
(Su et al., 2013)	MEF Matrigel	Pax6, Olig2, Tuj1, HOXB4, HB9, Islet1, Lhx3, ChAT, electrophysiology																				
(Qu et al., 2014)	Matrigel / Vitronectin-laminin-fibronectin	Pax6, Sox1, Zic1, Oct4, Nanog, HB9, Tuj1, ChAT, MAP2, Btx, Syn1, SV-2, electrophysiology																				
(Du et al., 2015)	MEF Matrigel	Sox1, Otx2, HOXA3, Nkx2.2, Olig2, Btx, ChAT, Map2, Islet1																				
(Hu et al., 2015)	Vitronectin	Nanog, Oct4, SSEA4, Sox1, Sox2, Tra-1-60, Tra-1-81, Nanog, Pax6, Olig2, HB9, Tuj1, ChAT																				

5.2 Aims & objectives of the chapter

Recently, companies have focused their attention on developing a stable protocol to derive MNs from human iPSCs. The main objective of this chapter is to characterise human iPSC-derived motor neuron progenitors (MNPs) which were kindly provided by Axol Bioscience (Cambridge, UK), as part of a beta testing collaboration. Determining the cholinergic potential of these cells is essential to substitute the previously used human neuroblastoma line SH-SY5Y to form a NMJ with human skeletal muscle (SkM). Finally, the substrates and media used to culture MNPs were used for SH-SY5Y to compare their effects on the two neuronal cell type used for the realisation of this thesis.

The aims of this chapter were:

- Culturing and differentiating MNPs into MNs for 35 days;
- Assessing cholinergic characteristics of iPSC-derived MNs
- Verifying the potential use of MNPs after multiple passages

The objectives of this chapter were:

- To thaw, plate and grow MNPs until ready for differentiation using a specific medium supplemented with neurotrophic factors, in order to use them for co-culture with human SkM;
- To use immunofluorescent staining to observe the positivity to the cholinergic markers ChAT and Islet 1;
- To freeze MNPs P1, re-thaw them and plate them as P2 in order to use them for differentiation and co-culture with human SkM.

5.3 Materials & Methods

Human MNPs from a healthy 74 years old male donor, their substrates and culture medium were kindly provided by Axol Bioscience (Cambridge, UK), and cultured according to the manufacturer's protocol as described in section 2.1.7. A copy of the protocol used for these cells can be found at the end of the Supplementary section, while updated versions of the protocols will be available at the following webpage: <https://www.axolbio.com/shop/product/human-ipsc-derived-motor-neuron-progenitors-5172>.

MNPs were cultured in monolayer to characterise their phenotype, both upon receiving the cells from Axol Bioscience (passage 1, P1), and after the cells were frozen down after the first expansion (P2). Finally, the cells at P1 were also differentiated and characterised for the positivity to cholinergic markers until day 35.

5.3.1 MNPs: expansion and differentiation at P1

The P1 cells were both cultured on their recommended substrate (SureBond™+ReadySet, Axol Bioscience, UK), as described in 2.1.7.2.

5.3.1.1 MNPs: positivity to cholinergic markers

Upon thawing, the cells were expanded on a layer of SureBond™ (2.1.7.1) until they reached 70% confluency (5-7 days). Then, they were detached according to the manufacturer's guidelines and seeded on SureBond™+ReadySet-coated glass. The cells were cultured up to 35 days, and fixed/immunostained at the following timepoints: 5, 7, 14, 21, 28 and 35 days. Bright-field images were taken after each medium change, and the cells were stained for cholinergic markers (ChAT and Islet1) as described in sections 2.3.1.6 and 2.3.1.7, respectively.

5.3.2 MNPs characterisation: expansion and differentiation at P2

The P1 batch of cells that was utilised for the full characterisation were frozen down to be used for further tests. The cells were cultured as above. Daily micrographs were taken to compare the morphology during the expansion stage with the P1 cells. Then, differentiation was induced upon seeding the progenitors on SureBond™+ReadySet-coated glass coverslips, in preparation for immunofluorescent staining.

5.4 Results

5.4.1 MNPs characterisation: expansion and differentiation at P1

The first batch of iPSC-derived MNPs P1 used for the characterisation were seeded on SureBond™-coated T25 flasks after thawing, and showed a viability of 77.8% prior to seeding for expansion.

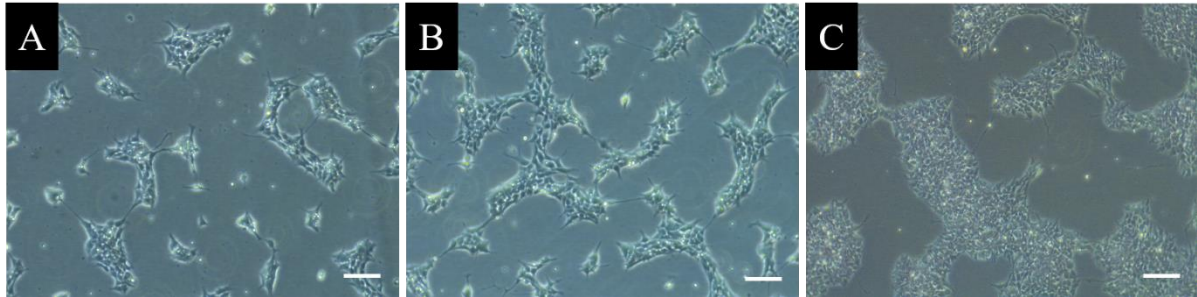


Figure 5.1. MNPs P1 proliferation after thawing. The cells were imaged at 24 (A), 48 (B) and 72 (C) hours after plating. Scale bars: 100 μ m.

The cells proliferated in clusters which increased in size gradually from day 1 (24h after seeding, **Figure 5.1A**) to day 2 (48h after seeding, **Figure 5.1B**) and day 3 (72h after seeding, **Figure 5.1C**). Cells seeded on gelatin, the substrate used for primary human SkM culture, did not survive after 24 hours (**Figure 5.2**), confirming that SureBond™ is a suitable substrate for the cells to adhere in culture.

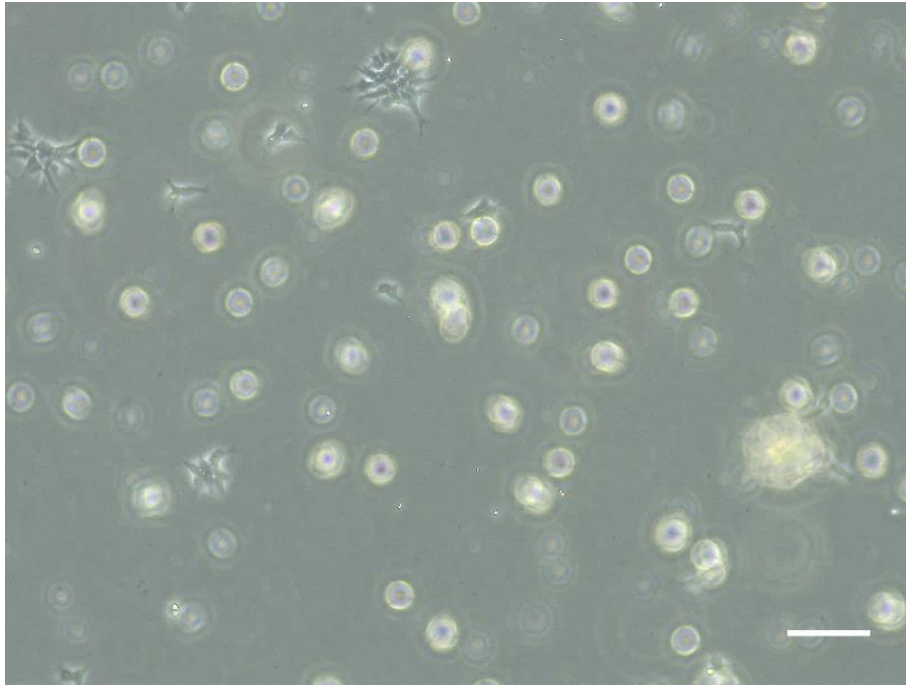


Figure 5.2. MNPs P1 did not adhere on gelatin upon thawing. Scale bar: 100 μm .

When the cells were 70% confluent, they were passaged and re-plated on SureBond™+ReadySet-coated glass coverslips. Bright-field images showed rapid generation of protrusions and neuronal extensions, enhancing the complexity of the neuronal network over time and suggesting that the differentiation process occurred rapidly and efficiently. As observed in **Figure 5.3**, within 48 hours from the beginning of the differentiation process, the cells proliferated and extended neurites in different directions. The amount of neurites visibly increased until day 10-12, after which the cells clumped in aggregates and seemed to form neurospheres (**Figure 5.4**). These spheres appeared greater in size and number until the neurons began to die in culture. The formation of aggregates may indicate that the substrate on which the cells were seeded was suboptimal. The culture was carried out until day 35 as the manufacturer suggested, despite the poor viability of the cells at that stage, and the change in morphology compared to earlier days (**Figure 5.5**).

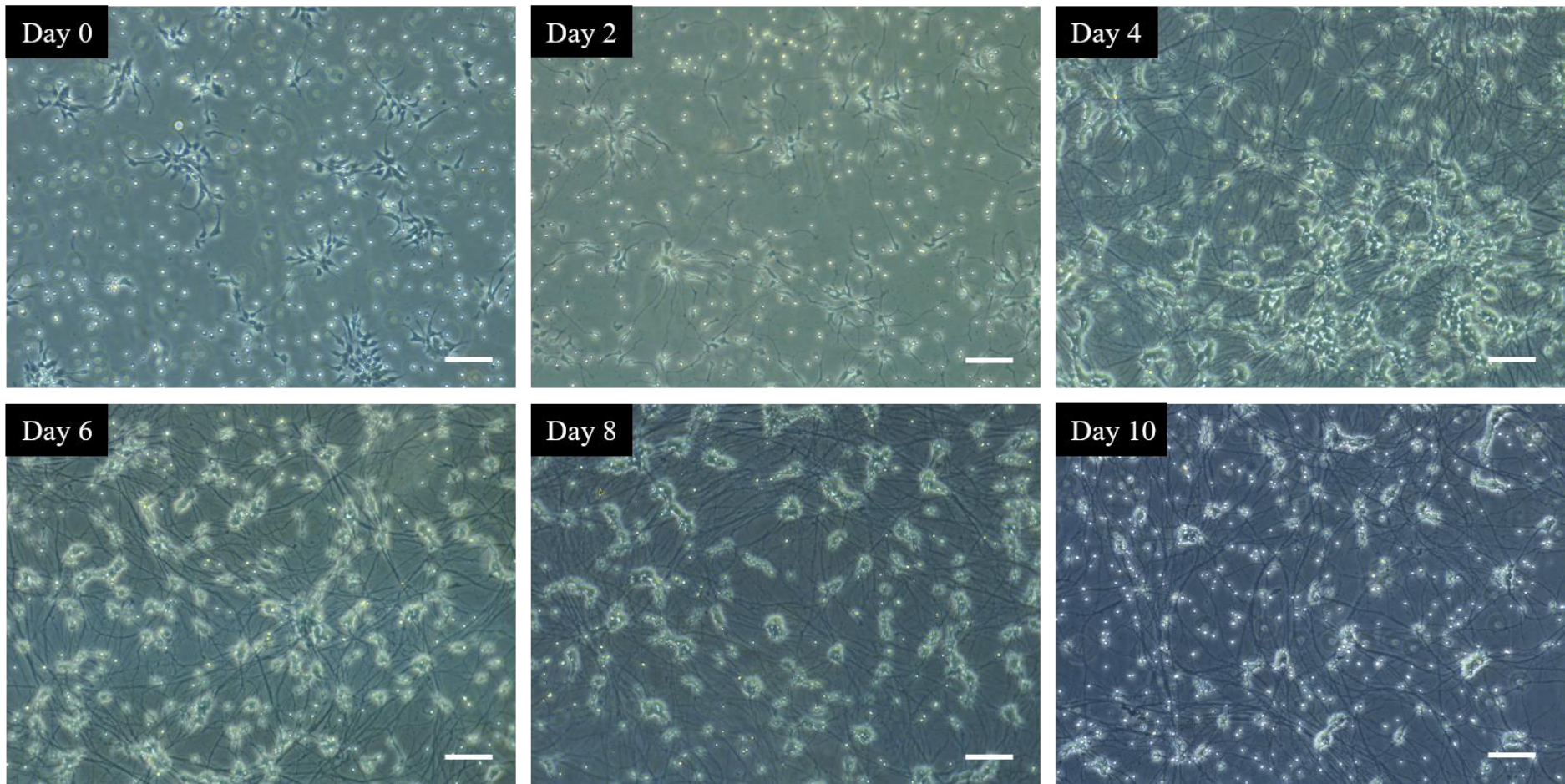


Figure 5.3. MNPs P1 differentiation in monolayer from day 0 to day 10. Scale bars: 100 μm.

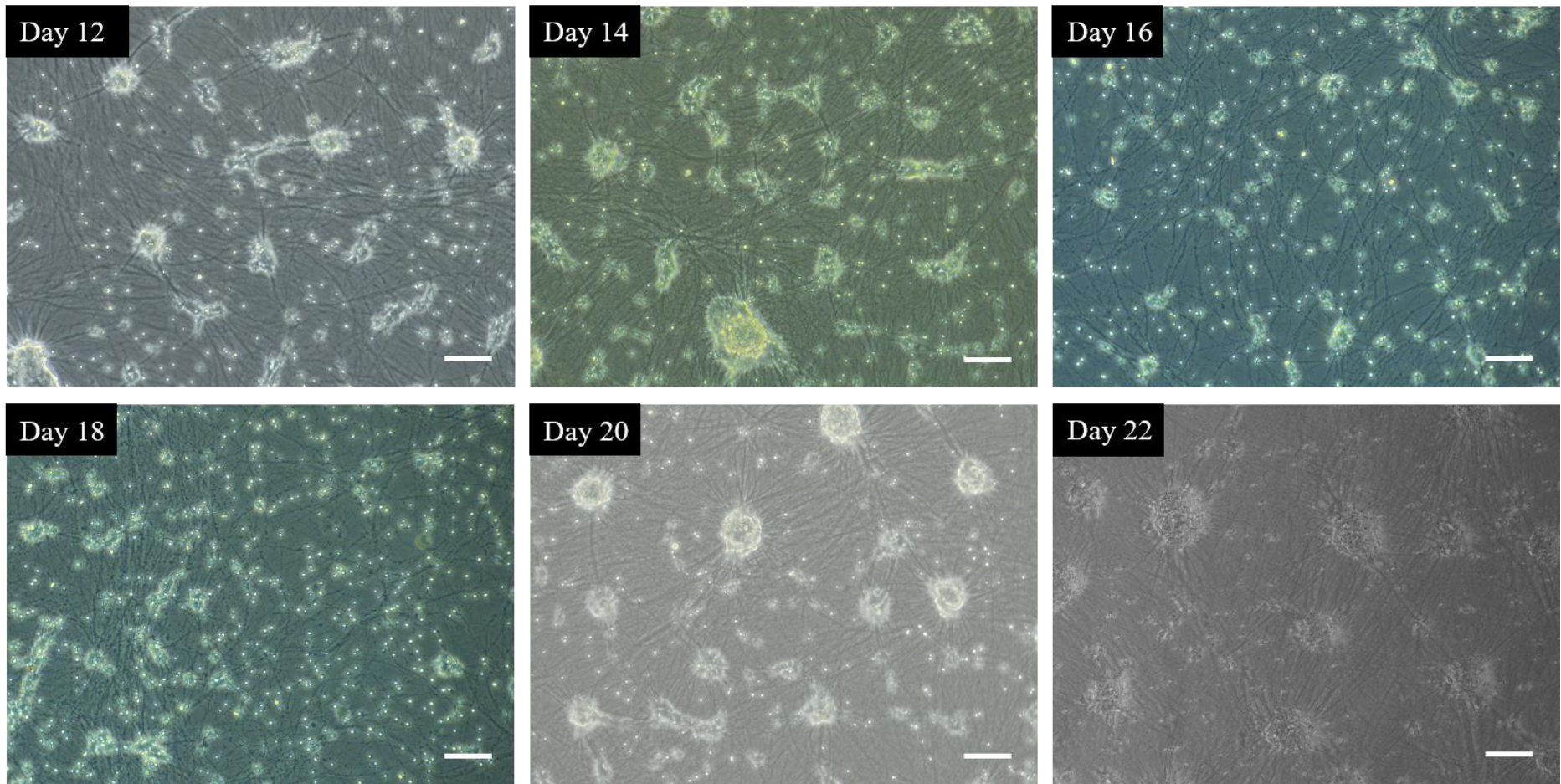


Figure 5.4. MNPs P1 differentiation in monolayer from day 12 to day 22. Scale bars: 100 μm .

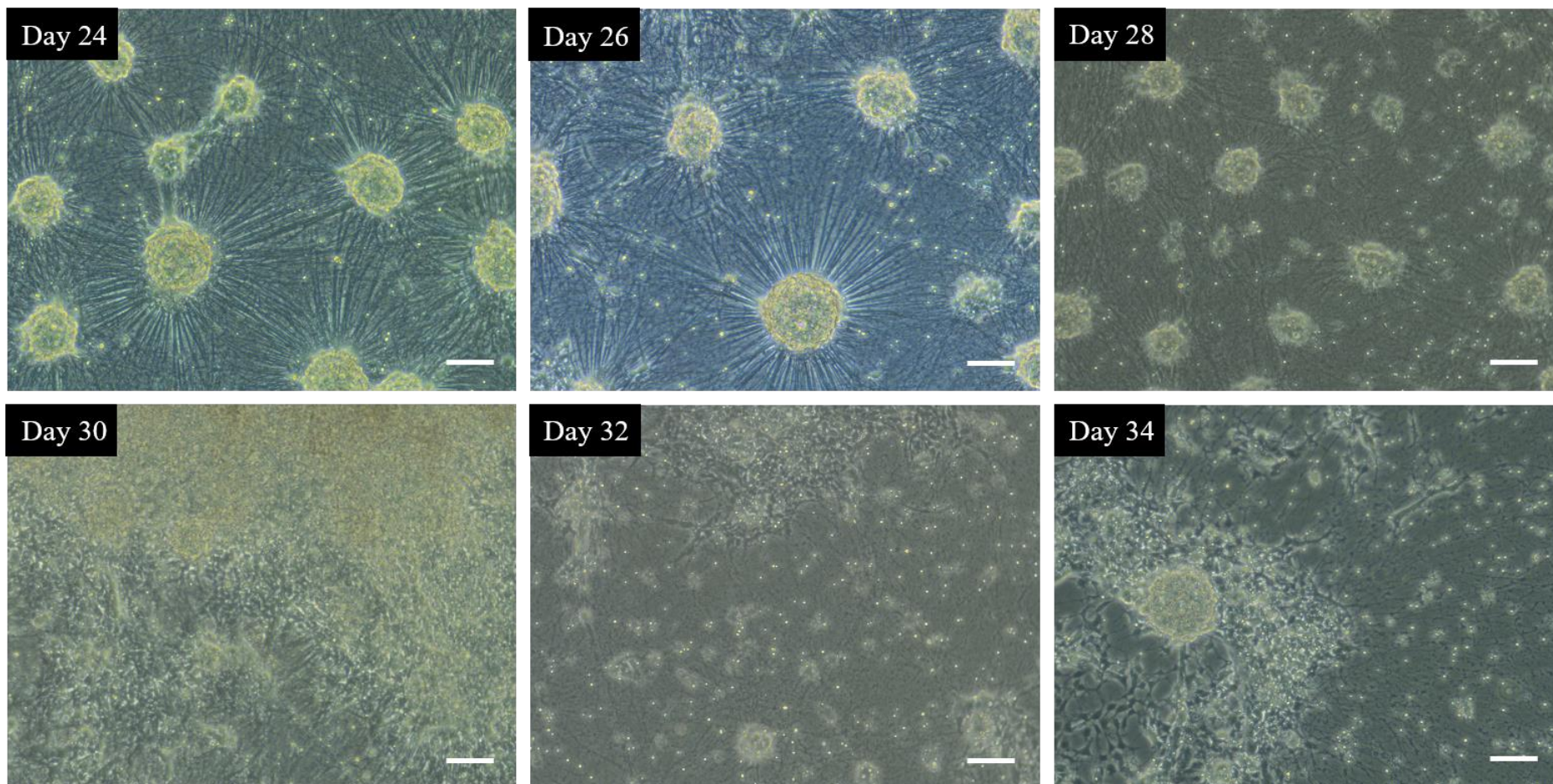


Figure 5.5. MNPs P1 differentiation in monolayer from day 24 to day 34. Scale bars: 100 μm .

5.4.1.1 MNPs characterisation: MN markers immunostaining

MNPs P1 that were expanded up to 35 days were also immunostained for the cholinergic markers ChAT and Islet 1. The cells appeared positive to both ChAT (**Figure 5.6**) and Islet 1 (**Figure 5.7**) at all timepoints, even though the observation of considerable cell death made imaging challenging after day 14. The staining appeared to be localised within the soma of the neurons, which was more and more clear as days passed and neurospheres formed. To confirm that, higher magnification images were taken and showed that both ChAT and Islet 1 are localised in the soma (**Figure 5.8** and **Figure 5.9**).

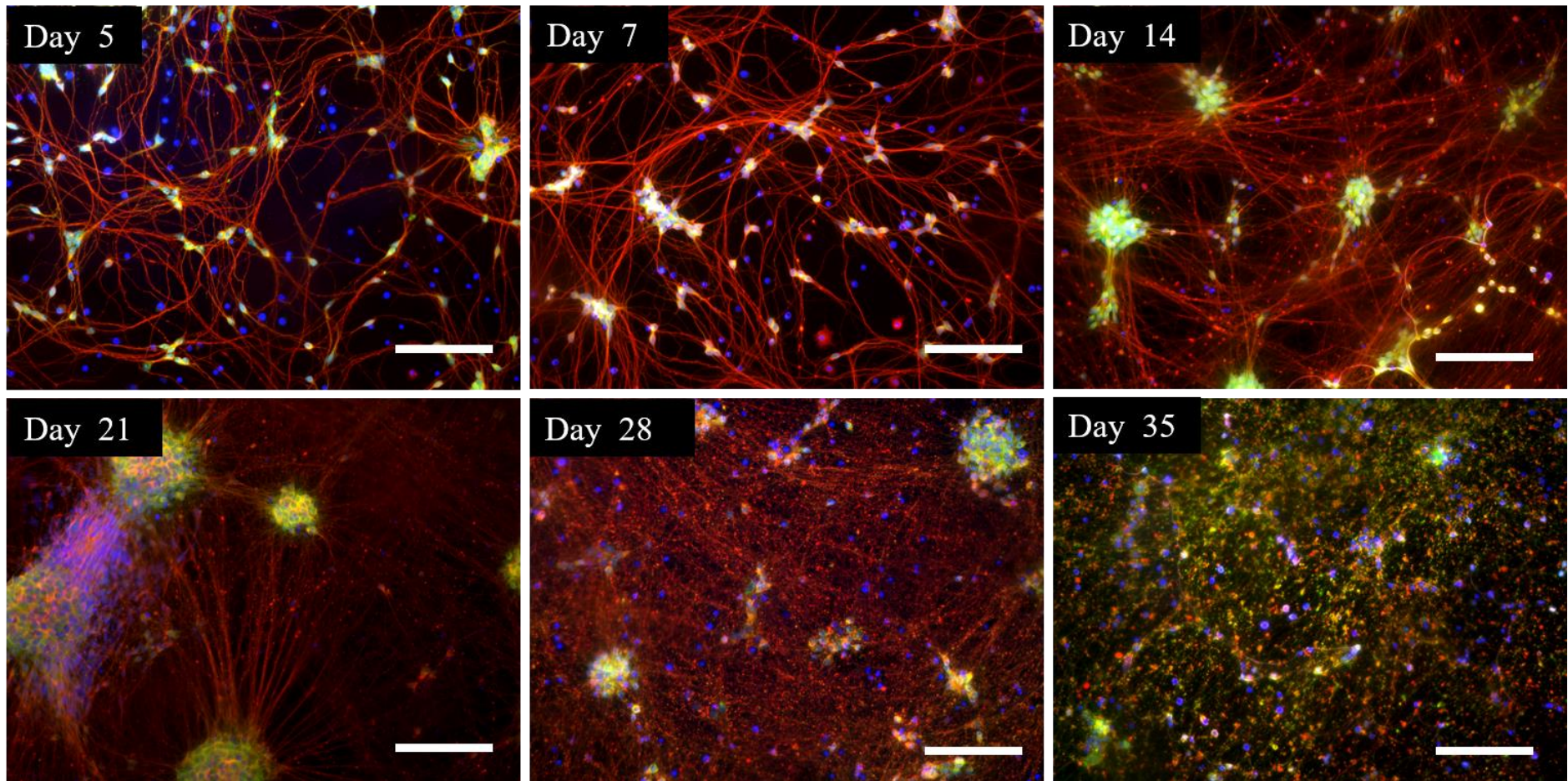


Figure 5.6. MNPs are positive to ChAT immunostaining from day 5 to day 35. The cells were immunostained for ChAT to identify the enzyme (green), β -III Tubulin for the cytoskeleton (red) and DAPI to counterstain the nuclei (blue). Scale bars: 50 μ m.

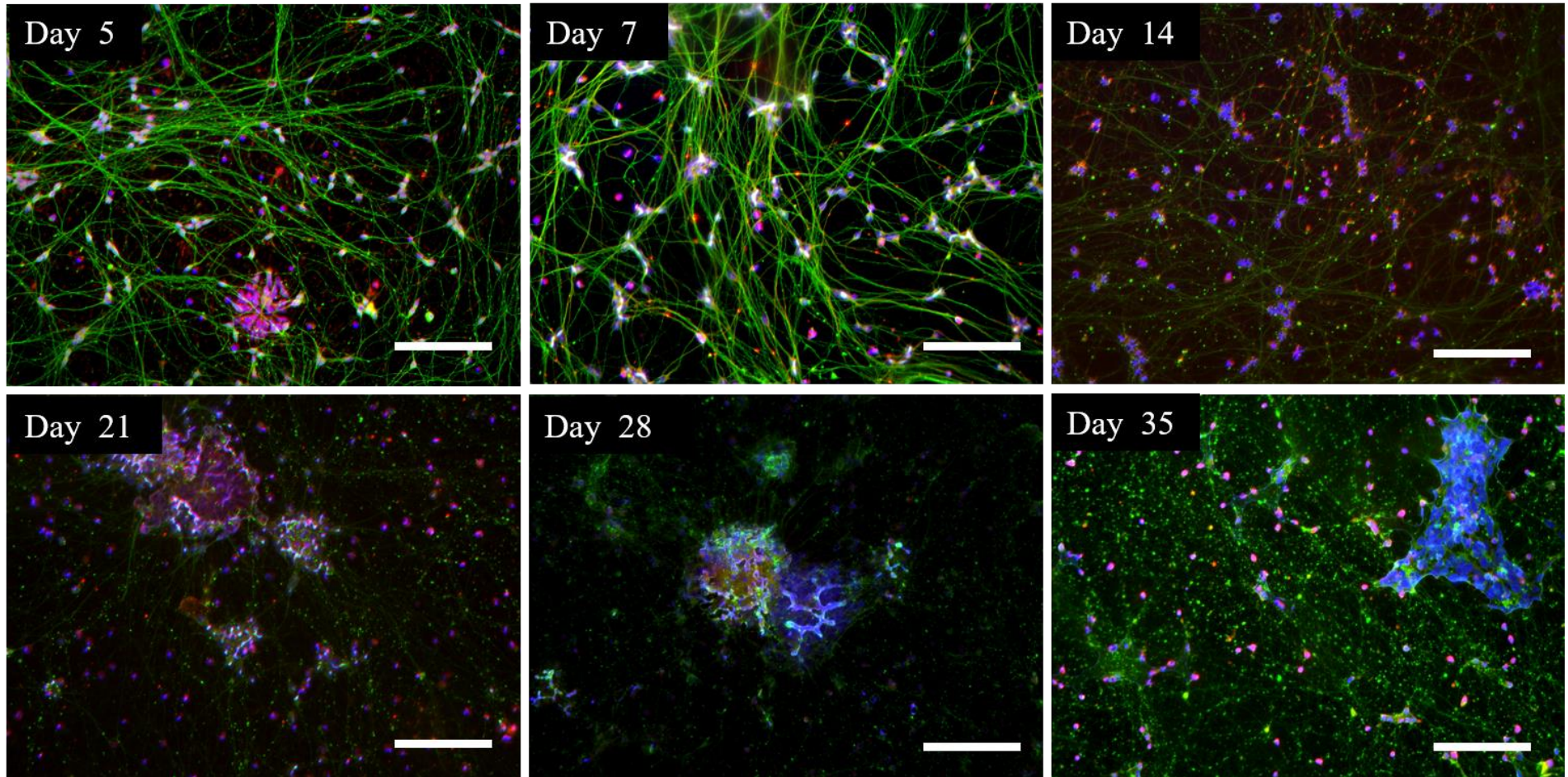


Figure 5.7. MNPs are positive to Islet 1 immunostaining at day 5, 7 and 14. The cells were immunostained for Islet 1 to identify the cholinergic marker (red), β -III Tubulin for the cytoskeleton (green) and DAPI to counterstain the nuclei (blue). Scale bars: 50 μ m.

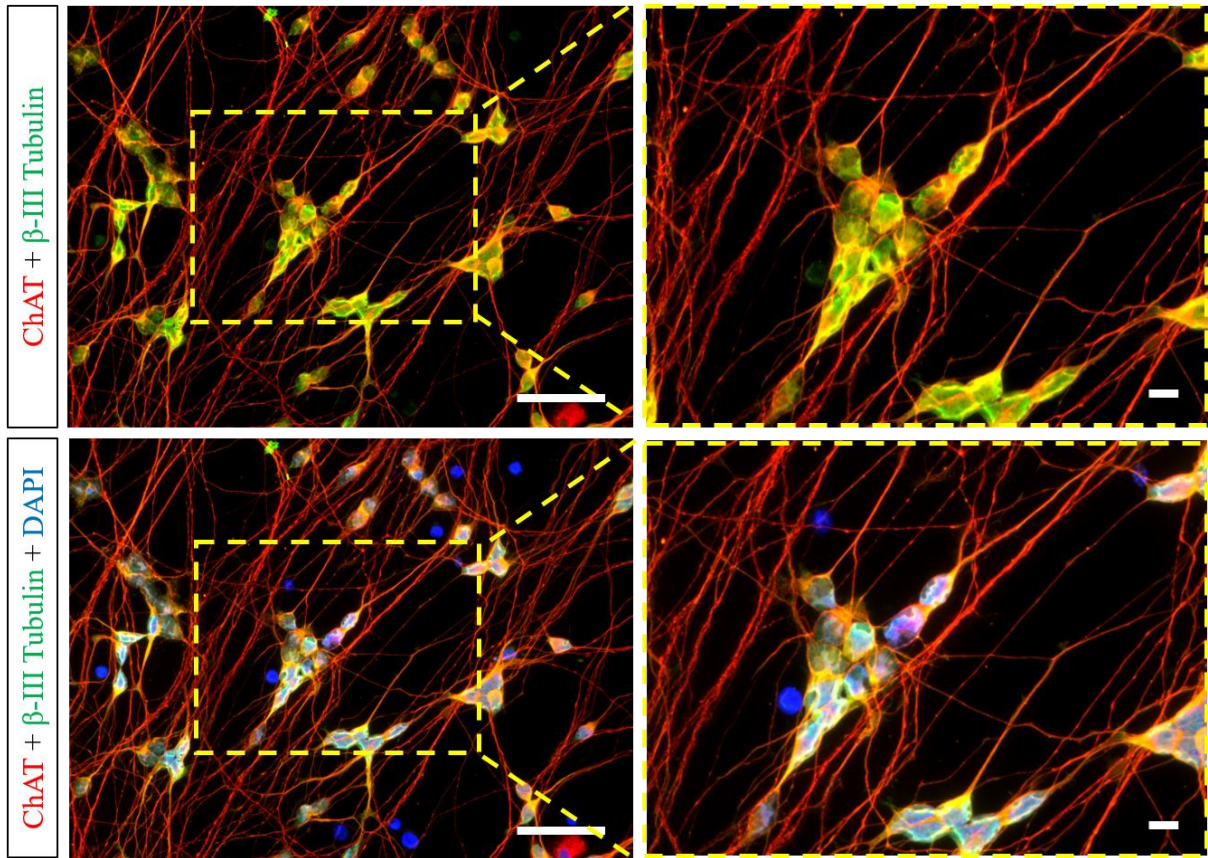


Figure 5.8. MNPs express the cholinergic marker ChAT in the nuclei after 5 days in MM. The cells were immunostained for ChAT to identify the enzyme (green), β -III Tubulin for the cytoskeleton (red) and DAPI to counterstain the nuclei (blue). Scale bars: 50 μ m.

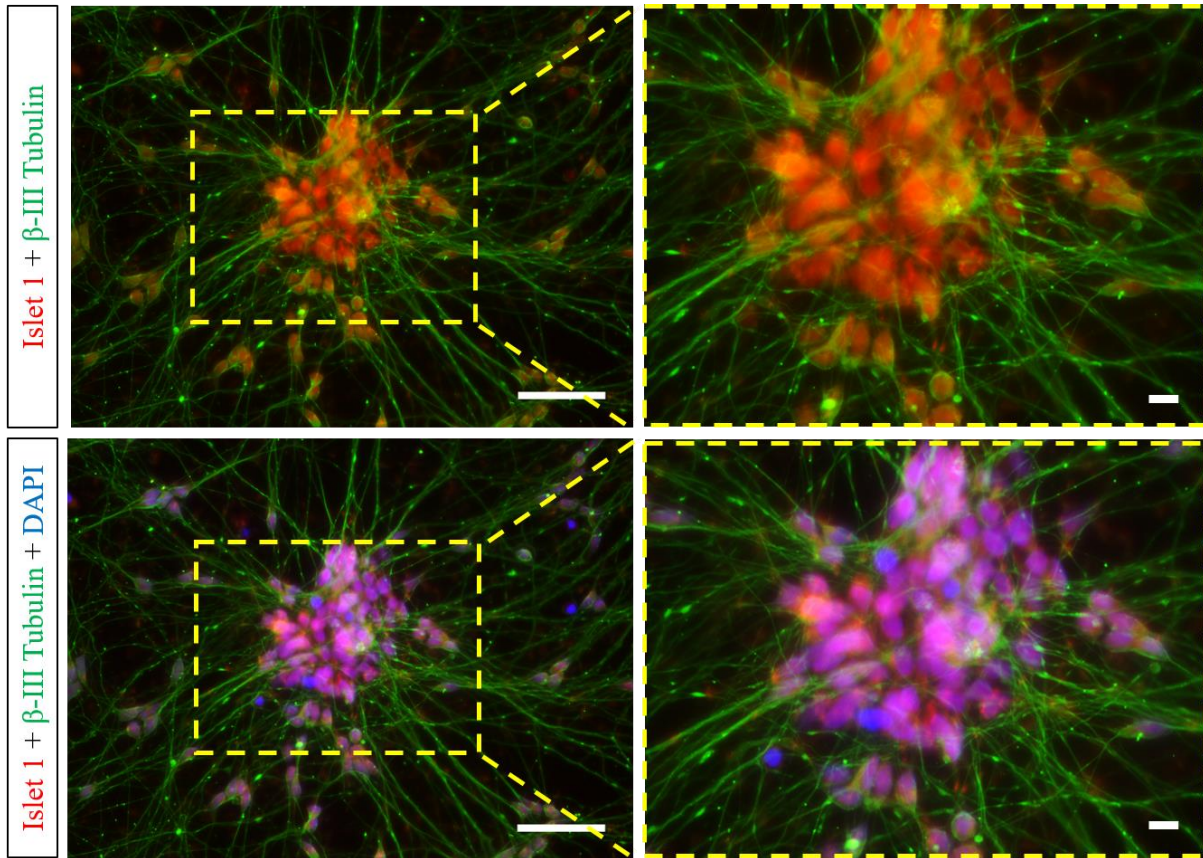


Figure 5.9. MNPs express the cholinergic marker Islet 1 in the nuclei after 5 days in MM. The cells were immunostained for Islet 1 (red), β -III Tubulin for the cytoskeleton (green) and DAPI to counterstain the nuclei (blue). Scale bars: 50 μ m.

5.4.2 MNPs characterisation: expansion and differentiation at P2

A comparison between MNPs at P1 (upon receiving from the supplier) and P2 (after they had been cultured, passaged and frozen down once) was briefly performed. After thawing, 36.8% of MNPs P1 were viable, and the viability of MNPs P2 was 50%. This may not be necessarily linked to the passage, since 77.8% of the previously used P1's were viable (see 5.3.1). The cells were expanded for 5 days, and proliferation as well as morphology were monitored daily. Images of the cells throughout the 5 days are shown in **Figure 5.10**. The morphology did not appear to vary across passage, indicating that the cells can be cultured after a first expansion and cryopreservation. Further marker characterisation would be necessary to ensure that the positivity to the previously investigated ChAT and Islet 1 is retained at passage 2.

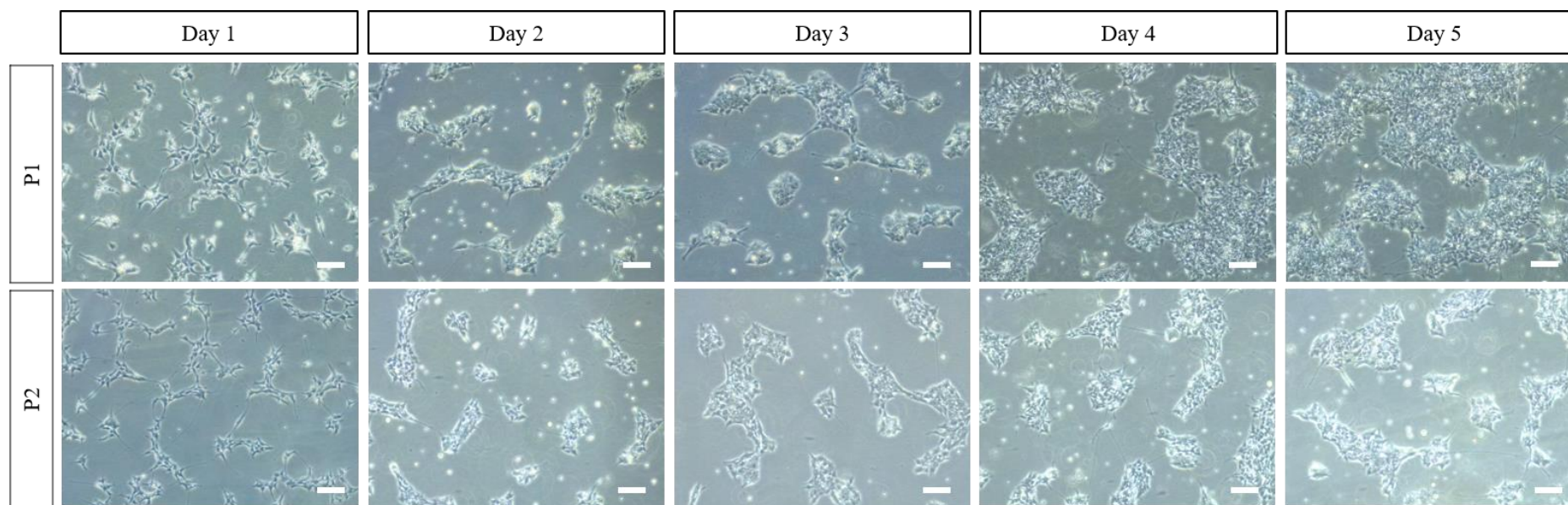


Figure 5.10. MNPs at passage P1 and P2 expansion upon thawing, from day 1 to day 5. Scale bars: 100 μm .

When the cells were plated for differentiation, they did not adhere to the substrate and died after 24h (**Figure 5.11**). This suggests that the multiple cryopreservation and passage steps influenced the ability of these cells to adhere, although this only represented one attempt to further expand and differentiate previously cultured MNPs.

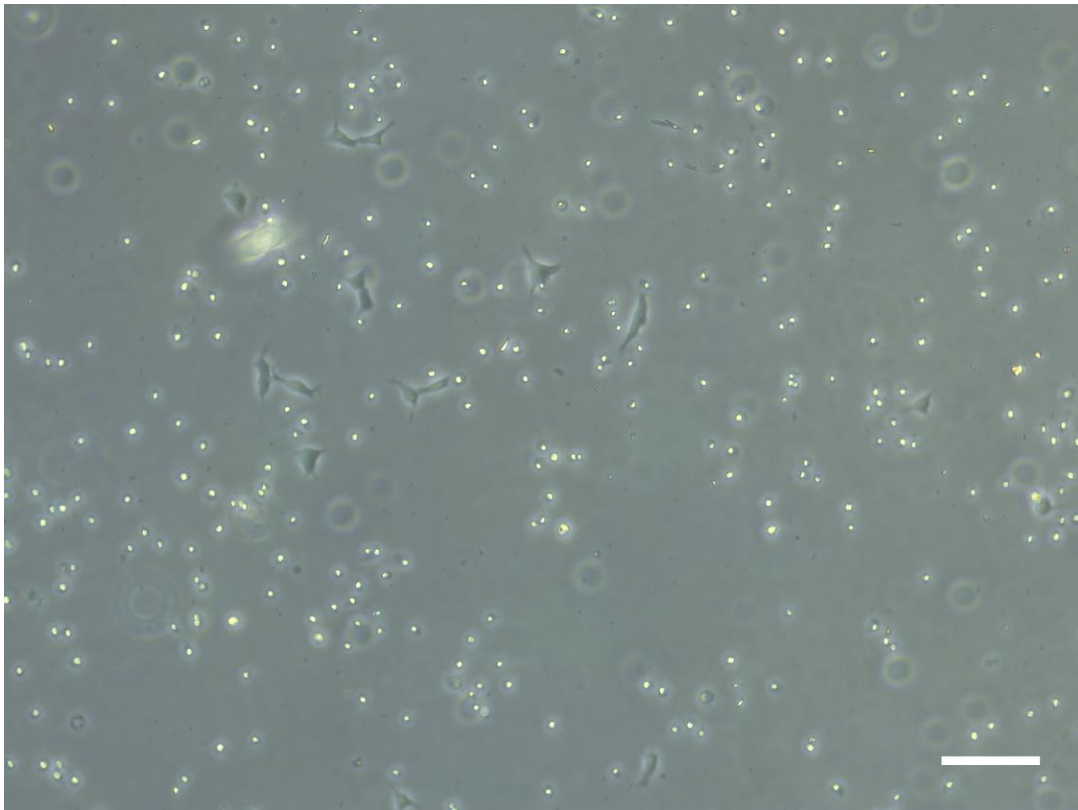


Figure 5.11. MNPs P2 did not adhere to SureBond™+ReadySet-coated glass after passage. Scale bar: 100 μm .

5.5 Discussion

The use of iPSCs recently allowed for the generation of human MNs (Demestre et al., 2015; Du et al., 2015). Several protocols were described in the literature, many of which require extensive times to produce MNs. Optimising the differentiation stage to minimise time-consuming and expensive procedures is still a priority in order to obtain a cholinergic population of MNs which is able to form a NMJ with human primary SkM cells *in vitro*. This chapter focused on the characterisation of commercially available MNPs, to assess their morphology in culture, their positivity to cholinergic markers, morphology upon re-freezing and re-thawing, and the effect of medium and substrate used for MNPs on SH-SY5Y.

5.5.1 MNPs can be cultured and differentiated into MN-like cells

Here we reported the differentiation of commercially available MNPs into MNs in 5 days. This protocol generated cells which presented a MN-like morphology in a timescale comparable to previous works (Hester et al., 2011; Karumbayaram et al., 2010). The cells were cultured for 35 days, although considerable cell death was noticeable after 14 days. Formation of neurospheres was also observed within the first 14 days, and such spheres appeared larger and more numerous as time in culture proceeded. Aggregates of neurons routinely form during the neuronal induction phase, where embryoid bodies are generated and selected to preserve a population of pluripotent cells (Su et al., 2013). Explants from an adult mouse brain were cultured *in vitro* in the absence of adhesion factors to create spheres of floating cells from which differentiated cells spread (Reynolds and Weiss, 1992). The neurospheres observed in this thesis were adherent rather than in suspension. In addition, neuronal projections extended from the spheres instead of undifferentiated cells, advises that the cell population constituting the aggregate was neuronal. However, the presence of such aggregates suggests that the differentiation conditions may still be suboptimal for these MNPs. MNs require other cell types to sustain their growth and function *in vivo* (Bear et al., 2001), thus highlighting the need to add other neuronal cell types (i.e. Schwann cells) to the culture.

5.5.2 MNPs cannot be differentiated at P2

Upon receiving MNPs from Axol Bioscience, the cells were plated for expansion and passaged so that they could be plated for experimental work. These cells were used at P1 for the characterisation up until day 35 and the co-culture with hSkM in 2D and in 3D (see Chapter 6).

To this date and the best of the author's knowledge, there are currently three commercially available types of human iPSC-derived MNs. The cost of a single vial is not negligible and the manufacturers recommend a single use. Thus, testing viability after re-freezing/re-thawing and the ability of the cells to adhere to SureBond™+ReadySet after a second passage is important. One attempt has been done in this work to re-use the cells at P2. During the expansion stage, the cells spacial organisation and morphology appeared similar to the same batch at P1 (**Figure 5.10**). However, after the second passage, MNPs P2 did not adhere on the coating used for final plating and differentiation (SureBond™+ReadySet), as shown in **Figure 5.11**. Whether this is dependant on the substrate itself or on the cells ability to adhere after a second passage, it remains unclear. More attempts should be performed to verify that the cells can or cannot be used after a second round of expansion. Since the manufacturer's protocol for the generation of these cells is unknown, it is challenging to identify stages at which the cells could be adapted for multiple uses. This would certainly be easier if the cells were generated in house, rather than purchased from a commercial provider, and it could be considered for future approaches.

5.5.3 MNPs express cholinergic markers ChAT and Islet 1

In order to use MNPs for the generation of an *in vitro* NMJ, such cells must have a cholinergic phenotype. Since the previously used SH-SY5Y cholinergic potential was highly debated in the literature (Korecka et al., 2013; Pählman et al., 1984), it was hypothesised that an iPSC-derived source of MNPs could be differentiated into MNs expressing cholinergic markers. In particular, the enzyme ChAT was used as it is responsible for the synthesis of ACh, the neurotransmitter released by MNs, that initiates contraction of SkM fibres (Guyton and Hall, 2005). ChAT was extensively utilised as a cholinergic marker (Du et al., 2015; Ebert et al., 2009; Egawa et al., 2012; Hu et al., 2010; Qu et al., 2014), and therefore considered a reliable approach to characterise MNPs. Upon differentiation in MM, the cells expressed ChAT in their nuclei at all timepoints, despite the cell death observed after 14 days. Images taken at the same exposure time showed increasing fluorescence intensity as the culture proceeded. The other marker utilised for the characterisation was Islet 1, involved in neuronal development (Li et al., 2014; Waclaw et al., 2017) and also previously used to identify cholinergic neurons (Dimos et al., 2008; Du et al., 2015; Ebert et al., 2009; Egawa et al., 2012; Reinhardt et al., 2013). The cells nuclei appeared positive to Islet 1 at all timepoints, most importantly after 5 days of differentiation. This is generally the time required for SkM to differentiate *in vitro*, therefore making these neurons suitable for a co-culture with SkM cells.

5.6 Chapter summary

In this chapter, the characterisation of iPSC-derived MNPs was carried out. The cells were expanded until they reached 70% confluence, before undergoing differentiation for a total of 35 days. Considerable cell death was observed after 14 days, and the formation of neurospheres was also evident within the first days in culture. The presence of aggregates may suggest that the developing MNs require additional cell populations to sustain their adhesion and differentiation, or that the substrate and differentiation medium (MM) still needs optimisation. Positivity to the cholinergic markers ChAT and Islet 1 was an encouraging result, showing that iPSC-derived MNPs can be differentiated into cholinergic MNs in as little as 5 days. Finally, using MNPs at P2 was not possible due to cell death after passage. This represents a disadvantage typical of iPSC cultures, whereby it is rarely possible to use cells after multiple freezing-thawing cycles or passages, thus increasing the cost and time required for these cultures.

Overall, the search for a suitable source of human MNs led to the characterisation of promising MNPs which can readily differentiate to neuronal cells which are positive to the neuronal morphological marker β -III Tubulin and the cholinergic markers ChAT and Islet 1. Therefore, these were considered valuable cells for primary co-cultures with human SkM, in order to fulfil the aim of this thesis and generate a human NMJ *in vitro*.

6 ESTABLISHING HUMAN MUSCLE-NERVE CO-CULTURES

6.1 Introduction

After establishing a chimeric co-culture using murine skeletal muscle (SkM) cells and a human neuroblastoma line, moving to primary human SkM and induced pluripotent stem cell-derived motor neurons (iPSC-derived MNs) has great potential for the generation of a human neuromuscular junction (NMJ) model. A human model would provide researchers with a system whereby primary cells could be used.

6.1.1 iPSC-derived MNs and human primary SkM co-cultures

Primary human muscle can be obtained by Bergstrom biopsy, both from healthy and diseased donors (Bergstrom, 1975). As for MNs, although a primary source is not available, the use of stem cells represents a great advantage and it allows to obtain such cells from a variety of donors, while not being derived from embryos or animals. Combining these two cell types would enable the generation of a model the biomimetics of which is closely representative of the *in vivo* environment. To do so, it is essential to determine the co-culture conditions. The substrates used for cellular adhesion, as well as the media utilised for growth and differentiation are essential criteria which are intrinsic to heterotypic cultures (Goers et al., 2014). Subsequently, a bidimensional (2D) co-culture must be successfully replicated in a three dimensional (3D) tissue engineered system, to closely replicate the *in vivo* microenvironment in which the cells physiologically interact. Finally, 3D models which are suitable for functional studies represent an ideal system in which muscle-nerve interactions can be investigated.

The literature mainly reported iPSC-derived MNs co-cultures using the murine myoblast line C2C12 (Du et al., 2015; Hester et al., 2011; Qu et al., 2014), rather than human-human systems. Human-based NMJ cultures were reported using fetal spinal stem cells and SkM stem cells (Guo et al., 2011) or ESC-derived MNs and primary SkM (Bakooshi et al., 2018). To the best of the authors knowledge, at this time there is only one work that reported NMJ formation between human iPSC-derived MNs and primary SkM, whereby the muscle counterpart was

also derived from iPSCs (Demestre et al., 2015). In addition, iPSC-derived MNs were co-cultured with immortalised primary SkM cells (Shimojo et al., 2015), although this was done in bidimensional conditions and not in a tissue engineering construct, as this work aimed to do. Establishing a human-human co-culture in a 3D environment is, indeed, a key aspect which would provide researchers with a representative model to investigate physiological and non-physiological aspects of the NMJ. Tissue engineered constructs such as collagen gels were previously utilised for SkM 3D cultures to allow for its maturation, differentiation and alignment (A. S. T. Smith et al., 2012). The same constructs were then utilised for muscle-nerve co-cultures, and allowed for the generation of a NMJ using rat primary cells (Smith et al., 2016). A recent work also reported a nerve-muscle co-culture in collagen-based constructs was used for functional studies looking at force generation within the gel (Morimoto et al., 2013). Similarly, fibrin gels were used both for SkM monocultures and functional studies, and as a platform to generate a primary rat NMJ (Martin et al., 2015).

6.2 Aims & objectives of the chapter

The main objective of this chapter is to co-culture human iPSC-derived motor neuron progenitors (MNPs) and human primary SkM. The aims are to optimise media, substrates and timing of the co-culture in monolayer, and thus establish a robust methodology for NMJ formation. Finally this monolayer model will be utilised to develop a 3D tissue engineered model of neuromuscular interaction.

The aims for this chapter were:

- Identifying co-culture conditions for hSkM and MNs;
- Co-culturing and differentiating hSkM and MNs in 2D;
- Assessing the positivity to pre- and post-synaptic proteins;
- Enhancing the expression of SkM markers by adding MNs to the culture;
- Co-culturing and differentiating hSkM and MNs in tissue engineered constructs;
- Increasing force generation in tissue engineered constructs by adding MNs to the culture.

The objectives for this chapter were:

- To culture hSkM on different substrates and differentiate using muscle and neuronal medium;
- To use immunofluorescent staining and myotube width measurement as indications of the differentiative stage and AChR expression of hSkM cultured in different conditions, and in the presence or absence of MNs;
- To use gene expression analysis as a measurements of SkM development and maturation when using different media for the differentiation, as well as MNs in co-culture;
- To co-culture hSkM and MNs in tissue engineered constructs and verify differentiation using immunofluorescent staining, observe cell distribution using confocal microscopy and cross sectional images, and to measure functional activity of SkM with electrical stimulation.

6.3 Materials & Methods

6.3.1 Human MNPs and human SkM co-culture

Human SkM cells were cultured, trypsinised and counted as previously described (2.1.4). SkM cells were seeded at a density of 10,000/cm², and expanded on gelatin and/or SureBond™+ReadySet-coated glass coverslips until 100% confluent in MGM. Then, the controls were differentiated in standard MDM, or in MN Maintenance Medium (MM, Axol Bioscience). For the co-culture, MNPs were seeded on the layer of SkM cells in MN Recovery Medium (RM, Axol Bioscience, supplemented with 10 µM Y-27632) and left to adhere for 4-6 hours. Then, the medium was changed to MM. Human MNPs, their substrates and culture medium were kindly provided by Axol Bioscience (Cambridge, UK), and expanded prior to the experiment according to the manufacturer's protocol (2.1.7). The co-culture was carried out for 5 days (hu028_1) and 4 days (hu020, hu027 and hu028_2) to ensure myotube formation and MN differentiation (identified by the presence of neurite projections). At the end of the experiment, the cells were fixed and stained for morphological markers (rhodamine phalloidin, β-III Tubulin and DAPI) and interaction (BTX and SV-2) immunostaining of the co-cultures were performed as previously described in Chapter 3.

The media formulations are summarised below in **Table 6.1** for clarity.

Table 6.1. Media abbreviations and compositions used for the MNPs & human primary SkM co-culture.

Medium name	Cells	Composition
Muscle Growth Medium (MGM)	hSKM	DMEM, 20% FBS, 1% P/S
Muscle Differentiation Medium (MDM)	hSKM	DMEM, 2% HS, 1% P/S
Recovery Medium (RM)	MNPs	RM, 10 µM Y-27632
Maintenance Medium (MM)	MNPs/Co-culture	MM, 0.5 µM RA, 5 ng/mL BDNF and 10 ng/mL CNTF

Since the co-cultures conditions were unique for different biopsy samples, a summary of the experimental setup is provided below in **Table 6.2**.

Table 6.2. Experimental setup for the MNPs/hu028_1 co-culture in monolayer. All samples were seeded both on SureBond™+ReadySet and gelatin.

Abbreviations: hSkM = human skeletal muscle; DMEM = Dulbecco’s Modified Eagle’s medium; FBS = fetal bovine serum; P/S = penicillin/streptomycin; HS = horse serum; MM = motor neuron maintenance medium; MN = motor neurons; RM = recovery medium; MNPs = motor neuron progenitors.

Plate ID	Sample name	Expansion		MNPs seeding	Differentiation		
		Hu028	MNPs		Hu028	MNPs	Co-culture
A	hSkM control	DMEM + 20% FBS + 1% P/S	/	/	DMEM + 2% HS + 1% P/S (5 days)	/	/
B	hSkM MM	DMEM + 20% FBS + 1% P/S	/	/	MM (5 days)	/	/
C	Co-culture MM	DMEM + 20% FBS + 1% P/S	RM + 10 μ M Y-27632 (24h), then RM for up to 6 days.	RM + 10 μ M Y-27632 (24h)	/	/	MM (5 days)
D	Co-culture (pre-differentiation)	DMEM + 20% FBS + 1% P/S	RM + 10 μ M Y-27632 (24h), then RM for up to 6 days.	RM + 10 μ M Y-27632 (24h)	DMEM + 2% HS + 1% P/S (24h)	/	MM (5 days)
E	MNPs control	/	RM + 10 μ M Y-27632 (24h), then RM for up to 6 days.	RM + 10 μ M Y-27632 (24h)	/	MM (5 days)	/

For the co-culture using hu020, hu027 and hu028_2, the setup was simplified and it is represented in **Figure 6.1**.

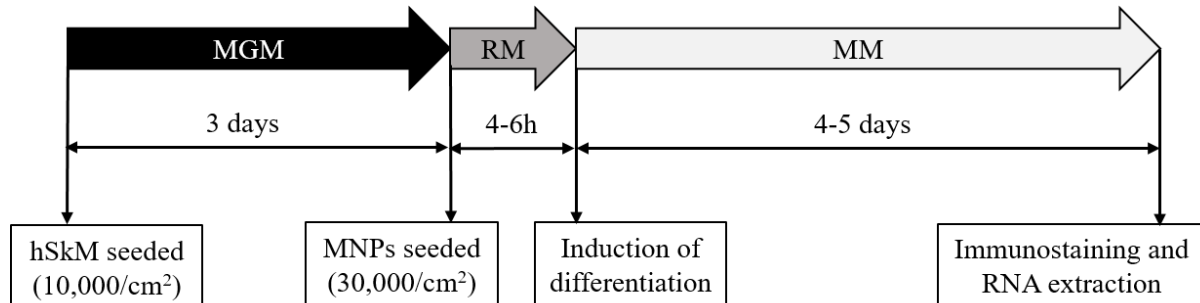


Figure 6.1. Co-culture protocol using hu020, hu027 and hu028_2 SkM cells. The muscle was seeded in MGM and expanded until confluent (3 days), then the MNPs were seeded on the layer of muscle in MN RM until adhesion was complete (4-6 hours). Finally, the cells were exposed to MM for 4-5 days to allow differentiation.

6.3.2 Human co-cultures in collagen/Matrigel® gels

Collagen constructs were generated using C2C12 myoblasts, with the method based around previous work from our group (Smith et al., 2016). Collagen hydrogels were formed by the addition of 85 % v/v type I rat tail collagen (First Link, UK; dissolved in 0.1 M acetic acid, protein at 2.035 mg/mL), with 10 % v/v of 10X minimal essential medium (MEM) (Gibco, UK). This solution was subsequently neutralised by the addition of 5 M and 1 M sodium hydroxide (NaOH) dropwise, until a colour change to cirrus pink was observed. The cells were added at a seeding density of 4×10^6 cells/mL in a 5 % v/v muscle growth medium (MGM) solution, before being transferred to the pre-sterilised inserts to set for 10-15 minutes at 37 °C. A scalpel blade was used to detach the constructs from the edges of the scaffolds, to ensure the only points of attachment were the posts. MGM was added for four days and changed daily, before being changed to muscle differentiation medium (MDM, DMEM, 2 % Horse Serum (HS), 1 % P/S) for a further 10 days in culture. Collagen/Matrigel® constructs were generated using human donor hu028_2 in removable 50 μ L scaffolds 3D printed via fused deposition modelling (FDM, see 2.2.3.2 for details). Gels were formed by the addition of 65 % v/v type I rat tail collagen, with 10 % v/v of 10X minimal essential medium (MEM) (Gibco, UK). This solution was subsequently neutralised by the addition of 5M and 1M sodium hydroxide (NaOH) dropwise, until a colour change to cirrus pink was observed. This was followed by the addition

of 20% v/v Corning® Matrigel® Matrix (Corning™ Matrigel™ Membrane Matrix). The cells were added at a seeding density of 4×10^6 cells/mL in a 5 % v/v MGM solution, before being transferred to the pre-sterilised inserts to set for 10-15 minutes in an incubator. MGM was added for four days and changed daily, before being changed to MDM for a further 10 days in culture. For co-culture gels, on the fourth day a new 50 μ L gel was prepared using the same protocol, but seeding MNPs into it at a density of 12×10^6 cells/mL. Upon removing MGM from the mould, and washing twice with sterile PBS, the gel was pipetted in the mould, ensuring total coverage around the previously set muscle gel. This was left in the incubator for 10-15 minutes to ensure setting, before adding MN RM (supplemented with 0.1 μ M RA and 10 μ M Y-27632) for 24h. On the fifth day, the medium was changed to MM (supplemented with 0.5 μ M RA, 5 ng/mL BDNF and 10 ng/mL CNTF) for a further 9 days to ensure differentiation.

6.3.3 Force measurement

To enable force measurement, constructs were prepared as follows. After being washed twice in PBS, one end of the construct was detached from the mould. The loose end of the construct was then attached to the force transducer (403A Aurora force transducer, Aurora Scientific, UK) using the eyelet present in the construct. The construct was covered (3 mL) with Krebs-Ringer-HEPES buffer solution (KRH; 10 mM HEPES, 138 mM NaCl, 4.7 mM KCl, 1.25 mM CaCl₂, 1.25 mM MgSO, 5 mM Glucose, 0.05% Bovine Serum Albumin in dH₂O, Merk, UK). Wire electrodes were positioned either side of the construct to allow for electric field stimulation. Impulses were generated using LabVIEW software (National Instruments, Berkshire, United Kingdom) connected to a custom-built amplifier. Maximal twitch force was determined using a single 3.6 v/mm, 1.2 ms impulse and maximal tetanic force was measured using a 1 second pulse train at 100 Hz and 3.6 v/mm, generated using LabVIEW 2012 software (National Instruments, UK). Data was acquired using a Powerlab system (ver. 8/35) and associated software (Labchart 8, AD Instruments, UK).

6.3.4 Confocal imaging

Confocal images were acquired using a Leiss LSM 880 microscope. All images were taken at 40x using an oil immersion objective. For tile scan images, a sequence of images of either 7x2 or 15x2 images were taken and then stitched together to create a single image. Z-stack images were taken longitudinally across the gel at 1.07 μ m thickness. Image analysis was

performed using the software Fiji (Java 1.6.0_24, available to download at <https://imagej.net/Fiji/Downloads>).

6.3.5 Cross sections preparation

The collagen/Matrigel® constructs were sectioned to perform morphological immunostaining. To do so, the gels were dehydrated over night in a 20% sucrose (Thermo Fisher Scientific, UK) solution in TBS 1x. The following day, the gels were layered on a glass slide (Superfrost® plus, Fisher, UK) covered in optimum cutting temperature medium (OCT, Thermo Fisher Scientific, UK) for adhesion. Then, isopentane (Merk, UK) which was previously cooled down with liquid N₂ was used to dip the glass slide and freeze the OCT and the embedded gels. A scalpel was used to cut the gel out of the OCT/isopentane matrix and place it on the microtome stage for sectioning. The sections were cut using a Shandon Cryotome SME (Thermo Fisher Scientific). The chamber temperature was set to -25°C and the sample temperature at -20°C. Sections 12 µm thick were placed on a new glass slide for immunostaining and imaging. Morphological staining was conducted as previously described (see sections 2.3.1.441 and 2.3.1.5).

6.4 Results

6.4.1 MNPs & human primary SkM co-culture in monolayer

The human MNP/SkM co-culture in monolayer was repeated four times, using three donors (hu020, hu027, and two different batches of hu028). Due to the variability in results, the outputs from these cultures are reported in two parts. In the first part, hu028 (batch_1) SkM cells were co-cultured with MNPs, both on the standard muscle substrate gelatin, and on the MNPs substrate SureBond™+ReadySet. Following the acquisition of these results, three co-cultures were performed on gelatin only (hu020, hu027 and hu028 (batch_2), as fewer myotubes were observed on SureBond™+ReadySet (see **Figure 6.4**).

6.4.2 Hu028_1 & MNPs co-culture in monolayer: preliminary cues on substrate and media compatibility

Co-culturing MNs with human primary SkM required extreme attention while expanding the two cell types in mono- and co-culture. First, different culture conditions were tested to identify what medium would allow more myotube formation, comparing the standard MDM and the MM used to induce MN maturation from MNPs.

Although MNPs did not adhere to gelatin (see **Figure 5.2**), the co-culture was performed on gelatin as well as SureBond™+ReadySet. As a result, MNPs adhered on the layer of hu028_1 myoblasts, indicating that the presence of a “neuronal-friendly” substrate is not a necessary requirement for co-cultures. Despite using standard MDM in Plate A, no myotube formation occurred on either substrate. However, when MM was used, a few myotubes formed (**Figure 6.2**), more abundant on gelatin than on SureBond™+ReadySet (**Figure 6.4**). Gelatin is commonly used to culture primary SkM, and the exact composition of SureBond™+ReadySet is unknown, thus suggesting that gelatin is a more suitable substrate than SureBond™+ReadySet.

In the co-culture **Figure 6.3** there was a notable increase in myotube number when the cells were either co-cultured or differentiated in MM as opposed to standard MDM (**Figure 6.4**).

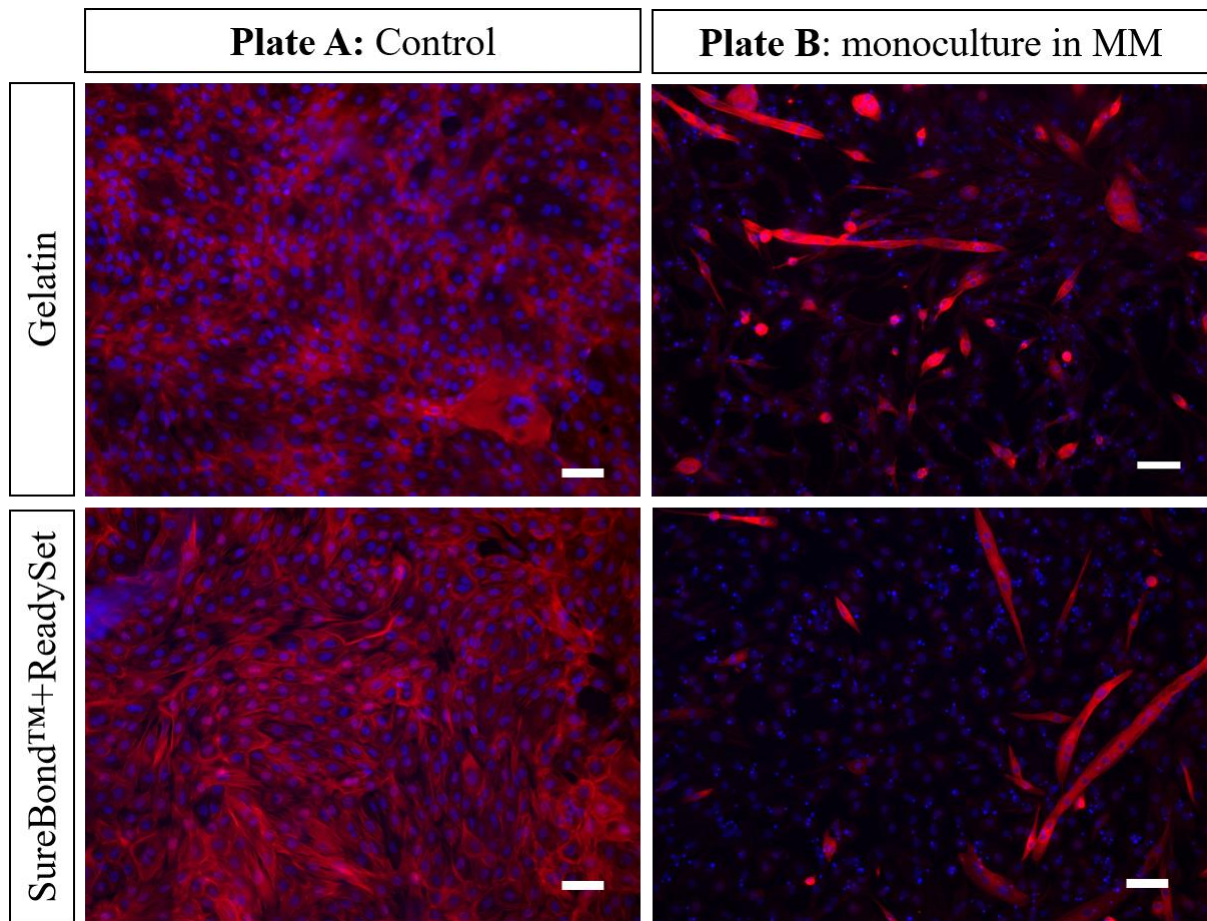


Figure 6.2. Human primary SkM cells hu028_1 cultured on gelatin and SureBond™+ReadySet. Plate A are muscle monocultures cultured in control conditions; plate B are muscle monocultures differentiated in MM. The cells were immunostained for morphological markers: rhodamine phalloidin was used to identify actin filaments in SkM cells (red) and the nuclei were counterstained with DAPI (blue). Scale bars: 100 μ m.

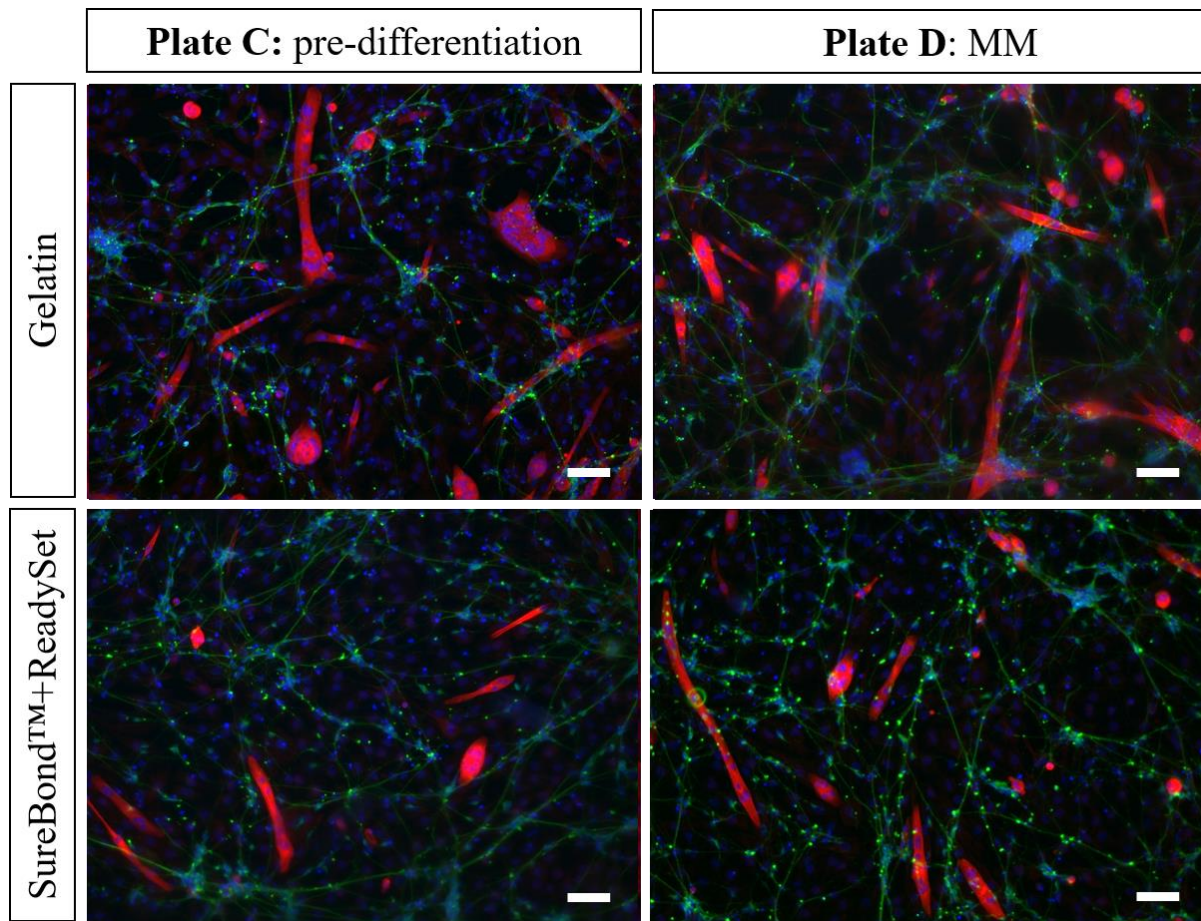


Figure 6.3. Human primary SkM cells hu028_1 and MNPs were co-cultured on gelatin and SureBond™+ReadySet. The SkM cells in plate C were pre-differentiated in MDM for 24h before adding MM to the co-culture. In plate D, the co-culture was differentiated with MM only. The cells were immunostained for morphological markers: rhodamine phalloidin was used to identify actin filaments in SkM cells (red), β -III Tubulin was used to highlight the cytoskeleton of the neurons (green), and the nuclei were counterstained with DAPI (blue). Scale bars: 100 μ m.

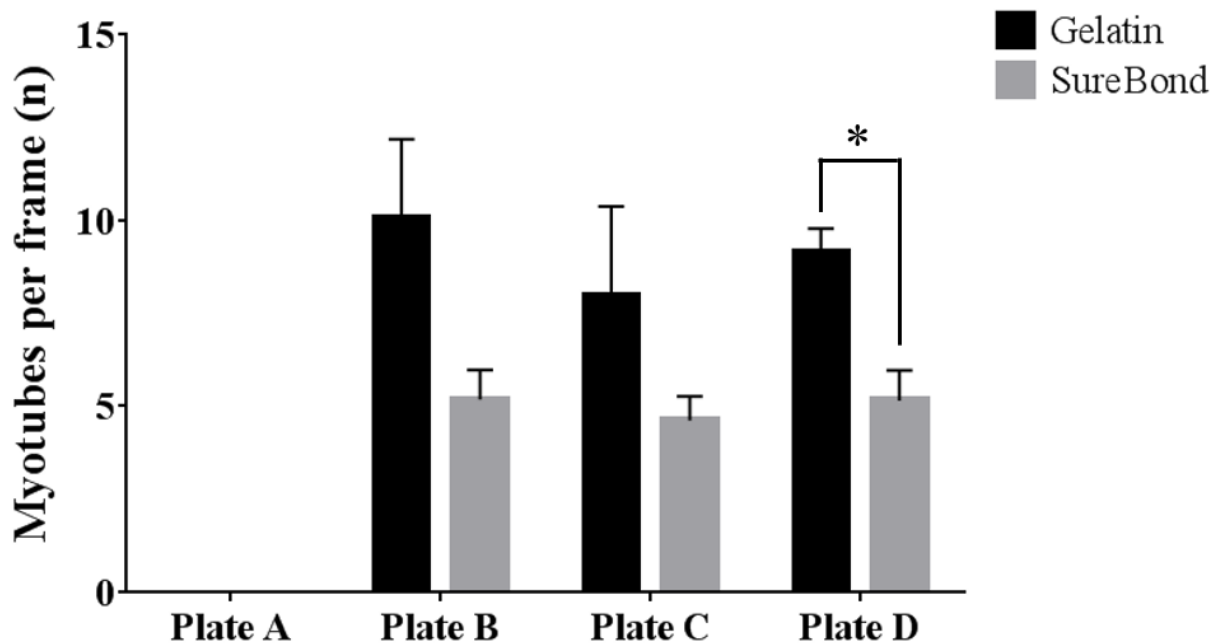


Figure 6.4. Number of hu028_1 myotubes per frame. The cells were differentiated in both standard and MM medium, on gelatin and SureBond™+ReadySet. The asterisk shows significant difference between samples: * = $p \leq 0.05$. This was found performing ANOVA and the Bonferroni post-hoc test. Results are shown as average \pm SD, n=3.

Despite the lack of differentiation in the muscle control, this experiment represented a valuable piece of information for future human primary co-cultures. In fact, it was interesting to observe the distribution of the MNPs around SkM fibres. At higher magnification, it was possible to notice how the neuritic extensions projected along the muscle fibres, as well as wrapped around them (**Figure 6.5**). This behavior was observed in all co-culture conditions.

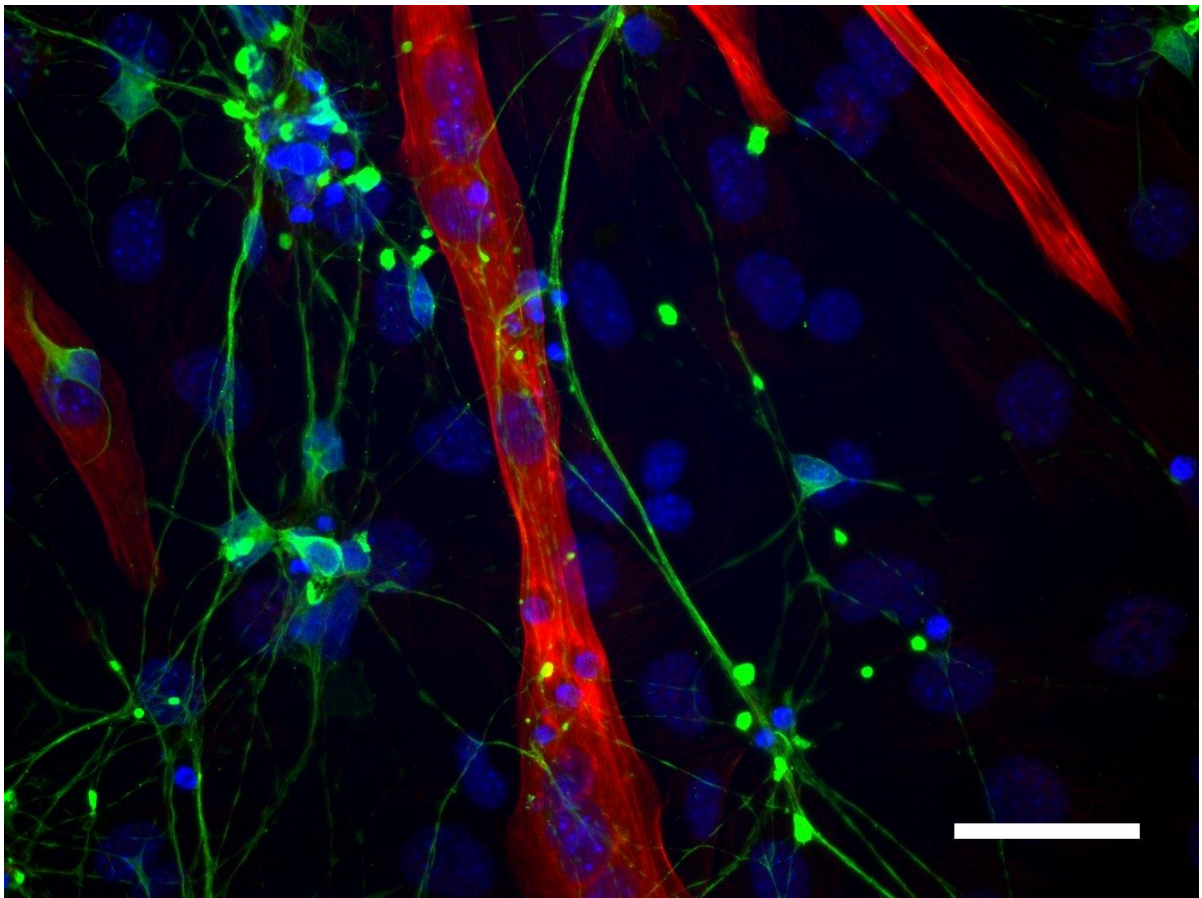


Figure 6.5. MNPs extend along and around hu028_1 myofibres (plate C). The cells were immunostained for morphological markers: rhodamine phalloidin was used to identify actin filaments in SkM cells (red), β -III Tubulin was used to highlight the cytoskeleton of the neurons (green), and the nuclei were counterstained with DAPI (blue). Scale bar: 100 μ m.

6.4.2.1 Hu020, hu027 and hu028_2 & MNPs co-culture: how do MNs affect SkM?

The second, third and fourth biological repeats of the co-culture were done using hu020, hu027 and hu028_2. This time, SkM cells were only seeded on gelatin as it was previously observed that MNPs adhere on the layer of SkM and therefore the presence of SureBond™+ReadySet as a substrate previously did not represent a crucial factor for the cells to proliferate in co-culture.

Morphological staining is shown in **Figure 6.6**. Donor hu020 did not differentiate in control conditions, just like the first repeat carried out with hu028_1 (**Figure 6.2**). This shows the unpredictable myogenic potential of primary cells. On the other hand, both hu027 and hu028_2 did differentiate in control conditions. When exposed to MM, hu020 formed myotubes which were comparable in number to the ones observed in the co-culture with MNs. The myotube width was quantified across all conditions and donors, and it is reported in **Figure 6.7**. The images show the difference in neuronal morphology when comparing between donors. The morphology of the MNs co-cultured with hu020 appeared comparable to what was previously observed (see Chapter 5). MNs on hu027 appeared to be peeling off during the mounting stage of the immunostaining, hence the spread morphology shown in **Figure 6.6**. Despite that, neurites can be observed extending along the direction of the muscle fibres. When MNs differentiated on hu028_2, they formed into cell aggregates from which neurites extended.

The 3 donors in monoculture (control), monoculture in MM and the co-cultures were also immunostained for pre- (SV-2) and post-synaptic (AChR) markers. All muscle donors expressed AChR's on their surface, both with or without neurons (**Figure 6.8**). The clusters appeared more sparse in control and MM conditions, and localised in the co-culture, as highlighted by the arrows in **Figure 6.8**. The MNs were stained by the anti-SV-2 antibody, but this also highlighted the cell body of the muscle fibres, indicating that aspecific binding occurred, and therefore suggesting the necessity to repeat this analysis in the future. However, MNs were clearly observed in close proximity to all SkM donors, but no overlap of the two markers was identified in this work.

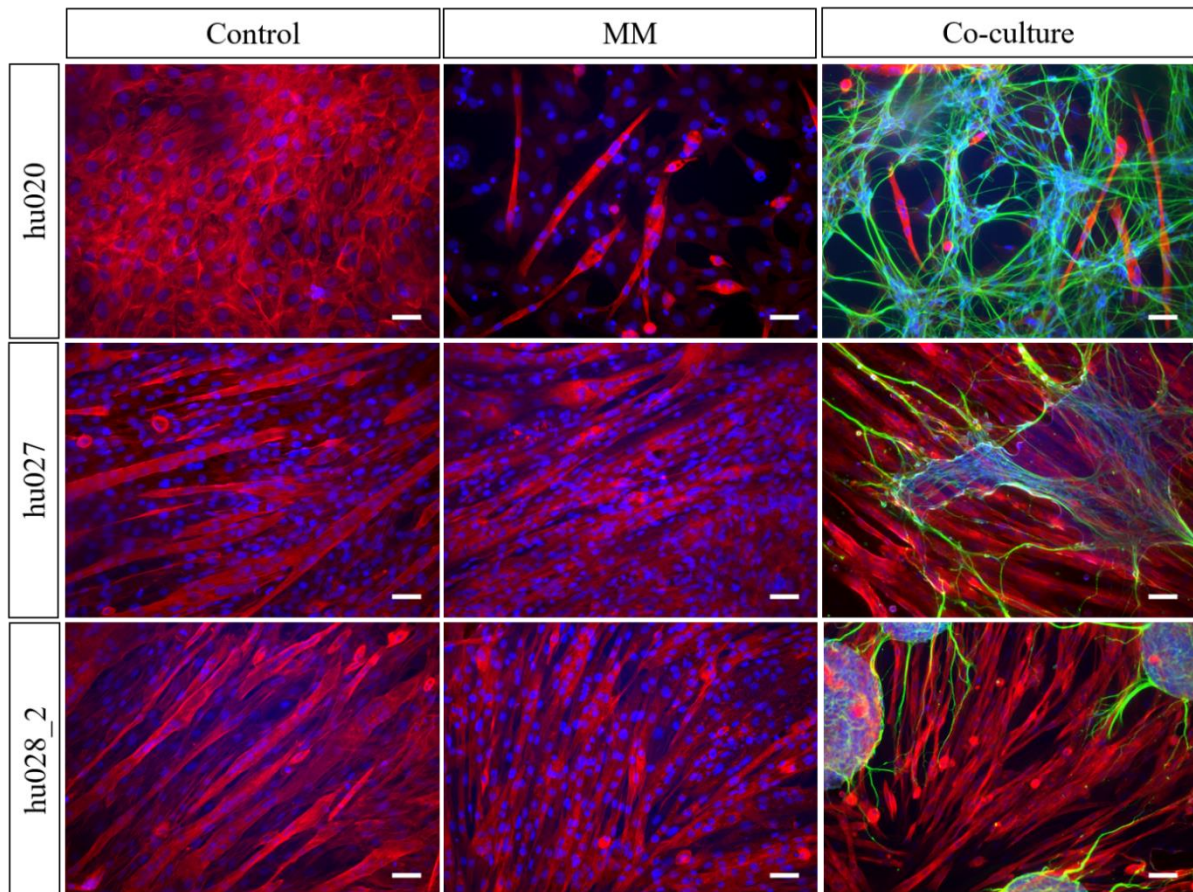


Figure 6.6. Human muscle-nerve co-cultures using hu020, hu027 and hu028_2 SkM cells and MNPs. The cells were immunostained for morphological markers: rhodamine phalloidin was used to identify actin filaments in SkM cells (red), β -III Tubulin was used to highlight the cytoskeleton of the neurons (green), and the nuclei were counterstained with DAPI (blue). Scale bars: 50 μ m.

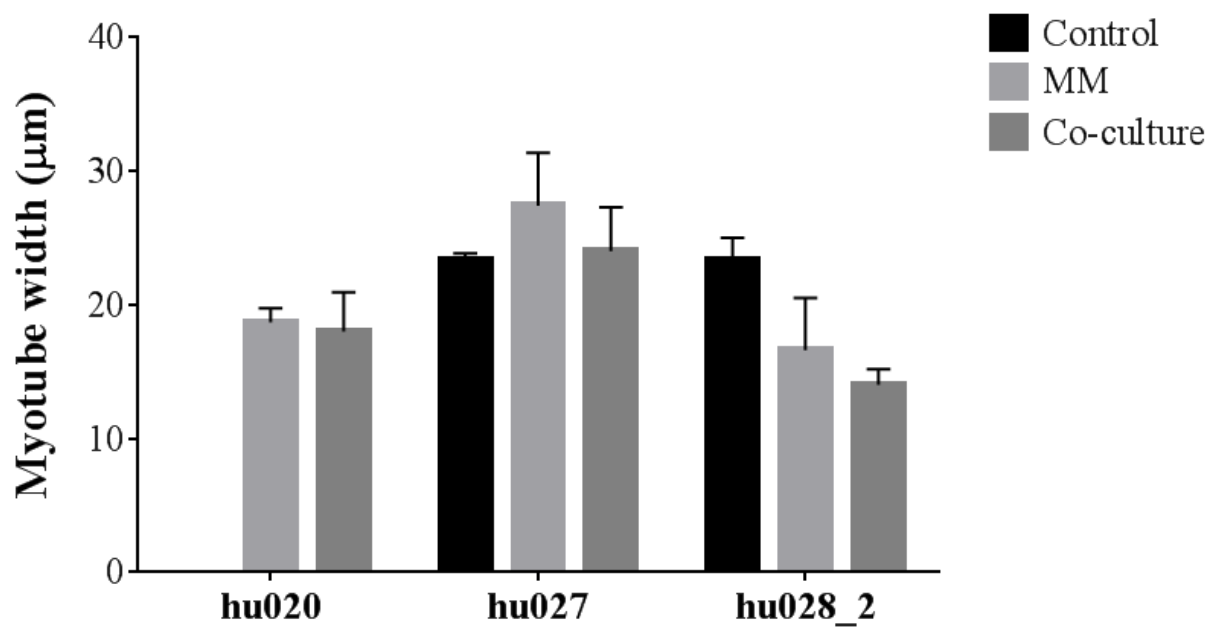


Figure 6.7. Myotube width (μm) of hu020, hu027 and hu028_2 in control, MM and co-culture conditions. The cells were cultured in control conditions (control), in Axol MM (MM) and in co-culture with MNPs in MM (co-culture). No statistical difference was observed within the same biopsy in different culture conditions when using 1 by 3 ANOVA. Results are shown as average \pm SD, n=3.

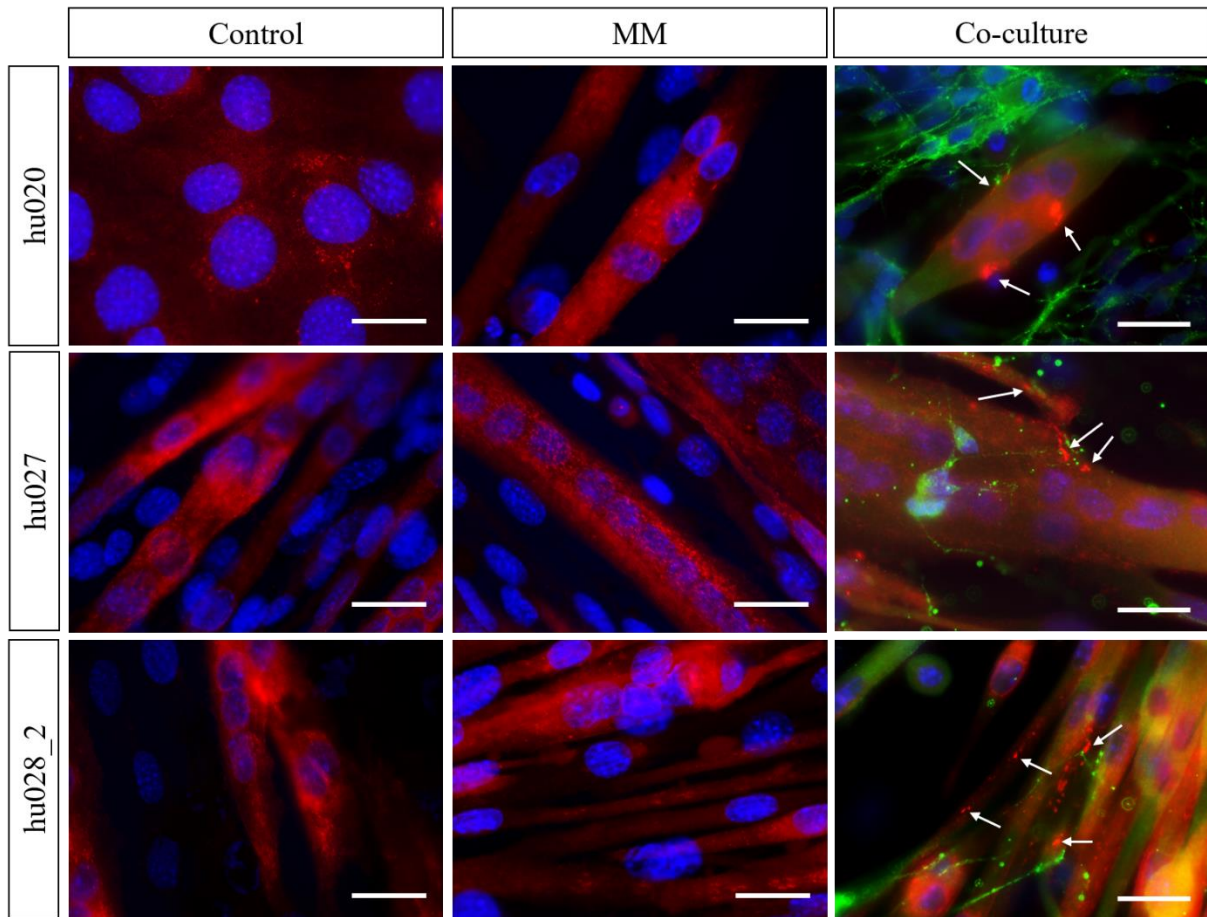


Figure 6.8. Interaction immunostaining of pre- and post-synaptic markers in human co-cultures. The cells were immunostained with pre- and post-synaptic markers: texas red-conjugated α -Bungarotoxin (BTX, red) was used for AChR clusters in all samples, synaptic vesicle 2 (SV-2) was used for ACh-releasing vesicles in iPSC-derived MNs (green) in the co-culture, and nuclei were counterstained with DAPI (blue). The arrows indicate AChR clusters on SkM fibres in co-culture. Scale bars: 25 μ m.

Gene expression analysis was carried out to investigate changes in MyHC8 (neonatal, **Figure 6.9**), MyHC7 (slow, **Figure 6.10**) and MyHC1 (fast, **Figure 6.11**) in both hu027 and hu028_2. Significant differences were observed in both biopsies and all genes, apart from MyHC1 expression in hu028_2. Generally, the cells expressed higher levels of the three genes when monocultured in MM. However, in the co-cultures with MNs, these levels of expression were depleted if compared to control or MM monocultures.

MyHC8 expression (**Figure 6.9**) in hu027 was 6-fold greater in MM cultures, than in control ($p < 0.001$). the decrease in expression from MM to the co-culture was also significant ($p < 0.0001$). Likewise, donor hu028_2 expressed 6 times more MyHC8 when cultured in MM, than in the control ($p < 0.0001$), and the decrease in co-culture was comparable to the one observed in hu027 cells ($p < 0.0001$). MyHC7 expression (**Figure 6.10**) showed a similar trend: the expression of MyHC7 in hu0274 doubled in MM ($p < 0.0001$) and was totally depleted in the co-culture ($p < 0.0001$ when compared to MM, $p = 0.0009$ when compared to the control). Hu028_2 cells showed comparable levels of expression in all samples, with a 2-fold increase from control to MM ($p < 0.0001$), a decrease from MM to co-culture ($p < 0.0001$) and from control to co-culture ($p = 0.001$). MyHC1 expression (**Figure 6.11**), which encodes for fast-twitching fibres, is affected in hu027, but not in hu028_2 cells. The increase in MyHC1 expression in hu027 cultured in MM, compared to the control, was 19 times higher ($p < 0.0001$), and then decreased when MNs were present in the culture ($p = 0.0142$ if compared to the control and $p < 0.0001$ if compared to MM). Interestingly, this great increase in MyHC1 expression was not observed in hu028_2, which maintained comparable levels of expression across all samples.

MyHC8

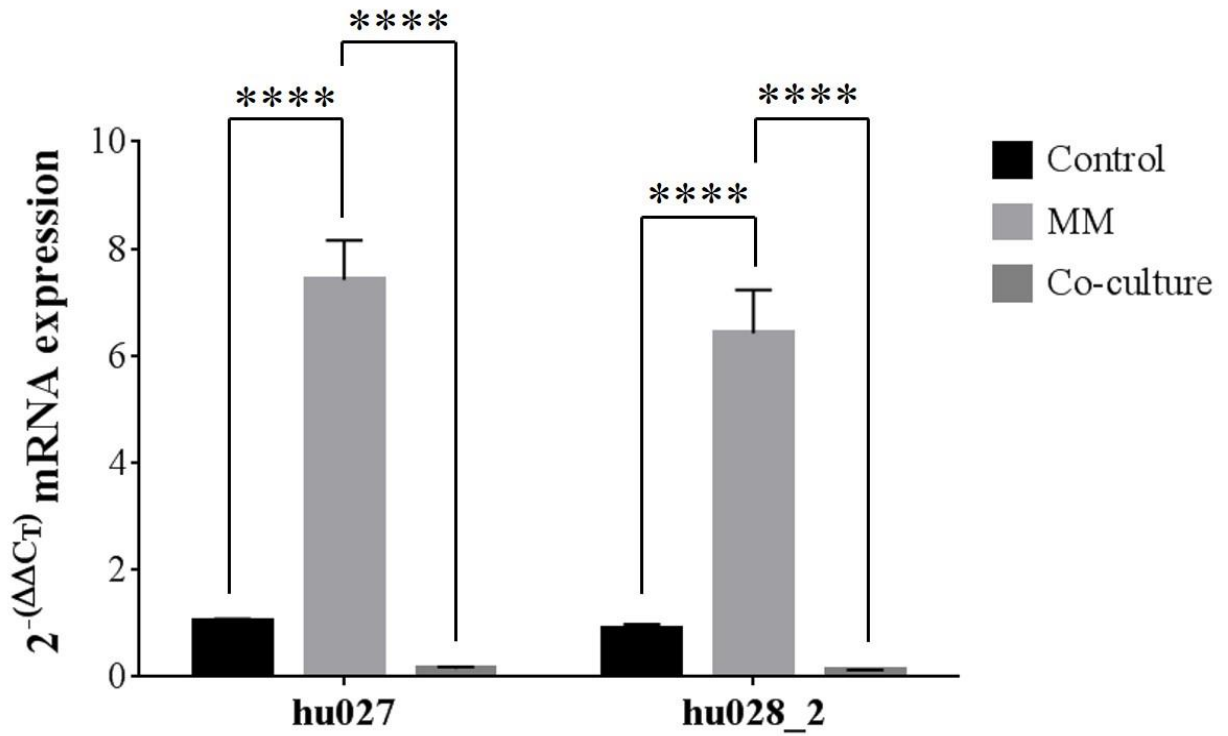


Figure 6.9. MyHC8 (neonatal) mRNA expression in human SkM hu027 and hu028_2. Asterisks show significant difference between samples: * = $p \leq 0.05$, ** = $p \leq 0.01$, *** = $p \leq 0.001$, **** = $p \leq 0.00001$ when using 1 by 3 ANOVA and the Bonferroni post-hoc analysis. Results are shown as average \pm SD, n=3.

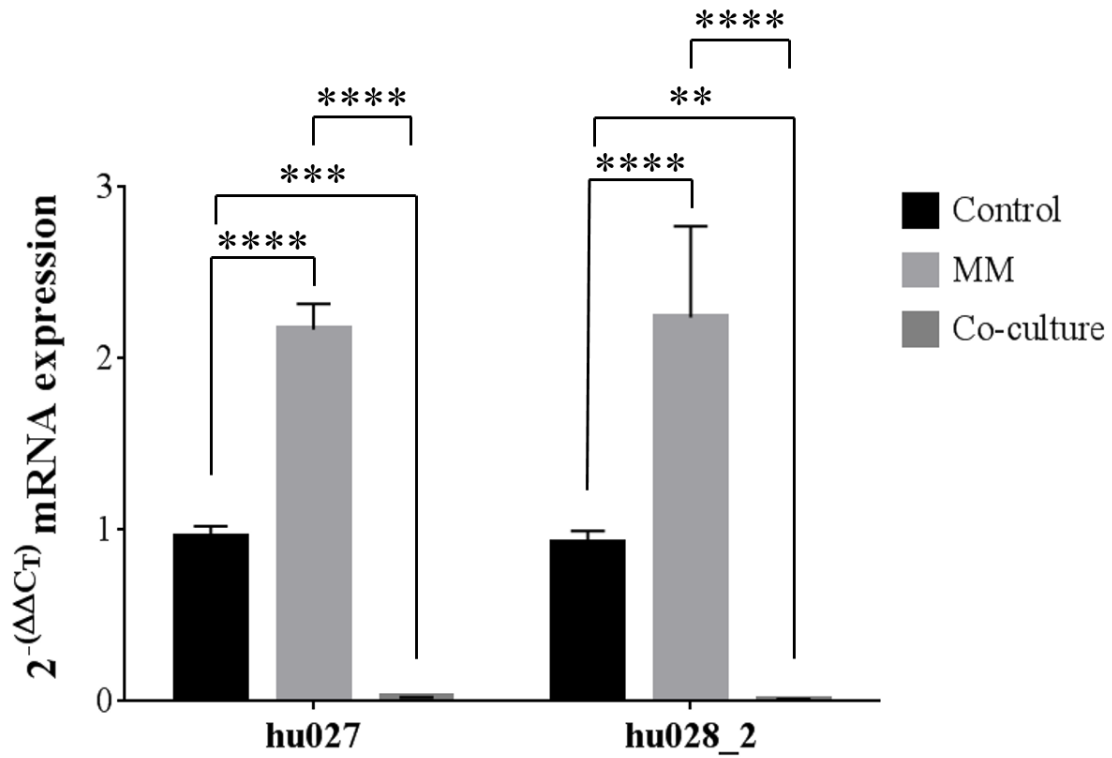


Figure 6.10. MyHC7 (fast) mRNA expression in human SkM hu027 and hu028_2. Asterisks show significant difference between samples: * = $p \leq 0.05$, ** = $p \leq 0.01$, *** = $p \leq 0.001$, **** = $p \leq 0.00001$ when using 1 by 3 ANOVA and the Bonferroni post-hoc analysis. Results are shown as average \pm SD, n=3.

MyHC1

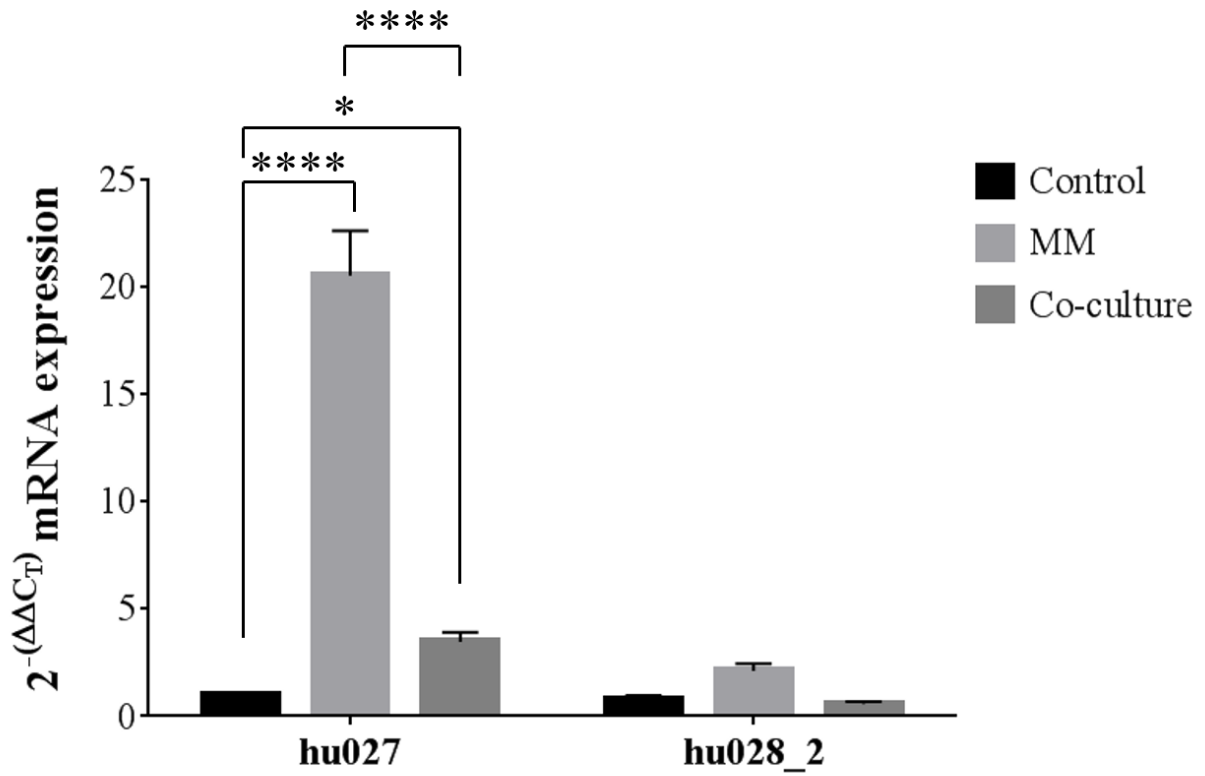


Figure 6.11. MyHC1 (fast) mRNA expression in human SkM hu027 and hu028_2. Asterisks show significant difference between samples: * = $p \leq 0.05$, ** = $p \leq 0.01$, *** = $p \leq 0.001$, **** = $p \leq 0.00001$ when using 1 by 3 ANOVA and the Bonferroni post-hoc analysis. Results are shown as average \pm SD, n=3.

6.4.3 The first attempt of a human muscle-nerve 3D co-culture

Upon co-culturing human-derived SkM cells and iPSC-derived MNs in monolayer, 3D tissue engineered constructs were used to attempt the establishment of a co-culture in a more complex, *in vivo*-like environment. Collagen gels based on previously shown constructs (see chapter 4.1) were scaled down from 500 to 50 μL in volume, and 20% Matrigel® was added to the mixture to enhance neuronal adhesion and extension. The neurons, instead of being seeded on top of the muscle gel as previously shown (Chapter 4), were seeded in a second gel which surrounded the first gel at day 4.

All gels gradually deformed throughout the 14-day period (**Figure 6.12**), and this was quantified as reported in **Figure 6.13**.

Morphological immunostaining showed differentiation of both hu028_2 and MNs within the gels. The use of both standard MDM and MM induced myotube formation in monoculture hu0285_2 gels (**Figure 6.14A** and **Figure 6.14B**). A gel with MNs only was also prepared to observe cell morphology and distribution within the matrix. The neurons extended neurites both in monoculture (**Figure 6.14C**) and in co-culture with hu028_2 (**Figure 6.14D**).

The myotube width of the cells in control conditions, or when the cells were differentiated in MM both in monoculture and co-culture is shown in **Figure 6.15**.

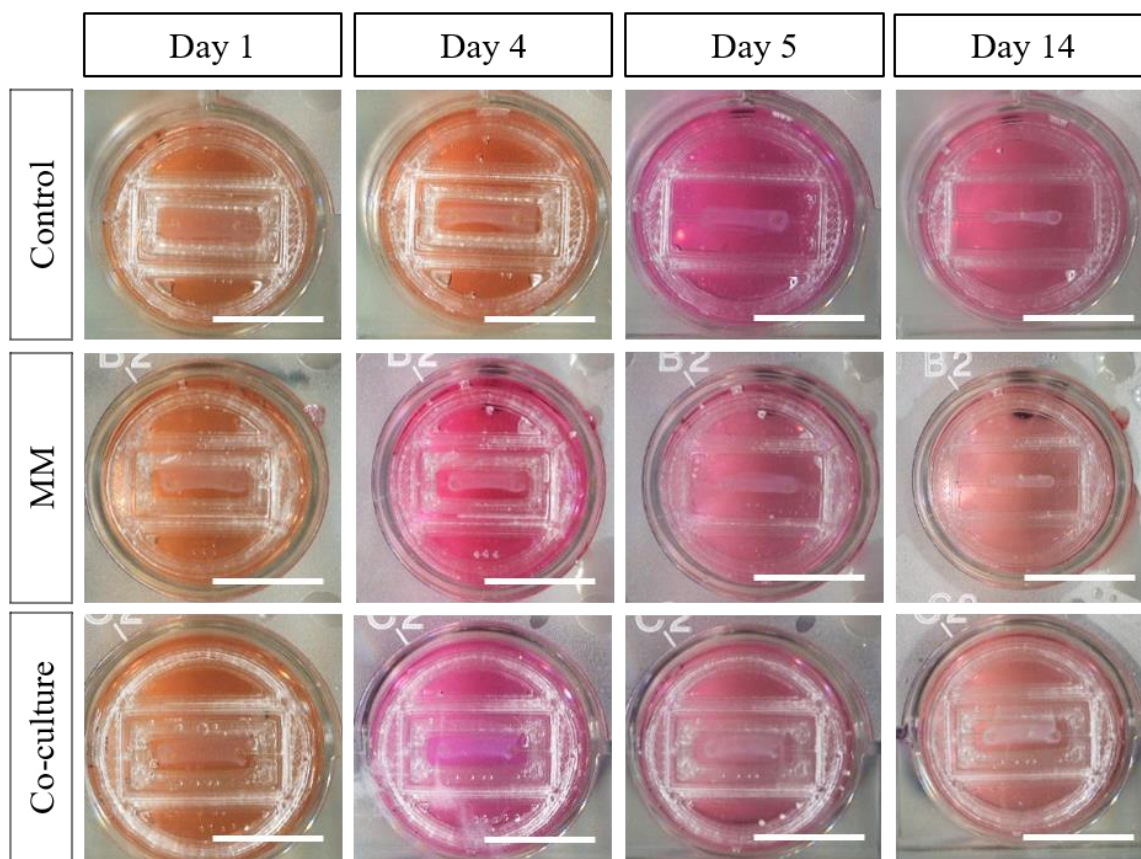


Figure 6.12. Collagen gels (50 μ L) with hu028_2 and MNs. Scale bars: 1 cm.

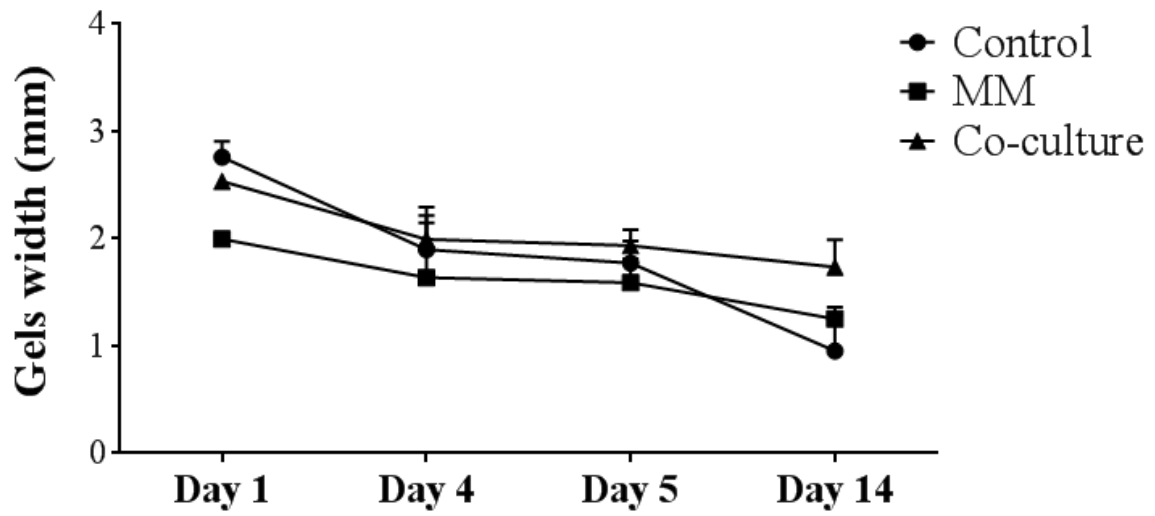


Figure 6.13. Collagen/Matrigel® gels deformation. Each gel was measured in the middle three times, and then averaged. Such values were then averaged to the other gels to obtain a final value. No difference was observed across the conditions at each timepoint when using the Student's t-Test. Results are shown as average \pm SD, n=2.

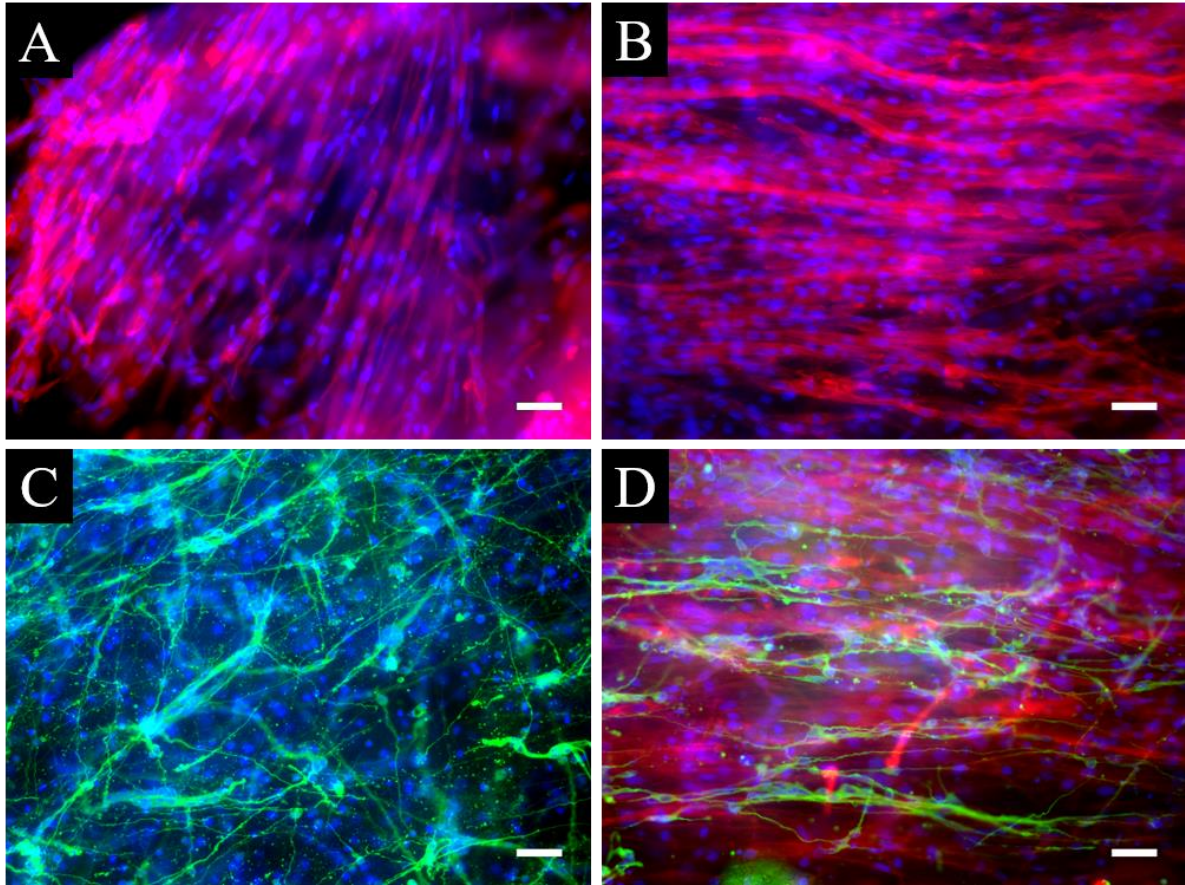


Figure 6.14. 3D culture of hu028_2 and MNs. The cells were immunostained for morphological markers: rhodamine phalloidin was used to identify actin filaments in SkM cells (red), β -III Tubulin was used to highlight the cytoskeleton of the neurons (green), and the nuclei were counterstained with DAPI (blue). Scale bars: 50 μ m.

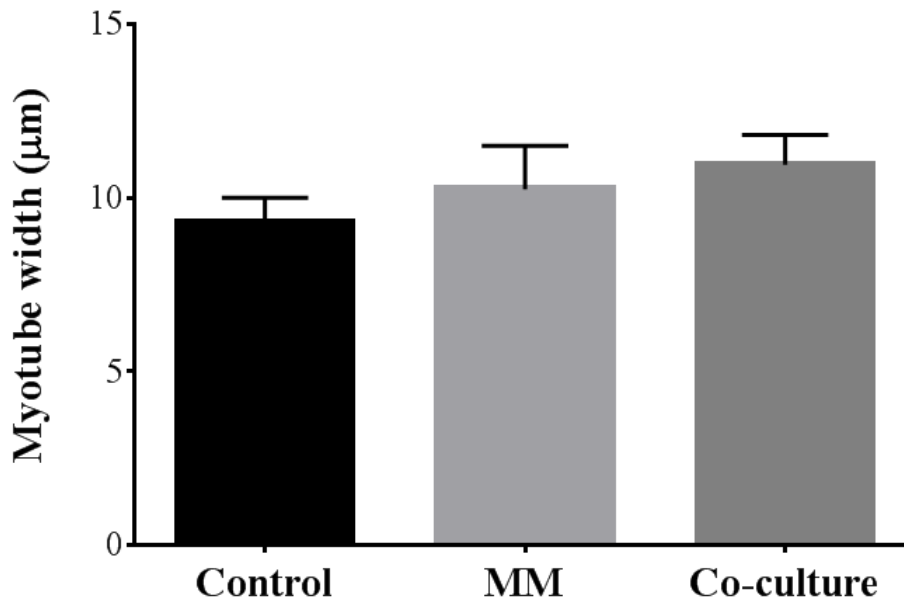


Figure 6.15. Myotube width (μm) of hu028_2 cultured in 50 μL collagen/Matrigel® gels. The myotube width was measured when the cells were cultured in control conditions (control), in MM (MM) and in co-culture with MNs (co-culture). No statistical differences were found across the conditions. Results are shown as average \pm SD, $n=1$.

The force traces generated from the electrical stimulation analysis are reported in **Figure 6.16**. One gel per condition was used to determine the force generated by the muscle within a control gel (hu028_2 monoculture), a MM gel (hu028_2 differentiated in MM) and a co-culture gel (hu028_2 and MNPs). During three tetanic stimuli, the maximum force generated by hu028_2 in the MM gel was higher than the one generated by the control gel. The co-culture gel generated the lowest amount of force (**Table 6.3**). Similarly, the co-culture gel generated a limited amount of force, if compared to control and MM conditions. However, upon administering a single stimulus to the gels, hu028_2 cells in control conditions generated more force than what the same cells in MM conditions did. Indeed, also upon single twitch stimulation, the signal from SkM in co-culture was merged to the background noise recorded.

Table 6.3. Maximum force (μN) generated by hu028_2 cells in 50 μL collagen/Matrigel® constructs. Results of the tetanus signal are shown as average, n=3 measurements from 1 gel per condition. The single twitch was repeated once per gel.

	Control	MM	Co-culture
Tetanus (100 Hz)	67.86 \pm 6.14	81.18 \pm 5.88	16.21 \pm 4.65
Single twitch (1 Hz)	36.27	22.59	4.07

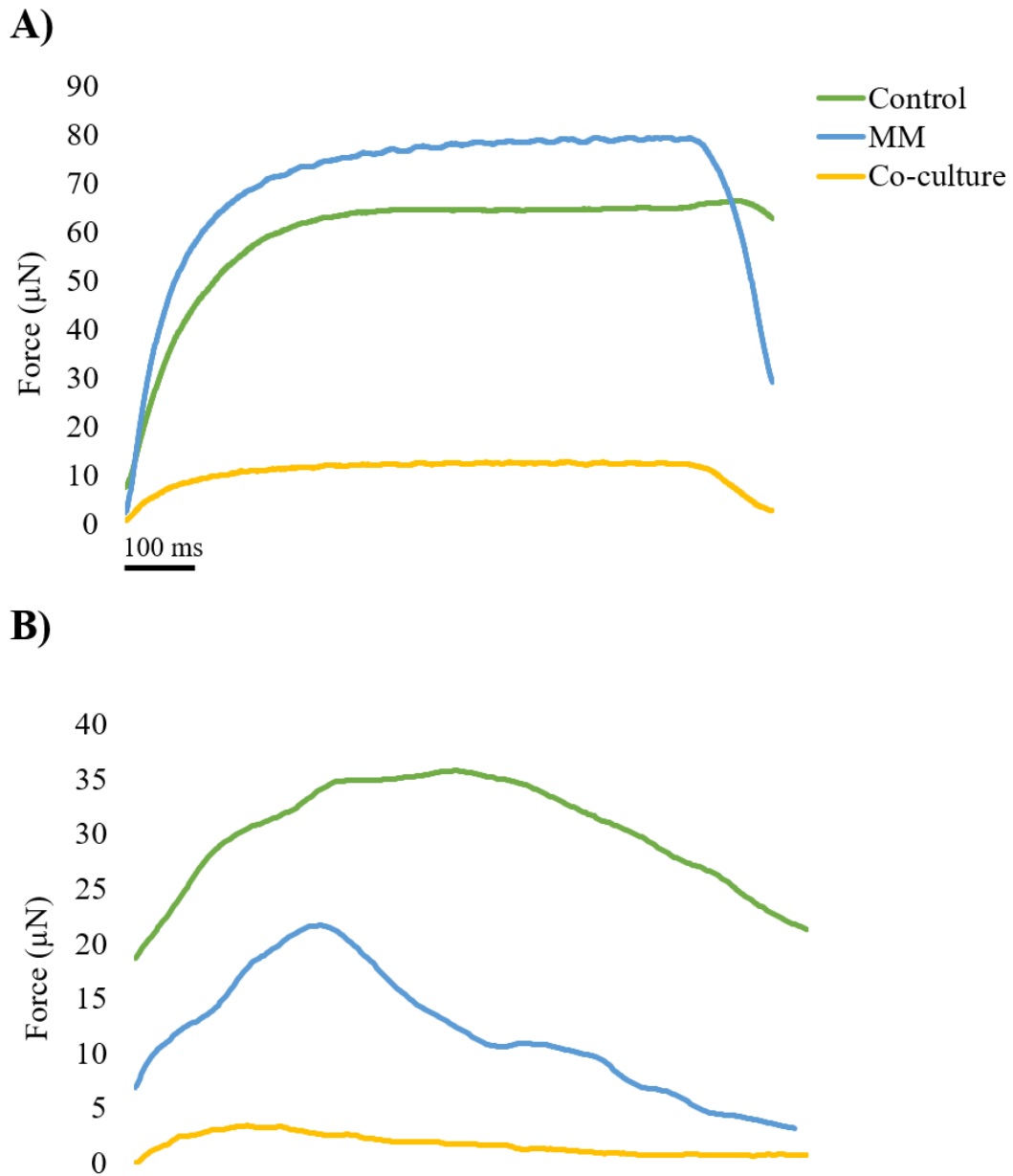


Figure 6.16. Contractility of hu028_2 cells in 50 μL collagen/Matrigel® gels. Maximal tetanic force (μN) was measured using a 1 second pulse train at 100 Hz and 3.6 v/mm (A) and maximal twitch force (μN) was determined using a single 3.6 v/mm, 1.2 ms impulse (B). The tetanus curves were generated by averaging the results from 3 stimuli on one gel. The single twitches were only repeated once per gel.

Subsequently, confocal imaging was utilised to determine the spacial organisation of the cells within the gel. Tile scans of all conditions are reported in **Figure 6.17**. Gels with hu028_2 monocultures, both control and MM, showed the presence of differentiated myotubes. The gel with MNs in monoculture also showed differentiation as generation of protrusions and neurite extension within the matrix. In co-culture conditions, the upper area showed a higher density of MNs, in accordance with the setup of the gel. Indeed, a second 50 μ L gel was set around the first SkM gel, thus showing the upper part of the tile scan predominantly made of neurons. The lower portion of the co-culture image shows myotubes and undifferentiated hu028_2 cells, suggesting that portion corresponds to the inner part of the gel.

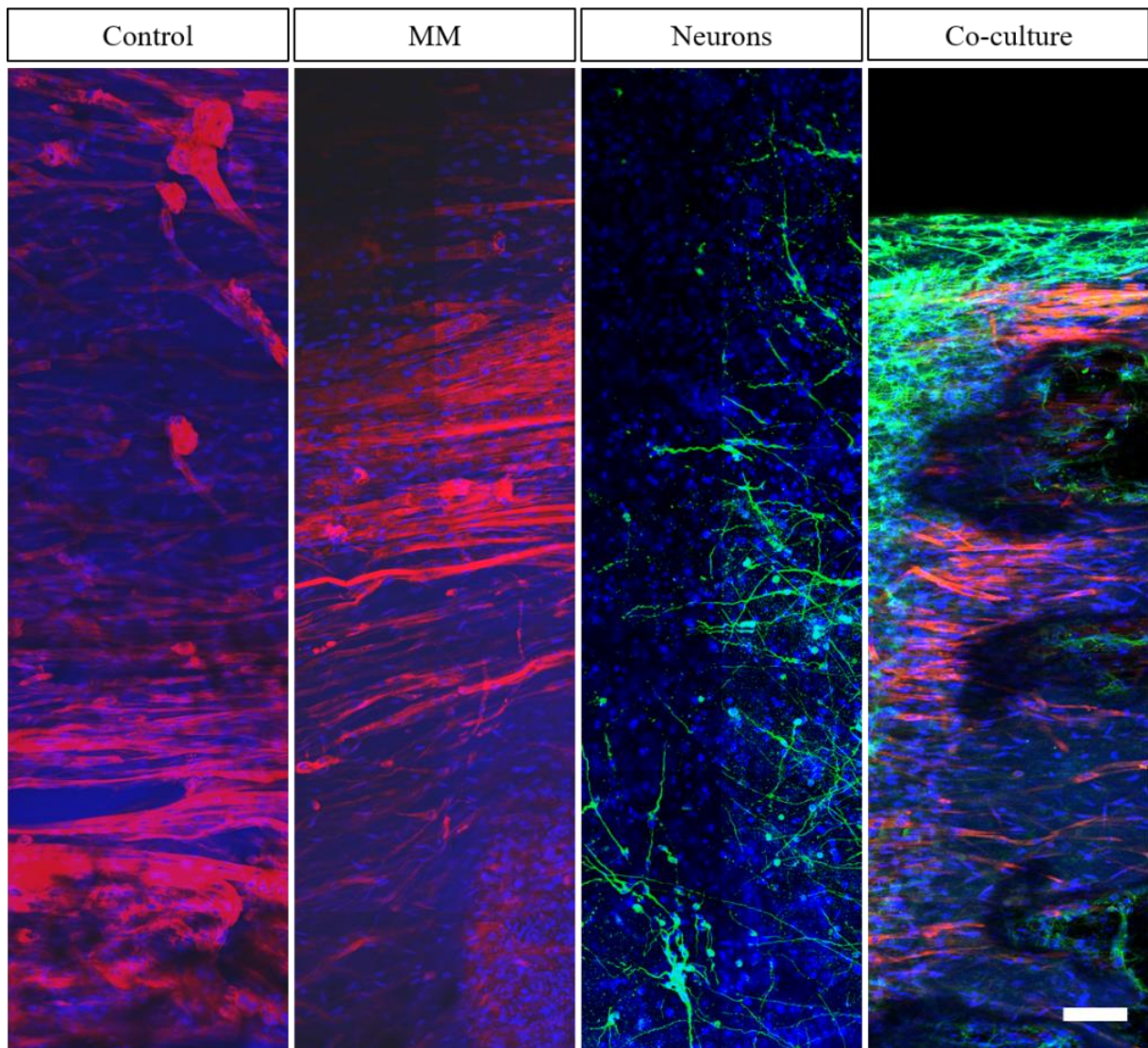


Figure 6.17. Tile scans of human 50 μ L collagen/Matrigel® constructs. The cells were immunostained for morphological markers: rhodamine phalloidin was used to identify actin filaments in SkM cells (red), β -III Tubulin was used to highlight the cytoskeleton of the neurons (green), and the nuclei were counterstained with DAPI (blue). Scale bar: 100 μ m.

A tile scan image of the co-culture gel shows the distribution of the cells at the interface between the outer neuronal gel and the inner muscle gel (**Figure 6.18**). Here, the separation of the channels showed the individual cell types across the full width of the gel. Although the β -III Tubulin immunostaining showed aspecific binding to the muscle fibres, it can be observed that the upper part of the image (corresponding to the outer section of the gel) was mainly characterised by the presence of MNs. On the contrary, the lower part of the image (corresponding to the inner, muscular portion of the gel) has a higher abundance of SkM cells.

The presence of both hu028_2 cells and MNs within the same snap shot of the tile scan also showed coexistence of the two cell types (**Figure 6.18**).

To verify this coexistence, 1.07 μ m thick sections of the gel were imaged (**Figure 6.19**). The Z stack began at the outer edge of the gel, within the neuronal gel region, whereby a high abundance of MNs was observed. The cells extended neurites within the matrix, suggesting differentiation (**Figure 6.19A** and **Figure 6.19B**). Image **C** shows the first visible myotubes, which are also reached by neurites (**D**), not just at the periphery of the muscle gel, but also within (**E** and **F**). Finally, observations on images **G** and **H** suggest that the abundance of myotubes at the opposite edge of the neuronal gel decreased, thus representing the other end of the outer neuronal gel, whereby less myotubes were observed.

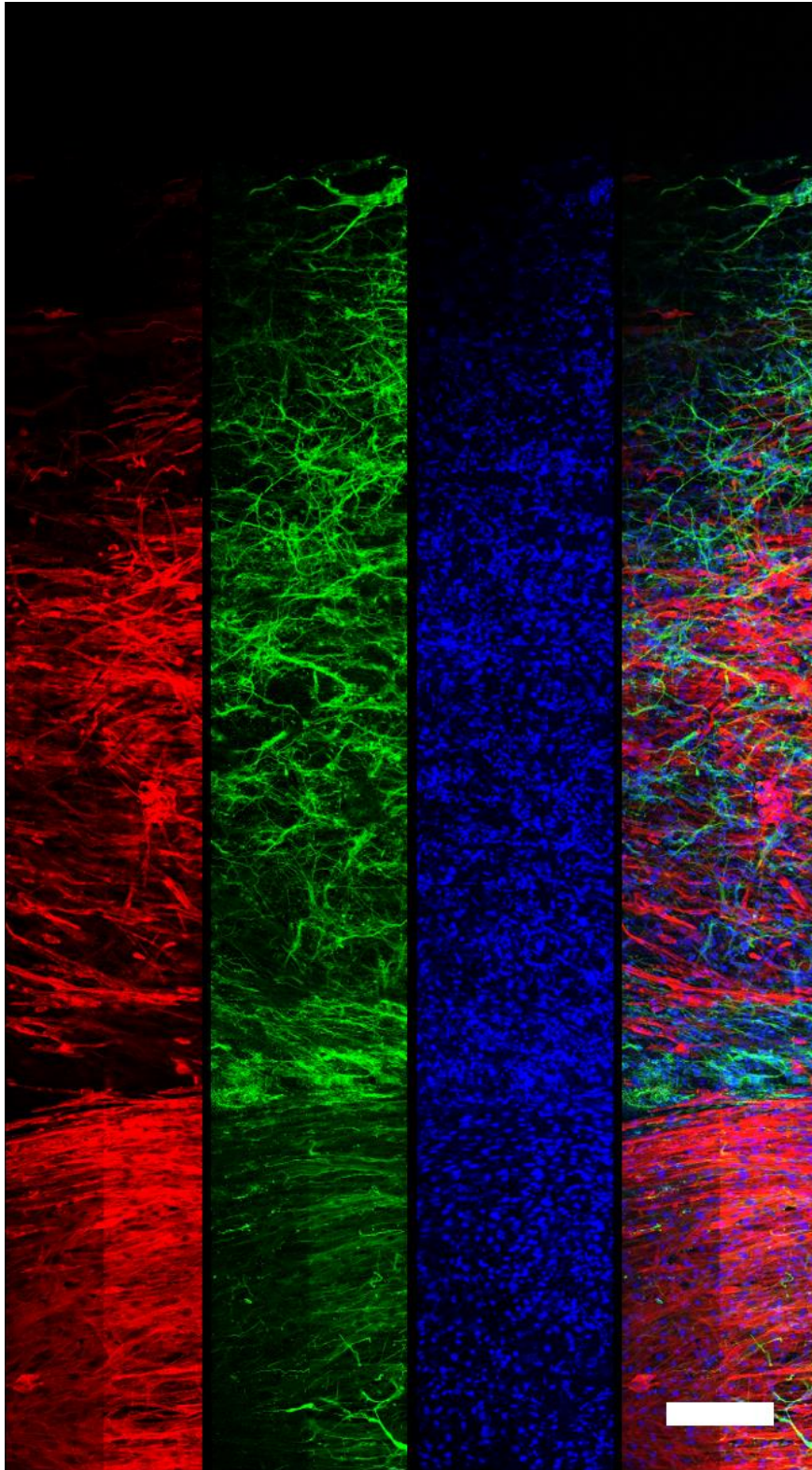


Figure 6.18. Morphological tile scan image of human co-culture gels. The cells were immunostained for morphological markers: rhodamine phalloidin was used to identify actin filaments in SkM cells (red), β -III Tubulin was used to highlight the cytoskeleton of the neurons (green), and the nuclei were counterstained with DAPI (blue). Scale bar: 100 μ m.

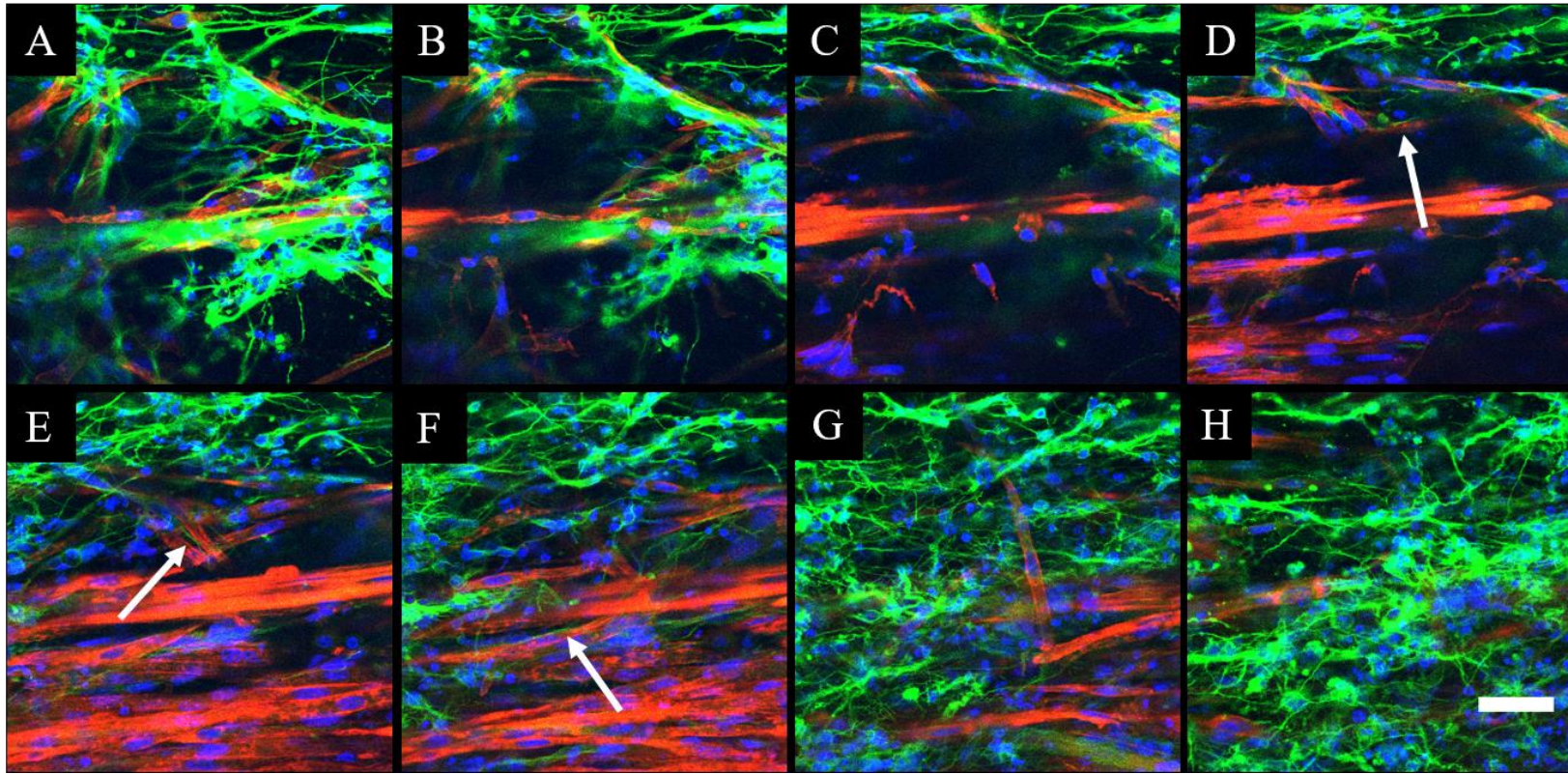


Figure 6.19. Z stack of co-culture gels acquired via confocal imaging. These 8 images were acquired running longitudinally across a 50 μ L collagen/Matrigel® co-culture gel (hu028_2 and MNPs), from the outer neuronal portion of the gel (A) to the interface between neuronal and muscle gel (D, E and F) until the other side of the neuronal gel (H). The cells were immunostained for morphological markers: rhodamine phalloidin was used to identify actin filaments in SkM cells (red), β -III Tubulin was used to highlight the cytoskeleton of the neurons (green), and the nuclei were counterstained with DAPI (blue). Scale bar: 100 μ m.

The distribution of the cells throughout the matrix was investigated by performing cross sections of the gels and immunostain them for morphological markers. As shown in **Figure 6.20**, a low magnification image (**A**) was taken to observe the general layout of the cells within the gel. Here, the neuronal, outer gel can be identified by the densely populated area at the edge of the gel. At higher magnification (image **B**), an empty inner area can be seen. A limited amount of muscle cells were visible within the muscle gel, however the edges of such gel were densely populated. Finally, an image of the edge between the two gels (**C**) shows a neuronal population confined within the outer gel and muscle cells, highlighted by white rectangles.

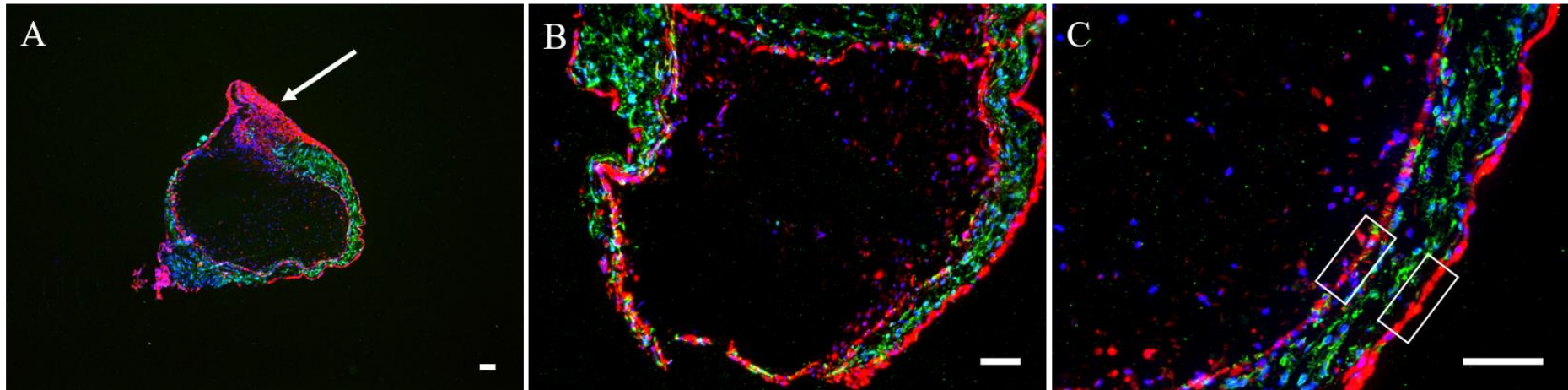


Figure 6.20. Cross sectional images of hu028_2 and MNs co-culture constructs. The cells were immunostained for morphological markers to identify their location across the gel: rhodamine phalloidin was used to identify actin filaments in SkM cells (red), β -III Tubulin was used to highlight the cytoskeleton of the neurons (green), and the nuclei were counterstained with DAPI (blue). Scale bar: 100 μ m.

6.5 Discussion

Since the discovery of a cocktail of factors which induces pluripotency in human fully differentiated cells (Yamanaka et al., 2007), the use of iPSCs to generate MNs increased. These cells were co-cultured in monolayer with the murine myoblast line C2C12 (Du et al., 2015) and a human myoblast cell line (Shimojo et al., 2015). However, the work carried out in this chapter highlights the optimisation of co-culture conditions for iPSC-derived MNs and human primary SkM cells. Despite the variability in SkM cells which is intrinsic in primary work, the progression of these co-cultures could lead to a better model for personalised medicine, whereby both SkM and skin are taken from the patient to generate an *in vitro* co-culture and test potential treatments before they are administered to the patient. First, the media and substrates used for the culture of MNPs were tested on human SkM cells. Then, 3 more donors were used to establish a 2D co-culture. Finally, the co-culture was performed in 3D tissue engineered constructs as part of preliminary work.

6.5.1 Substrate and media compatibility for human SkM co-cultures with human MNs

The co-culture optimisation carried out in Chapter 3 with C2C12 and SH-SY5Y showed that a layer of confluent myoblasts is crucial for the generation of myotubes. The principle behind this section is that the differentiation medium for iPSC-derived MNs (MM) will be used in the co-culture, and that the substrates on which neurons and SkM cells grow differ. While primary muscle grows on gelatin, MNPs require SureBond™+ReadySet to adhere and proliferate. Thus, it was necessary to establish the effects of the neuronal media and substrate on SkM cells, to optimise the co-culture conditions. Although the donor used in this section (hu028_1) did not differentiate in the control conditions, myotube formation was observed when the muscle was monocultured and co-culture with MNPs in MM. This indicates that the neurotrophic factors which supplement MM were beneficial to the myogenicity of this particular donor, even though desmin positivity was not investigated. A study on mouse embryos found that BDNF and CNTF enhanced muscle survival in aneural SkM cultures (Kablar and Belliveau, 2005). The co-cultures in this section were established using 2 approaches: plate C, where a pre-differentiation in MDM was carried out for 24h, before using MM, and plate D, where the cells were directly exposed to MM. This approach aimed to determine whether the exposure to gold standard MDM would affect myotube formation. Interestingly, when quantifying the number of myotubes per frame, no difference appeared across samples, indicating that the pre-

differentiation step was not necessary. No myotubes formed in the control, but hu028_1 exposed to MM in mono and co-cultures, showed some myotube formation. All samples were cultured on gelatin and on SureBond™+ReadySet. The trend across all samples showed that myotube formation was predominant in samples cultured on gelatin. Previous research indicated gelatin as a suitable substrate for primary SkM cultures (Brady et al., 2008). Even though the difference between the substrates was not significant, this information represented an important cue on how substrates can influence SkM differentiation. As a consequence, SureBond™+ReadySet was not used for subsequent co-cultures with MNs, as it was hypothesised that the neurons would have adhered on the layer of confluent myoblasts, rather than on the underneath substrate. In addition, previous work reported in the supplementary section, showed that long-term cultures of SkM on SureBond™ caused lower Desmin positivity and differentiation (**Figure S9.9**).

6.5.2 Human muscle-nerve co-cultures in 2D: cues on SkM maturation and the influence of MNs

The setup of iPSC-derived MNPs with three different SkM donors (hu020, hu027 and hu028_2) was established based on previous work (see supplementary **Figure S9.6** and **Figure S9.7**) SureBond™+ReadySet, the substrate used to culture MNPs for differentiation into MNs, was not used for this work as it had previously shown to reduce myotube formation and hinder myogenicity (**Figure S9.9**). Therefore, all co-cultures established in this section were based on gelatin as a substrate for muscle growth and differentiation. We hypothesised that the confluent layer of myoblasts would have provided the neurons with a substrate to adhere to, since it was extensively reported that myoblasts require cell-cell contact in order to fuse into myotubes. Thus, the neurons would not be in direct contact with the underlying substrate, whether this is gelatin or SureBond™+ReadySet. Although donor hu020 did not differentiate in the control, the presence of myotubes when the cells were differentiated in MM suggests that this medium can be used for myotube formation and it is more effective than conventional MDM. This was not surprising, considering that neurotrophic factors have been shown to be beneficial to SkM cells in terms of survival (Mousavi et al., 2002) and contraction (Matthews et al., 2009).

In the co-cultures, low magnification images allowed for the observation of the distribution of MNs on myotubes. The variability in the cells distribution can be attributed to the different substrates (i.e. SkM donors) the cells are seeded onto. The specific factor that is crucial for

these changes remains unclear, but we hypothesised that a more or less myogenic myoblast population could affect neuronal adhesion. The ECM of MNs comprises fibronectin, laminin, vitronectin, collagens and proteoglycans (Letourneau et al., 1994). Therefore, when culturing embryonic- or iPSC-derived MNs, surface coatings are required. The literature reported the use of Matrigel® (Sun et al., 2012; H Wichterle et al., 2002), mouse embryonic fibroblasts (MEFs) (Dimos et al., 2008; Ebert et al., 2009; Karumbayaram et al., 2010) or combinations of more substrates (Du et al., 2015; Reinhardt et al., 2013). These substrates are necessary for the neurons to adhere and interact with the underlying matrix. However, such substrates can be expensive, are animal-derived and vary in composition. The vast use of MEFs suggests that fibroblasts, which are responsible for the production of ECM components, favour neuronal adhesion. The distribution of MNs on donor hu020 appeared homogeneous and the neuronal network developed like in the monocultures previously established in Chapter 5. The low number of myotubes in hu020/MN co-cultures may suggest that the myogenic population in hu020 was lower, also confirmed by the lack of differentiation in control conditions. Fewer myogenic cells imply that a great portion of cells were non-myogenic cells, such as fibroblasts. Since these are the cells responsible for the production of ECM, having a less myogenic population compared to the other donors (hu027 and hu028_2) meant for the neurons that more ECM components were present in the culture and allowed them to adhere and extend neurites. In fact, where a higher number of myotubes was observed, MNs started to peel off the surface or rolled-up into neurospheres. These outcomes reinforce the need to continue to optimise co-culture conditions to favour NMJ formation, potentially by adding Schwann cells, which can support and stabilise MNs in culture (Bear et al., 2001).

The neuromuscular interaction immunostaining did not show any colocalisation of AChR and SV-2. This may be due to the necessity of improving the culture niche for both SkM and MNs so that a closer interaction can be identified. Colocalisation of pre- and post-synaptic markers was reported in mouse co-cultures (Toma et al., 2015; Umbach et al., 2012a) and in human MNs/murine SkM (C2C12) (Qu et al., 2014). In a human iPSC-derived MN co-culture with iPSC-derived SkM, the proximity between neurons and muscle was identified by β -III Tubulin and BTX staining (Demestre et al., 2015). Although this did not show pre- and post-synaptic interaction using BTX and SV-2, it highlighted how close the two cell types were, which is comparable to what was observed in this work. In addition, the observation of a more punctate

appearance of the BTX staining in co-culture, rather than in control or MM conditions, suggests that the presence of the neurons had an effect on the clustering of the receptors.

Investigating gene expression of MyHC's provides researchers with information on fibre composition, development and maturation, as specific isoforms coincide with specific sets of contractile and metabolic properties (Delbono, 2010). Adding MNs to a SkM culture aimed to enhance the expression of MyHC's which are related to such conditions. This analysis revealed that the use of MM enhanced the expression of MyHC8, MyHC7 and MyHC1. These markers identify genes which are expressed during the embryonic/fetal phase or regeneration (MyHC8 and MyHC7) and late fetal (MyHC1) in human (Schiaffino et al., 2015). The expression of MyHC8 in adult SkM is specific to specialised muscles, and MyHC7 encodes for type I fibres. The higher expression of these markers when the cells were cultured in MM indicates that the medium composition was ideal for muscle maturation in all 3 genes, with the exception of MyHC1 expression in hu028_2. Although the complete composition of MM is unknown to us, the supplementation with BDNF and CNTF may have influenced gene expression. The reduction in gene expression in the co-cultures was unexpected, and the reasons behind these results are poorly understood. However, it was reported that during regeneration, the switch from fast fibres (MyHC1) to slow fibres (MyHC7) can be controlled by neuronal activity, thus implying that when MNs are present, a higher production of slow fibres is expected instead of fast ones (Esser et al., 1993). Preliminary results conducted in this thesis showed a reduction of both fast and slow fibres gene expression, thus requiring further studies to investigate more markers and SkM donors.

6.5.3 The first attempt to establish a human muscle-nerve co-culture in 3D

Animal models of the NMJ have elucidated several aspects of it, such as its structure and function, or protein changes which cause pathological conditions. Mice have been particularly useful for their size and relatively manageable for handling and analysis (for an extensive review see Webster, 2018). However, it was recently shown that the NMJ in lower animals and in humans differs under many aspects. For instance, the morphology is different, human NMJ's are stable throughout the adult lifespan, if compared to humans, and the proteome is not entirely conserved (Jones et al., 2017). Therefore, developing a human model of the NMJ represents a great advantage over animal models, not just because understanding the physiology of the same species is more accurate using that species' tissues, but also because using patient-specific SkM

and MNs would closely mimic one's particular pathology. Previous models were mainly generated in a 2D environment, whereby the cell-cell and cell-matrix interactions were limited, and the applicability for functional studies was also a challenge. Here, a single, but crucial attempt to generate a 3D model of the NMJ using human cells was carried out. First, a novel, biocompatible collagen construct was used, adapted from previous work which proved the suitability of this system for SkM tissue engineering (Smith et al., 2016) and NMJ studies (Smith, 2012). Immunofluorescent staining highlighting the morphology of the cells within the construct, showing differentiation of both hSkM and iPSC-derived MNs, in monoculture and in co-culture. In particular, SkM myoblasts fused into aligned myotubes both in standard MDM and in MM, conventionally used for the differentiation of MNPs into MNs. This confirmed the outcome previously obtained in 2D. Although there was no significant change in matrix remodeling or myotube width, the differentiation in MM did have an effect on the functionality of the muscle. The augmented force generation when the muscle was differentiated in MM, and reduced when in co-culture, reflect the 2D gene expression results which showed a net increase in gene expression when different donors were cultured in MM. This confirmed the maturation increase due to the medium composition, but did not explain why the addition of the neurons depleted force generation. This outcome may be due to the mechanics of the system. When adding a second gel around the first one, further deformation was impaired and the cells were not able to pull on either side of the construct as they could do in control or MM conditions. A previous model of the NMJ using primary rat cells showed an increase in force generation when MNs were co-cultured with SkM conditions (Martin et al., 2015), thus suggesting that seeding the cells on the surface of the gel may be a more suitable approach to maximise twitching. Subsequently, a combination of confocal microscopy and cross sections were used to gather information on the distribution of the cells within the gel. Confocal imaging appeared to be misleading when determining the location of the cells and their interaction within the matrix. Due to the sample preparation for this type of analysis, the gels were pressed between the glass slide and the coverglass, thus filling the necrotic gap in the middle of the gel and giving a non-realistic view of cell-cell proportion. In previous work, cross sections of collagen-only constructs with primary rat cells, the distribution of the muscle cells appeared homogeneous, whereas the amount of MNs was limited and confined to the top edge of the gel (Smith, 2012). In this work, the same analysis revealed an empty area in the centre of the gel, distribution of muscle cells along the outer edges of both the inner, muscle gel, and the outer, neuron gel. Compared to previous work (Smith, 2012), these results, although not conducted

the same way, showed a totally different cell distribution, but a much greater portion of neurons and neuronal extension. Necrotic areas in the middle of the gel were previously observed (Juhas and Bursac, 2014) and a population of fibroblasts was identified among the cells which migrated towards the periphery of the construct. This distinction was not performed in this work, but immunostaining using specific markers could provide more information on the distribution of different cell types. This represents a promising starting point whereby the interactions between SkM and MNs are favoured, even though further optimisation and repeats are necessary.

6.6 Chapter summary

The co-culture work carried out in this chapter provided important information regarding media and substrate compatibility, and the influence of iPSC-derived MNs on human primary SkM cultures. Utilising 3 different donors, one of which was used in 2 batches, was crucial and highlighted how variable primary cultures can be. Here lays the challenge of this work, establishing a primary co-culture which allows for differentiation of 2 very diverse cell types in a well-defined environment. The first part of the chapter highlighted that the medium used for the differentiation of MNPs into MNs was beneficial to the differentiation of SkM. This was further confirmed in the second part of the chapter. This difference was not only visible from a morphological point of view, but reflected on the expression pattern of 3 MyHC's. These appear at different stages during SkM development and can be used to address the effects of the different culture conditions on muscle maturation. Although moving from cell lines to primary cells was a great progression, the lower variability observed in the morphology of MNs in co-cultures highlighted the necessity to further optimise the co-culture conditions. Future work may be focused on introducing a third cell types into the system, in order to support MNs and enhance muscle-nerve interactions. When translating the co-culture from 2D to a 3D system, the differentiation of both SkM and MNs was obtained, and neither the myotube width or the matrix remodeling were impaired by the use of neuronal medium or the presence of the neurons themselves, if compared to a standard muscle-only gel. Areas of proximity between the two cell types were identified, thus showing migration of the cells within the matrix. In fact, both aligned myotubes and extended neuronal projections formed in co-culture gels. The interface between SkM and MNs showed that both cell types coexisted in a 3D environment which is suitable for their differentiation.

7 GENERAL DISCUSSION

The investigations conducted in this thesis allowed for the generation of muscle-nerve co-cultures using different cell sources and culture conditions. Initial optimisation and proof of concept work was conducted using a murine myoblast cell line, C2C12, which is widely used for SkM studies, and a human neuronal cell line, SH-SY5Y. The ultimate aim of this work was to establish a human-human muscle-nerve co-culture. Thus, C2C12 were eventually replaced by primary human SkM, and SH-SY5Y by a human stem cell source of MNs. Culturing these cells both in monolayer and in 3D tissue engineered constructs, enabled for the development of a system which potentially promotes NMJ formation. This model could be used *in vitro* as a tool for drug screening studies, as well as to understand the mechanisms underpinning physiology and pathophysiology of the NMJ.

To date, common NMJ models are either based on the use of animals, animal-derived cells, or human embryonic stem cells (Lu et al., 2015; H Wichterle et al., 2002). The initial chimeric co-culture using C2C12 and SH-SY5Y cells was essential to generate information and expertise in the culture of heterogeneous cell types in monolayer and in two different kinds of 3D tissue engineered constructs. These constructs were shown to be suitable for SkM culture as they resemble the mechanical structure of the musculoskeletal tissue, allowing for the cells to mature and align in an *in vivo*-like matrix (Player et al., 2014). In addition, muscle-nerve co-cultures were also performed within these constructs to generate a NMJ *in vitro*. However, 3D co-cultures using human SkM and human MNs were not reported, to the best of our knowledge. The generation of pluripotent stem cells from an adult cell source allowed for the differentiation of several cell types including cardiomyocytes (BurrIDGE et al., 2015), SkM (Maffioletti et al., 2015), endothelial cells (Patsch et al., 2016), hepatocytes (Si-Tayeb et al., 2010), pancreatic β cells (Zhang et al., 2009), lung epithelial cells (Huang et al., 2014) and different types of neurons (Chambers et al., 2009; Ma et al., 2011; Shi et al., 2012). This was achieved without requiring embryos and expensive, time-consuming procedures. Although some challenges still remain, protocols for the generation of MNs from iPSCs were reported (Du et al., 2015; Karumbayaram et al., 2010). Such protocols show common features (i.e. the use of neurotrophic factors or similar coating solutions), but mostly differ in terms of the length of the neuronal induction/differentiation steps, and the concentrations of supplements and media composition. Therefore, the reproducible generation of MNs which are suitable for commercial use is still

limited. Establishing a collaboration with Axol Bioscience (Cambridge, UK) was a crucial aspect for the completion of this work. Axol provided us with iPSC-derived MNs in order to characterise the cells and co-culture them with human SkM. After determining that the cells can be cultured for extensive periods of time, and that they express two commonly tested cholinergic markers, they were co-cultured with primary human SkM in monolayer and in collagen/Matrigel® hydrogels.

The final aim of this work was to establish a human 3D *in vitro* model of the NMJ. This was achieved partially by utilising human sources of SkM and MNs within a 3D environment. Future studies would be essential to further investigate the interactions between the cells and complete the model using an additional neuronal population which sustains MNs both *in vivo* and *in vitro*.

7.1 Key findings

The use of C2C12 for studies on SkM physiology and co-culture with neurons is extensively reported (Blau et al., 1985; Burattini et al., 2004). Also, SH-SY5Y were used as a cholinergic neuronal population which made them suitable for preliminary studies in this work (Adem et al., 1987; Pählman et al., 1984). The differentiation of SH-SY5Y cells requires the use of RA in culture, which is linked to development and neuronal outgrowth within the nervous system (Rhinn and Dolle, 2012). However, the effect of RA on C2C12 appears to be controversial in the literature, as some reported that it promotes muscle differentiation (Albagli-Curiel et al., 1993), others believed that it caused an atrophic phenotype (Pardo-Figueres, 2017) or reduced its maturation (El Haddad et al., 2017). Thus, the first aim of this thesis was to establish optimal conditions for the co-culture of C2C12 and SH-SY5Y in a 2D environment, by testing the mostly used concentration for SH-SY5Y differentiation (10 μM), and dilutions of it (5 and 1 μM). Testing a medium to use in the co-culture, supplemented with different concentrations of RA, allowed for the definition of a medium which can be used to achieve both muscle and neuronal differentiation. The data collected in this work suggested that by lowering the concentration of RA, longer neurites and wider myotubes form in monoculture. Interestingly, when the cells were co-cultured, these values increased and were comparable to the control for C2C12, and higher than the control for SH-SY5Y. Thus, the concentration of RA used for both SH-SY5Y monoculture and the co-culture with C2C12 was 1 μM . Another crucial aspect that was observed was the distribution of the cells in culture. SkM is a highly aligned tissue *in vivo*,

where several fibres are bundled together to form a greater structure which contracts all together in the same direction. Monolayer cultures do not allow for control on cell alignment, although small areas of aligned myotubes were observed. When SH-SY5Y are monocultured, they spread across the culture well and extend neurites in all directions, whereas when seeded on a layer of C2C12 myoblasts, the process of differentiation induces the cells to align to the direction of the myotubes. The behaviour of the neurons suggests that the myofibres represent a topographical cue for them to follow, and this happened even in monolayer cultures.

In terms of interaction between C2C12 and SH-SY5Y cells in monolayer, the immunostaining with BTX (to highlight AChR's) and SV-2 (for the ACh-transporting vesicles) showed limited colocalisations areas of the two markers. Observing these colocalisations would have indicated a close interaction of the two cell types, via a link between the vesicles which are responsible for the release of the neurotransmitter on the pre-synaptic cells, and their own receptor on the post-synaptic membrane. It was then hypothesised that the use of a supplement could increase the incidence of these interactions and could be used when culturing the cells in 3D tissue engineered constructs. The addition of agrin to the differentiation stage was thought to be beneficial to C2C12 maturation, verified by looking at common developmental and differentiation gene expression. Agrin is a main component of the NMJ, where it promotes the aggregation of AChR's in the middle of the muscle fibre surface (Daniels, 2012). Aggregation of AChR's is essential for NMJ formation, as these aggregates are the binding site for the neurotransmitter ACh, which is released by MNs to induce depolarisation of the post-synaptic membrane, release of intracellular Ca^{2+} and, eventually, muscle contraction (Wu et al., 2010). The addition of agrin in muscle-nerve co-cultures was reported (Martin et al., 2015), but a comparison between the presence and absence of the compound appeared to be an important piece of information while developing optimal co-culture conditions. The results obtained in this work showed that adding agrin to a C2C12/SH-SY5Y co-culture increased the expression of MyoG, if compared to a C2C12 monoculture with agrin. The same effect was observed in MyHC3 and MyHC8, where the sole addition of SH-SY5Y to the culture increased MyHC8 expression compared to a monoculture with agrin, and was comparable to the co-culture with agrin. This suggests that agrin promoted the expression of development-related genes, particularly in the co-culture. No significant changes in MyHC7 (slow fibres), MyHC1 (fast) and MyHC2 (faster) were found, indicating that the addition of agrin had an impact on the early

stages of muscle maturation, but not on the postnatal definition of the type of muscle fibre which were generated.

Monolayer cultures are a simple way to gather information on the cells behaviour within a simple environment. However, cells naturally develop in 3D matrices which are rich in growth factors and ECM structures. Culturing cells in 3D is crucial to develop and *in vitro* model, as this allows researchers to study cell-cell and cell-matrix interactions in a microenvironment which closely mimics the *in vivo* conditions (Edmondson et al., 2014). Multiple constructs can serve this purpose, but in order to choose which ones are suitable for muscle-nerve co-cultures, it is necessary to address a few key points. First, the 3D constructs must allow the cells to align to resemble the native architecture of the muscle. This can be achieved by having a gel which is attached to two anchor points, creating tension in the gel which results in cell alignment (Khodabakus and Baar, 2009). This can be achieved by using previously described collagen- and fibrin-based gels. Second, the type of matrix that constitutes the gel is crucial as it should represent what the native environment is like. Collagen is a suitable material as it represents the most abundant protein in the muscle ECM, and is also present in the setting where neurons outgrow (Gillies and Lieber, 2012). Fibrin is also a good candidate as it has been previously shown to allow muscle maturation and differentiation (Martin et al., 2015), and was used for muscle-nerve co-cultures to establish an *in vitro* NMJ. Finally, these constructs can also be used to perform functional studies (Martin et al., 2015), which is particularly important when trying to reproduce such a complex interaction as the NMJ is. The co-culture of C2C12 and SH-SY5Y cells in 500 μ L collagen gels and in fibrin gels was achieved in this work. C2C12 matured into aligned myotubes both in the monoculture and in the co-culture with the neurons. Similarly to what was observed in monolayer, SH-SY5Y also aligned, suggesting that the anchor points were also beneficial to neuronal alignment as they were for the muscle. The 3D nature of the gels hindered imaging with a traditional fluorescent microscope, therefore the only cue about cell-cell interaction was achieved by observing how the cells sit on different focal planes. This implies that there is no close interaction between C2C12 and SH-SY5Y within collagen or fibrin gels. During the culture, remodelling of the matrix was observed in both systems, with a peak of bigger deformation at the point of adding the neurons to the culture. This may suggest that the decrease in serum concentration which is intrinsic in the use of differentiation medium triggered a bigger response in muscle differentiation, therefore resulting in higher matrix remodelling. However, at the end of the culture, both control and co-

culture gels appeared comparable in terms of gel width and also myotube width. Thus, the addition of the neurons did not appear to be significant for muscle differentiation within these matrices. Further optimisation brought to the use of additional compounds within collagen gels, particularly Matrigel®, which was considered for subsequent experiments involving 3D tissue engineered constructs. This product is commonly used to culture primary neurons and its rich composition encourages adhesion and differentiation, therefore making it suitable for the aim of this work.

Following the optimisation of C2C12/SH-SY5Y co-cultures, the availability of a human source of MNs allowed for characterisation of such neurons and their use in muscle-nerve co-cultures. While replacing C2C12 with human primary SkM is fairly easy and available, finding a source of human MNs was much more challenging. The culture conditions and characteristics of C2C12 and SH-SY5Y are known, whereas newly developed cells still require investigation to determine their phenotype, positivity to certain markers and behaviour in co-cultures. iPSC-derived MNPs were acquired by Axol Bioscience as part of a β -testing collaboration. The cells were expanded following the manufacturer's protocols for up to 5-7 days, showing variable viability after thawing (77.8% the first batch, 36.8% the second batch). The cells adhered and proliferated in culture, forming agglomerates of cells which expanded until they reached 70% confluency and were ready to be plated for differentiation. The progenitors which underwent only one passage (P1) were cultured for 35 days, whereas the ones which were frozen down and re-thawed (P2), died after the second passage and could not be further differentiated. Although this was only attempted once, it may indicate that these cells are not yet optimised to undergo several passages and be used for multiple experiments. This represents a limitation to this date, but colony selection and immortalisation of the cells may result in the use of these cells for a prolonged period of time. MNs P1 were immunostained for cholinergic markers which are commonly used to identify acetylcholine-releasing neurons, ChAT (Hu et al., 2010) and Islet 1 (Kablur and Rudnicki, 1999). These were expressed by the cells at all timepoints (5, 7, 14, 21, 28 and 35 days). However, cell death was increasingly observed during the culture, and the formation of neurospheres around day 7 led to belief that the substrate on which the cells are routinely cultured (SureBond™+ReadySet) may not be optimal. Alternatively, the seeding density could be adjusted to achieve both neuronal proliferation/differentiation and prevent cell-cell aggregation, which suggests that the cells are not fully adhering to the substrate.

Preliminary work was performed to test adherence and differentiation of human SkM to the substrate used for MN cultures, in the presence of neuronal differentiation medium (MM). The culture of hu028_1 was achieved both on gelatin and SureBond™+ReadySet, even though a higher number of myotubes was observed on gelatin. Different conditions in mono and co-culture led to base future co-cultures on gelatin only, in order to enhance myotube formation. Since the confluent layer of myoblasts will not allow MNs to adhere to the underneath substrate, the presence of SureBond™+ReadySet underneath the muscle layer was a secondary aspect to consider. Also, previous work had shown that SureBond™+ReadySet hindered desmin positivity and led to progressive muscle death, if compared to gelatin (for supplementary work, see appendix). Thus, subsequent repeats were conducted using gelatin only as a substrate.

Keeping MNs in culture for more than 5 days was not necessary when establishing co-cultures with human primary SkM. The timing of primary co-cultures is challenging, as the rate at which these MNs grow is known, but muscle donors are variable in that aspect. In order to achieve muscle differentiation, a fully confluent layer of myoblasts must form. Since the growth rates of different biopsies are different, and MNPs must be seeded on the myoblast layer on the same day, some biopsies may have not been 100% confluent before the neurons were seeded on them. This may be the reason why hu028_1 and hu020 did not differentiate in control conditions. However, the fact that both these donors did differentiate when cultured in MM suggests that the components within this medium had a pro-myogenic effect on a less myogenic population than hu027 and hu028_2. In fact, gene expression analysis showed that the MyHC8, MyHC7 and MyHC8 were highly expressed when hu027 and hu028_2 were differentiated in MM, if compared to the control, with the exception of hu028_2's MyHC1 expression, which was unvaried. These results suggest that the composition of MM, which is unknown to us, was beneficial to the muscle and enhanced its developmental marker, as well as markers for fast and slow-twitching fibres. Potentially, the addition of certain neurotrophic factors to MM played a role in this increase in gene expression, although the same medium was used for the co-culture with MNs and this significantly decreased MyHC8, MyHC7 and MyHC1 levels. Unexpectedly, the co-culture with the neurons depleted completely MyHC8 and MyHC7 if compared to the control, even though MyHC1 expression in hu027 increased. When in co-culture with the different donors, the neurons adhered differently. The phenotype observed when in co-culture with hu028_1 and hu020 was comparable to the previously established monocultures. However, the cells on donor hu027 appeared to be densely proliferating in

separated areas and peeling off during the immunostaining process. In addition, all neurons on donor hu028_2 formed into neurospheres, similarly to what was partially observed in long-term neuronal monocultures. These results indicate that the donor to donor variability is, at this stage, a determining factor when establishing human muscle-nerve co-cultures. Although variability is intrinsic in primary cultures, further optimisation of such cultures may reduce the impact on cell-cell interactions. As for the interaction between pre- and post-synaptic proteins (SV-2 and AChR, respectively), clusters of AChR's were found in hu020, hu027 and hu028_2, across all conditions. However, the presence of MNs appeared to enhance clustering, which was visible as highly stained areas on the muscle fibre, if compared to the sparse punctate staining that was observed in control conditions. On the neuronal side, the SV-2 antibody positively stained the MNs, but aspecific staining was also noticeable where myotubes appeared green (yellow in the merged images). Repeating this immunostaining would be important to determine whether the SV-2 antibody is suitable for such analysis, or other markers can be used for the same purpose (e.g. synapsin).

When moving from a 2D to a 3D human muscle-nerve co-culture, more challenges were faced. Despite conducting preliminary studies with C2C12 and SH-SY5Y cell lines at the beginning of this thesis, the different cell types and engineering of the constructs utilised required further investigation. Encouraging results came from the morphological immunostaining, which showed the generation of aligned myotubes and extended neuronal projections within collagen/Matrigel® constructs. This showed the suitability of the gel for such cultures, and the coexistence of the two cell types in a complex environment. A great amount of information was also obtained by performing cross sections of the gels and observe the distribution of them within the matrix. This represented a unique attempt to co-culture primary hSkM and iPSC-derived MNs, however multiple slices across the middle of the gel showed that the cells are distributed in promiximity of one-another, leaving an empty area in the middle of the construct. The repetition of such experiments by varying the neuronal seeding procedures or the timing at which these are seeded (for instance, after myotubes are already formed), would provide more information on the best approach to obtain a homogeneous distribution of cells and optimal conditions for them to interact. The novelty of this work is reflected on the functional data which was acquired from the 3D human co-cultures. These results did not show an increase in force generation when MNs were present, which reflects what was previously observed in monolayer, where the gene expression of muscle development and maturity markers was

depleted in the co-culture. However, this depletion was evident when comparing co-culture conditions with a muscle monoculture in MM, and less strong if compared to the control. Similarly, a higher degree of force was generated by muscle differentiated in MM. However, the single twitch showed higher force in the control, if compared to MM conditions.

All in all, this isolated attempt represented the first system in which human primary SkM and iPSC-derived MNs were co-cultured in 3D, allowing for the acquisition of functional data. Future work may focus on the optimisation of the model and the investigation of potential interactions between the two cell types, identified as NMJ.

7.2 Future directions

The work conducted in this thesis shows muscle-nerve co-cultures which aimed to ‘humanise’ previously reported models. The use of a mouse-human chimera was firstly achieved to optimise co-culture conditions and observe the engineering aspect which relates to the use of 3D constructs. The subsequent use of primary human SkM and MNs further improved the system by utilising more suitable cell sources than cell lines. Despite the few attempts to establish a NMJ both in 2D and in 3D, interactions between SkM and MNs still appear to be challenging. Adding Matrigel® to the collagen gel matrix was a promising modification to the original protocol, as the numerous factors which are intrinsic to Matrigel® would be beneficial for neuronal outgrowth, which is why this coating is routinely used for primary neuronal cultures (Umbach et al., 2012b). Schwann cells are known to cover a support role for MNs *in vivo*, (Bear et al., 2001) thus representing an optimal candidate for future cultures. Providing MNs with an additional cell type which can sustain their growth and differentiation could be crucial for neuronal functionality within complex 3D matrices. In addition, humanising the system leads to the fulfilment of the 3R’s (reduce, refine, replace), for which much more can be done. These cultures are still based on the use of animal-derived serum, but promising MNs were previously generated in serum-free conditions (Egawa et al., 2012), and the addition of certain growth factors may sustain the muscle when doing the same. Similarly, the gelatin used for the expansion of primary SkM, and the collagen that constitutes the 3D matrix of the gels are also animal-derived. Future work may focus on completely substitute these compounds with synthetic counterparts or human recombinant ones. Likewise, the growth factors and ECM components found in Matrigel® are variable and could be replaced by defined, synthetic products.

The real potential of this model, once fully optimised, lies in the generation of a platform which can be of interest for pharmaceutical companies which are developing new treatments. There is great interest in replacing animal models with human alternatives for preliminary studies, thus making the work conducted in this thesis a key progression in the process of generating such models. To do so, the constructs preparation would need some further optimisation to ensure that the protocols are kept consistent (e.g. specific amount of NaOH for neutralisation) and the gels can be prepared using high throughput methods. Although this co-culture does not represent a fully formed organism as an animal model would, this NMJ model has more potential for future applications. For instance, they could represent personalised co-cultures for patients who are affected by neurodegenerative diseases for which, to this date, no treatment is available (**Figure 7.1**). These patients often undergo ineffective treatments which have major consequences on their wellbeing. However, by deriving MNs from the patient's skin or blood, their neurons could be closely studied and therapies could be tested to predict their effectiveness. Furthermore, SkM could also be derived using the same technology, thus avoiding biopsies which may be detrimental in patients affected by neurodegenerative or muscular diseases. It has been recently shown (Demestre et al., 2015) that it is possible to generate both SkM and MNs from healthy and affected individuals, however the following step would be to transfer this to a 3D culture system. Stem cell researchers are also in the process of optimising transdifferentiation protocols through which the fully differentiated cells used as donors, can be directly differentiated into the final cell type without undergoing a de-differentiation process. This would significantly decrease the amount of time required for the generation of either MNs or SkM, while simplifying protocols and reducing the use of reagents.

Overall, the models proposed in this thesis are suitable for neuromuscular co-cultures and may be the key to a personalised *in vitro* model of the NMJ.

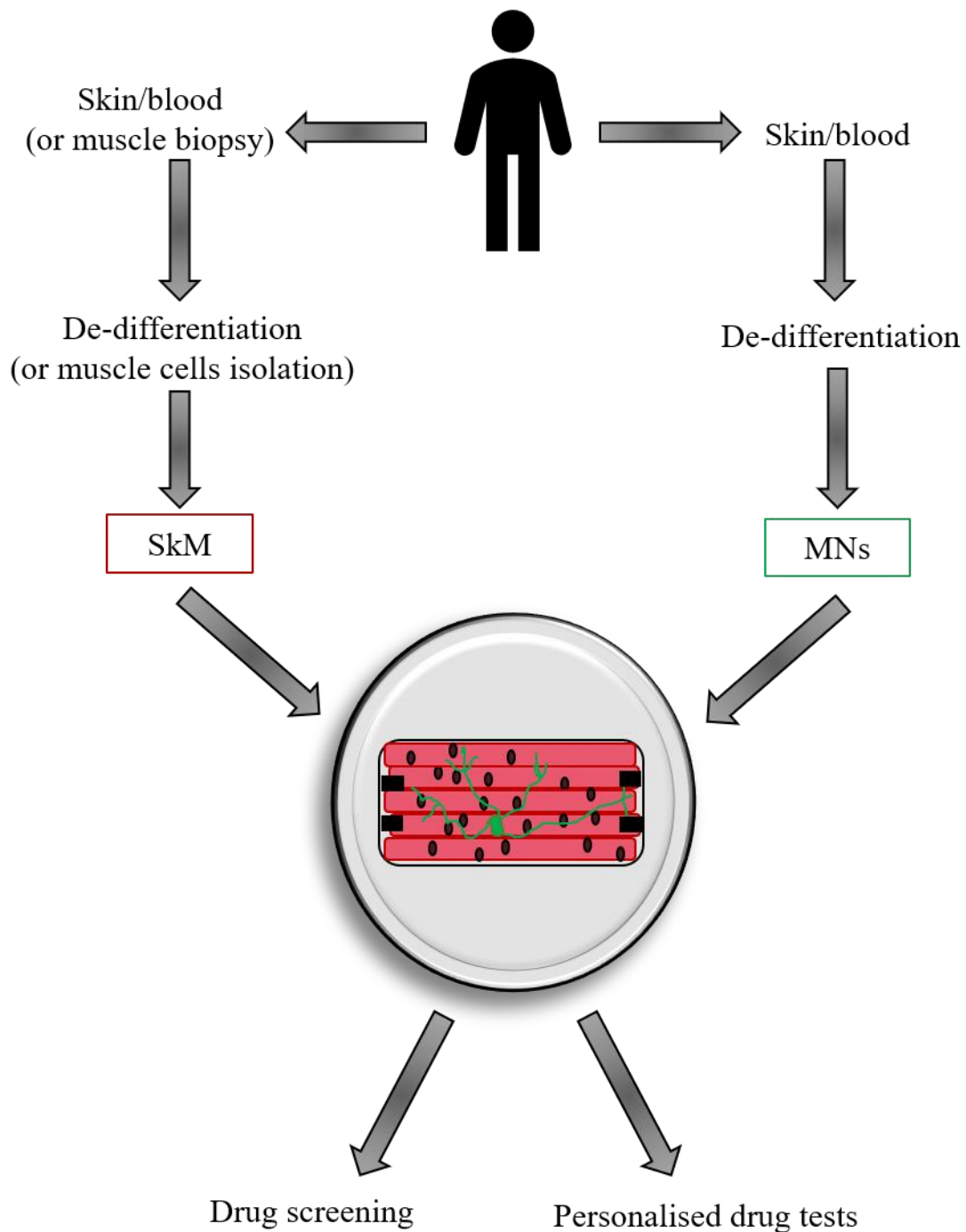


Figure 7.1. Process to develop a personalised 3D muscle-nerve in vitro model. Skin or blood could be taken from the patient to derive both SkM and MNs (via de-differentiation and differentiation, or transdifferentiation). The cells would then be co-cultured in the 3D tissue engineered construct to test novel therapeutics or treatments which the patients could start.

7.3 Conclusions

This thesis focussed on the development of a human model of the NMJ using tissue engineered constructs. The importance of creating this model lies on its being a representative system for *in vitro* testing and personalised drug screening. Avoiding the use of cell lines, animal cells or ESCs would not only help reduce, refine and replace the use of animals in research, but also provide researchers with a complex system which would help underpinning the physiological features of this fascinating tissue interface. A chimeric co-culture was an important step to take to determine cell behaviour and tissue engineering challenges when working with SkM and MNs. Although the primary 3D co-cultures presented the author with several challenges, the preliminary results presented in the second part of this work set the grounds for more optimisation to be carried out in the future. Growing interest from the scientific community, particularly from drug developing companies, makes this model's optimisation a necessary leap to take in future studies.

8 BIBLIOGRAPHY

- Abou Neel, E.A., Cheema, U., Knowles, J.C., Brown, R.A., Nazhat, S.N., 2006. Use of multiple unconfined compression for control of collagen gel scaffold density and mechanical properties. *Soft Matter* 2, 986–992.
- Acheson, A., Conover, J.C., Fandi, J.P., DeChiara, T.M., Russell, M., Thadani, A., Squinto, S.P., Yancopoulos, G.D., Lindsay, R.M., 1995. A BDNF autocrine loop in adult sensory neurons prevents cell death. *Lett. to Nat.* 374, 450–453.
- Adem, a, Mattsson, M.E., Nordberg, A., Pählman, S., 1987. Muscarinic receptors in human SH-SY5Y neuroblastoma cell line: regulation by phorbol ester and retinoic acid-induced differentiation. *Brain Res.* 430, 235–242.
- Albagli-Curiel, O., Carnac, G., Vandromme, M., Vincent, S., Crepieux, P., Bonnieu, A., 1993. Serum-induced inhibition of myogenesis is differentially relieved by retinoic acid and triiodothyronine in C2 murine muscle cells. *Differentiation.* 52, 201–210.
- Alberts, B., Johnson, A., Lewis, J., Raff, M., Roberts, K., Walter, P., 2002. *Molecular biology of the cell*, 4th ed.
- Alovskaya, a, Alekseeva, T., Phillips, J.B., King, V., Brown, R., 2007. Fibronectin, collagen, fibrin - components of extracellular matrix for nerve regeneration. *Top. Tissue Eng.* 3, 1–27.
- Andrews, P.W., Damjanov, I., Simon, D., Banting, G.S., Carlin, C., Dracopoli, N.C., Fogh, J., 1984. Pluripotent embryonal carcinoma clones derived from the human teratocarcinoma cell line Tera-2. Differentiation in vivo and in vitro. *Lab. Invest.* 50, 147–162.
- Arber, S., Han, B., Mendelsohn, M., Smith, M., Jessell, T.M., Sockanathan, S., 1999. Requirement for the homeobox gene Hb9 in the consolidation of motor neuron identity. *Neuron* 23, 659–674.

- Arnold, H.H., Gerharz, C.D., Gabbert, H.E., Salminen, A., 1992. Retinoic acid induces myogenin synthesis and myogenic differentiation in the rat rhabdomyosarcoma cell line BA-Han-1C. *J. Cell Biol.* 118, 877–887.
- Asakura, A., Komaki, M., Rudnicki, M.A., 2001. Muscle satellite cells are multipotential stem cells that exhibit myogenic, osteogenic, and adipogenic differentiation. *Differentiation* 68, 245–253.
- Bach, A.D., Beier, J.P., Stern-Staeter, J., Horch, R.E., 2004. Skeletal muscle tissue engineering. *J. Cell. Mol. Med.* 8, 413–422.
- Bakooshli, M.A., Lippmann, E.S., Mulcahy, B., Tung, K., Pegoraro, E., Ahn, H., Ginsberg, H., Zhen, M., Ashton, R.S., Gilbert, P.M., 2018. A 3D model of human skeletal muscle innervated with stem cell-derived motor neurons enables epsilon-subunit targeted myasthenic syndrome studies.
- Barany, M., 1967. ATPase Activity of Myosin Correlated with Speed of Muscle Shortening. *J. Gen. Physiol.* 50, 197–218.
- Barik, A., Lu, Y., Sathyamurthy, A., Bowman, A., Shen, C., Li, L., Xiong, W. -c., Mei, L., 2014. LRP4 is critical for neuromuscular junction maintenance. *J. Neurosci.* 34, 13892–13905.
- Bear, M., Connors, B., Paradiso, M., 2001. *Neuroscience exploring the brain*, 3rd ed, Lippincott Williams & Wilkins.
- Beauchamp, J.R., Heslop, L., Yu, D.S.W., Tajbakhsh, S., Kelly, R.G., Wernig, A., Buckingham, M.E., Partridge, T.A., Zammit, P.S., 2000. Expression of CD34 and Myf5 defines the majority of quiescent adult skeletal muscle satellite cells. *J. Cell Biol.* 151, 1221–1233.
- Bell, G.H., Emslie-Smith, D., Patterson, C., 1980. *Textbook of physiology*, 10th ed. Churchill Livingstone, Edinburgh; New York.
- Bergstrom, J., 1975. Percutaneous needle biopsy of skeletal muscle in physiological and clinical research. *Scand. J. Clin. Lab. Invest.* 35, 609–616.

- Bhatheja, K., Field, J., 2006. Schwann cells: origins and role in axonal maintenance and regeneration. *Int. J. Biochem. Cell Biol.* 38, 1995–1999.
- Bian, W., Bursac, N., 2012. Soluble miniagrin enhances contractile function of engineered skeletal muscle. *FASEB J.* 26, 955–965.
- Bian, W., Bursac, N., 2009. Engineered skeletal muscle tissue networks with controllable architecture. *Biomaterials* 30, 1401–1412.
- Bianchi, F., Malboubi, M., Li, Y., George, J.H., Jerusalem, A., Szele, F., Thompson, M.S., Ye, H., 2018. Rapid and efficient differentiation of functional motor neurons from human iPSC for neural injury modelling. *Stem Cell Res.* 32, 126–134.
- Biedler, J.L., Helson, L., Spengler, B. a, 1973. Morphology and growth, tumorigenicity, and cytogenetics of human neuroblastoma cells in continuous culture morphology and growth, tumorigenicity, and cytogenetics of human neuroblastoma cells in continuous culture. *Cancer Res.* 33, 2643–2652.
- Binder, M.D., Hirokawa, N., Uwe, W., 2009. *Encyclopedia of neuroscience*. Springer.
- Bischoff, R., 1974. Enzymatic liberation of myogenic cells from adult rat muscle. *Anat. Rec.* 180, 645–661.
- Blau, H.M., Pavlath, G.K., Hardeman, E.C., Chiu, C.P., Silberstein, L., Webster, S.G., Miller, S.C., Webster, C., 1985. Plasticity of the differentiated state. *Science* 230, 758–766.
- Boonen, K.J.M., Langelaan, M.L.P., Polak, R.B., van der Schaft, D.W.J., Baaijens, F.P.T., Post, M.J., 2010. Effects of a combined mechanical stimulation protocol: Value for skeletal muscle tissue engineering, *Journal of Biomechanics*.
- Brady, M. a., Lewis, M.P., Mudera, V., 2008. Synergy between myogenic and non-myogenic cells in a 3D tissue-engineered craniofacial skeletal muscle construct. *J. Tissue Eng. Regen. Med.* 2, 408–417.
- Brown, D.M., Parr, T., Brameld, J.M., 2012. Myosin heavy chain mRNA isoforms are

- expressed in two distinct cohorts during C2C12 myogenesis. *J. Muscle Res. Cell Motil.* 32, 383–390.
- Buckingham, M., Relaix, F., 2007. The role of Pax genes in the development of tissues and organs: Pax3 and Pax7 regulate muscle progenitor cell functions. *Annu. Rev. Cell Dev. Biol.* 23, 645–673.
- Burattini, S., Ferri, R., Battistelli, M., Curci, R., Luchetti, F., Falcieri, E., 2004. C2C12 murine myoblasts as a model of skeletal muscle development: morpho-functional characterization. *Eur. J. Histochem.* 48, 223–233.
- Burden, S.J., Yumoto, N., Zhang, W., 2013. The role of MuSK in synapse formation and neuromuscular disease. *Cold Spring Harb. Perspect. Biol.* 5, 1–12.
- Burgess, R.W., Nguyen, Q.T., Young-Jin, S., Lichtman, J.W., Sanes, J.R., 1999. Alternatively spliced isoforms of nerve- and muscle-derived agrin: Their roles at the neuromuscular junction. *Neuron* 23, 33–44.
- Burrige, P.W., Matsa, E., Shukla, P., Lin, Z.C., Churko, J.M., Ebert, A.D., Lan, F., Diecke, S., Huber, B., Mordwinkin, N.M., Plews, J.R., Abilez, O.J., Cui, B., Gold, J.D., Wu, J.C., 2015. Chemically defined and small molecule-based generation of human cardiomyocytes. *Nat. Methods* 11, 855–860.
- Chambers, S.M.S.M., Fasano, C.A.C.A., Papapetrou, E.P., Tomishima, M., Sadelain, M., Studer, L., 2009. Highly efficient neural conversion of human ES and iPS cells by dual inhibition of SMAD signaling. *Nature* 461, 275–280.
- Charge, S.B.P., Rudnicki, M.A., 2004. Cellular and molecular regulation of muscle regeneration. *Physiol. Rev.* 84, 209.
- Clagett-dame, M., McNeill, E.M., Muley, P.D., 2006. Role of all-trans retinoic acid in neurite outgrowth and axonal elongation. *J. Neurobiol.* 66, 677–686.
- Colquhoun, D., Sakmann, B., 1998. From muscle endplate to brain synapses: A short history of synapses and agonist-activated ion channels. *Neuron* 20, 381–387.

- Cossu, G., Borello, U., 1999. Wnt signaling and the activation of myogenesis in mammals. *EMBO J.* 18, 6867–6872.
- Daniels, M.P., 2012. The role of agrin in synaptic development, plasticity and signaling in the central nervous system. *Neurochem. Int.* 61, 848–853.
- DeChiara, T.M., Bowen, D.C., Valenzuela, D.M., Simmons, M. V, Poueymirou, W.T., Thomas, S., Kinetz, E., Compton, D.L., Rojas, E., Park, J.S., Smith, C., DiStefano, P.S., Glass, D.J., Burden, S.J., Yancopoulos, G.D., 1996. The receptor tyrosine kinase MuSK is required for neuromuscular junction formation in vivo. *Cell* 85, 501–512.
- DeLapeyriere, O., Henderson, C.E., 1997. Motoneuron differentiation, survival and synaptogenesis. *Curr. Opin. Genet. Dev.* 7, 642–650.
- Delbono, O., 2010. Myosin - still a good reference for skeletal muscle fibre classification? *J. Physiol.* 588, 9.
- Delli Carri, A., Onorati, M., Castiglioni, V., Faedo, A., Camnasio, S., Toselli, M., Biella, G., Cattaneo, E., 2013. Human pluripotent stem cell differentiation into authentic striatal projection neurons. *Stem Cell Rev. Reports* 9, 461–474.
- Demestre, M., Orth, M., Fohr, K.J., Achberger, K., Ludolph, A.C., Liebau, S., Boeckers, T.M., 2015. Formation and characterisation of neuromuscular junctions between hiPSC derived motoneurons and myotubes. *Stem Cell Res.* 15, 328–336.
- Dennis, R.G., Kosnik, P.E., 2000. Excitability and isometric contractile properties of mammalian skeletal muscle constructs engineered in vitro. *Vitr. Cell. Dev. Biol. - Anim.* 36, 327.
- Dimos, J.T., Rodolfa, K.T., Niakan, K.K., Weisenthal, L.M., Mitsumoto, H., Chung, W., Croft, G.F., Saphier, G., Leibel, R., Golland, R., Wichterle, H., Henderson, C.E., Eggan, K., 2008. Induced pluripotent stem cells generated from patients with ALS can be differentiated into motor neurons. *Science* (80-.). 321, 1218–1221.
- Dixon, T.A., Cohen, E., Cairns, D.M., Rodriguez, M., Mathews, J., Jose, R.R., Kaplan, D.L.,

2018. Bioinspired three-dimensional human neuromuscular junction development in suspended hydrogel arrays. *Tissue Eng. Part C Methods* 24, 346–359.
- Dolmetsch, R., Geschwind, D.H., 2013. The human brain in a dish: the promise of iPSC-derived neurons. *Cell* 145, 831–834.
- Du, Z.-W., Chen, H., Liu, H., Lu, J., Qian, K., Huang, C.-L., Zhong, X., Fan, F., Zhang, S.-C., 2015. Generation and expansion of highly pure motor neuron progenitors from human pluripotent stem cells. *Nat. Commun.* 6, 6626.
- Dusterhoft, S., Pette, D., 1990. Effects of electrically induced contractile activity on cultured embryonic chick breast muscle cells. *Differentiation* 44, 178–184.
- Eastwood, M., McGrouther, D.A., Brown, R.A., 1994. A culture force monitor for measurement of contraction forces generated in human dermal fibroblast cultures: evidence for cell-matrix mechanical signalling. *Biochim. Biophys. Acta - Gen. Subj.* 1201, 186–192.
- Eastwood, M., Mudera, V.C., McGrouther, D.A., Brown, R.A., 1998. Effect of precise mechanical loading on fibroblast populated collagen lattices: morphological changes. *Cell Motil. Cytoskeleton* 40, 13–21.
- Ebert, A.D., Yu, J., Rose, F.F., Mattis, V.B., Lorson, C.L., Thomson, J. a., Svendsen, C.N., 2009. Induced pluripotent stem cells from a spinal muscular atrophy patient. *Nature* 457, 277–280.
- Edmondson, R., Broglie, J.J., Adcock, A.F., Yang, L., 2014. Three-dimensional cell culture systems and their applications in drug discovery and cell-based biosensors. *Assay Drug Dev. Technol.* 12, 207–218.
- Egawa, N., Kitaoka, S., Tsukita, K., Naitoh, M., Takahashi, K., Yamamoto, T., Adachi, F., Kondo, T., Okita, K., Asaka, I., Aoi, T., Watanabe, A., Yamada, Y., Morizane, A., Takahashi, J., Ayaki, T., Ito, H., Yoshikawa, K., Yamawaki, S., Suzuki, S., Watanabe, D., Hioki, H., Kaneko, T., Makioka, K., Okamoto, K., Takuma, H., Tamaoka, A., Hasegawa, K., Nonaka, T., Hasegawa, M., Kawata, A., Yoshida, M., Nakahata, T., Takahashi, R.,

- Marchetto, M.C.N., Gage, F.H., Yamanaka, S., Inoue, H., 2012. Drug Screening for ALS Using Patient-Specific Induced Pluripotent Stem Cells. *Sci. Transl. Med.* 4, 145ra104.
- El Haddad, M., Notarnicola, C., Evano, B., El Khatib, N., Blaquièrre, M., Bonniou, A., Tajbakhsh, S., Hugon, G., Vernus, B., Mercier, J., Carnac, G., 2017. Retinoic acid maintains human skeletal muscle progenitor cells in an immature state. *Cell. Mol. Life Sci.* 74, 1923–1936.
- El Omri, A., Han, J., Kawada, K., Ben Abdrabbah, M., Isoda, H., 2012. Luteolin enhances cholinergic activities in PC12 cells through ERK1/2 and PI3K/Akt pathways. *Brain Res.* 1437, 16–25.
- Elkabetz, Y., Panagiotakos, G., G., A., Socci, N.D., Tabar, V., Studer, L., 2008. Human ES cell-derived neural rosettes reveal a functionally distinct early neural stem cell stage. *Genes Dev.* 22, 152–165.
- Encinas, M., Iglesias, M., Liu, Y., Wang, H., Muhaisen, A., Ceña, V., Gallego, C., Comella, J.X., 2000. Sequential treatment of SH-SY5Y cells with retinoic acid and brain-derived neurotrophic factor gives rise to fully differentiated, neurotrophic factor-dependent, human neuron-like cells. *J. Neurochem.* 75, 991–1003.
- Engler, A.J., Griffin, M.A., Sen, S., Bönnemann, C.G., Sweeney, H.L., Discher, D.E., 2004. Myotubes differentiate optimally on substrates with tissue-like stiffness: Pathological implications for soft or stiff microenvironments. *J. Cell Biol.* 166, 877–887.
- Ericson, J., Thor, S., Edlund, T., Jessell, T.M., Yamada, T., 1992. Early stages of motor neuron differentiation revealed by expression of homeobox gene *Islet-1*. *Science* (80-.). 256, 1555–1560.
- Esser, K., Gunning, P., Hardeman, E., 1993. Nerve-dependent and -independent patterns of mRNA expression in regenerating skeletal muscle. *Dev. Biol.*
- Flanagan-Steet, H., Fox, M.A., Meyer, D., Sanes, J.R., 2005. Neuromuscular synapses can form in vivo by incorporation of initially neuronal postsynaptic specializations. *Development* 132, 4471–4481.

- Forster, J.I., Köglsberger, S., Trefois, C., Boyd, O., Baumuratov, a S., Buck, L., Balling, R., Antony, P.M. a, 2016. Characterization of differentiated SH-SY5Y as neuronal screening model reveals increased oxidative vulnerability. *J. Biomol. Screen.*
- Franzini-Armstrong, C., Peachy, L.D., 1981. Striated muscle-contraction and control mechanisms. *J. Cell Biol.* 91.
- Gillies, A.R., Lieber, R.L., 2012. Structure and function of the skeletal muscle extracellular matrix. *Muscle nerve* 44, 318–331.
- Goers, L., Freemont, P., Polizzi, K.M., 2014. Co-culture systems and technologies: taking synthetic biology to the next level. *J. R. Soc. Interface* 11, 20140065–20140065.
- Goldspink, G., Scutt, A., Loughna, P.T., Wells, D.J., Jaenicke, T., Gerlach, G.F., 1992. Gene expression in skeletal muscle in response to stretch and force generation. *Am. J. Physiol.* 262, R356-63.
- Gomes, A., Potter, J.D., Szczesna-Cordary, D., 2002. The role of Troponin in muscle contraction. *Life* 323–333.
- Gray, H., 1960. *Anatomy of the human body.*, The Anatomical Record.
- Greene, L.A., Tischler, A.S., 1976. Establishment of a noradrenergic clonal line of rat adrenal pheochromocytoma cells which respond to nerve growth factor. *Proc. Natl. Acad. Sci.* 73, 2424–2428.
- Grefte, S., Vullings, S., Kuijpers-Jagtman, A.M., Torensma, R., Von Den Hoff, J.W., 2012. Matrigel, but not collagen I, maintains the differentiation capacity of muscle derived cells in vitro. *Biomed. Mater.* 7.
- Grey, M., 2011. Bio-engineering of muscle tissue in culture: influence of neural, cartilage or kidney cells and the effect of retinoic acid on muscle cell growth.
- Griffith, L.G., Swartz, M.A., 2006. Capturing complex 3D tissue physiology in vitro. *Nat. Rev. Mol. Cell Biol.* 7, 211.

- Guo, X., Gonzalez, M., Stancescu, M., Vandeburgh, H., Hickman, J., 2011. Neuromuscular Junction Formation between Human Stem cell- derived Motoneurons and Human Skeletal Muscle in a Defined System. *Biomaterials* 32, 9602–9611.
- Guyton, C.A., Hall, E.J., 2005. *Textbook of medical physiology*, 11th ed. Elsevier.
- Halevy, O., Lerman, O., 1993. Retinoic acid induces adult muscle cell differentiation mediated by the retinoic acid receptor- α . *J. Cell. Physiol.* 154, 566–572.
- Hall, E.J., 2016. *Guyton and Hall Textbook of Medical Physiology*, 13th ed. Elsevier.
- Hamade, A., Deries, M., Begemann, G., Bally-Cuif, L., Genêt, C., Sabatier, F., Bonniou, A., Cousin, X., 2006. Retinoic acid activates myogenesis in vivo through Fgf8 signalling. *Dev. Biol.* 289, 127–140.
- Hanna, J., Saha, K., Jaenisch, R., 2010. Somatic cell reprogramming and transitions between pluripotent states: facts, hypotheses, unresolved issues. *Cell* 143, 508–525. <https://doi.org/10.1016/j.cell.2010.10.008>.Somatic
- Heckman, C.J., Enoka, R.M., 2004. *Physiology of the motor neuron and the motor unit, Handbook of Clinical Neurophysiology*. Elsevier B.V.
- Henriquez, J.P., Webb, A., Bence, M., Bildsoe, H., Sahores, M., Hughes, S.M., Salinas, P.C., 2008. Wnt signaling promotes AChR aggregation at the neuromuscular synapse in collaboration with agrin. *Proc. Natl. Acad. Sci. U. S. A.* 105, 18812–18817.
- Hesser, B.A., Henschel, O., Witzemann, V., 2006. Synapse disassembly and formation of new synapses in postnatal muscle upon conditional inactivation of MuSK. *Mol. Cell. Neurosci.* 31, 470–480.
- Hester, M.E., Murtha, M.J., Song, S., Rao, M., Miranda, C.J., Meyer, K., Tian, J., Boulting, G., Schaffer, D. V, Zhu, M.X., Pfaff, S.L., Gage, F.H., Kaspar, B.K., 2011. Rapid and efficient generation of functional motor neurons from human pluripotent stem cells using gene delivered transcription factor codes. *Mol. Ther.* 19, 1905–1912.

- Hill, E.J., Jiménez-González, C., Tarczyluk, M., Nagel, D.A., Coleman, M.D., Parri, H.R., 2012. NT2 derived neuronal and astrocytic network signalling. *PLoS One* 7, 1–10.
- Hoch, W., 1999. Formation of the neuromuscular junction. Agrin and its unusual receptors. *Eur. J. Biochem.* 265, 1–10.
- Hong-rong, X., Lin-sen, H., Guo-yi, L., 2010. SH-SY5Y human neuroblastoma cell line: in vitro cell model of dopaminergic neurons in Parkinson's disease. *Chin Med J* 123, 1086–1092.
- Hounoum, B.M., Vourc, P., Felix, R., Corcia, P., Patin, F., Guéguinou, M., Potier-cartereau, M., Vandier, C., Raoul, C., Andres, C.R., Mavel, S., Blasco, H., 2016. NSC-34 motor neuron-like cells are unsuitable as experimental model for glutamate-mediated excitotoxicity. *Fr* 10, 1–12.
- Howard, B.D., Melega, W.P., 1981. Acetylcholine Metabolism in PC12, A Clonal Cell Line on Secretory Cells BT - Cholinergic Mechanisms: Phylogenetic Aspects, Central and Peripheral Synapses, and Clinical Significance, in: Pepeu, G., Ladinsky, H. (Eds.), . Springer US, Boston, MA, pp. 133–142.
- Hu, B.-Y., Weick, J.P., Yu, J., Ma, L.-X., Zhang, X.-Q., Thomson, J. a., Zhang, S.-C., 2010. Neural differentiation of human induced pluripotent stem cells follows developmental principles but with variable potency. *Proc. Natl. Acad. Sci.* 107, 4335–4340.
- Hu, B., Zhang, S., 2009. Differentiation of spinal motor neurons from pluripotent human stem cells. *Nat. Protoc.* 4, 1295–1304.
- Hu, W., He, Y., Xiong, Y., Lu, H., Chen, H., Hou, L., Qiu, Z., Fang, Y., Zhang, S., 2015. Derivation, expansion, and motor neuron differentiation of human-induced pluripotent stem cells with non-integrating episomal vectors and a defined xenogeneic-free culture system. *Mol. Neurobiol.*
- Huang, E.J., Reichardt, L.F., 2009. Neurotrophins: roles in neuronal development and function. *Annu Rev Neurosci* 24, 677–736.

- Huang, S.X.L., Naimul Islam, M., O'Neill, J., Hu, Z., Yang, Y.-G., Chen, Y.-W., Mumau, M., Green, M.D., Vunjak-Novakovic, G., Bhattacharya, J., Snoeck, H.-W., 2014. Highly efficient generation of airway and lung epithelial cells from human pluripotent stem. *Nat Biotechnol* 32, 84–91.
- Huang, Y.-C.Y., Dennis, R.R.G.R.R.G., Larkin, L., Baar, K., 2005. Rapid formation of functional muscle in vitro using fibrin gels. *J. Appl. Physiol.* 98, 706–713.
- Huxley, H.E., 1953. Electron microscope studies of the organisation of the filaments in striated muscle. *Biochim. Biophys. Acta* 12, 387–394.
- Iacovitti, L., Stull, N.D., Jin, H., 2001. Differentiation of human dopamine neurons from an embryonic carcinomal stem cell line. *Brain Res.* 912, 99–104.
- Ichikawa, T., Ajiki, K., Matsuura, J., Misawa, H., 1997. Localization of two cholinergic markers , choline acetyltransferase and vesicular acetylcholine transporter in the central nervous system of the rat : in situ hybridization histochemistry and immunohistochemistry 13, 23–39.
- Imberti, B., Tomasoni, S., Ciampi, O., Pezzotta, A., Derosas, M., Xinaris, C., Rizzo, P., Papadimou, E., Novelli, R., Benigni, A., Remuzzi, G., Morigi, M., 2015. Renal progenitors derived from human iPSCs engraft and restore function in a mouse model of acute kidney injury. *Sci. Rep.* 5, 8826.
- Irintchev, A., Zeschnigk, M., Starzinski-Powitz, A., Wernig, A., 1994. Expression pattern of M-cadherin in normal, denervated, and regenerating mouse muscles. *Dev. Dyn.* 199, 326–337.
- Jones, J.M., Player, D.J., Martin, N.R.W., Capel, A.J., Lewis, M.P., Mudera, V., 2018. An assessment of myotube morphology, matrix deformation, and myogenic mRNA expression in custom-built and commercially available engineered muscle chamber configurations. *Front. Physiol.* 9, 1–9.
- Jones, R.A., Harrison, C., Eaton, S.L., Llaverro Hurtado, M., Graham, L.C., Alkhamash, L., Oladiran, O.A., Gale, A., Lamont, D.J., Simpson, H., Simmen, M.W., Soeller, C., Wishart,

- T.M., Gillingwater, T.H., 2017. Cellular and molecular anatomy of the human neuromuscular junction. *Cell Rep.* 21, 2348–2356.
- Joshi, S., Guleria, R., Pan, J., DiPette, D., Singh, U.S., 2006. Retinoic acid receptors and tissue-transglutaminase mediate short-term effect of retinoic acid on migration and invasion of neuroblastoma SH-SY5Y cells. *Oncogene* 25, 240–247.
- Juhas, M., Bursac, N., 2014. Roles of adherent myogenic cells and dynamic culture in engineering muscle function and maintenance of satellite cells. *Biomaterials* 35, 9438–9446.
- Kablar, B., Belliveau, A.C., 2005. Presence of neurotrophic factors in skeletal muscle correlates with survival of spinal cord motor neurons. *Dev. Dyn.* 234, 659–669.
- Kablar, B., Rudnicki, M.A., 1999. Development in the absence of skeletal muscle results in the sequential ablation of motor neurons from the spinal cord to the brain. *Dev. Biol.* 208, 93–109.
- Kalman, B., Monge, C., Bigot, A., Mouly, V., Picart, C., Boudou, T., 2015. Engineering human 3D micromuscles with co-culture of fibroblasts and myoblasts. *Comput. Methods Biomech. Biomed. Engin.* 18, 1960–1961.
- Kanning, K.C., Kaplan, A., Henderson, C.E., 2010. Motor Neuron Diversity in Development and Disease.
- Karumbayaram, S., Novitch, B.G., Patterson, M., Umbach, J. a., Richter, L., Lindgren, A., Conway, A.E., Clark, A.T., Goldman, S. a., Plath, K., Wiedau-Pazos, M., Kornblum, H.I., Lowry, W.E., 2009. Directed differentiation of human-induced pluripotent stem cells generates active motor neurons. *Stem Cells* 27, 806–811.
- Karumbayaram, S., Novitch, B.G., Patterson, M., Umbach, J. a, Richter, L., Conway, A., Clark, A., Goldman, S. a, Plath, K., 2010. Directed differentiation of human induced pluripotent stem cells generates active motor neurons. *Stem Cells* 27, 806–811.
- Kasa, P., Dobo, E., Wolff, J.R., 1991. Cholinergic innervation of the mouse superior cervical

- ganglion: light- and electron-microscopic immunocytochemistry for choline acetyltransferase. *Cell Tissue Res.* 265, 151–8.
- Khodabukus, A., Baar, K., 2014. The effect of serum origin on tissue engineered skeletal muscle function. *J. Cell. Biochem.* 115, 2198–2207.
- Khodabukus, A., Baar, K., 2009. Regulating fibrinolysis to engineer skeletal muscle from the C2C12 cell line. *Tissue Eng. Part C. Methods* 15, 501–511.
- Khodabukus, A., Paxton, J.Z., Donnelly, K., Baar, K., 2007. Engineered muscle: a tool for studying muscle physiology and function. *Exerc. Sport Sci. Rev.* 35, 186–191.
- Khodabukus, A., Prabhu, N., Wang, J., Bursac, N., 2018. In vitro tissue-engineered skeletal muscle models for studying muscle physiology and disease 1701498, 1–20.
- Kim, D.-S., Ross, P.J., Zaslavsky, K., Ellis, J., 2014. Optimizing neuronal differentiation from induced pluripotent stem cells to model ASD. *Front. Cell. Neurosci.* 8.
- Kim, N., Stiegler, A.L., Cameron, T.O., Hallock, P.T., Gomez, A.M., Huang, J.H., Hubbard, S.R., Dustin, M.L., Burden, S.J., 2008. Lrp4 Is a Receptor for Agrin and Forms a Complex with MuSK. *Cell* 135, 334–342.
- Kjaer, M., 2004. Role of extracellular matrix in adaptation of tendon and skeletal muscle to mechanical loading. *Physiol. Rev.* 84, 649–698.
- Kjær, M., 2004. Role of Extracellular Matrix in Adaptation of Tendon and Skeletal Muscle to Mechanical Loading. *Physiol Rev* 84, 649–698.
- Kleinman, H.K., Martin, G.R., 2005. Matrigel: Basement membrane matrix with biological activity. *Semin. Cancer Biol.* 15, 378–386.
- Korecka, J. a., van Kesteren, R.E., Blaas, E., Spitzer, S.O., Kamstra, J.H., Smit, A.B., Swaab, D.F., Verhaagen, J., Bossers, K., 2013. Phenotypic Characterization of Retinoic Acid Differentiated SH-SY5Y Cells by Transcriptional Profiling. *PLoS One* 8.
- Langer, R., Vacanti, J.P., 1993. Tissue engineering. *Science* (80-.). 260, 920–926.

- Langlois, A., Duval, D., 1997. Differentiation of the human NT2 cells into neurons and glia. *Methods Cell Sci.* 19, 213–219.
- Larkin, L.M., Meulen, J.H.V.A.N.D.E.R., Dennis, R.G., Kennedy, J.B., 2005. Functional evaluation of nerve-skeletal muscle constructs engineered in vitro. *Vitr. cell* 42, 75–82.
- Lee, G., Papapetrou, E.P., Kim, H., Chambers, S.M., Mark, J., Fasano, C. a, Ganat, Y.M., Menon, J., Viale, A., Tabar, V., Sadelain, M., Studer, L., 2010. Modeling pathogenesis and treatment of familial dysautonomia using patient specific iPSCs 461, 402–406.
- Lee, V.M., Andrews, P.W., 1986. Differentiation of NTERA-2 clonal human embryonal carcinoma cells into neurons involves the induction of all three neurofilament proteins. *J. Neurosci.* 6, 514–521.
- Legay, C., Mei, L., 2017. Moving forward with the neuromuscular junction. *J. Neurochem.* 142, 59–63.
- Letourneau, P.C., Condic, M.L., Snow, D.M., 1994. Interactions of developing neurons with the extracellular matrix. *J Neurosci* 14, 915–928.
- Lewis, M.P., Machell, J.R., Hunt, N.P., Sinanan, a C., Tippett, H.L., 2001. The extracellular matrix of muscle--implications for manipulation of the craniofacial musculature. *Eur. J. Oral Sci.* 109, 209–21.
- Li, R., Wu, F., Ruonala, R., Sapkota, D., Hu, Z., Mu, X., 2014. Isl1 and Pou4f2 form a complex to regulate target genes in developing retinal ganglion cells. *PLoS One* 9.
- Li, X.-J., Du, Z.-W., Zarnowska, E.D., Pankratz, M., Hansen, L.O., Pearce, R. a, Zhang, S.-C., 2005. Specification of motoneurons from human embryonic stem cells. *Nat. Biotechnol.* 23, 215–221.
- Li, X., Krawetz, R., Liu, S., Meng, G., Rancourt, D.E., 2009. ROCK inhibitor improves survival of cryopreserved serum/feeder-free single human embryonic stem cells. *Hum. Reprod.* 24, 580–589.

- Liao, J.K., Seto, M., Noma, K., 2009. Rho kinase (ROCK) inhibitors. *J Cardiovasc Pharmacol* 50, 17–24.
- Lieber, R.L., 2009. *Skeletal muscle structure, function and plasticity*, 3rd ed. Lippincott Williams & Wilkins.
- Lodish, H., Berk, A., Matsudaira, P., Kaiser, C.A., Krieger, M., Scott, M.P., Zipursky, L.S., Darnell, J., 2015. *Molecular Cell Biology*, 5th ed, Statewide Agricultural Land Use Baseline 2015. W.H.Freeman & Co Ltd.
- Lodish, H., Berk, A., Zipursky, S.L., Matsudaira, P., Baltimore, D., Darnell, J., 2000. *Molecular cell biology*, 4th ed. W.H.Freeman & Co Ltd.
- Lu, D., Chen, E.Y.T., Lee, P., Wang, Y.-C., Ching, W., Markey, C., Gulstrom, C., Chen, L.-C., Nguyen, T., Chin, W.-C., 2015. Accelerated neuronal differentiation toward motor neuron lineage from human embryonic stem cell line (H9). *Tissue Eng. Part C. Methods* 21, 242–52.
- Lumley, J.S., Craven, J.L., Aitken, J.T., 1980. *Essential Anatomy*, 3rd ed. Churchill Livingstone, New York.
- Lund, A.W., Yener, B., Stegemann, J.P., Plopper, G.E., 2009. The natural and engineered 3D microenvironment as a regulatory cue during stem cell fate determination. *Tissue Eng. Part B. Rev.* 15, 371–380.
- Ma, L., Liu, Y., Zhang, S.-C., 2011. Directed differentiation of dopamine neurons from human pluripotent stem cells BT - human pluripotent stem cells: methods and protocols, in: Schwartz, P.H., Wesselschmidt, R.L. (Eds.), . Humana Press, Totowa, NJ, pp. 411–418.
- Ma, W., Tavakoli, T., Derby, E., Serebryakova, Y., Rao, M.S., Mattson, M.P., 2008. Cell-extracellular matrix interactions regulate neural differentiation of human embryonic stem cells. *BMC Dev. Biol.* 8, 1–13.
- Machida, S., Spangenburg, E.E., Booth, F.W., 2004. Primary rat muscle progenitor cells have decreased proliferation and myotube formation during passages. *Cell Prolif.* 37, 267–277.

- MacIntosh, B.R., Gardiner, P.F., McComas, A.J., 2006. *Skeletal muscle: form and function*, II. ed. USA.
- Maden, M., Graham, A., Zile, M., Gale, E., 2000. Abnormalities of somite development in the absence of retinoic acid. *Int. J. Dev. Biol.* 44, 151–159.
- Maffioletti, S.M., Gerli, M.F.M., Ragazzi, M., Dastidar, S., Benedetti, S., Loperfido, M., VandenDriessche, T., Chuah, M.K., Tedesco, F.S., 2015. Efficient derivation and inducible differentiation of expandable skeletal myogenic cells from human ES and patient-specific iPS cells. *Nat. Protoc.* 10, 941.
- Maffioletti, S.M., Sarcar, S., Henderson, A.B.H., Mannhardt, I., Pinton, L., Moyle, L.A., Steele-Stallard, H., Cappellari, O., Wells, K.E., Ferrari, G., Mitchell, J.S., Tyzack, G.E., Kotiadis, V.N., Khedr, M., Ragazzi, M., Wang, W., Duchen, M.R., Patani, R., Zammit, P.S., Wells, D.J., Eschenhagen, T., Tedesco, F.S., 2018. Three-dimensional human iPSC-derived artificial skeletal muscles model muscular dystrophies and enable multilineage tissue engineering. *Cell Rep.* 23, 899–908.
- Maier, O., Böhm, J., Dahm, M., Brück, S., Beyer, C., Johann, S., 2013. Neurochemistry International Differentiated NSC-34 motoneuron-like cells as experimental model for cholinergic neurodegeneration. *Neurochem. Int.* 62, 1029–1038.
- Manabe, Y., Miyatake, S., Takagi, M., Nakamura, M., Okeda, A., Nakano, T., Hirshman, M.F., Goodyear, L.J., Fujii, N.L., 2012. Characterization of an acute muscle contraction model using cultured C2C12 myotubes. *PLoS One* 7.
- Marangi, P.A., Forsayeth, J.R., Mittaud, P., Erb-Vögtli, S., Blake, D.J., Moransard, M., Sander, A., Fuhrer, C., 2001. Acetylcholine receptors are required for agrin-induced clustering of postsynaptic proteins. *EMBO J.* 20, 7060–7073.
- Martin-Ibañez, R., Unger, C., Strömberg, A., Baker, D., Canals, J.M., Hovatta, O., 2008. Novel cryopreservation method for dissociated human embryonic stem cells in the presence of a ROCK inhibitor. *Hum. Reprod.* 23, 2744–2754.
- Martin, N.R.W., 2012. A tissue engineering human skeletal muscle model for use in exercise

sciences. University of Bedfordshire.

Martin, N.R.W., Passey, S.L., Player, D.J., Khodabukus, A., Ferguson, R. a., Sharples, A.P., Mudera, V., Baar, K., Lewis, M.P., 2013. Factors affecting the structure and maturation of human tissue engineered skeletal muscle. *Biomaterials* 34, 5759–5765.

Martin, N.R.W., Passey, S.L., Player, D.J., Mudera, V., Baar, K., Greensmith, L., Lewis, M.P., 2015. Neuromuscular Junction Formation in Tissue-Engineered Skeletal Muscle Augments Contractile Function and Improves Cytoskeletal Organization. *Tissue Eng. Part A* 21.

Martin, N.R.W., Turner, M.C., Farrington, R., Player, D.J., Lewis, M.P., 2017. Leucine elicits myotube hypertrophy and enhances maximal contractile force in tissue engineered skeletal muscle in vitro. *J. Cell. Physiol.* 232, 2788–2797.

Matthews, V.B., Åström, M.B., Chan, M.H.S., Bruce, C.R., Krabbe, K.S., Prelovsek, O., Åkerström, T., Yfanti, C., Broholm, C., Mortensen, O.H., Penkowa, M., Hojman, P., Zankari, A., Watt, M.J., Bruunsgaard, H., Pedersen, B.K., Febbraio, M.A., 2009. Brain-derived neurotrophic factor is produced by skeletal muscle cells in response to contraction and enhances fat oxidation via activation of AMP-activated protein kinase. *Diabetologia* 52, 1409–1418.

Matusica, D., Fenech, M.P., Rogers, M., Rush, R.A., 2008. Characterization and use of the NSC-34 cell line for study of neurotrophin receptor trafficking 565, 553–565.

McConville, J., Vincent, A., 2002. Diseases of the Neuromuscular junction: Myasthenia Gravis. *Curr. Opin. Pharmacol.* 2, 296–301.

McMahan, U.J., Horton, S.E., Werle, M.J., Honig, L.S., Kroger, S., Ruegg, M.A., Escher, G., 1992. No Title. *Curr. Opin. Cell Biol.* 4, 869–874.

Mey, J., McCaffery, P., 2004. Retinoic acid signaling in the nervous system of adult vertebrates. *Neuroscientist* 10, 409–421.

Miralles, F., 2016. Modelling the response to low-frequency repetitive nerve stimulation of

- myasthenia gravis and Lambert–Eaton myasthenic syndrome. *Med. Biol. Eng. Comput.* 54, 1761–1778.
- Molina, W., Reyes, E., Joshi, N., Barrios, A., Hernandez, L., 2010. Maturation of the neuromuscular junction in masseters of human fetus. *Rom. J. Morphol. Embryol.* 51, 537–541.
- Morimoto, Y., Kato-Negishi, M., Onoe, H., Takeuchi, S., 2013. Three-dimensional neuron-muscle constructs with neuromuscular junctions. *Biomaterials* 34, 9413–9419.
- Mosesson, M.W., 2005. Fibrinogen and fibrin structure and functions. *J. Thromb. Haemost.* 3, 1894–1904.
- Mouly, V., Aamiri, A., Bigot, A., Cooper, R.N., Di Donna, S., Furling, D., Gidaro, T., Jacquemin, V., Mamchaoui, K., Negroni, E., Perie, S., Renault, V., Silva-Barbosa, S.D., Butler-Browne, G.S., 2005. The mitotic clock in skeletal muscle regeneration, disease and cell mediated gene therapy. *Acta Physiol Scand* 184, 3–15.
- Mousavi, K., Miranda, W., Parry, D.J., 2002. Neurotrophic factors enhance the survival of muscle fibers in EDL, but not SOL, after neonatal nerve injury. *AJP Cell Physiol.* 283, C950–C959.
- Murphy, N.P., Ball, S.G., Vaughan, P.F.T., 1991. Potassium- and carbachol-evoked release of [3H]Noradrenaline from human neuroblastoma cells, SH-SY5Y. *J. Neurochem.* 56, 1810–1815.
- Nakashima, H., Ohkawara, B., Ishigaki, S., Fukudome, T., Ito, K., Tsushima, M., Konishi, H., Okuno, T., Yoshimura, T., Ito, M., Masuda, A., Sobue, G., Kiyama, H., Ishiguro, N., Ohno, K., 2016. R-spondin 2 promotes acetylcholine receptor clustering at the neuromuscular junction via Lgr5. *Sci. Rep.* 6, 1–14.
- Necker, R., 2004. Distribution of choline acetyltransferase and NADPH diaphorase in the spinal cord of the pigeon. *Anat. Embryol. (Berl).* 208, 169–181.
- Nerem, R.M., 1992. Tissue engineering in the USA. *Med. Biol. Eng. Comput.* 30, CE8–CE12.

- Noah, E., Winkel, R., Schramm, U., Kühnel, W., 2002. Impact of innervation and exercise on muscle regeneration in neovascularized muscle grafts in rats, *Annals of anatomy*.
- Olson, E.N., Klein, W.H., 1994. bHLH factors in muscle development: dead lines and commitments, what to leave in and what to leave out. *Genes Dev.* 8, 1–8.
- Ostrovidov, S., Ahadian, S., Ramon-Azcon, J., Hosseini, V., Fujie, T., Parthiban, S.P., Shiku, H., Matsue, T., Kaji, H., Ramalingam, M., Bae, H., Khademhosseini, A., 2017. Three-dimensional co-culture of C2C12/PC12 cells improves skeletal muscle tissue formation and function. *J. Tissue Eng. Regen. Med.* 11, 582–595.
- Ostrovidov, S., Hosseini, V., Ahadian, S., Fujie, T., Parthiban, S.P., Ramalingam, M., Bae, H., Kaji, H., Khademhosseini, A., 2014. Skeletal muscle tissue engineering: methods to form skeletal myotubes and their applications. *Tissue Eng. Part B Rev.* 20, 403–436.
- Påhlman, S., Hoehner, J.C., Nånberg, E., Hedborg, F., Fagerström, S., Gestblom, C., Johansson, I., Larsson, U., Lavenius, E., Ortoft, E., 1995. Differentiation and survival influences of growth factors in human neuroblastoma. *Eur. J. Cancer* 31A, 453–8.
- Påhlman, S., Ruusala, a I., Abrahamsson, L., Mattsson, M.E., Esscher, T., 1984. Retinoic acid-induced differentiation of cultured human neuroblastoma cells: a comparison with phorbol ester-induced differentiation. *Cell Differ.* 14, 135–144.
- Pardo-Figueres, M. de las M., 2017. Designing neuronal networks with chemically modified substrates: an improved approach to conventional in vitro neural systems. Loughborough University.
- Passey, S., Martin, N., Player, D., Lewis, M.P., 2011. Stretching skeletal muscle in vitro: Does it replicate in vivo physiology? *Biotechnol. Lett.* 33, 1513–1521.
- Patsch, C., Challet-meylan, L., Thoma, E.C., Urich, E., Sullivan, J.F.O., Grainger, S.J., Kapp, F.G., Sun, L., Xia, Y., Florido, M.H.C., He, W., Pan, W., Prummer, M., Warren, R., Jakob-roetne, R., Certa, U., Jagasia, R., Freskgård, P., Kling, D., Huang, P., Zon, L.I., Chaikof, E.L., Robert, E., Graf, M., Iacone, R., Cowan, C.A., 2016. Generation of vascular endothelial and smooth muscle cells from human pluripotent stem cells. *Nat. Cell Biol.*

17, 994–1003.

Pette, D., Staron, R.S., 2000. Myosin isoforms, muscle fiber types, and transitions. *Microsc. Res. Tech.* 50, 500–509.

Pevny, L.H., Sockanathan, S., Placzek, M., Lovell-Badge, R., 1998. A role for SOX1 in neural determination. *Development* 125, 1967–1978.

Pfaff, S.L., Mendelsohn, M., Stewart, C.L., Edlund, T., Jessell, T.M., 1996. Requirement for LIM homeobox gene *Isl1* in motor neuron generation reveals a motor neuron-dependent step in interneuron differentiation. *Cell* 84, 309–320.

Player, D.J., 2013. An in Vitro Model for Assessment of Skeletal Muscle Adaptation Following Exercise Related Physiological Cues. University of Bedfordshire.

Player, D.J., Martin, N.R.W., Passey, S.L., Sharples, a. P., Mudera, V., Lewis, M.P., 2014. Acute mechanical overload increases IGF-I and MMP-9 mRNA in 3D tissue-engineered skeletal muscle. *Biotechnol. Lett.* 36, 1113–1124.

Podrygajlo, G., Tegenge, M.A., Gierse, A., Paquet-Durand, F., Tan, S., Bicker, G., Stern, M., 2009. Cellular phenotypes of human model neurons (NT2) after differentiation in aggregate culture. *Cell Tissue Res.* 336, 439–452.

Powell, C. a, Smiley, B.L., Mills, J., Vandeburgh, H.H., 2002. Mechanical stimulation improves tissue-engineered human skeletal muscle. *Am. J. Physiol. Cell Physiol.* 283, C1557–C1565.

Presgraves, S.P., Ahmed, T., Borwege, S., Joyce, J.N., 2004. Terminally differentiated SH-SY5Y cells provide a model system for studying neuroprotective effects of dopamine agonists. *Neurotox. Res.* 5, 579–598.

Purves, D., Augustine, G.J., Fitzpatrick, D., Hall, W.C., Lamantia, A.-S., Mcnamara, J.O., Willians, S.M., 2004. *Neuroscience*, Sunderland.

Qazi, T.H., Mooney, D.J., Pumberger, M., Geißler, S., Duda, G.N., 2015. Biomaterials based

- strategies for skeletal muscle tissue engineering: Existing technologies and future trends. *Biomaterials* 53, 502–521.
- Qu, Q., Li, D., Louis, K.R., Li, X., Yang, H., Sun, Q., Crandall, S.R., Tsang, S., Zhou, J., Cox, C.L., Cheng, J., Wang, F., 2014. High-efficiency motor neuron differentiation from human pluripotent stem cells and the function of Islet-1. *Nat. Commun.* 5, 3449.
- Reijntjes, S., Francis-West, P., Mankoo, B.S., 2010. Retinoic acid is both necessary for and inhibits myogenic commitment and differentiation in the chick limb. *Int. J. Dev. Biol.* 54, 125–134.
- Reinhardt, P., Glatza, M., Hemmer, K., Tsytsyura, Y., Thiel, C.S., Höing, S., Moritz, S., Parga, J. a, Wagner, L., Bruder, J.M., Wu, G., Schmid, B., Röpke, A., Klingauf, J., Schwamborn, J.C., Gasser, T., Schöler, H.R., Sternecker, J., 2013. Derivation and expansion using only small molecules of human neural progenitors for neurodegenerative disease modeling. *PLoS One* 8, e59252.
- Reynolds, B.A., Weiss, S., 1992. Nervous system generation of neurons and astrocytes from isolated cells of the adult mammalian central nervous system. *Science* (80-). 255, 1707–1710.
- Rhinn, M., Dolle, P., 2012. Retinoic acid signalling during development. *Development* 139, 843–858.
- Rimington, R., Capel, A., Fleming, J., Player, D., Mudera, V., Jones, J., Ferguson, R., Baker, L., Turner, M., Lewis, M., Martin, N., 2018a. 50uL Mould LS.
- Rimington, R., Capel, A., Fleming, J., Player, D., Turner, M., Baker, L., Martin, N., Ferguson, R., Mudera, V., Jones, J., Lewis, M., 2018b. 500 uL Mould.
- Rimington, R.P., Capel, A.J., Christie, S.D.R., Lewis, M.P., 2017. Biocompatible 3D printed polymers via fused deposition modelling direct C 2 C 12 cellular phenotype in vitro. *Lab Chip* 17, 2982–2993.
- Rudnicki, M.A., Schnegelsberg, P.N.J., Stead, R.H., Braun, T., Arnold, H.-H., Jaenisch, R.,

1993. MyoD or Myf-5 is required for the formation of skeletal muscle. *Cell* 75, 1351–1359.
- Sakar, M.S., Neal, D., Boudou, T., Borochin, M.A., Li, Y., Weiss, R., Kamm, R.D., Chen, C.S., Asada, H.H., 2012. Formation and optogenetic control of engineered 3D skeletal muscle bioactuators. *Lab Chip* 12, 4976–4985.
- Sandri, M., 2008. Signaling in Muscle Atrophy and Hypertrophy. *Physiology* 23, 160–170.
- Sarkanen, J.R., Nykky, J., Siikanen, J., Selinummi, J., Ylikomi, T., Jalonen, T.O., 2007. Cholesterol supports the retinoic acid-induced synaptic vesicle formation in differentiating human SH-SY5Y neuroblastoma cells. *J. Neurochem.* 102, 1941–1952.
- Sato, M., Ito, A., Kawabe, Y., Nagamori, E., Kamihira, M., 2011. Enhanced contractile force generation by artificial skeletal muscle tissues using IGF-I gene-engineered myoblast cells. *J. Biosci. Bioeng.* 112, 273–278.
- Schaeffer, L., De Kerchove D’Exaerde, A., Changeux, J.P., 2001. Targeting transcription to the neuromuscular synapse. *Neuron* 31, 15–22.
- Schiaffino, S., Reggiani, C., 2011. Fiber types in mammalian skeletal muscles. *Physiol. Rev.* 91, 1447–531.
- Schiaffino, S., Rossi, A.C., Smerdu, V., Leinwand, L.A., Reggiani, C., 2015. Developmental myosins: Expression patterns and functional significance. *Skelet. Muscle* 5, 1–14.
- Schmidt, C.E., Leach, J.B., 2003. Neural Tissue Engineering: Strategies for Repair and Regeneration. *Annu. Rev. Biomed. Eng.* 5, 293–347.
- Schmittgen, T.D., Livak, K.J., 2008. Analyzing real-time PCR data by the comparative CT method. *Nat. Protoc.* 3, 1101.
- Schubert, D., LaCorbiere, M., Klier, F.G., Steinbach, J.H., 1980. The modulation of neurotransmitter synthesis by steroid hormones and insulin. *Brain Res.* 190, 67–79.
- Sciote, J.J., Morris, T.J., 2000. Skeletal muscle function and fibre types: The relationship

- between occlusal function and the phenotype of jaw-closing muscles in human. *J. Orthod.* 27, 15–30.
- Scott, I.G., Åkerman, K.E.O., Heikkilä, J.E., Kaila, K., Andersson, L.C., 1986. Development of a neural phenotype in differentiating ganglion cell-derived human neuroblastoma cells. *J. Cell. Physiol.* 128, 285–292.
- Sharples, A.P., Player, D.J., Martin, N.R.W., Mudera, V., Stewart, C.E., Lewis, M.P., 2012. Modelling in vivo skeletal muscle ageing in vitro using three-dimensional bioengineered constructs. *Aging Cell* 11, 986–995.
- Shi, Y., Kirwan, P., Livesey, F.J., 2012. Directed differentiation of human pluripotent stem cells to cerebral cortex neurons and neural networks. *Nat. Protoc.* 7, 1836–1846.
- Shimojo, D., Onodera, K., Doi-Torii, Y., Ishihara, Y., Hattori, C., Miwa, Y., Tanaka, S., Okada, R., Ohyama, M., Shoji, M., Nakanishi, A., Doyu, M., Okano, H., Okada, Y., 2015. Rapid, efficient, and simple motor neuron differentiation from human pluripotent stem cells. *Mol. Brain* 8, 1–15.
- Shirasaki, R., Pfaff, S.L., 2002. Transcriptional codes and the control of neuronal identity. *Annu. Rev. Neurosci.* 25, 251–281.
- Si-Tayeb, K., Noto, F.K., Nagaoka, M., Li, J., Battle, M.A., Duris, C., North, P.E., Dalton, S., Duncan, S., 2010. Highly efficient generation of human hepatocyte-like cells from induced pluripotent stem cells. *Hepatology* 51, 297–305.
- Singh, V.K., Saini, A., Kalsan, M., Kumar, N., Chandra, R., 2016. Describing the Stem Cell Potency: The Various Methods of Functional Assessment and In silico Diagnostics. *Front. Cell Dev. Biol.* 4.
- Sleeman, M.W., Anderson, K.D., Lambert, P.D., Yancopoulos, G.D., Wiegand, S.J., 2000. The ciliary neurotrophic factor and its receptor, CNTFR alpha. *Pharm. Acta Helv.* 74, 265–272.
- Smith, A. S.T., Passey, S., Greensmith, L., Mudera, V., Lewis, M.P., 2012. Characterization

- and optimization of a simple, repeatable system for the long term in vitro culture of aligned myotubes in 3D. *J. Cell. Biochem.* 113, 1044–1053.
- Smith, A.S.T., 2012. Development and characterisation of a novel myotube-motoneuron 3D co-culture system.
- Smith, A.S.T., Passey, S., Greensmith, L., Mudera, V., Lewis, M.P., 2012. Characterization and optimization of a simple, repeatable system for the long term in vitro culture of aligned myotubes in 3D. *J. Cell. Biochem.* 113, 1044–1053.
- Smith, A.S.T., Passey, S.L., Martin, N.R.W., Player, D.J., Mudera, V., Greensmith, L., Lewis, M.P., 2016. Creating interactions between tissue-engineered skeletal muscle and the peripheral nervous system. *Cells Tissues Organs* 202, 143–158.
- Smith, A.S.T., Shah, R., Hunt, N.P., Lewis, M.P., 2010. The role of connective tissue and extracellular matrix signaling in controlling muscle development, function, and response to mechanical forces. *Semin. Orthod.* 16, 135–142.
- Smith, G.M., Liu, Y., Hong, J.W., 2013. Neuronal Cell Culture, *Methods in Molecular Biology*.
- Son, E., Ichida, J., Wainger, B., Toma, J., 2011. Conversion of Mouse and Human Fibroblasts into Functional Spinal Motor Neurons. *Cell Stem Cell* 9, 205–218.
- Son, Y.J., Thompson, W.J., 1995. Nerve sprouting in muscle is induced and guided by processes extended by schwann cells. *Neuron* 14, 133–141.
- Southam, K.A., King, A.E., Blizzard, C.A., McCormack, G.H., Dickson, T.C., 2013. Microfluidic primary culture model of the lower motor neuron-neuromuscular junction circuit. *J. Neurosci. Methods* 218, 164–169.
- Strohman, R.C., Bayne, E., Spector, D., Obinata, T., Micou-eastwood, J., Maniotis, A., 1990. Myogenesis and histogenesis of skeletal muscle on flexible membranes in vitro. *Vitr. Cell. Dev. Biol.* 26, 201–208.
- Su, H., Wang, L., Cai, J., Yuan, Q., Yang, X., Yao, X., Wong, W.M., Huang, W., Li, Z., Wan,

- J.B., Wang, Y., Pei, D., So, K.F., Qin, D., Wu, W., 2013. Transplanted motoneurons derived from human induced pluripotent stem cells form functional connections with target muscle. *Stem Cell Res.* 11, 529–539.
- Sun, Y., Huang, Z., Liu, W., Yang, K., Sun, K., Xing, S., Wang, D., Zhang, W., Jiang, X., 2012. Surface coating as a key parameter in engineering neuronal network structures in vitro. *Biointerphases* 7, 1–14.
- Takahashi, K., Yamanaka, S., 2006. Induction of Pluripotent Stem Cells from Mouse Embryonic and Adult Fibroblast Cultures by Defined Factors. *Cell* 126, 663–676.
- Tanabe, Y., William, C., Jessell, T.M., 1998. Specification of motor neuron identity by the MNR2 homeodomain protein. *Cell* 95, 67–80.
- Tatsumi, R., Sheehan, S.M., Iwasaki, H., Hattori, A., Allen, R.E., 2001. Mechanical stretch induces activation of skeletal muscle satellite cells in vitro. *Exp. Cell Res.* 267, 107–114.
- Ten Broek, R.W., Grefte, S., Von Den Hoff, J.W., 2010. Regulatory factors and cell populations involved in skeletal muscle regeneration. *J. Cell. Physiol.* 224, 7–16.
- Thomson, J.A., Itskovitz-eldor, J., Shapiro, S., Waknitz, M.A., Swiergiel, J.J., Jones, J.M., 1998. Embryonic stem cell lines derived from human blastocysts 282, 1145–1147.
- Toma, J.S., Shettar, B.C., Chipman, P.H., Pinto, D.M., Borowska, J.P., Ichida, J.K., Fawcett, J.P., Zhang, Y., Eggan, K., Rafuse, V.F., 2015. Motoneurons derived from induced pluripotent stem cells develop mature phenotypes typical of endogenous spinal motoneurons. *J. Neurosci.* 35, 1291–1306.
- Tong, Z., Seira, O., Casas, C., Reginensi, D., Homs-Corbera, A., Samitier, J., Del Río, J.A., 2014. Engineering a functional neuro-muscular junction model in a chip. *RSC Adv.* 4.
- Turner, M.C., Player, D.J., Martin, N.R.W., Akam, E.C., Lewis, M.P., 2018. The effect of chronic high insulin exposure upon metabolic and myogenic markers in C2C12 skeletal muscle cells and myotubes. *J. Cell. Biochem.*

- Umbach, J. a., Adams, K.L., Gundersen, C.B., Novitch, B.G., 2012a. Functional neuromuscular junctions formed by embryonic stem cell-derived motor neurons. *PLoS One* 7, 3–8.
- Umbach, J. a., Adams, K.L., Gundersen, C.B., Novitch, B.G., 2012b. Functional neuromuscular junctions formed by embryonic stem cell-derived motor neurons. *PLoS One* 7.
- Ungrin, M.D., Joshi, C., Nica, A., Bauwens, C., Zandstra, P.W., 2008. Reproducible, ultra high-throughput formation of multicellular organization from single cell suspension-derived human embryonic stem cell aggregates. *PLoS One* 3.
- Vandenburgh, H., Kaufman, S., 1979. In vitro model for stretch-induced hypertrophy of skeletal muscle. *Science* 203, 265–268.
- Vandenburgh, H.H., Karlisch, P., Farr, L., 1988. Maintenance of highly contractile tissue-cultured avian skeletal myotubes in collagen gel. *Vitr. Cell. Dev. Biol. - Anim.* 24, 166–174.
- Vitte, J., Attali, R., Warwar, N., Gurt, I., Melki, J., 2009. Spinal muscular atrophy. *Adv Exp Med Biol* 652, 237–246.
- Waclaw, R.R., Ehrman, L.A., Merchan-Sala, P., Kholi, V., Nardini, D., Capbell, K., 2017. Foxo1 is a downstream effector of Isl1 in direct pathway striatal projection neuron development within the embryonic mouse telencephalon. *Mol cell neurosci* 80, 44–51.
- Wallace, G., 1989. Agrin-induced extracellular apparatus specializations contain cytoplasmic, membrane, components of the postsynaptic apparatus. *Methods*.
- Weatherbee, S.D., Anderson, K. V., Niswander, L.A., 2006. LDL-receptor-related protein 4 is crucial for formation of the neuromuscular junction. *Development* 133, 4993–5000.
- Webster, R.G., 2018. Animal models of the neuromuscular junction, vitally informative for understanding function and the molecular mechanisms of congenital myasthenic syndromes. *Int. J. Mol. Sci.* 19.

- Wehrle, U., Düsterhöft, S., Pette, D., 1994. Effects of chronic electrical stimulation on myosin heavy chain expression in satellite cell cultures derived from rat muscles of different fiber-type composition. *Differentiation* 58, 37–46.
- Weiss, A., McDonough, D., Wertman, B., Acakpo-Satchivi, L., Montgomery, K., Kucherlapati, R., Leinwand, L., Krauter, K., 1999. Organization of human and mouse skeletal myosin heavy chain gene clusters is highly conserved. *Proc. Natl. Acad. Sci. U. S. A.* 96, 2958–63.
- Weiss, A., Schiaffino, S., Leinwand, L.A., 1999. Comparative sequence analysis of the complete human sarcomeric myosin heavy chain family: implications for functional diversity. *J. Mol. Biol.* 290, 61–75.
- Wheeler, H.E., Wing, C., Delaney, S.M., Komatsu, M., Dolan, M.E., 2015. Modeling chemotherapeutic neurotoxicity with human induced pluripotent stem cell-derived neuronal cells. *PLoS One* 10.
- Wichterle, H., Lieberam, I., Porter, J.A., Jessell, T.M., 2002. Directed differentiation of embryonic stem cells into motor neurons. *Cell* 110, 385–397.
- Wichterle, H., Wichterle, H., Lieberam, I., Lieberam, I., Porter, J. a, Porter, J. a, Jessell, T.M., Jessell, T.M., 2002. Directed differentiation of embryonic stem cells into motor neurons. *Cell* 110, 385–97.
- Wijesekera, L.C., Leigh, P.N., 2009. Amyotrophic lateral sclerosis. *Orphanet J. Rare Dis.* 4, 3.
- Winter, J., Schmidt, C., 2002. *Biomimetic Strategies and Applications in the Nervous System.*
- Witzemann, V., 2006. Development of the neuromuscular junction. *Cell Tissue Res.* 326, 263–271.
- Wu, H., Xiong, W.C., Mei, L., 2010. To build a synapse: signaling pathways in neuromuscular junction assembly. *Development* 137, 1017–33.
- Xiao, Y., Grieshammer, U., Rosenthal, N., 1995b. Regulation of a muscle-specific transgene

- by retinoic acid. *J. Cell Biol.* 129, 1345–1354.
- Xun, Z., Lee, D.Y., Lim, J., Canaria, C.A., Barnebey, A., Yanonne, S.M., McMurray, C.T., 2012. Retinoic acid-induced differentiation increases the rate of oxygen consumption and enhances the spare respiratory capacity of mitochondria in SH-SY5Y cells. *Mech. Ageing Dev.* 133, 176–185.
- Yamanaka, S., 2012. Perspective induced pluripotent stem cells: past, present, and future. *STEM* 10, 678–684.
- Yamanaka, S., Takahashi, K., Tanabe, K., Ohnuki, M., Narita, M., Ichisaka, T., Tomoda, K., 2007. Induction of pluripotent stem cells from adult human fibroblasts by defined factors. *Cell* 131, 861–72.
- Yasin, R., Van Beers, G., Nurse, K.C.E., Al-Ani, S., Landon, D.N., Thompson, E.J., 1977. A quantitative technique for growing human adult skeletal muscle in culture starting from mononucleated cells. *J. Neurol. Sci.* 32, 347–360.
- Yi, H., Xie, B., Liu, B., Wang, X., Xu, L., Liu, J., Li, M., Zhong, X., Peng, F., 2018. Derivation and identification of motor neurons from human urine-derived induced pluripotent stem cells. *Stem Cells Int.* 2018.
- Yonemura, S., Kitani-yasuda, T., Tsukita, S., 1993. The 220-kD protein colocalizing with cadherins in non-epithelial cells is identical to ZO-1, a tight junction-associated protein in epithelial cells: cDNA cloning and immunoelectron microscopy. *J. Cell Biol.* 121, 491–502.
- Yun, M.L., Jung, O.L., Jung, J.H., Ji, H.K., Park, S.H., Ji, M.P., Kim, E.K., Suh, P.G., Hyeon, S.K., 2008. Retinoic acid leads to cytoskeletal rearrangement through AMPK-Rac1 and stimulates glucose uptake through AMPK-p38 MAPK in skeletal muscle cells. *J. Biol. Chem.* 283, 33969–33974.
- Zeng, H., Guo, M., Martins-Taylor, K., Wang, X., Zhang, Z., Park, J.W., Zhan, S., Kronenberg, M.S., Lichtler, A., Liu, H.X., Chen, F.P., Yue, L., Li, X.J., Xu, R.H., 2010. Specification of region-specific neurons including forebrain glutamatergic neurons from human

induced pluripotent stem cells. *PLoS One* 5, 1–11.

Zhang, D., Jiang, W., Liu, M., Sui, X., Yin, X., Chen, S., Shi, Y., Deng, H., 2009. Highly efficient differentiation of human ES cells and iPS cells into mature pancreatic insulin-producing cells. *Cell Res.* 19, 429–438.

Zhang, S.C., Wernig, M., Duncan, I.D., Brustle, O., Thomson, J.A., 2001. In vitro differentiation of transplantable neural precursors from human embryonic stem cells. *Nat. Biotechnol.* 19, 1129–1133.

Zhang, W., Coldefy, A.S., Hubbard, S.R., Burden, S.J., 2011. Agrin binds to the N-terminal region of Lrp4 protein and stimulates association between Lrp4 and the first immunoglobulin-like domain in muscle-specific kinase (MuSK). *J. Biol. Chem.* 286, 40624–40630.

Zhu, G.H., Huang, J., Bi, Y., Su, Y., Tang, Y., He, B.C., He, Y., Luo, J., Wang, Y., Chen, L., Zuo, G.W., Jiang, W., Luo, Q., Shen, J., Liu, B., Zhang, W.L., Shi, Q., Zhang, B.Q., Kang, Q., Zhu, J., Tian, J., Luu, H.H., Haydon, R.C., Chen, Y., He, T.C., 2009. Activation of RXR and RAR signaling promotes myogenic differentiation of myoblastic C2C12 cells. *Differentiation* 78, 195–204.

Zigova, T., Willing, A.E., Tedesco, E.M., Borlongan, C. V., Saporta, S., Snable, G.L., Sanberg, P.R., 1999. Lithium chloride induces the expression of tyrosine hydroxylase in hNT neurons. *Exp. Neurol.* 157, 251–258.

9 SUPPLEMENTARY INFORMATION

9.1 APPENDIX A: SH-SY5Y neurites alignment to C2C12 myotubes

In C2C12/SH-SY5Y co-cultures in 3D tissue engineered constructs, SH-SY5Y were shown to extend neurites along the same direction as C2C12 myofibres. This alignment was quantified and is reported in **Table S9.1** below.

Table S9.1. Angle difference between the orientation of C2C12 muscle fibres and SH-SY5Y neurites.

	Angle difference
Fibrin gels	5.18 ± 1.16
Collagen gels	13.68 ± 8.28

9.2 APPENDIX B: Human skeletal muscle & SH-SY5Y co-culture

As an intermediate step between the chimeric C2C12/SH-SY5Y co-culture and the human primary one, human donor hu035 was co-cultured with SH-SY5Y in monolayer. Myotube formation was observed in all conditions. However, a higher number of myotubes was present when hu035 were monocultured in NDM or in the co-culture with the same medium. SH-SY5Y extended neurites in all conditions, but it was not possible to quantify their length due to imaging limitations. However, the neurites in co-culture, differentiated in MN MM, did not show the typical SH-SY5Y morphology that was previously reported in Chapter 3, nor compared to the monoculture or the co-culture with C2C12 cells.

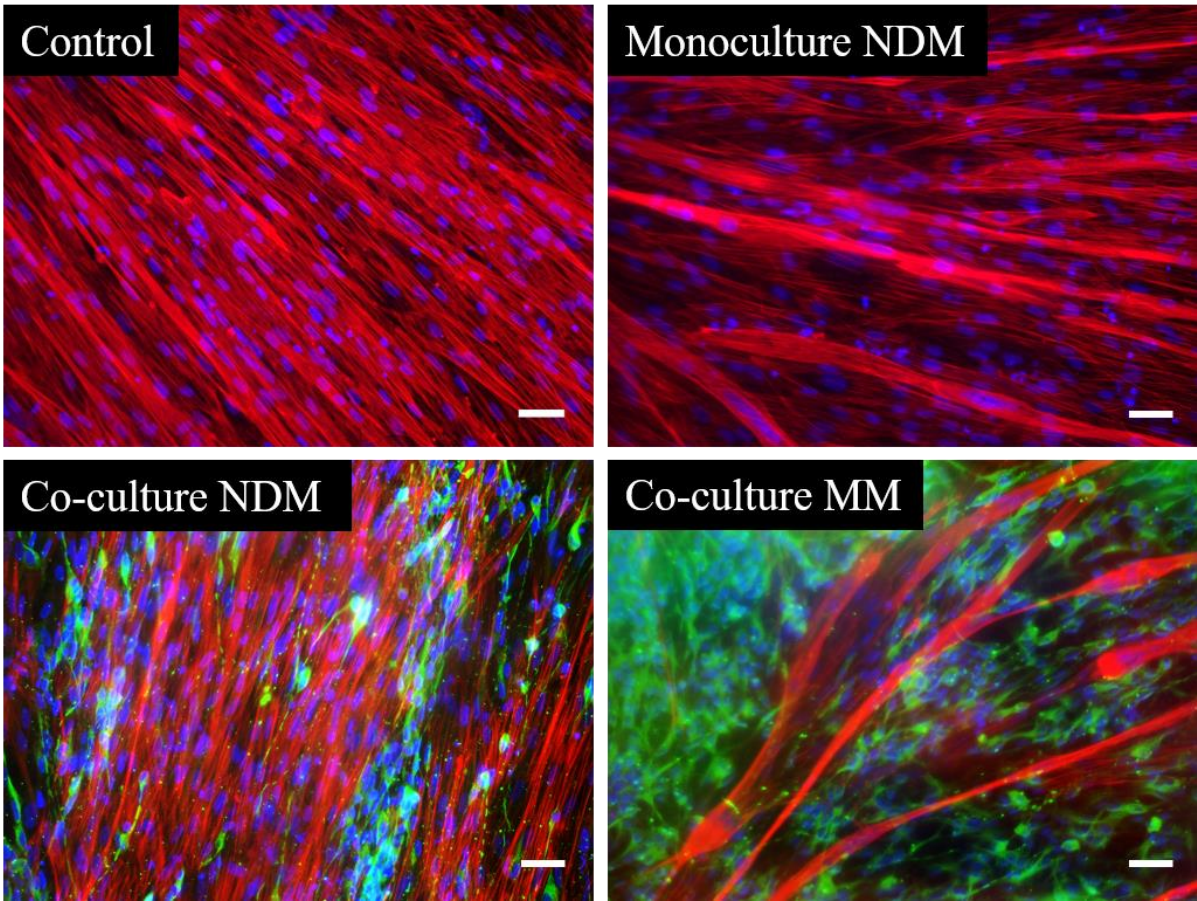


Figure S9.1. hu035 and SH-SY5Y co-culture in monolayer. The cells were immunostained for morphological markers: rhodamine phalloidin was used to identify actin filaments in SkM cells (red) and the nuclei were counterstained with DAPI (blue). Scale bars: 100 μ m.

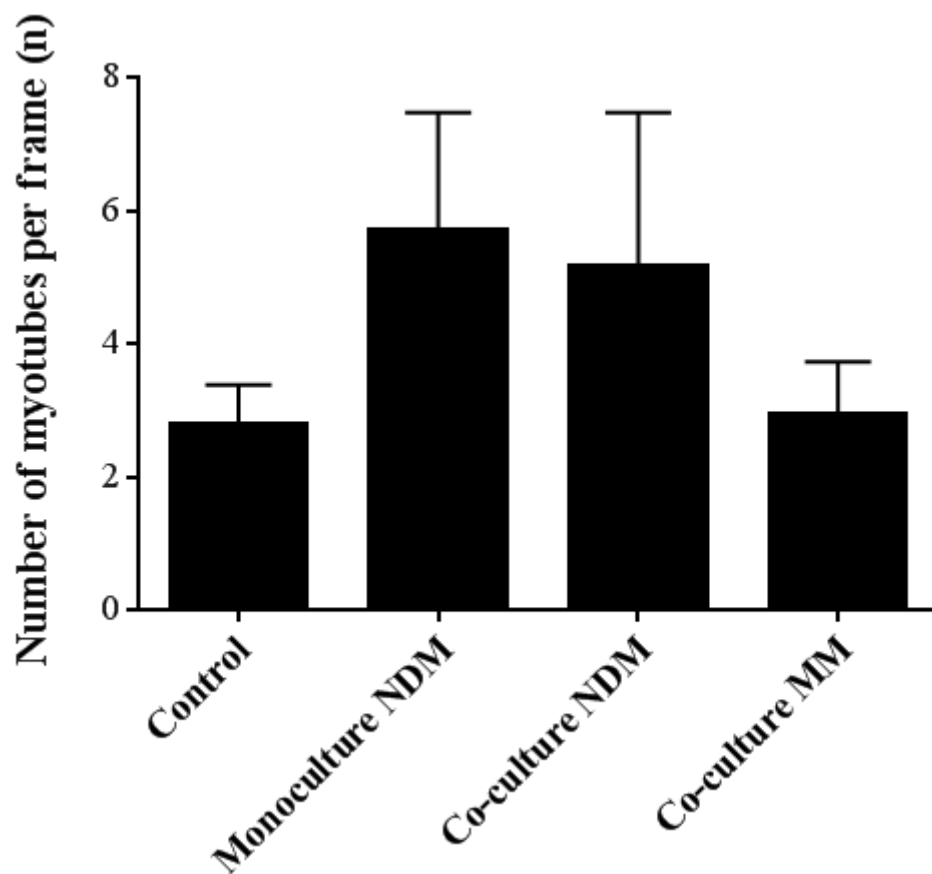


Figure S9.2. Number of hu035 myotubes per frame (n). Results are shown as average \pm SD, n=3.

9.3 APPENDIX C: SH-SY5Y vs iPSC-derived MNs comparison

To perform a comparison between the previously utilised neuroblastoma line SH-SY5Y and the hereby characterised MNPs, ChAT immunostaining and culture of SH-SY5Y in the conditions which are ideal for MNPs were performed. The cells were immunostained for the cholinergic marker ChAT as previously described (2.3.1.6). The MNPs characterised in this Chapter were cultured according to the manufacturer’s recommendations. These conditions differ from the culture and differentiation of SH-SY5Y neuroblastoma cells. A summary of the media compositions for either cell types can be found in **Table S9.2**. SH-SY5Y were expanded in standard conditions and seeded for the experiment in the respective experimental conditions. The differentiation was induced the day after plating, and was carried out for 5 days as required for standard differentiation conditions in NDM.

Table S9.2. Culture conditions for SH-SY5Y cells and MNPs.

Cells	Substrate	Growth Medium	Differentiation Medium
SH-SY5Y	Tissue culture plastic/glass	NGM: Glutamax 10% NFBS 1% P/S	NDM: Glutamax 2% NFBS 1 μ M RA 1% P/S
MNPs	SureBond™ for growth stage, SureBond™+ReadySet for differentiation stage	MN RM: Axol RM supplemented with 0.1 μ M RA and 10 μ M Y-27632 for adhesion, then RM with 0.1 μ M RA only	MM: Axol MM supplemented with 0.5 μ M RA, 5 ng/mL BDNF, 10 ng/mL CNTF

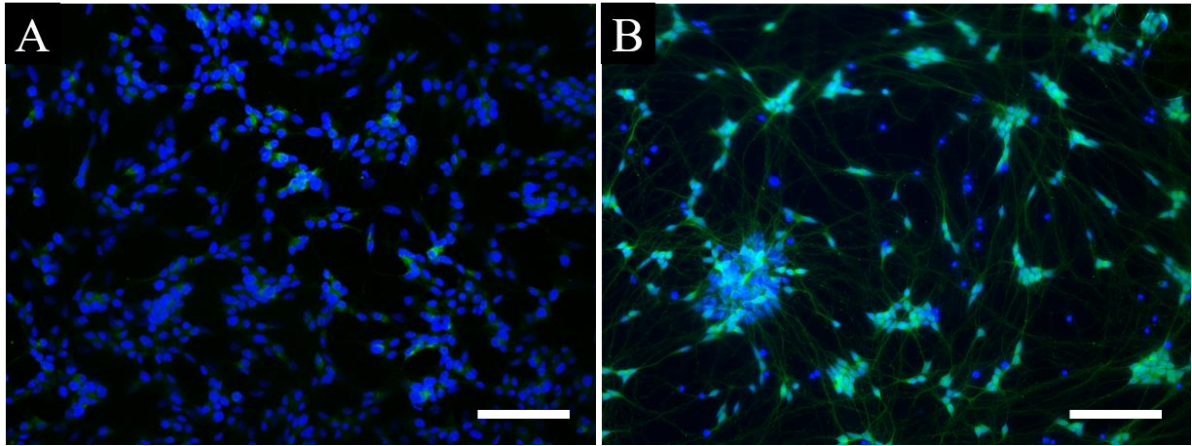


Figure S9.3. Positivity to ChAT immunostaining in SH-SY5Y and MNs. SH-SY5Y (A) and MNPs (B) were cultured and differentiated in their respective standard conditions. The cells were immunostained for ChAT (green) and the nuclei were counterstained with DAPI (blue). Scale bars: 100 μ m.

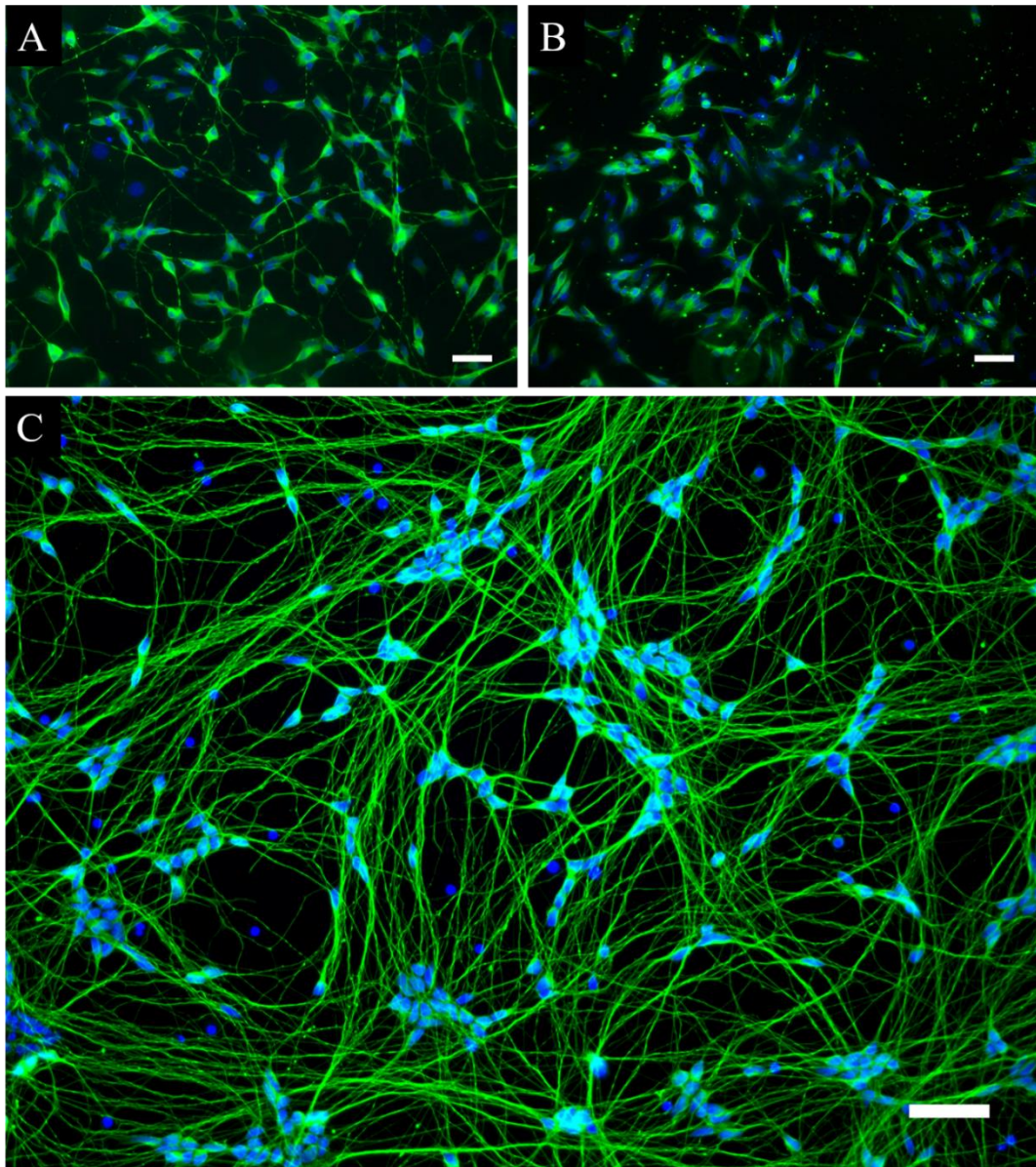


Figure S9.4. Morphological difference between SH-SY5Y and iPSC-derived MNs. SH-SY5Y cells cultured in standard conditions (A) and in iPSC-derived MNPs conditions (B). The cells were then immunostained for morphological markers: β -III Tubulin was used for the cytoskeleton (green) and DAPI was used to counterstain the nuclei (blue). Scale bars: 50 μ m.

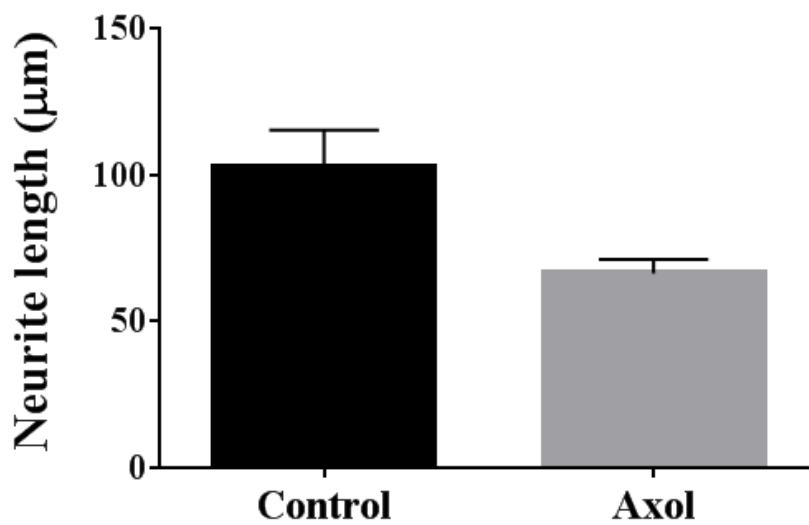


Figure S9.5. SH-SY5Y neurite length (μm) in different culture conditions. The neurite length was quantified in control culture and differentiation conditions (control), and in the conditions in which MNPs were cultured and differentiated (Axol). Results are shown as average \pm SD, $n=3$.

9.4 APPENDIX D: Media and substrate for human MNs: compatibility for hSkM

A preliminary experiment was carried out to investigate the effect of the neuronal substrate SureBond™+ReadySet on primary hSkM. This was compared to control condition being gelatin, as this is normally used as a coating solution for primary muscle cultures. Furthermore, differentiation was carried out using conventional MDM for cells expanded on gelatin, and neuronal differentiation medium (MM) for both gelatin and SureBond™+ReadySet. The formulation of the MM used for this experiment differed from the one used in Chapters 5 and 6. However, important information was gathered regarding media compatibility and how the substrate affects proliferation, differentiation and desmin positivity of hSkM cells.

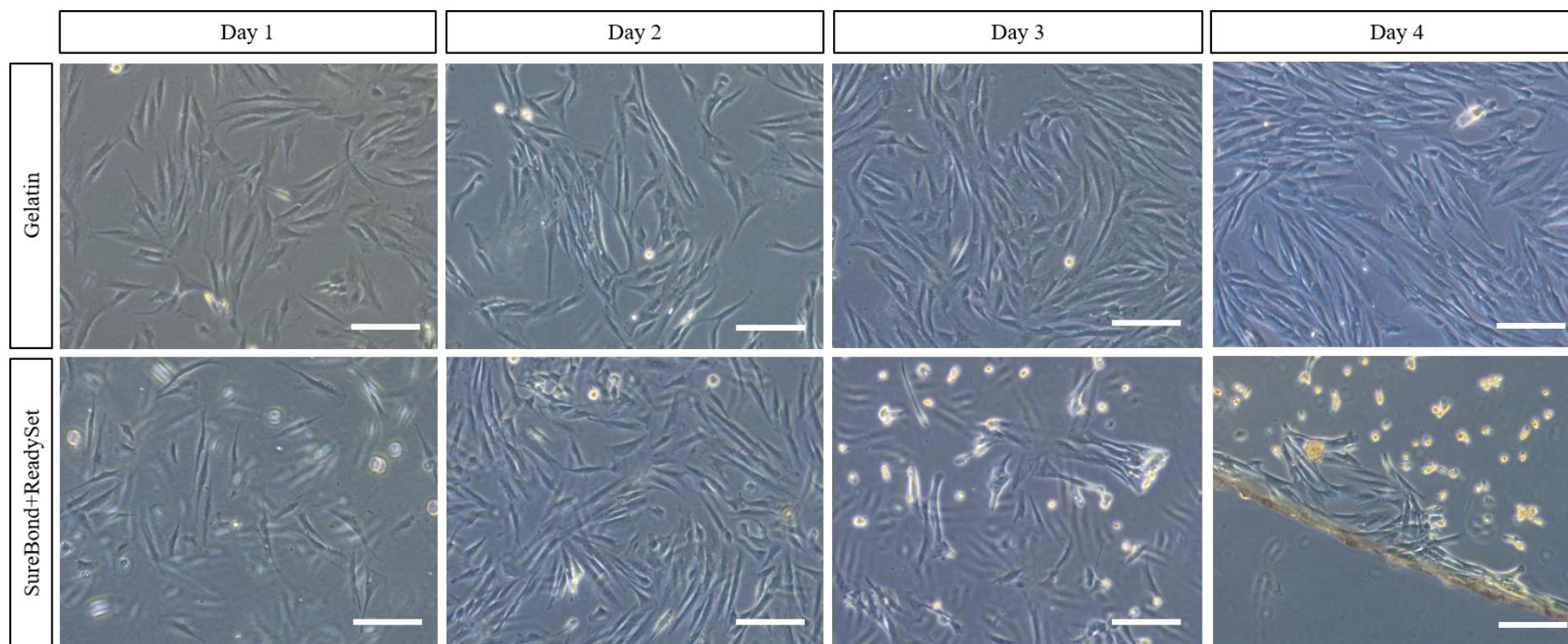


Figure S9.6. hu029 proliferation on gelatin and SureBond™+ReadySet over a period of 4 days. Scale bars: 100 μm .

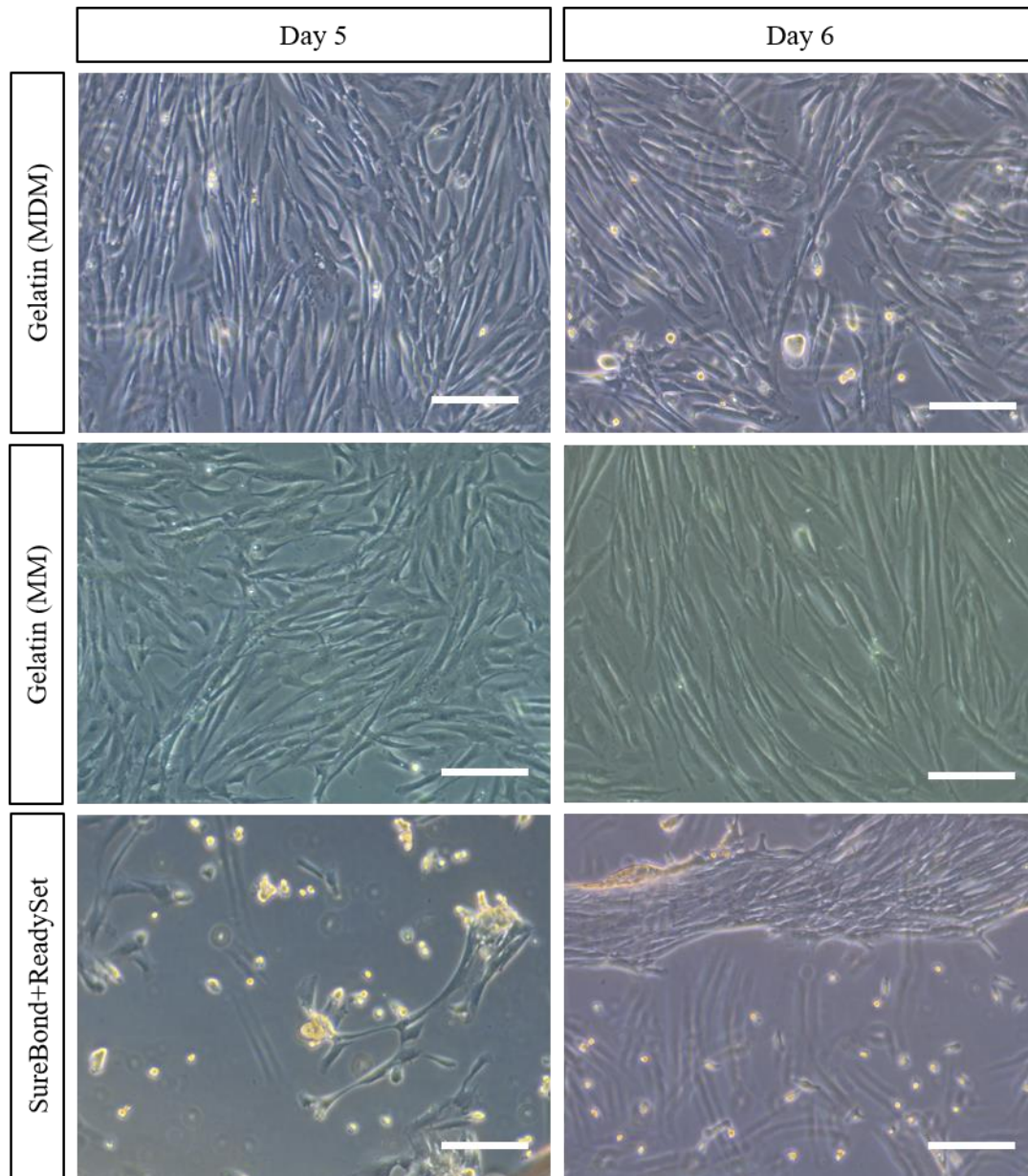


Figure S9.7. hu029 differentiation on gelatin (in control conditions, MDM and neuronal medium, MM) and SureBond™+ReadySet (in neuronal MM). Scale bars: 100 μ m.

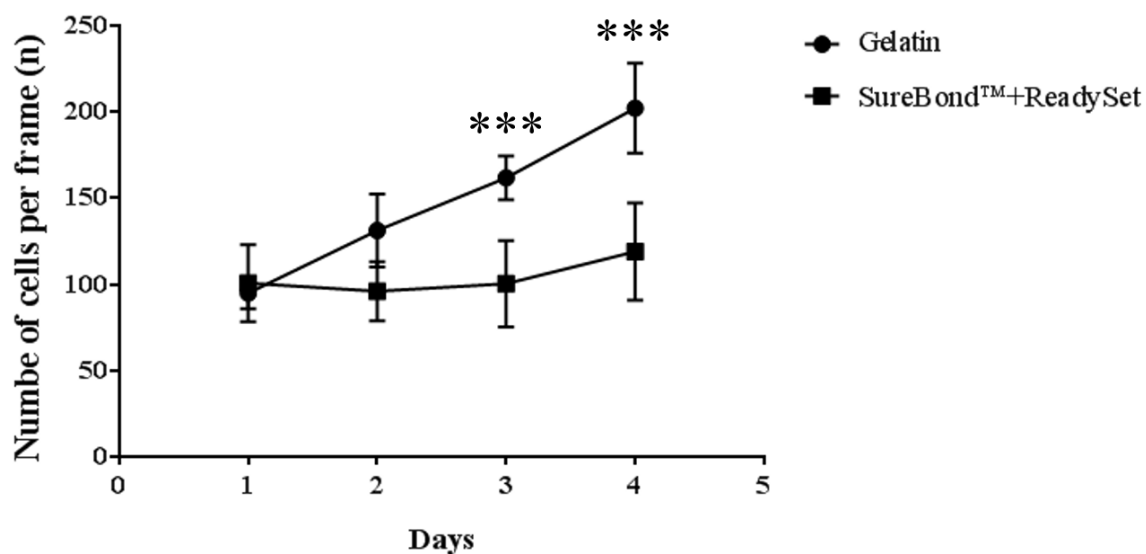


Figure S9.8. Number of hu029 cells per frame (n) during proliferation on gelatin or SureBond™+ReadySet. Human primary SkM cells hu029 were cultured on both gelatin- and SureBond™+ReadySet-coated glass coverslips. The cells were seeded in MGM and expanded until they were confluent (day 4). The number of cells/frame was quantified daily and averaged across 3 wells in the same conditions. The asterisks show significant differences between the two substrates (***) = $p \leq 0.001$). Results are shown as average \pm SD, n=3.

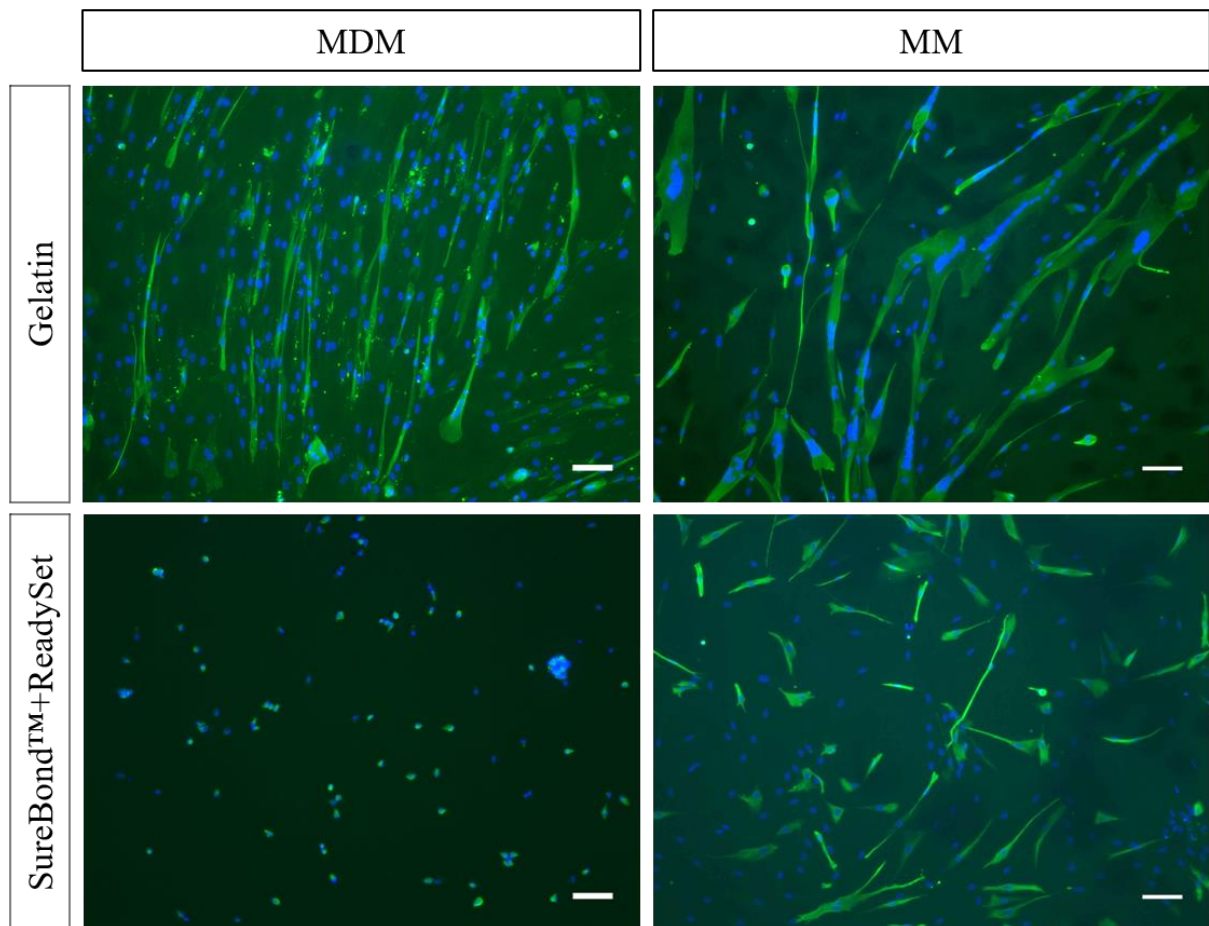


Figure S9.9. Desmin positivity of hu029 cells cultured on gelatin or SureBond™+ReadySet, and differentiated in either MDM or MM. Myogenic cells were immunostained with desmin (green) and the nuclei with DAPI (blue). Scale bars: 100 μ m.

9.5 APPENDIX E: Culture of Human iPSC-Derived Motor Neuron Progenitors

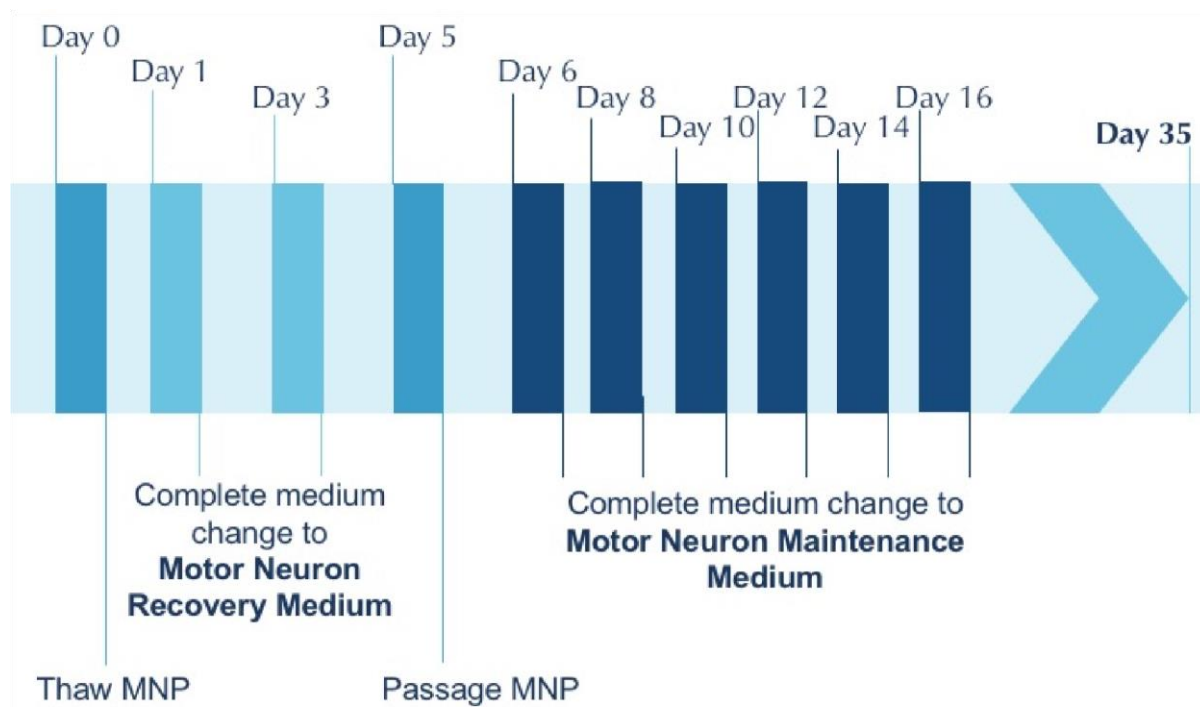
Product Information

Catalog. No.	Product Name	Format	Stock Conc.	Storage on Arrival	Thawing Instructions	Storage Once Thawed
ax0070	Human iPSC-Derived Motor Neuron Progenitors	TBC cells/vial	N/A	Liquid Nitrogen	Follow protocol	N/A
ax0071	Motor Neuron Recovery Medium	30 mL	1x	-80°C	Overnight at 4°C	Once thawed store aliquot at 4°C for up to 1 week
ax0072	Motor Neuron Maintenance Medium	200 mL	1x	-80°C	Overnight at 4°C	Once thawed store aliquot at 4°C for up to 1 week
ax0041+	SureBond+Ready Set	SureBond 3 x 120 µL ReadySet 2 x 10 mL	SureBond 50x ReadySet 1x	SureBond -80°C ReadySet 4°C	SureBond Overnight at 4°C ReadySet N/A	SureBond Store at 4°C for up to 2 weeks ReadySet Store at 4°C for up to 1 month
ax0041XF	SureBond-XF	1 mL	200x	4°C	N/A	Store at 4°C for up to 1 month
ax0041	SureBond	3 x 120 µL	50x	-80°C	Overnight at 4°C	Store at 4°C for up to 2 weeks

ax0044	Unlock	25 mL	1x	Aliquot & store at -80°C for 5 months	Overnight at 4°C	Once thawed store aliquot at 4°C for up to 1 week
--------	--------	-------	----	---------------------------------------	------------------	---

Additional Reagents		
Product Name	Provider	Catalog No.
Retinoic acid	Sigma-Aldrich	R2625
Brain-Derived Neurotrophic Factor (BDNF)	Peprtech	450-02
Ciliary Neurotrophic Factor (CNTF)	Peprtech	450-13
Rock Inhibitor (Y27632 hydrochloride)	Selleck Chemicals	S1049

These reagents must be added fresh for each use to each aliquot of medium.



Important!

Axol Neural Cell Culture Media

DOES NOT contain antibiotics or antifungal agents. Axol Bioscience does not recommend the use of antimicrobial agents such as penicillin, streptomycin and amphotericin. Antimicrobial agents should not be necessary if proper aseptic technique is adopted

Preparation of Reagents

Preparation of Motor Neuron Recovery Medium

- Upon receipt aliquot and store **Motor Neuron Recovery Medium** at or below - **80°C** protected from light.
- When ready to use, thaw an aliquot of **Motor Neuron Recovery Medium** overnight at **4°C** in the dark.
- **Motor Neuron Recovery Medium** requires supplement with retinoic acid before use.
- Prepare **Motor Neuron Recovery Medium** by adding the following concentration of retinoic acid:

Growth Factor	Stock Concentration	Final Concentration	50 mL Medium
Retinoic acid	1 mM	0.1 μ M	5 μ L

During thawing and passaging **Motor Neuron Recovery Medium** should be supplemented with rock inhibitor (Y27632 hydrochloride) to a final concentration of 10 μ M.

Preparation of Motor Neuron Maintenance Medium

- Upon receipt aliquot and store **Motor Neuron Maintenance Medium** at or below **-80°C** protected from light.
- When ready to use, thaw an aliquot of **Motor Neuron Maintenance Medium** overnight at **4°C** in the dark.
- **Motor Neuron Maintenance Medium** requires supplement with 3 compounds before use.
- Prepare **Motor Neuron Maintenance Medium** by adding the following factors fresh each time:

Growth Factor	Stock Concentration	Final Concentration	50 mL Medium
Retinoic acid	1 mM	0.5 μ M	25 μ L
Brain-Derived Neurotrophic Factor (BDNF)	10 μ g/mL	5 ng/mL	25 μ L
Ciliary Neurotrophic Factor (CNTF)	10 μ g/mL	10 ng/mL	50 μ L

SureBond Coating Solution (required for plating during recovery)

- Upon receipt store **SureBond** at **-80°C**.
- Thaw the **SureBond** coating solution overnight at **4°C**.
- Calculate the total surface area that requires coating.
- Dilute the **SureBond** stock solution (50x) in D-PBS (1x) (without calcium or magnesium) to make 1x working solution e.g. **120 μ L** in **6 mL**.

- Coat the surface of your culture vessel with the **SureBond** 1x working solution. We recommend coating at a volume of **200 μL per cm^2** . • Incubate your culture vessel **overnight** at **37°C**.

SureBond-XF Coating Solution (required for final plating on plastic)

- Upon receipt store **SureBond-XF** at **4°C**.
- Calculate the total surface area that requires coating.
- Dilute the **SureBond-XF** stock solution (200x) in Dulbecco's-PBS (1x) (D-PBS without calcium or magnesium) to make 1x working solution e.g. **30 μL in 6 mL**.
- Coat the surface of your culture vessel with the **SureBond-XF** 1x working solution. We recommend coating at a volume of **200 μL per cm^2** however, please optimize for your experiments.

SureBond+ReadySet Coating Solution (required for final plating on glass)

- Upon receipt store **SureBond** at or below **-80°C** and store **ReadySet** at **4°C**.
- Thaw the **SureBond** coating solution overnight at **4°C**.
- Calculate the total surface area that requires coating.
- Pre-coat your culture vessel with **ReadySet** at a volume of **250 μL per cm^2** .
- Incubate at **37°C** for **45 minutes**.
- Wash the plate thoroughly **four times** using an equal volume of sterile ddH₂O (e.g. if 250 μL of **ReadySet**, use 250 μL sterile ddH₂O). During each wash rock the dish to ensure thorough washing.
- Do not let the **ReadySet** dry out following washing, proceed straight to coating with **SureBond**.
- Dilute the **SureBond** stock solution (50x) in D-PBS (1x) (without calcium or magnesium) to make 1x working solution e.g. **120 μL in 6 mL**.
- Coat the surface of your culture vessel with the **SureBond** 1x working solution. We recommend coating at a volume of **200 μL per cm^2** .
- Incubate for **1 hour** at **37°C**.

Important!

Make sure that the coating does not evaporate.

Do not let the **SureBond** or **SureBond-XF** coating dry out before seeding the cells.

DO NOT wash the vessel after coating with **SureBond** or **SureBond-XF**.

Unlock (required for passaging)

- Upon receipt aliquot and store **Unlock** at or below **-80°C** protected from light.
- Stored at **-80°C**, the reagent is stable for 6 months from date of manufacture.

Culture of Human iPSC-Derived Motor Neuron Progenitors

Thawing and Plating

The day before thawing **iPSC-Derived Motor Neuron Progenitors**

- Thaw an aliquot of **Motor Neuron Recovery Medium** overnight at **4°C**.
- Prepare culture vessels by coating with **SureBond overnight**, Matrigel™ or Geltrex (prepared before seeding in accordance with manufacturer's instructions) prior to thawing cells.
- T-25 flasks or 60 mm dishes are recommended for initial plating of iPSC-Derived Motor Neurons after thawing.

On the day of thawing **Human iPSC-Derived Motor Neuron Progenitors**.

- Prepare **Motor Neuron Recovery Medium** by adding rock inhibitor (Y27632 hydrochloride) to a final concentration of 10µM and retinoic acid to a final concentration of 0.1 µM.
- Pre-warm all media and culture vessels to **37°C** before use.
- Add 4 mL of **Motor Neuron Recovery Medium** into a 15 mL sterile conical tube
- To thaw the cells – transfer the vial of cells from storage by transporting the vial buried in dry ice. Remove the vial from dry ice and transfer it to a **37°C** water bath.
- Quickly thaw the vial of cells in a **37°C** water bath. Do not completely submerge the vial (only up to 2/3rd of the vial). Remove the vial before the last bit of ice has melted, after 2-3 minutes.
- **Do not shake the vial during thawing.**
- Take the vial of cells to a biological safety cabinet, spraying the vial and hood thoroughly with 70% ethanol and wiping with an autoclaved paper towel before placing the vial in the hood.
- Using a P1000 pipette, gently, drop-wise add the cell suspension into the 15 mL sterile conical tube containing **Motor Neuron Recovery Medium**. Gently wash the cryogenic vial with **1 mL** of warm **Motor Neuron Recovery Medium** and transfer this to the 15 mL sterile conical tube.
- Centrifuge cells at **200 x g** for **5 minutes** at **room temperature**.
- Carefully aspirate and discard the supernatant with a pipette.

- Using a P1000 pipette, gently resuspend the cell pellet in **1 mL** of **Motor Neuron Recovery Medium** until they are in a single cell suspension.
- Perform a cell count to ensure optimal seeding density.
- Remove the coating solution and add an appropriate volume of medium to the culture vessel. Do not let the culture vessel dry out.
- Plate the resuspended cells drop-wise and evenly at a density ranging from **100,000 - 150,000 cells/cm²**.
- Gently rock the culture vessel back and forth to ensure an even seeding density.
- Incubate the cells at **37°C, 5% CO₂**.
- The day after plating, replace all of the medium with fresh pre-warmed, **37°C, Motor Neuron Recovery Medium** without rock inhibitor (Y27632 hydrochloride).
- **Every 2 days** replace all of the medium with fresh pre-warmed, **37°C, Motor Neuron Recovery Medium** (without rock inhibitor (Y27632 hydrochloride)). Passage the **iPSC-Derived Motor Neuron Progenitors** at **day 5** or **day 7**, depending on confluency.

Passaging and Maintenance of Human iPSC-Derived Motor Neuron Progenitors

- When the culture is 70 % confluent, it is ready to undergo passaging.

The day before passaging **iPSC-Derived Motor Neuron Progenitors**

- Thaw an aliquot of **Unlock** and **Motor Neuron Maintenance Medium** overnight at **4°C** before use and store at **4°C**.
- **Pre-Coat Culture Vessels:** Make sure to pre-coat the surface of your culture vessel that the cells will be passaged into. If continuing to expand **iPSC-Derived Motor Neuron Progenitors**, pre-coat culture vessels with **SureBond-XF** (for plastic culture vessels), **SureBond+ReadySet** (for glass culture vessels) or Matrigel™ (prepared before seeding in accordance with manufacturer's instructions).

On the day of passaging **Human iPSC-Derived Motor Neuron Progenitors**

- Prepare **Motor Neuron Maintenance Medium** by adding rock inhibitor (Y27632 hydrochloride) to a final concentration of 10µM and retinoic acid to a final concentration of 0.5 µM, BDNF to a final concentration of 5 ng/mL and CNTF to a final concentration of 10 ng/mL.
- Pre-warm all media and culture vessels to **37°C** before use.

- Remove all spent medium from cell culture vessels.
- Gently rinse the surface of the cell layer once with the Dulbecco's-PBS (1x) (D-PBS, without calcium or magnesium, **2 mL D-PBS (1x) per 10 cm² culture surface area**).
- Discard the D-PBS.
- To detach the cells from a coating of **SureBond** use **Unlock**.
- Add **1 mL per 10cm²** of culture surface area of cold/room temperature **Unlock**. Evenly distribute it over the entire cell layer. Incubate the cells for **5 minutes** at **37°C**.
- Use a P1000 pipette to transfer the cells drop-wise into a 15 mL sterile conical tube add gently **four volumes** of pre-warmed, **37°C**, **Motor Neuron Maintenance Medium**. (For example if 1 mL of **Unlock** is used, then add 4 mL of the medium to stop the reaction). Gently pipette up and down a few times to disperse the medium.
- Centrifuge cells at **200 x g** for **5 minutes** at **room temperature**.
- Carefully aspirate and discard the supernatant with a pipette.
- Using a P1000 pipette, gently resuspend the cell pellet in **1 mL** of **Motor Neuron Maintenance Medium** until they are in a single cell suspension.
- Perform a cell count to ensure optimal seeding density.
- Remove the coating solution and add an appropriate volume of medium to the culture vessel. Do not let the culture vessel dry out.
- Plate the resuspended cells drop-wise and evenly at a density of **100,000 cells/cm²**.
- The day after plating, replace all of the medium with fresh pre-warmed, **37°C**, **Motor Neuron Maintenance Medium** without rock inhibitor (Y27632 hydrochloride).
- **Every 2 days** remove and replace all of the medium with fresh pre-warmed, **37°C**, **Motor Neuron Maintenance Medium** (without rock inhibitor (Y27632 hydrochloride)).

Note

Terminally differentiated iPSC-Derived Motor Neurons can be cultured for up to 35 days

- **iPSC-Derived Motor Neurons** should be culture for a minimum of 19-35 days.